Methods of Cancer Diagnosis, Therapy, and Prognosis

Volume 3
Gastrointestinal Carcinoma

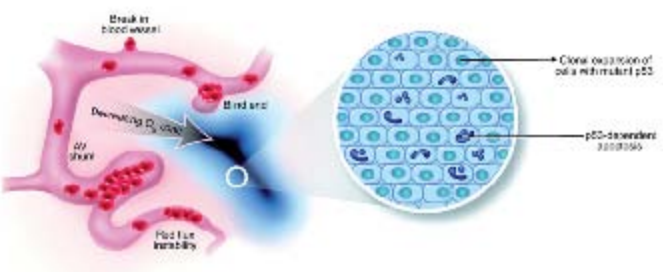

M.A. Hayat
Editor

Springer

Gastrointestinal Carcinoma

Methods of Cancer Diagnosis, Therapy, and Prognosis

Volume 3

For other titles published in this series, go to
www.springer.com/series/8172

Methods of Cancer Diagnosis, Therapy, and Prognosis

Volume 3

Gastrointestinal Carcinoma

Edited by

M.A. Hayat
Department of Biological Sciences,
Kean University, Union, NJ, USA

Springer

Editor
M.A. Hayat
Department of Biological Sciences
Kean University
Union, NJ
USA

ISBN 978-1-4020-8899-5 e-ISBN 978-1-4020-8900-8

Library of Congress Control Number: 2008930172

Printed on acid-free paper

9 8 7 6 5 4 3 2 1

springer.com

New technology, for better or for worse, will be used, as that is our nature.

Lewis Thomas

You have been given the key that opens the gates of heaven; the same key opens the gates of hell.

Writing at the entrance to a Buddhist temple

Authors and Co-Authors of Volume 3

Nicole B. Baril
Southern California Permanente Medical Group,
Kaiser Foundation Hospital,
Riverside, 10800 Magnolia Avenue
Riverside, CA 92505
E-mail: Nicole.B.Baril@kp.org

Laurent Bedenne
Fédération Francophone de Cancérologie Digestive, Faculté de Médecine,
BP 87900, 21079 Dijon-Cedex, France

Martin Béhé
Department of Nuclear Medicine,
Radboud University Nijmegen Medical Center, Postbus 9101, 6500 HB
Nijmegen, The Netherlands
E-mail: M.Gotthardt@nucmed.umcn.nl

Thomas M. Behr
Department of Nuclear Medicine,
Radboud University Nijmegen Medical Center, Postbus 9101, 6500 HB
Nijmegen, The Netherlands
E-mail: M.Gotthardt@nucmed.umcn.nl

Oliver Bouché
Service d'Hépato-Gastroentérologie,
CHU Robert Debré, avenue du Général Koenig, 51092 Reims Cedex, France

Kanika A. Bowen
Department of Surgery,
University of Texas, Medical Branch,
301 University Blvd., Galveston,
TX 77555

Bruno Buecher
Centre Hospitalier Universitaire
Hotel-Dieu, 44093 Nantes Cedex 01,
France

Halagowder Devaraj
Unit of Biochemistry,
Department of Zoology,
University of Madras, Guindy Campus,
600 025 Chennai, India
E-mail: hdrajum@yahoo.com

Niranjali Devaraj
Unit of Biochemistry, Department of Zoology, University of Madras, Guindy Campus, 600 025 Chennai, India

Michel Ducreux
Institut Gustave-Roussy, 39, Rue Camille Desmoulins, 94805 Villejuif, Cedex,
France

Jacqueline Duffour
CRLC Val d'Aurelle, Parc Euromedecine,
34298 Montpellier cedex 5, France
E-mail: jduffour@valdorel.fnclcc.fr

Turkkan Evrensel
Uludag University Medical School,
Department of Medical Oncology,
Gorukle-16059, Bursa, Turkey

Levente Ficsor
Department of Internal Medicine,
Semmelweis Egyetem II. Sz.
Belgyogyaszati Klinika, Sejtanalitika
Laboratorium, 1086 Budapest
Szentkiralyi utca 46, Hungary
E-mail: ficsorl@bel2.sote.hu

Eric François
Centre Antoine Lacassagne Nice,
06189 Nice Cedex 02, France

Yoshitaka Fujii
Nagoya City University Medical School,
Department of Surgery II, Kawasumi 1,
Mizuho-cho, Mizuho-ku, Nagoya,
467-8601, Japan

Mitsuhiro Fujishiro
University of Tokyo,
Department of Gastroenterology,
Graduate School of Medicine,
7-3-1 Hongo, Bunkyo-ku,
Tokyo 1138655, Japan
E-mail: mtfujish-kkr@umin.ac.jp

Kanwar R.S. Gill
Division of Gastroenterology and
Hepatology, Mayo Clinic,
4500 San Pablo Road, Jacksonville,
FL 32224, USA
E-mail: Gill.kanwarRupinder@mayo.edu

Takehiko Gokan
Department of Radiology, Showa
University School of Medicine,
1-5-8 Hatanodai, Shinagawa-ku,
Tokyo 142-8555, Japan

Martin Gotthardt
Department of Nuclear Medicine,
Radboud University Nijmegen Medical
Center, Postbus 9101,
6500 HB Nijmegen, The Netherlands
E-mail: M.Gotthardt@nucmed.umcn.nl

David Y. Graham
577 Matsushima, Kurashiki,
Okayama Prefacture 701-0192, Japan

Ken Haruma
577 Matsushima, Kurashiki,
Okayama Prefacture 701-0192, Japan

Tadateru Hasuo
Division of Surgical Pathology,
Department of Biomedical Informatics,
Kobe University, Graduate School
of Medicine, Kobe, Japan

M.A. Hayat
Department of Biological Sciences,
Kean University, 1000 Morris Avenue,
Union, NJ 07083, USA
E-mail: ehayat@kean.edu

Tatsuya Higashi
Department of Nuclear Medicine and
Diagnostic Imaging,
Kyoto University Graduate School
of Medicine, 54, Kawahara-cho,
Shogoin, Sakyo-ku, 606-8507
Kyoto, Japan
E-mail: higashi@kuhp.kyoto-u.ac.jp

Atsushi Imagawa
Tsuyama Central Hospital, Department
of Gastroenterology, 1756 Kawasaki
Tsumaya-City, Okayama,
7080841, Japan
E-mail: imagawa-gi@umin.ac.jp

Hideyuki Ishiguro
Nagoya City University Medical School, Department of Surgery II, Kawasumi 1, Mizuho-cho, Mizuho-ku, Nagoya, 467-8601, Japan
E-mail: h-ishi@med.nagoya-cu.ac.jp

Yoshihiro Kakeji
Department of Surgery and Science, Graduate School of Medical Sciences, Kyushu University, Maidashi 3-1-1, Higashi-ku,
Fukuoka 812-8582, Japan
E-mail: kakeji@surg2.med.kyushu-u.ac.jp

Masaaki Kawahara
Department of Radiology, Showa University School of Medicine, 1-5-8 Hatanodai, Shinagawa-ku, Tokyo 142-8555, Japan

Seigo Kitano
Department of Surgery I, Oita University, Faculty of Medicine, 1-1 Idaigaoka, Yufu,
Oita 879-5593, Japan
E-mail: kitano@med.oita-u.ac.jp

A. Anand Kumar
Unit of Biochemistry, Department of Zoology, University of Madras, Guindy Campus,
600 025 Chennai, India

Ender Kurt
Uludag University Medical School, Department of Medical Oncology, Gorukle-16059, Bursa, Turkey
E-mail: ekurt@uludag.edu.tr

Meral Kurt
Uludag University Medical School, Department of Radiation oncology, Gorukle-16059, Bursa, Turkey

Yoshiyuki Kuwabara
Nagoya City University Medical School, Department of Surgery II, Kawasumi 1, Mizuho-cho, Mizuho-ku, Nagoya, 467-8601, Japan

Jean-Louis Legoux
Service d'Hépato-Gastroentérologie, Hôpital du Haut Lévêque, 5 avenue de Magellan, 33604 Pessac, France

Naoko Maeda
Division of Surgical Pathology, Department of Biomedical Informatics, Kobe University, Graduate School of Medicine, Kobe, Japan

Yoshihiko Maehara
Department of Surgery and Science, Graduate School of Medical Sciences, Kyushu University, Maidashi 3-1-1, Higashi-ku,
Fukuoka 812-8582, Japan

Osman Manavoglu
Uludag University Medical School, Department of Medical Oncology, Gorukle-16059, Bursa, Turkey

Chantal Milan
Service d'Hepato - Gastroenterologie - Chu - Le Bocage, Dijon Cedex, France

Bela Molnar
Semmelweis Egyetem II. Sz. Belgyogyaszati Klinika, Sejtanalitika Laboratorium, 1086 Budapest Szentkiralyi utca 46, Hungary

Masaru Morita
Department of Surgery and Science, Graduate School of Medical Sciences, Kyushu University, Maidashi 3-1-1, Higashi-ku, Fukuoka 812-8582, Japan

Toshio Morohoshi
First Department of Pathology, Showa University School of Medicine, 1-5-8 Hatanodai, Shinagawa-ku, Tokyo 142-8555, Japan

Hideji Nakamura
Division of Hepatobiliary and Pancreatic Medicine, Department of Internal Medicine, Hyogo College of Medicine, 1-1 Mukogawa-cho, Nishinomiya, Hyogo 663-8501, Japan
E-mail: nakamura@hyo-med.ac.jp

Korefumi Nakamura
Division of Surgical Pathology, Department of Biomedical Informatics, Kobe University, Graduate School of Medicine, Kobe, Japan

Cristina Nanni
Nuclear Medicine Service- PET Unit, Policlinico S. Orsola-Malpighi, Bologna University, Bologna, Italy

Nobuyuki Ohike
First Department of Pathology, Showa University School of Medicine, 1-5-8 Hatanodai, Shinagawa-ku, Tokyo 142-8555, Japan
E-mail: ohike@med.showa-u.ac.jp

Eiji Oki
Department of Surgery and Science, Graduate School of Medical Sciences, Kyushu University, Maidashi 3-1-1, Higashi-ku, Fukuoka 812-8582, Japan

Yasuhiro Omori
Division of Surgical Pathology, Department of Biomedical Informatics, Kobe University, Graduate School of Medicine, Kobe, Japan

Lutfi Ozkan
Uludag University Medical School, Department of Radiation Oncology, Gorukle-16059, Bursa, Turkey

Nathan W. Pearlman
Department of Surgery, University of Colorado, Health Sciences Center, C311 University Hospital, 4200 E. 9th Avenue, Denver, CO 80262
E-mail: Nathan.Pearlman@uchsc.edu

Zhihai Peng
Department of Gastrointestinal Medical Oncology, Unit 426, The University of Texas M.D. Anderson Cancer Center, 1515 Holcombe Blvd., Houston, TX 77030, USA

Jean-Luc Raoul
Centre Eugène Marquis, CS 44229–35062 Rennes Cedex, France

Taylor S. Riall
Department of Surgery, University of Texas, Medical Branch, 301 University Blvd., Galveston, TX 77555, USA
E-mail: tsriall@utmb.edu

Philippe Rougier
Institut Gustave-Roussy, 39, Rue Camille Desmoulins, 94805 Villejuif, Cedex, France

Domenico Rubello
Nuclear Medicine Service- PET Unit, S. Maria della Misericordia Hospital, Viale Tre Martiri, 140, 45100 Rovigo, Italy
E-mail: domenico.rubello@libero.it

Noriaki Sadanaga
Department of Surgery and Science, Graduate School of Medical Sciences, Kyushu University, Maidashi 3-1-1, Higashi-ku, Fukuoka 812-8582, Japan

Shin-ya Satake
Division of Surgical Pathology,
Department of Biomedical Informatics,
Kobe University, Graduate School
of Medicine, Kobe, Japan

Lana Y. Schumacher
Stanford University School of Medicine
Department of Surgery
300 Pasteur Drive H-3591
Stanford, CA 94035

Jean-François Seitz
Institut Paoli-Calmettes, Marseille,
France

Shuho Semba
Division of Surgical Pathology,
Department of Biomedical Informatics,
Kobe University, Graduate School
of Medicine, Kobe, Japan

Akiko Shiotani
577 Matsushima, Kurashiki, Okayama
Prefacture 701-0192, Japan
E-mail: shiotani@med.kawasaki-m.ac.jp

Norio Shiraishi
Department of Surgery I,
Oita University, Faculty of Medicine,
1-1 Idaigaoka, Yufu, Oita 879-5593, Japan

Ayako Sugihara
Department of Pathology,
Meiwa General Hospital, Hyogo, Japan

Nobuyoshi Sugito
Nagoya City University Medical School,
Department of Surgery II,
Kawasumi 1, Mizuho-cho, Mizuho-ku,
Nagoya, 467-8601, Japan

Manabu Takahashi
Pathology Division, Ebara Hospital,
Tokyo 142-8555, Japan

Yasuhiko Tomita
Department of Pathology, Osaka University,
Graduate School of Medicine,
Yamada-Oka 22,
Suita, 565-0871,
Osaka Japan
E-mail: yt@molpath.med.osaka-u.ac.jp

Hirokazu Uyama
Department of Gastroenterology and
Hepatology,
Osaka University Graduate School of
Medicine, Yamada-oka 2-2, Suita, 565-
0871, Osaka, Japan

Denis Vetter
CHU Hopital Civil, 67091 Strasbourg
cedex, France

Timothy Woodward
Division of Gastroenterology and
Hepatology, Mayo Clinic,
4500 San Pablo Road, Jacksonville,
FL 32224, USA

Sherry M. Wren
Palo Alto Veterans Health Care System,
Department of Surgery, G112 3801
Miranda Avenue, Palo Alto,
CA 94304, USA
E-mail: swren@stanford.edu

Keping Xie
Department of Gastrointestinal Medical
Oncology, Unit 426, The University
of Texas M.D. Anderson Cancer Center,
1515 Holcombe Blvd., Houston,
TX 77030, USA
E-mail: kepxie@mail.mdanderson.org

Kazuhiro Yasuda
Department of Surgery I,
Oita University, Faculty of Medicine,
1-1 Idaigaoka, Yufu,
Oita 879-5593, Japan

Marc Ychou
CRLC Val d'Aurelle, Parc Euromedecine,
34298 Montpellier cedex 5, France

Hiroshi Yokozaki
Division of Pathology,
Department of Pathology and
Microbiology, Kobe University
Graduate School of Medicine,
7-5-1 Kusunoki-cho,
Chuo-ku,
Kobe 650-0017,
Japan
E-mail: hyoko@med.kobe-u.ac.jp

Preface

Each year, tens of millions of people are diagnosed worldwide with cancer, and more than half of these patients eventually die from this disease. The severity of the burden of cancer becomes really clear by knowing that there were ~10, 862, 496 new cancer cases (excluding skin cancer) in the world in 2002, and the number of deaths caused by this disease in the same year was ~ 6,723,887 (GLOBOCAN). The number of deaths due to cancer in the United States was estimated to be 559, 650 (Am. Cancer Soc.). Cancer is caused by both external factors (tobacco, chemicals, radiation, and infectious organisms) and internal factors (inherited mutations, hormones, immune conditions, and mutations that occur from metabolism).

All cancer types caused by cigarette smoking and heavy use of alcohol can be prevented. Currently, ~ 5 million people are killed annually worldwide by tobacco use, and by 2030, this number will increase to ~ 10 million, with 70% of deaths occurring in developing countries.

This volume contains detailed discussion of methods of diagnosis, therapy, and prognosis of gastrointestinal cancers, while Volumes 1 and 2 detail similar aspects of breast cancer, and lung and prostate cancers, respectively. The following data indicate the burden (seriousness) of gastrointestinal cancer, liver cancer, and colorectal cancers globally and in the United States. (Table 1) Surgical and molecular therapies and prognostic markers for gastrointestinal stromal tumors are discussed in this volume. Role of anticancer drugs and monoclonal antibodies specific for these tumors are also discussed. Imaging modality assessing the effect of anticancer imatinib on these tumors is included. Diagnostic and prognostic markers of clinical outcomes using chemotherapy and hormone replacement therapy for gastric adenocarcinoma are detailed. Also, are discussed immunohistochemistry of esophageal cancer progression, and diagnostic and therapeutic methodologies for biliary tumors. Immunohistochemistry of esophageal squamous cell carcinoma is included. Screening and multimodality therapies for advanced gastric cancer and response to chemotherapy are presented. Gastrointestinal cancer response to chemotherapy using the gene microrrays method is included. Photodynamic therapy and stenting for hilar cholangiocarcinoma are also discussed in this volume. In addition, discussion on the use of laparoscopy and ultrasound fine needle aspiration esophagectomy and

TABLE 1. Comparative rates of incidence and mortality of gastrointestinal cancers, liver cancer, and colorectal cancer between worldwide and the United States.

Name of Cancer	Incidence	Mortality
Colorectal cancer (worldwide)	923, 152	529, 978
Colorectal cancer (U.S.A)	153, 760	52, 180
Stomach cancer (worldwide)	933, 937	700, 349
Liver cancer (worldwide)	626, 162	598, 321
Liver cancer (U.S.A)	19, 160	16, 780
Pancreatic cancer (worldwide)	232, 306	227, 023
Pancreatic cancer (U.S.A)	37, 170	33, 370

granulocytic sarcoma of the small intestine is included. In addition, the role of hepatoma-derived growth factor in carcinogenesis and prognosis of pancreatic ductal cancer is discussed. Use of the FDG-PET technique in the prognosis of pancreatic cancer is also explained. Advantages of the application of chemotherapy to patients with unresectable locally-advanced pancreatic cancer are detailed.

This volume has been prepared through the efforts of 74 contributors representing eight countries. I am indebted to them for their promptness in accepting my suggestions. Strictly uniform style of manuscript writing has been accomplished. The very high quality of each chapter made my work as the editor an easy one. The methods presented here offer much more detailed, tested information than is available in scientific journals. Each chapter provides unique practical information based on the clinical expertise of the authors. The chapters contain the most up-to-date information, and hopefully the volume will be published expediously.

I am grateful to the Board of Trustees of Kean University and its president, Dr. Dawood Farahi and Vice President, Dr. Kristie Reilly for recognizing the importance of scholarship in an institution of higher education, and providing resources to complete this project. I am thankful to Betsy Mathew for her expert help in completing this volume.

M.A. Hayat
May 30, 2008

Contents

Contents of Volume 1 and 2

Volume 1

Volume 2

1
Introduction: Gastrointestinal Cancer

M.A. Hayat

INTRODUCTION

Cancer inflicts an enormous global burden of disease, which becomes apparent by considering the data shown in Table 1.1. In many countries, cancer ranks as the second most common cause of death following cardiovascular diseases. More deadly than AIDS, malaria or tuberculosis, is cancer. Cancer causes ~ 6.7 million deaths globally per year compared with a death toll of ~ 5 million from AIDS, malaria, and tuberculosis combined. Approximately, 10.9 million new cases of cancer are reported globally, and 24.6 million persons are alive with cancer (within 3 years of diagnosis). The most commonly diagnosed cancer types and causes of cancer death globally are shown in Table 1.1. The most prevalent cancer survivals in the world are breast cancer patients (4.4 million, up to 5 years following diagnosis) (http://caonline.amcancersoc.org/cgi/content/full/55/2/74). Estimated new cases of cancer and deaths caused by this disease in the United States are indicated in Table 1.2.

GASTROINTESTINAL CANCER

Approximately, 4,177,674, cases of gastrointestinal cancer are diagnosed each year with 2,440,563 deaths globally (Table 1.3). It is estimated that 261,800 cases of gastrointestinal cancer were reported in 2007 in the United States, resulting in 133,430 deaths (Table 1.4). In the same year 112,340 cases of colon cancer and 41,420 cases of rectal cancer were estimated to have occurred. In 2005, the number of newly diagnosed gastric cancer in the United States was estimated to be 22,000 and 11,500 deaths. These data clearly indicate that gastrointestinal cancer is one of the most commonly diagnosed malignancies and mortalities. The prognosis of upper gastrointestinal tract cancer at presentation is poor with 5 year survival rates of 20–22% for gastric cancer, 8–15% for esophageal cancer, and only 4% for pancreatic cancer. The reason for the low rate of survival is that many patients already have locally infiltrating cancer, lymph node metastases or distant metastases at the time of presentation.

TABLE 1.1. Global incidence and mortality cases of major cancer types. (Am. Cancer Soc.).

	Incidence	Mortality
1. Lung	1.35 million	1.18 million
2. Breast	1.15 million	410,712
3. Colorectal	1 million	529,000
4. Stomach	934,000	700,000
5. Liver	626,000	598,000

TABLE 1.2. Estimated new cases of cancer and deaths in the United States. (Am. Cancer Soc.).

	New Cases	Deaths
Respiratory system	229,400	164,840
Digestive system	271,250	134,710
Genital system	306,380	55,740
Breast	180,510	40,910
Urinary system	120,400	27,340
Leukemia	44,240	21,790
Lymphoma	71,380	19,730
Brain & other nervous system	20,500	12,740
Skin	65,050	10,850
Multiple Myeloma	19,900	10,790
Oral cavity & pharynx	34,360	7,550
Soft tissue (including heart)	9,220	3,560
Endocrine system	35,520	2,320
Bones & joints	2,370	1,330
Eye & orbit	2,340	220

Gastrointestinal Stromal Tumors (GISTs)

GISTs constitute the most common primary mesenchymal tumors of the digestive tract, and comprise ~ 5% of all sarcomas. They occur in older adults (median age 55–60 years) and rarely in children. These tumors are found throughout the intestinal tract: stomach (60%), small intestine (35%), and rectum, esophagus, omentum, and mesentrum (< 5%), and rarely in retroperitonium. The tumors are metastatic in omentum and mesentry (Miettinen and Lasota, 2006). GISTs originate from intestilial of Cajal or related stem cells. Tumor size and mitotic activity are the best predictive prognostic features. The most common presentation of these tumors is gastrointestinal bleeding, vague upper abdominal pain, and the presence of an abdominal mass. GISTs may also cause altered bowel function, bowel obstruction or perforation, dysphagia, and fever.

TABLE 1.3. Estimated global cases of gastrointestinal cancers and deaths.

	New Cases	Deaths
Stomach cancer	1,833,937	700,349
Colorectal cancer	1,023,152	528,978
Liver cancer	626,162	598,321
Esophagus cancer	462,117	385,892
Pancreas Cancer	232,306	227,023
Totals	4,177,674	2,440,563

It should be noted that GISTs do not constitute a single uniform entity, but represent a group of closely related neoplasms. Thus, molecular classification of these tumors is necessary to achieve correct diagnosis, effective clinical management, and correct interpretation of clinical results. Most GISTs express Kit (CD117), CD34, and heavy caldesmon, and some are positive for smooth muscle actin and desmin. Familial GISTs occur in patients with inheritable germline kit or platelet-derived growth factor receptor alpha (PDGFRA) mutations; central to the tumorgenesis of GISTs are gain-of-function mutations in Kit or alternative PDGFRA protooncogenes. These mutant

TABLE 1.4. Estimated new gastrointestinal cancer cases and deaths in 2007 in the United States. (Am. Cancer Soc.).

	New Cases	Deaths
Colorectal	153,760	52,180
Pancreatic	37,170	33,370
Stomach	21,260	11,210
Liver	19,160	16,780
Esophagus	15,560	13,940
Gallbladder & other biliary	9,250	3,250
Small intestine	5,640	2,700
Total	261,800	133,430

genes confer constitutive kinase activity to drive tumor development, which is the rationale for using imatinib mesylate (a selective tyrosine kinase inhibitor) for targeted therapy.

Based on the combination of mitotic rate and tumor size, the NIH stratified patients with GISTs into four risk categories, irrespective of tumor site (Fletcher *et al*., 2002). Significant prognostic heterogeneity exists in the high-risk category of the NIH scheme. Huang *et al*. (2007) have proposed a modified classification, recommending that GISTs with tumor size > 5 cm and mitosis > 10/50 high power fields be specified as the risk level IV category. This observation is basically in agreement with the study by Miettinen *et al*. (2005) which indicated that tumor- specific mortality was relatively low for tumors > 10 cm with mitotic activity which behave worse than their large but mitotically inactive counterparts. Such GISTs are highly lethal with a priority for genetic analysis to assess the suitability of postoperative adjuvant imatinib therapy.

Kit/PDGFRA tyrosine kinase inhibitor imatinib mesylate is used for the treatment of metastatic GISTs. This treatment improves the survival of patients with not only metastatic but also inoperable malignant GISTs, especially those whose tumors have Kit exon 11 mutations. For example, Nilsson *et al*. (2007) show that 1 year of imatinib (400 mg/day p.o.) (orally) treatment after radical surgery for high grade GIST reduces the risk of recurrent disease.

Imatinib is thought to up-regulate and down-regulate genes in GISTs. Imatinib induces insulin-like growth factor binding protein-3 (IGFBP-3) in GIST cell lines and human tumor tissues obtained early in the patient's treatment (Trent *et al*., 2006). Thus, it is suggested that IGFBP-3 is an early marker of antitumor activity of imatinib in GISTs. However, the usefulness of this drug for GISTs is controversial with regard to its resistance in patients with this cancer. The disagreement also relates to the dose of imatinib (ranging from 400 to 800 mg/day) used and the role of Kit exon 9 mutations and Kit exon 11 mutations (Heinrich *et al*., 2006; Debiec-Rychter *et al*., 2006). It should be noted that the exact role of adjuvant imatinib in GIST is not fully known, and is currently being investigated in ongoing trials. Surgery continues to be the treatment of choice for non-metastatic GISTs.

Gastric Cancer

Gastric cancer is the fourth most common cancer in the world. The incidence and mortality of this cancer are one of the highest in some parts of the world, e.g., China. Poor survival of patients with locally advanced gastric cancer is due to distant metastasis and incomplete resection. Local regional recurrence can also be involved in diminished disease-free survival. Although the incidence of gastric adenocarcinomas is declining, it is still one of the most common causes of cancer deaths worldwide. In 2002, 934,000 new gastric cancer cases were diagnosed worldwide with an estimated 700,000 deaths. In the United States and other Western countries, the incidence of gastrointestinal junction adenocarcinoma has risen faster than other gastrointestinal adenocarcinomas during the last quarter century.

As stated earlier, gastric cancer is a disease with a high rate of mortality and a limited number of effective curative options. However, several surgical

procedures, including radical gastrectomy with modified DI lymphadenectomy, endoscopic mucosal resection, and pylorus-preserving gastrectomy (PPG), have been developed for treating early gastric cancer. According to Hiki *et al.* (2006), clinical outcomes of surgical treatment were comparable for gastric cancer patients who underwent laparoscopy-assisted PPG and those treated with conventional PPG. Laparoscopy is used because it is less invasive and thus results in better postoperative quality of life, especially immediately after the procedure, as compared with conventional open operation. Better quality of life is associated with less postoperative pain and disability, earlier return of bowel function, shorter durations of hospitalization, and better cosmetic results. According to Moehler *et al.* (2005), the combination of irinotecan with continuous leucovorin-5-fluorouracil represents a potentially valuable treatment option for metastatic gastric cancer, but requires further evaluation. Di Lauro *et al.* (2007) also suggest the use of irinotecan, docetaxel, and oxaliplatin as a combination therapy for treating metastatic gastric or gastroesophageal junction adenocarcinoma, although this treatment resulted in neutropaenia, diarrhea, mucositis, and vomiting in some of the patients. It needs to be noted that despite recent advances in chemotherapy of metastatic gastric cancer, the survival advantage is marginal and no regimen has emerged that could be considered standard. Low response rate and less than favorable toxicity are some of the problems. Although combinations of various drugs are being tried, survival is still very poor. Some of the combinations of recently developed agents used in the first-line treatment of metastatic gastric cancer are mentioned above.

Esophageal Cancer

Human esophageal cancer is the eighth most frequently diagnosed cancer and the sixth most frequent cause of cancer death in the world. Globally, both esophageal and gastric cancers account for an estimated 1.4 million new cases and 1.1 million deaths, which are more than colorectal and breast cancers combined. Approximately, 386,000 (5.7% of the total cancers) deaths annually are attributed to esophageal malignancy worldwide. It was estimated that in 2007, 15,560 patients were diagnosed with esophageal cancer in the United States, with an estimated 13,940, deaths from this disease (Table 1.4).

At least two epithelial subtypes occur in the esophagus: esophageal squamous cell carcinoma and esophageal adenocarcinoma. Most esophageal cancers are squamous cell carcinoma that accounts for ~ 90% of this cancer, and arises in the middle and low-third of the esophagus. Rates of esophageal adenocarcinoma have been increasing during the last 2 decades, while those of the esophageal squamous cell carcinoma have been decreasing, suggesting distinct etiologies between these two subtypes. Esophageal cancer has a very poor survival: 16% of the cases in the United States and 10% in Europe. The 5-year survival rate of this cancer has improved only slightly during the past 3 decades. However, multimodel therapy followed by esophagectomy have increased 5-year survival to 30–40% in selected patient groups, but accurate detection of the presence of distant metastasis (M stage) is necessary to decide whether esophagectomy or chemotherapy should be offered to the patient (see later). An association

between cigarette smoking and increased risk of esophageal cancer has been found (Freedman *et al*., 2007). Alcohol use is also associated with this cancer, and obesity may also play a role in the development of this malignancy.

Treatments

Esophageal cancer patients generally have a poor prognosis because many of them already have locally unresectable or metastatic disease at presentation. It is estimated that 30–50% of patients at the time of presentation will have advanced stage (Stage IV) disease. Clinical outcome of this cancer is the most dismal among many types of digestive tumors because it is asymptomatic at early stage. Preoperative investigations commonly performed for staging of esophageal cancer include endoscopic ultrasonography (EUS), computed tomography (CT), ultrasound of the neck and abdomen, chest radiography, and bronchoscopy. EUS is the most important modality for evaluating local invasion of tumor into esophageal wall (the T stage) and regional lymph node involvement (the N stage).

Treatments of esophageal cancer include surgery, chemotherapy, neoadjuvant treatment with chemotherapy, radiation therapy alone or in combination with chemotherapy, photodynamic therapy, and stent placement. The choice of the treatment for individual patients should be based on the physician's ability to correctly define the extent of local, regional, and distance disease. The role of surgical treatment in palliation is limited, and is reserved for those patients who may derive some curative benefit from the intervention (Wren *et al*., 2002). Resectioning is recommended only for those patients with no evidence of metastasis. Appropriate staging can avoid the risk of operation for these patients who have little chance of cure. Positron emission tomography (PET) scan is effective for nonoperative staging (Wren *et al*., 2002). Correct staging helps to decide which patients should be offered adjuvant therapy and which patients will be operated on. Before deciding the type of treatment, a physical examination and fine-needle aspiration of suspicious lymph nodes in the cervical area are recommended. Also, a staging computed tomography (CT) scan of the chest, abdomen, and pelvis area can be carried out. EUS identifies patients with advanced local-regional disease (T3 N1) for entrance into neoadjuvant treatment. Subsequently, PET can also be used to assess response to chemotherapy and radiation.

Multimodel programs that include chemotherapy and radiation are being increasingly used for the treatment of these patients. Concurrent chemoradiation is an effective strategy for radiosensitization and control of micrometastatic disease. This combined treatment is also more effective than radiation alone in palliating dysphagia (Harvey *et al*., 2004). Recently, O'Connor *et al*. (2007) have recommended the use of oxaliplatin in combination with 5-fluorouracil and radiation in patients with locally advanced esophageal carcinoma (Stage II or III). Oxaliplatin is an important chemotherapeutic agent that is approved by the U.S. Food and Drug Administration for the treatment of advanced colorectal cancer. These authors recommend the following doses: oxaliplatin 85 mg/m^2, protracted-infusion 5-FU, 180 mg/m^2, and radiation, 50.4 Gy. According to these authors, the toxicities are modest and include pneumonitis and pulmonary fibrosis. In contrast, toxicities

associated with cisplatin-based concurrent chemoradiotherapy are more serious and include emesis, nephrotoxicity, esophagitis, mucositis, myelosuppression, delayed nausea, malnutrition, dehydration, weight loss and fluid electrolyte imbalances.

Oxaliplatin in combination with capecitabine has also been used for metastatic disease. Oxaliplatin (130 mg/m^2) can be used intravenously once a day and capecitabine (1,000 mg/m^2) orally twice daily on days 1–14 in a 21-day cycle (van Meerten*et al*., 2007). The frequency of toxicity is relatively low and quality of life is maintained during the treatment. This treatment can be given on an outpatient basis, and is thought to be less toxic than cisplatin-based therapy.

Vagal sparing esophagectomy therapy is recommended for intramucosal adenocarcinoma of the esophagus (Oh *et al*., 2006). (Intramucosal carcinoma arising in Barrett's esophagus is a complication of the common entity gastroesophageal reflux disease, and occurs after a long history of reflux). This method results in complete removal of all malignant and premalignant tissues, and preserves gastrointestinal innervations and blood supply to the gastric conduit while removing all of Barrett's mucosa and eliminating the risk of unrecognized dysplasia or synchronous cancers. This procedure also has lower morbidity, no mortality, and shorter hospital stay compared with standard types of resection.

Analysis of microvessel factors in biopsy specimens of tumors is useful for predicting the outcome of treatments. For patients with T_{2-3} esophageal cancers, hotspot microvessel density (MVD), total microvessel number (TN)/ total tumor area (TA), and total microvessel parameters (TP) are useful predictors for overall survival (Zhang *et al*., 2006). These combinations provide reliable assessment of chemoradiation. Using these protocols and a computer-assisted image analysis system for biopsy specimens, outcome of patients with this cancer treated with chemoradiation can be predicted (Zhang *et al*., 2006). This method produces low variability and high reproducibility (by minimizing intraobservor and interobservor variations in microvessel counting) for evaluating tumor vasculature.

The available data concerning the treatments for esophageal cancer are conflicting. An agreement is lacking, for example, on whether surgery alone or multimodel therapy is most effective for patients with locally advanced esophageal cancer. Because there are few long-term survivors with this disease, it is important to consider health-related quality of life when selecting a treatment. According to Graham *et al*. (2006), the optimal treatment for locally invasive esophageal cancer consists of chemoradiation followed by surgery to achieve improvement in quality-adjusted life expectancy of 40 days compared with surgery alone (15 days).

Pancreatic Cancer

Pancreatic cancer is the fourth leading cause of cancer-related deaths in both sexes, and has the highest death to incidence ratio of all types of cancers. The prognosis of patients with this disease remains very poor, with a 5-year survival rate of less than 5% after diagnosis. The incidence of pancreatic cancer continues to increase in the United States, and the yearly incidence of this cancer is estimated to be four cases per million. In 2007,

approximately 37,170 new cases were diagnosed and 33,370 patients died in the United States, yielding a relative mortality rate of 89.8%. In Europe, 73,700 cases of pancreatic adenocarcinoma were reported. Poor prognosis of this cancer is related to a high incidence of tumor cell invasion and metastasis. In spite of recent improvements in diagnostic techniques, this cancer is diagnosed at an advanced stage in most patients. Because of the combination of late stage disease presentation (localized: 8%, regional: 26%, and metastatic: 52%), intrinsic resistance to conventional treatments, and very low accessibility to resection, pancreatic cancer has the worst overall prognosis among solid tumors. Smoking and alcoholism are risk factors for this cancer.

Unquestionable evidence of malignancy of pancreatic endocrine tumors is shown by gross invasion of adjacent organs and metastasis in the regional lymph nodes or other distant sites. Among these patients, approximately one-third are diagnosed as having locally advanced stage radiographically confined to the pancreas and surrounding tissues (Ikeda *et al*., 2007). The most common metastatic sites are the liver, lung and peritoneum.

Genetic, histological, and clinical studies have identified three different preneoplastic lesions as potential precursors of pancreatic ductal adenocarcinoma that comprises > 90% of pancreatic cancer. Intraductal papillary mucinous neoplasms arise in the main pancreatic duct or its major branches, pancreatic intraepithelial neoplasias originate within intralobular ducts, and mucinous cystic neoplasms are mucin-producing epithelial neoplasms with a characteristic ovarian type stroma. These preneoplastic lesions represent progressive stages of the disease (Maitra *et al*., 2005). Pancreatic ductal carcinoma comprises up to 70% of all cases of pancreatic cancers, and has the worst prognosis.

As stated earlier, pancreatic adenocarcinomas arise from proliferative premalignant pancreatic intraepithelial neoplasia (PanIN) of the ductal epithelium. PanIN lesions begin as low cuboidal epithelial cells that become columnar owing to increased mucin production (Cruz-Monserrate *et al*., 2007). This is followed by nuclear atypia and increased proliferation, leading to luminal shedding and/or invasion into the stroma (Hruban *et al*., 2001). These morphological changes are accompanied by increased genetic abnormalities, including activation of K-ras, loss of tumor suppressors (e.g., p16, p53, and DPC4), and upregulation of telomerases (Hruban *et al*., 2000). Recent immunohistochemical studies have shown the upregulation and altered localization of intefrin $\alpha 6\beta 4$ (Cruz-Monserrate *et al*., 2007). Integrins are receptors for extracellular matrices that transmit mechanical and biochemical signals to regulate cellular functions including cell proliferation. PanIN lesions can also be found in patients with chronic pancreatitis, and these patients have an increased risk of developing pancreatic cancer (Malka *et al*., 2002).

Treatments

A number of chemotherapeutic agents, such as gemcitabine, paclitaxel, capecitabine, bevacizumab, gefitinib, and erlotinib, in conjunction with radiotherapy have been tried against pancreatic cancer (Czito *et al*., 2006). Among all the targeted agents that have been studied in patients with pancreatic cancer, erlotinib

(an epidermal growth factor receptor tyrosine kinase inhibitor) has shown a modest benefit in survival for patients (J. Bendell and R.H Goldberg, 2007, personal communication). According to Bria *et al*. (2007), platinum/gemcitabine combinations appear to improve progression-free survival and the overall response rate to standard treatments, and thus can be considered for use for selected pancreatic cancer patients. However, no marked improvement of survival has been found. Recently, Ikeda *et al*. (2007) have tried S-1, a novel orally administered drug, concurrently with radiotherapy against locally-advanced pancreatic cancer. A phase II trial of this drug is now underway. In patients with locally-advanced pancreatic cancer, the concurrent external beam radiation and 5-fluorouracil therapy may offer a survival benefit in comparison with either of these two therapies alone.

Apart from surgery there is no effective therapy for pancreatic cancer, but even patients who undergo surgery often die within 1 year postoperatively. Resection is associated with high morbidity and mortality. The 5-year survival rate after surgical resection remains poor, ranging from 26% for patients with pancreatic adenocarcinoma to 70% for patients with ampullary carcinoma. Alternatively, palliative pancreaticoduodenectomy compared with traditional surgical palliation has been suggested for patients with advanced locoregional disease to improve survival (Lillemoe *et al*., 1996). Nevertheless, surgical resection of pancreatic cancer or adenocarcinoma or periampullarea provides almost no possibility of relatively long-term survival.

Gene silencing by RNA interference (RNAi) holds a promising therapeutic potential to suppress gene expression in mammalian cells. RNAi can be directed against pancreatic cancer through various pathways, including the inhibition of overexpressed oncogenes, suppression of tumor growth, metastasis, and enhancement of apoptosis. In combination with chemoradiation agents, RNAi can also attenuate the chemoradiation resistance of pancreatic cancer (Chang, 2007). Moreover, RNAi has been used for defining the loss of function of endogenous genes in pancreatic cancer. RNAi applications in pancreatic cancer require further exploration.

Aneuploidy and increased genetic instability, manifesting as losses, gains, and amplifications are common characteristics of pancreatic cancer (Kallioniemi, 2007). Using microarray-based copy number surveys, genes concealed in these aberrations can be uncovered, which provides targets for the development of diagnostic and therapeutic approaches.

REFERENCES

Bria, E., Milella, M., Gelibter, A., Cuppone, F., Pino, M.S., Ruggeri, E.M., Carlini, P., Nistico, C., Tersoli, E., Cognetti, F., and Giannarelli, D. 2007. Gemcitabine-based combinations for inoperable pancreatic cancer: have we made progress? *Cancer 110*: 525–533.

Chang, H. 2007. RNAi-mediated knockdown of target genes: a promising strategy for pancreatic cancer research. *Cancer Gene Ther. 14*: 677–685.

Cruz-Monserrate, Z., Qiu, S., Evers, B.M., and O'connor, K.L. 2007. Upregulation and redistribution of integrin α6β4 expression occurs at an early stage in pancreatic adenocarcinoma progression. *Mod. Pathol. 20*: 656–667.

Czito, B.G., Willett, C.G., Bendell, J.C., Morse, M.A., Tyler, D.S., Fernando, N.H., Mantyh,

C.R., Blobe, G.C., Honeycutt, W., Yu, D., Clary, B.M., Pappas, T.N., Ludwig, K.A., and Hurwitz, H.I. 2006. Increased toxicity with gefitinib, capecitabine, and radiation therapy in pancreatic and rectal cancers: phase I trial results. *J. Clin. Oncol. 24*: 565–662.

Debiec-Rychter, M., Sciot, R., Le Cesne, A., Schlemmer, M., Hohenberger, P., Van Oosterom, A.T., Blay, J.Y., Leyvraz, S., Stui, M., Casali, P.G., Zalcberg, J., Verweij, J., Van Glabbeke, M., Hagemeijer, A., and Judson, I. 2006. KIT mutations and dose selection for imatinib in patients with advanced gastrointestinal stromal tumors. *Eur. J. Cancer 42*: 1093–1103.

Di Lauro, L., Nunziata, C., Arena, M.G., Foggi, P., Sperduti, I., and Lopez, M. 2007. Irinotecam, docetaxel, and oxaliplatin combination in metastatic gastric or gastroesophageal junction adenocarcinoma. *Brit. J. Cancer 97*: 593–597.

Fletcher, C.D., Berman, J.J., Corless, C., Gorstein, F., Lasota, J., Longley, B.J. Miettinen, M., O'Leary, T.J., Remotti, H., Rubin, B.P., Shmookler, B., Sobin, L.H., and Weiss, S.W. 2002. Diagnosis of gastrointestinal stromal tumors: a consensus approach. *Hum. Pathol. 33*: 459–465.

Freedman, N.D., Abnet, C.C., Leitzmann, M.F., Mouw, T., Subar, A.F., Hollenbeck, A.R., and Schatzkin, A. 2007. 2007. A prospective study of tobacco, alcohol, and the risk of esophageal and gastric cancer subtypes. *Am. J. Epidemiol. 165*: 1–10.

Graham, A.J., Shrive, F.M., Ghali, W.A., Manns, B.J., Grondin, S.C., Finley, R.J., and Clifton, J. 2006. Defining the optimal treatment of locally advanced esophageal cancer: a systematic review and decision analysis. *Ann. Thorac. Sur. 83*: 1257–1264.

Harvey, J.A., Bessell, J.R., Beller, E.,Thomas, J., Gotley, D.C., Burmeister, B.H., Walpole, E.T., Thomson, D.B., Martin, I., Doyle, L., Burmeister, E., and Smithers, B.M. 2004. Chemoradiation therapy is effective for the palliative treatment of malignant dysphagia. *Dis. Esophagus 17*: 260–265.

Heinrich, M., Corless, C.L., Blanke, C.D., Demetri, G.D., Joensuu, H., Roberts, P., Burton L., Eisenberg, B., Von Mehren, M., Fletcher, C., Sandau, K., McDougall, K., Ou, W.B., Chen, C.J., and Fletcher, J. 2006. Molecular correlates of imatinib resistance in gastrointestinal stromal tumors. *J. Clin. Oncol. 24*: 4764–4774.

Hiki, N., Shimoyama, S., Yamaguchi, H., Kubota, K., and Kaminishi, M. 2006. Laparoscopy-assisted pylorus-preserving gastrectomy with quality controlled lymph node dissection in gastric cancer operation. *J. Am. Coll. Surg. 203*: 162–169.

Hruban, R.H., Goggins, M., Parsons, J., and Kern, S.E. 2000. Progression model for pancreatic cancer. *Clin. Cancer Res. 6*: 2969–2972.

Hruban, R.H., Adsay, N.V., Albores-Saavedra, J., Compton, C., Garrett, E.S., Goodman, S.N., Kern, S.E., Klimstra, D.S., Klöppel, G., Longnecker, D.S., Lüttges, J., and Offerhaus, G.J. 2001. Pancreatic intraepithelial neoplasia: a new nomenclature and classification system for pancreatic duct lesions. *Am. J. Surg. Pathol. 25*: 579–586.

Huang, H.Y., Li, C.F., Huang, W.W., Hu, T.H., Lin, C.N., Uen, Y. H., Hsiung, C.Y., and Lu, D. 2007. A modification of NIH consensus criteria to better distinguish the highly lethal subset of primary localized gastrointestinal stromal tumors: a subdivision of the original high-risk group on the bases of outcome. *Surgery 141*: 748–756.

Ikeda, M., Okusaka, T., Ito, Y., Cleno, H., Morizane, C., Furuse, J., Ishii, H., Kawashima, M., Kagani, Y., and Ikeda, H. 2007. A phase I trial of S-1 with concurrent radiotherapy for locally-advanced pancreatic cancer. *Brit. J. Cancer. 96*: 1650–1655.

Kallioniemi, A. 2007. Molecular characterization of novel amplification target genes in pancreatic cancer. *Cellul. Oncol.*: 103–113.

Lillemoe, K.D., Cameron, J.L., Yeo, C.J., Sohn, T.A., Nakeeb, A., Sauter, P.K., Hruban, R.H., Abrams, R.A., and Pitt, H.A. 1996. Pancreaticoduodenectomy. Does it have a role in the palliation of pancreatic cancer? *Ann. Surg. 223*: 718–725.

Maitra, A., Fukushima, N., Takaori, K., and Hruban, R.H. 2005. Precursors to invasive pancreatic cancer. *Adv. Anat. Pathol. 12*: 81–91.

Malka, D., Hammel, P., Maire, F., Rufat, P., Madeira, I., Pessione, F., Lévy, P., and Ruszniewski, P. 2002. Risk of pancreatic adenocarcinoma in chronic pancreatitis. *Gut 51*: 849–852.

van Meerten, E., Eskens, F.A., van Gameron, E.C., Doorn, L., and van der Gaast, A. 2007. First-line treatment with oxaliplatin and capecitabine in patients with advanced or metastatic esophageal cancer: a phase II study. *Br. J. Cancer 96*: *1348–52.*

Miettinen, M., and Lasota, J. 2006. Gastrointestinal stromal tumors: review on morphology, molecular pathology, prognosis, and differential diagnosis. *Arch. Pathol. Lab. Med. 130*: 1466–1478.

Miettinen, M., Sobin, L.H., and Lasota, J. 2005. Gastrointestinal stromal tumors of the stomach: a clinicopathologic, immunohistochemical and molecular genetic study of 1765 cases with long-term follow-up. *Am. J. Surg. Pathol. 29*: 52–68.

Moehler, M., Eimermacher, A., Siebler, J., Hohler, T., Wein, A., Menges, M., Flieger, D., Junginger, T., Geer, T., Gracien, E. Galle, P.R., and Heike, M. 2005. Randomized phase II evaluation of irinotecan plus high-dose 5-fluorouracil and leucovorin (ILF) vs. 5-fluorouracil, leucovorin, and etoposide (ELF) in untreated metastatic gastric cancer. *Brit. J. Cancer 92*: 2122–2128.

Nilsson, B., Sjolund, K., Kindbloom, L.-G., Meis-Kindblom, J.M., Bumming, P., Nilsson, O., Andersson, J., and Ahlman, H. 2007. Adjuvant imatinib treatment improves recurrence-free survival in patients with high-risk gastrointestinal stromal tumors (GIST). *Brit. J. Cancer 96*: 1656–1658.

O'Connor, B.M., Chadha, M.K., Pande, A., Lombardo, J.C., Nwogu, C.E., Nava, H.R., Yang, G., and Javle, M.M. 2007. Concurrent oxaliplatin, 5-flourouracil, and radiotherapy in the treatment of locally advanced esophageal carcinoma. *Cancer J. 13*: 119–124.

Oh, D.S., Hagen, J.A., Chandrasoma, P.T., Dunst, C.M., DeMeester, S.R., Alavi, M., Brenner, C.G., Lipham, J., Rozetto, C., Cote, R., and DeMesster, T.R. 2006. Clinical biology and surgical therapy of intramucosal adenocarcinoma of the esophagus. *J. Am. Coll. Surg. 203*: 152–161.

Trent, J.C., Ramdas, L., Dupart, J., Hunt, K., Macapinlac, H., Taylor, E., Hu, L., Salvado, A., Abbruzzese, J.L., Pollock, R., Benjamin, R.S., and Zhang, W. 2006. Early effects of imatinib mesylate on the expression of insulin-like growth factor binding protein-3 and positron emission tomography in patients with gastrointestinal stromal tumor. *Cancer 107*: 1898–1908.

Wren, S.M., Stinjins, and Srinivas, S. 2002. Positron emission tomography in the initial staging of esophageal cancer. *Arch. Surg. 137*: 1001–1007.

Zhang, S.-C., Hironoka, S., Ohtsu, A., Yoshida, S., Hasebe, T., Fukayama, M., and Ochiai, A. 2006. Computer-assisted analysis of biopsy specimen microvessels predicts the outcome of esophageal cancers treated with chemoradiotherapy. *Clin. Cancer Res. 12*: 1735–1741.

2
Metastatic Gastrointestinal Cancer: Safety of Cisplatin Combined with Continuous 5-FU Versus Bolus 5-FU and Leucovorin (Methodology)

Jacqueline Duffour, Olivier Bouché, Philippe Rougier, Chantal Milan, Laurent Bedenne, Jean-François Seitz, Bruno Buecher, Jean-Louis Legoux, Michel Ducreux, Denis Vetter, Jean-Luc Raoul, Eric François, and Marc Ychou

INTRODUCTION

Esophageal, gastric, and pancreatic cancers remain frequent digestive carcinomas, and are among the main causes of cancer death worldwide. At the metastatic stage, the prognosis is very poor in most cases. Most of the 5-Fluorouracile (5-FU) based regimens are widely used in esophageal and gastric locations and were common for pancreatic cancer before the advent of gemcitabine. Attempts to improve the antitumor efficacy of 5-FU in the gastrointestinal cancers have included biomodulation with various agents such as folinic acid, previously tested by Machover *et al*. (1986) and Poon *et al*. (1991) in colorectal cancer treatment. The combination of 5-Fluorouracil with cisplatin has proven to significantly increase the efficacy and survival of patients. The synergistic activity of this latter combination has been demonstrated in both experimental models by Etienne *et al*. (1991) and clinical studies by Kim *et al*. (1993). The association of 5-FU with cisplatin is still widely used in advanced gastric cancer; the FP regimen (using 5-FU 800–1,000 mg/m^2/day in continuous infusion for 5 days with cisplatin 100 mg/m^2/day on day 2) has been well documented in three large phase II trials reported by Lacave *et al*. (1991), Rougier *et al*. (1994), and Ohtsu *et al*. (1994), and yielded overall response rate of 41%, 43%, and 43%, respectively, with median survival times of 10.6, 9, and 7 months, respectively.

In advanced pancreatic carcinoma, the same FP regimen has been explored in a monocentric phase II study by Rougier *et al*. (1993). The response rate was 26.5% with a median survival of 7 months. At the time of commencing our study, this FP schedule was evaluated in two phase III trials, one in advanced gastric cancer by Vanhoefer *et al*. (2000) and another in advanced pancreatic cancer by Ducreux *et al*. (2002). Finally the combination 5-FU-cisplatin was considered to be the standard treatment in esophageal location, based on the randomized phase II study by Bleiberg *et al*. (1997). Recently, various authors as

Mitry *et al*. (2004) or Bouché *et al*. (2004) replaced the 5-FU monthly regimen by LV5FU2 in the combination 5-FU-cisplatin in advanced gastric and esophagogastric locations. They showed a similar efficacy. The modulation of the combination 5-FU/cisplatin with folinic acid (FLP regimen) has also been previously tested by Ychou *et al*. (1996) in patients with metastatic gastric cancer. This regimen using leucovorin 200 mg/m^2/day (given as a short infusion of 15 min) followed by 5-FU (400 mg/m^2/day for 5 days given as a 1 h infusion) with cisplatin (100 mg/m^2 on day 2), achieved equivalent results in terms of efficacy to those reported above with FP regimen by Lacave *et al*. (1991), Rougier *et al*. (1994), and Ohtsu *et al*. (1994) with better tolerance.

Considering the limited efficacy of these treatments in these gastrointestinal locations, we think that it is important to give priority to the quality of life during the short survival. So, we propose to compare in a randomized trial the safety (primary objective), clinical efficacy, and quality of life (secondary objectives) of FLP vs. FP as a first line chemotherapy in patients with metastatic esophageal, gastric and pancreatic carcinoma, three cancers tending to show a positive response to these molecules.

PATIENTS AND METHODS

Patient selection. The eligibility criteria were as follows: patients with histologically proven carcinoma of the esophagus, the stomach or the pancreas were eligible. They must have measurable metastatic disease (≥15 mm), no indication of radiotherapy and/or surgery and no prior chemotherapy for metastatic disease. In the case of adjuvant chemotherapy, regimen did not contain cisplatin. All patients had age ≤75 years, World Health Organization (WHO) performance status < 2, adequate baseline organ function defined as neutrophile count ≥1,500/mm^3, platelet count ≥100,000/mm^3 and creatinine level <1.25 normal level. In the cases where the patient was older than 70 years and/or creatinine level was between 1 and 1.25 times the normal limit, creatinine clearance had to be > 60 ml/mm. Ineligibility criteria included severe uncontrolled comorbidities and brain metastases. Written informed consent approved by the local Ethical Committee was given by all the participants before they entered the study.

Stratification and randomisation. Patients were stratified according to institution, performance status (WHO 0 vs. 1), and prior adjuvant chemotherapy. The type of primary tumor (esophageal adenocarcinoma, vs. esophageal squamous cell carcinoma, vs. gastric adenocarcinoma, vs. pancreatic adenocarcinoma) was defined as stratification's factor too. Patients were then randomly assigned to receive either FP regimen (arm A) or FLP regimen (arm B), by the FFCD data center (Dijon center, France), using the minimization technique.

Treatment plan. Treatment–A. 5-FU-cisplatin (FP) regimen consisted of 5-FU at a dose of 800 mg/m^2/day in continuous infusion for 5 consecutive days and cisplatin at 100 mg/m^2 in a 1 h perfusion on day 1 or day 2.

Treatment–B. 5-FU-cisplatin-leucovorin (FLP) regimen consisted of leucovorin at a dose of 100 mg/m^2/day in bolus for 5 consecutive days, followed by 5-FU at 350 mg/m^2/day in a 1 h infusion from day 1 to day 5 and cisplatin at 100 mg/m^2 given on day 1 or day 2.

The cycles were repeated every 28 days whatever the treatment. In case of no grade 3–4 (WHO grading) hematological and diarrhea toxicity at the first cycle, the dose of 5-FU was increased for the following cycles at 1,000 mg/m^2/day in arm A and 400 mg/m^2 in arm B. Treatment was continued until the disease progression in all patients and doses were adapted to the toxicity; a reduction of 25% was planned in case of hematological and/or digestive toxicity greater or equal to grade 3 during the interval between two cycles. Cycles were delayed until toxicity levels normalized. In the FLP arm, cisplatin could be stopped if renal, neurological, or otological toxicity precluded further administration. The protocol treatment was stopped for tumor progression, grade 4 life threatening toxicity, or at the patient's request.

Pretreatment evaluation, follow-up, and response evaluation. Baseline evaluation included a complete medical history and physical examination, standard biological tests, ECG, chest X-ray, and computed tomographic scan of the measurable metastatic lesions. The patients were monitored before each cycle of chemotherapy, including assessment of clinical toxicity, blood cell count, serum chemistry, physical examination, and quality of life assessment according to Spitzer's index (1981). Hospitalization durations were noted during and after the treatment. Between the first and the second cycle, blood cell count was performed every week, so as to increase the dose of 5-FU at the second cycle. Toxicities were evaluated and graded according to WHO criteria. Tumor response was assessed by computed tomographic scan every two cycles of chemotherapy (every 2 months) in both arms and at the end of the treatment. After completion of the treatment, the patients with tumor response or stable disease were evaluated every 2 months until documented disease progression. WHO criteria were used to define the response and the response duration. Computed tomographic scans were performed 4 weeks later to confirm the response. The computed tomographic scans of patients who achieved an objective response were centrally reviewed by an external panel of radiologists.

Statistical considerations. The aim of this study was to detect a difference of at least 15% (20–5%) in grade 3–4 toxicity (better tolerance expected in the FLP group), while observing a difference of $< 15\%$ in the objective response rate (ORR) between the two regimens. The study was designed so as to require 116 patients per arm to provide at least 80% power in a one-sided test (with a α risk of 5%). After 1 year of recruitment, an independent committee was able to stop the trial in case of too severe toxicity. The Mantel-Haenszel test was used to compare toxicity and responses between arms, using stratification on tumor location. Progression-free survival and overall survival were calculated, using the Kaplan-Meier method, from the date of inclusion to progression (relapse, second cancer, or cancer death) and death from any cause, respectively. The log-rank test was used to identify the prognostic factors, and the Cox proportional hazard model was used for all multivariate analyses. All analyses were based on the intent-to-treat principle.

RESULTS

From April 1995 to April 1998, 232 patients with metastatic esophageal, gastric, or pancreatic carcinoma from 28 institutions

(classified in three classes according to their size) were randomized. Six patients were ineligible (3%), four patients because of incorrect histology, one patient was not metastatic (liver angioma) and one patient had been treated with cisplatin previously.

The two arms (113 patients per arm) of the study were well balanced for the main characteristics: age, sex, prior adjuvant chemotherapy, performance status, location of primary tumor, number of metastatic sites, and chronology of metastases. The study comprised 173 men and 53 women; the mean age of the patient population was 60 years. The repartition of primary tumor was as follows: 19 squamous cell carcinoma of the esophagus, 19 esophageal adenocarcinoma, 91 gastric, and 97 pancreatic adenocarcinoma. Most of the patients (98%) had never received prior adjuvant chemotherapy. WHO performance status was good (0 or 1) in almost all the patients (225/226).

Toxicity and dose-intensity. There were ten protocol violations: four patients received FP treatment in place of FLP, one patient (allocated in the arm B) started the FP regimen and then continued with the FLP regimen and five patients were treated with additional radiotherapy (a tongue cancer, discovered 10 days after the inclusion, received radiotherapy). One ineligible patient (receiving FLP regimen) was included by mistake despite having a poor WHO performance status (2). Two hundred and twenty-three patients were assessable for treatment description and toxicity. The median number of cycles before progression was 3 (SE = 0.3) in arm A (range 1–12) and 3 (SE = 0.2) in arm B (range 1–11) and a total of 387 and 412 cycles were administered in arm A and B, respectively.

Toxicities were assessed for the first cycle and then for the whole range of cycles before progression. Overall, 78.4% and 69.6% of the patients treated by FP and FLP regimens, respectively, experienced WHO grade 3–4 toxic reactions ($p = 0.17$). Hematological toxicity was very similar in the two groups. The major toxicity was neutropenia (FP = 35.1% and FLP = 33.0%). Although severe anemia was more marked in arm B (24.1% vs. 15.3%), there was no significant difference between the two groups. The occurrence of nausea/vomiting was common with the use of high dose cisplatin and was not statistically different between the two groups (arm A = 25.2%, arm B = 33.0%). The only significantly different toxicity between the two arms was mucositis, with 16.2% of the patients with grade 3–4 in arm A vs. 4.5% in arm B ($p = 0.009$). In spite of the use of cisplatin, nephrotoxicity and hearing loss were very mild, regardless of arm, and serious ototoxicity showed minor differences (not statistically significant) between the two arms (0.9% in arm B vs. 1.8% in arm A).

The toxicity profile was assessed according to the type of primary tumor. Compared with the other sites (esophageal adenocarcinoma, squamous cell carcinoma or pancreatic adenocarcinoma), patients with gastric cancer developed the greatest grade 3–4 toxicities (81.4% vs. 57.9%, 72.2% and 70.5%, respectively $p = 0.04$). Severe hematological toxicity (60.4% whose 53.8% neutropenia) was very high in this location, compared with the other sites (31.6% and 26.3% in esophageal adenocarcinoma, 33.3% and 11.1% in squamous cell carcinoma and 36.8% and 21.1% in pancreatic location, respectively ($p = 0.0003$ and $p = 0.0001$). Severe digestive toxicity occurred

for 41.1% of the patients with pancreatic cancers, 21.1% of those with esophageal adenocarcinoma, 22.2% with squamous cell carcinoma and 34.1% with gastric cancer ($p = 0.10$).

These adverse effects were responsible for treatment interruptions in 11.5% of the cycles in arm A and 15.9% of the cycles in arm B. The occurrence of treatment interruption due to toxicity was very similar in the three sites (10.5%, 11.1%, and 11.5% of cycles in esophageal adenocarcinoma, squamous cell carcinomas and pancreatic cancer, respectively); patients with gastric cancer stopped their chemotherapy because of toxicity in 17.6% of cycles.

There were six toxic deaths: two in arm A and four in arm B. Two were due to neutropenic sepsis (arm B), two due to renal failure (one in arm A and one in arm B), one due to severe diarrhea (arm B), and one due to ischemic attack (arm A, in a patient with predisposing factors). Administration delays were necessary in 22.5% of the cycles (arm A) and 25% of the cycles (arm B). The duration of the delay was similar in the two arms: less than or equal to 3 days in 9.6% of the cycles in arm A vs. 10.1% in arm B, between 4 and 7 days in 9.0% of the cycles in arm A vs. 11.2% in arm B, greater or equal to 15 days in 1.6% and 1.2% of the cycles in arms A and B, respectively. Delays >15 days were only reported in patients with esophageal adenocarcinoma and gastric cancer (3.9% and 3.1% of the cycles respectively). The median doses of 5-FU and cisplatin received before progression, were respectively 831 and 95.7 mg/m^2/day in arm A representing a dose intensity of 89% and 95.7%, and 361.5 and 96.8 mg/m^2/day in the arm B i.e., a dose intensity of 94.3% and 96.8%, respectively.

Response rate. All patients were assessed for response. The objective response rate, initially assessed by investigators, was identical in the two groups (20.4%). It remained quite similar after external review at 18.6% (95% confidence interval (CI) 11.4–25.8) in arm A, not significantly different from 15% (95% CI 8.5–21.6) in arm B, ($p = 0.59$). Two complete responses were observed in each arm (21 objective responses in arm A vs. 17 in arm B). Twenty nine patients achieved stable disease in arm A, compared with 28 in arm B. The objective responses observed in patients were 7/19 (36.8%) with esophageal adenocarcinoma, 4/19 (21%) with esophageal squamous cell carcinoma, 18/91 (19.8%) with gastric cancer and 9/97 (9.3%) with pancreatic cancer. The median duration of objective response was 23.9 weeks (SE = 9.3) in arm A, which did not significantly differ from 24 weeks (SE = 4.3) in arm B ($p = 0.51$). Median duration of response was similar ($p = 0.22$) in the different sites of primary tumor: 27.7 weeks (SE = 32.3) in esophageal adenocarcinoma, 16.4 weeks (SE = 11.5) in esophageal squamous cell carcinoma, 24.0 weeks (SE = 6.2) in gastric cancer and 22.8 weeks (SE = 6.2) in pancreatic carcinoma.

Survival. Median overall survivals were not statistically different ($p = 0.83$) at 24 weeks (SE = 3.6) with FP and 24.7 weeks (SE = 3.6) with FLP. The 1- and 2-year survival rates were 21.5 % (SE = 3.9) and 6.7 % (SE = 2.5), respectively in arm A and 17.3 % (SE = 3.6) and 2.8 % (SE = 1.9) in the arm B. Considering the survival according to the location of the primary tumor, median overall survival was worst for pancreatic carcinoma (16.6 weeks, SE = 2.1) than for esophageal adenocarcinoma (31.3 weeks, SE = 1.9), esophageal

squamous cell carcinoma (20.6 weeks, SE = 1.1) and gastric cancer (39.7 weeks, SE = 4.1).

The only statistically significant predictors of survival in univariate analysis were tumor location ($p < 0.0001$) and performance status ($p = 0.0013$). The number of metastatic sites was not a statistically significant factor, but there was a trend towards better survival ($p = 0.062$) when the disease was not very extensive. Survival in the treatment groups was compared after adjustment for these prognostic factors. The FLP regimen was not superior to the FP regimen in terms of survival ($p = 0.28$) and the main factors correlated with poor survival were the location of primary tumor in pancreas ($p = 0.0002$) and the age of the patients ($p = 0.045$). Considering the median progression free survival, the two regimens did not differ significantly, 12.4 (SE = 2.6) and 12.1 (SE = 2.6) weeks with FP and FLP, respectively ($p = 0.91$). The 1- and 2- year survival rates were 9.4% (SE = 2.8) and 3.5% (SE = 1.8), respectively in the FP arm and 5.3% (SE = 2.1) and 1.2 % (SE = 1.1) in the FLP arm. As observed above, the progression free survival was worst ($p = 0.002$) for the pancreatic carcinoma, with a median survival time of 8.6 weeks (SE = 4.2), than for the other locations: 16 weeks (SE = 4.3) for esophageal adenocarcinoma, 13.4 weeks, (SE = 3.4) for esophageal squamous cell carcinoma and 20 weeks, (SE 3.6) for gastric cancer.

Quality of life was fairly well assessed until the sixth cycle (48 weeks) as questionnaire filling rates during the first six cycles were: 97.9%, 100%, 86.7%, 90.0%, 80.9% and 78.4%, respectively. During this period, there was no difference in Spitzer's scores between the two arms. From the seventh cycle, global quality of life data were available for only 34.3% of the patients; therefore, they could not be analyzed due to insufficient numbers.

The mean duration of hospital stay (during or after treatment) was not statistically different between the two arms: 38.3 days (SE = 2.8) in arm A compared to 35.2 days (SE = 0.6) in arm B ($p = 0.24$). When converted to days per month of life, the mean duration remained similar: 8.1 days (SE = 0.7) for arm A and 7.4 days (SE = 0.6) for arm B, ($p = 0.42$). The total duration of hospital stay was shorter in pancreatic location (29.8 days, SE = 2.3) than in esophageal adenocarcinoma (42.5 days, SE = 7.5), esophageal squamous cell carcinoma (36.2 days, SE = 5.0) and gastric cancer (43.0 days, SE = 3.1), but these differences were not observed when the duration of hospital stay was converted to days per month of life (7.3 days, SE = 1.6) in esophageal adenocarcinoma, 7.5 days (SE = 1.5) in esophageal squamous cell carcinoma, 7.3 days (SE = 0.7) in gastric cancer and 8.3 days (SE = 0.7) in pancreatic location.

DISCUSSION

The primary objective of this phase III randomized study was to compare the tolerance between FLP and FP regimen in metastatic esophageal, gastric, and pancreatic carcinomas. The overall safety of these chemotherapies is very similar to most previous studies; grade 3–4 neutropenia and digestive toxicity occurred in about 30% and 20% of the patients with gastric and pancreatic cancers, respectively, as observed by Rougier *et al.* (1993, 1994), Vanhoefer *et al.* (2000), Ducreux *et al.* (2002), and Andre *et al.*

(1996). Maximum severe toxicity was very similar in the two arms; only mild and particularly severe mucositis was statistically lower with FLP regimen. This could be explained by the duration of the injection (1-h infusion instead of 120 h) combined with the lower dose of 5-FU (350–400 mg/m^2) in this arm. Similar observations had already been made by Ychou *et al*. (1996) when using the same FLP regimen (with 1-h injection) showing no grade 3–4 mucositis in metastatic gastric cancer. Other worst toxicities (particularly neutropenia and digestive toxicities) are in the range reported by Vanhoefer *et al*. (2000) with a 5-FU/cisplatin regimen in gastric cancer (respectively 35% and 32%). Gastric cancer cases were associated with the highest toxicity, which is a common observation.

Regarding the efficacy in terms of response, survival, quality of life, and hospital stays (which represent secondary objectives), no significant differences were found between the FP and FLP regimens. Our study confirms the activity of the combination cisplatin-5-FU in the esophageal adenocarcinoma location, in terms of response rate (37%), which is slightly better than the 33% observed by Ilson *et al*. (1995). This efficacy, albeit real (19.8%) in metastatic squamous cell esophageal cancer, is less significant than the one of 35% observed by Bleiberg *et al*. (1997). However, the number of patients with esophageal cancer was too small to draw any valid conclusions.

Concerning the gastric location, the efficacy in terms of response rate observed in this trial (19.8%) is lower than that reported in previous phase II non randomized studies (Lacave *et al*., 1991; Rougier *et al*., 1994; Ohtsu *et al*., 1994; Ychou *et al*., 1996) using the same regimens; these studies showed response rates ranging from 41% to 52%. This can be due to a more selected population included in those phase II non-randomized trials. By contrast, the response rate reported in our trial concerns a non-selected population, coming from a great number of centers (including non-specialized ones). However, this response rate is far from the one reported by Kim *et al*. (1993) in a phase III trial (51%) (unconfirmed by external review) but equivalent to that of 20% recently reported by Vanhoefer *et al*. (2000) using FP regimen. Recently, a slightly better response rate (27%) was obtained by Bouché *et al*. (2004) in this condition with a combination LV5FU2-cisplatin. In terms of survival, the overall median survival of 40 weeks in our trial is in the same range as that obtained by previous studies (9–11 months) and it is better than the 7.2 months reported by Vanhoefer *et al*. (2000).

As for pancreatic location, efficacy of FP or/and FLP (with an overall response rate of 9.3% and a median overall survival of 116 days) is rather disappointing but similar to that reported in a trial conducted by Ducreux *et al*. (2002) testing continuous 5-FU (1,000 mg/m^2/day for 5 days) plus cisplatin (100 mg/m^2) 1 day vs. 5-FU (500 mg/m^2/day for 5 days). This study showed a slight advantage for the FP protocol compared with 5-FU alone, with a response rate of 12% and 112 days of median survival. In this location, gemcitabine is now widely used but has never been compared to a combination of 5-FU/cisplatin in a randomized trial, even if tolerance to gemcitabine was shown to be more favorable in two studies reported by Philip *et al*. (2001) and Colucci *et al*. (2002).

The quality of life data showed no differences between the study arms during the first six cycles; this is consistent with the similar duration of hospital stays reported in the two arms.

In conclusion, FLP regimen is substantially equivalent to FP as regards safety and quality of life as well as for antitumor efficacy in advanced gastric, pancreatic, and esophageal cancers; the only slight advantage of FLP in this study concerns mucositis. Based on these results, FLP could, at most, be an alternative to FP when appropriate. However, recent data in gastrointestinal cancers show that oral administration of 5-FU in combination schedules would replace intravenous administration of 5-FU in future trials.

Acknowledgements. This work was supported by Lederlé company and randomization and data center: FFCD (Fondation Française de Cancérologie Digestive).

REFERENCES

Andre, T., Lotz, J.P., Bouleuc, C., Azzouzi, K., Houry, S., Hannoun, L., See, J., Esteso, A., Avenin, D., and Izrael, V. 1996. Phase II trial of 5-fluorouracil, leucovorin and cisplatin for treatment of advanced pancreatic adenocarcinoma. *Ann. Oncol. 7*: 173–178.

Bleiberg, H., Conroy, T., Paillot, B., Lacave, A.J., Blijham, G., Jacob, J.H., Bedenne, L., Namer, M., De Besi, P., Gay, F., Collette, L., and Sahmoud, T. 1997. Randomised phase II study of cisplatin and 5-fluorouracil (5-FU) versus cisplatin alone in advanced squamous cell oesophageal cancer. *Eur. J. Cancer 33*: 1216–1220.

Bouché, O., Raoul, J.L., Bonnetain, F., Giovannini, M., Etienne, P.L., Lledo, G., Arsene, D., Paitel, J.F., Guerin-Meyer, V., Mitry, E., Buecher, B., Kaminsky, M.C., Seitz, J.F., Rougier, P., Bedenne, L., and Milan, C. 2004. Randomized multicenter phase II trial of a biweekly regimen of fluorouracil and leucovorin (LV5FU2), LV5FU2 plus cisplatin, or LV5FU2 plus irinotecan in patients with previously untreated metastatic gastric cancer: a Federation Francophone de Cancerologie Digestive Group Study–FFCD 9803. *J. Clin. Oncol. 22*: 4319–4328.

Colucci, G., Giuliani, F., Gebbia, V., Biglietto, M., Rabitti, P., Uomo, G., Cigolari, S., Testa, A., Maiello, E., and Lopez, M., 2002. Gemcitabine alone or with cisplatin for the treatment of patients with locally advanced and/or metastatic pancreatic carcinoma: a prospective, randomized phase III study of the Gruppo Oncologia dell'Italia Meridionale. *Cancer 94*: 902–910.

Ducreux, M., Rougier, P., Pignon, J.P., Douillard, J.Y., Seitz, J.F., Bugat, R., Bosset, J.F., Merouche, Y., Raoul, J.L., Ychou, M., Adenis, A., Berthault-Cvitkovic, F., and Luboinski, M. 2002. A randomised trial comparing 5-FU with 5-FU plus cisplatin in advanced pancreatic carcinoma. *Ann. Oncol. 13*: 1185–1191.

Etienne, M.C., Bernard, S., Fischel, J.L., Formento, P., Gioanni, J., Santini, J., Demard, F., Schneider, M., and Milano, G. 1991. Dose reduction without loss of efficacy for 5-fluorouracil and cisplatin combined with folinic acid. In vitro study on human head and neck carcinoma cell lines. *Br. J. Cancer 63*: 372–377.

Ilson, D.H., Sirott, M., Saltz, L., Heelan, R., Huang Y, Keresztes, R., and Kelsen, D.P. 1995. A phase II trial of interferon alpha-2A, 5-fluorouracil, and cisplatin in patients with advanced esophageal carcinoma. *Cancer 75*: 2197–2202.

Kim, N.K., Park, Y.S., Heo, D.S., Suh, C., Kim, S.Y., Park, K.C, Kang, Y.K., Shin, D.B., Kim, H.T., Kim, H.J., Kang, W.K., Suh, C.I., and Bang, Y.J. 1993. A phase III randomized study of 5-fluorouracil and cisplatin versus 5-fluorouracil, doxorubicin, and mitomycin C versus 5-fluorouracil alone in the treatment of advanced gastric cancer. *Cancer 71*: 3813–3818.

Lacave, A.J., Baron F.J., Anton, L.M., Estrada, E., De Sande, L.M., Palacio, I., Esteban, E., Gracia, J.M., Buesa, J.M., Fernandez, O.A., and Baron, G.M. 1991. Combination chemotherapy with cisplatin and 5-fluorouracil 5-day infusion in the therapy of advanced gastric cancer: a phase II trial. *Ann. Oncol. 2*: 751–754.

Machover, D., Goldschmidt, E., Chollet, P., Metzger, G., Zittoun J., Marquet, J., Vandenbulcke, J.M., Misset, J.L., Schwarzenberg, L., and Fourtillan,

J.B. 1986. Treatment of advanced colorectal and gastric adenocarcinomas with 5-fluorouracil and high-dose folinic acid. *J. Clin. Oncol. 4*: 685–696.

Mitry, E., Taieb, J., Artru, P., Boige, V., Vaillant, J.N., Clavero-Fabri, M.C., Ducreux, M., and Rougier, P. 2004. Combination of folinic acid, 5-fluorouracil bolus and infusion, and cisplatin (LV5FU2-P regimen)in patients with advanced gastric or gastrooesophageal junction carcinoma. *Ann. Oncol. 15*: 765–769.

Ohtsu, A., Shimada, Y., Yoshida, S., Saito, H., Seki, S., Morise, K., and Kurihara, M. 1994. Phase II study of protracted infusional 5-fluorouracil combined with cisplatinum for advanced gastric cancer: report from the Japan Clinical Oncology Group (JCOG). *Eur. J. Cancer 30A*: 2091–2093.

Philip, P.A., Zalupski, M.M., Vaitkevicius, V.K., Arlauskas, P., Chaplen, R., Heilbrun, L.K., Adsay, V., Weaver, D., and Shields, A.F. 2001. Phase II study of gemcitabine and cisplatin in the treatment of patients with advanced pancreatic carcinoma. *Cancer 92*: 569–577.

Poon, M.A., O'Connell, M.J., Wieand, H.S., Krook, J.E., Gerstner, J.B., Tschetter, L.K., Levitt, R., Kardinal, C.G., and Mailliard, J.A. 1991. Biochemical modulation of fluorouracil with leucovorin: confirmatory evidence of improved therapeutic efficacy in advanced colorectal cancer. *J. Clin. Oncol. 9*: 1967–1972.

Spitzer, W., Dobson, A., and Hall, J. 1981. Measuring the quality of life of cancer patients: a concise QL-Index for use by physicians. *J. Chronic Dis. 34*: 585–597.

Rougier, P., Zarba, J.J., Ducreux, M., Basile, M., Pignon, J.P., Mahjoubi, M., Benahmed, M., Droz, J.P., Cvitkovic, E., and Armand, J.P. 1993. Phase II study of cisplatin and 120-hour continuous infusion of 5-fluorouracil in patients with advanced pancreatic adenocarcinoma. *Ann. Oncol. 4*: 333–336.

Rougier, P., Ducreux, M., Mahjoubi, M., Pignon, J.P., Bellefqih, S., Oliveira, J., Bognel, C., Lasser, P., Ychou, M., Elias, D., Cvitkovic, E., Armand, J.P., and Droz J.P. 1994. Efficacy of combined 5-fluorouracil and cisplatinum in advanced gastric carcinomas. A phase II trial with prognostic factor analysis. *Eur. J. Cancer 30A*: 1263–1269.

Vanhoefer, U., Rougier, P., Wilke, H., Ducreux, M.P., Lacave, A.J., Van Cutsem, E., Planker, M., Santos, J.G., Piedbois, P., Paillot, B., Bodenstein, H., Schmoll, H.J., Bleiberg, H., Nordlinger, B., Couvreur, M.L., Baron, B., and Wils, J.A. 2000. Final results of a randomized phase III trial of sequential high-dose methotrexate, fluorouracil, and doxorubicin versus etoposide, leucovorin, and fluorouracil versus infusional fluorouracil and cisplatin in advanced gastric cancer: a trial of the European Organization for Research and Treatment of Cancer Gastrointestinal Tract Cancer Cooperative Group. *J. Clin. Oncol. 18*: 2648–2657.

Ychou, M., Astre, C., Rouanet, P., Fabre, J.M., Saint-Aubert, B., Domergue, J., Ribard, D., Ciurana, A.J., Janbon, C., and Pujol, H. 1996. A phase II study of 5-fluorouracil, leucovorin and cisplatin (FLP) for metastatic gastric cancer. *Eur. J. Cancer 32A*: 1933–1937.

3
Gastrointestinal Cancer: Endoscopic Submucosal Dissection (Methodology)

Atsushi Imagawa

INTRODUCTION

Endoscopic submucosal dissection (ESD) is a new method of endoscopic therapy for treating early gastrointestinal neoplasms. This technique has been developed to achieve an *en-bloc* resection of specimens larger than 20 mm in diameter and has contributed to making a histopathological diagnosis more precise than the conventional method known as endoscopic mucosal resection (EMR).

However, a major drawback of ESD is its high rate of perforation. It requires high levels of endoscopic skill and experience because it is one of the most complex and lengthy endoscopic procedures in use. Nevertheless, these drawbacks are being gradually overcome through intensive study and efforts by Japanese endoscopists who have treated early gastrointestinal neoplasms and are focusing on early gastric cancer (EGC). It is necessary to fully understand this treatment method because it is expected to become a standard technique and gradually spread world-wide. Therefore, I elaborate on the actual method of ESD, mainly in regard to EGC.

INDICATIONS

The indications for ESD for EGC in our hospital are intramucosal invasion of the intestinal type, in accordance with the World Health Organization (WHO) classification. No size limitation is applied for lesions without ulceration, whereas for ulcerated lesions the maximum diameter is 30 mm. It has been reported that there is no incidence, or only a very low incidence, of lymph node metastasis under these circumstances (Gotoda *et al*., 2000).

METHOD AND DISCUSSION

There are many reports on the use of diazepam, flunitrazepam, midazolam, and propofol as sedative medications in endoscopic procedures. Deep sedation during ESD is necessary because of the complexity of this procedure, and recently the use of propofol in particular has been increasing. Hence, we usually select propofol for sedation in this lengthy procedure. Propofol is a very useful medication for reducing patient's anxiety, discomfort, and pain during treatment. It

is administered by non-anesthesiologists, including endoscopists and nurses who are trained in administering propofol sedation under the supervision of an anesthesiologist. The initial dose of propofol is 1.0–1.4 mg/kg, this being followed by additional bolus doses, if required. After the initial dose, the propofol is administered at 1.0–2.0 mg/kg/h continuously during the procedure. Additional doses (0.4–0.6 mg/kg) are administered if the patient begins to move. Supplemental oxygen, at 2 l/min by nasal cannula, and Pentazocine (15 mg, i.m.) are administered just before starting the procedure. However, propofol use has the risk of increasing the incidence of cardio-respiratory complications because of the difficulties associated with controlling its narrow dose range. Therefore, blood pressure has to be recorded every 5 min, and electrocardiogram (ECG), heart rate, and peripheral oxygen saturation (SpO_2) also have to be measured continuously during the procedure. In addition, we are trying to use the BIS (Bispectral index) monitor method to objectively evaluate the patient's sedation by brain wave measurements for risk avoidance.

In carrying out a safe ESD, selecting the injection solution before the incision is very important. Various solutions for the submucosal injection, such as glycerin solution (glyceol: 10% glycerin and 5% fructose in a normal saline solution), sodium hyaluronate, and normal saline, have been used. For a gastric lesion, we usually select glyceol with a small amount of indigo carmine and epinephrine because it is possible to maintain a sufficient protrusion with this mixture. In contrast, the esophageal and colonic mucosal walls are thinner than the gastric wall. We usually select sodium hyaluronate for esophageal and colonic lesions because it maintains the mucosal elevation of these lesions better than other solutions (Fujishiro *et al*., 2004).

A single-channel endoscope (Olympus GIF-Q260J; Olympus Optical, Tokyo) with a water jet system is usually selected. When the lesion makes the ESD procedure difficult to perform, a multi-bending scope together with a water jet system (the "M-scope," Olympus GIF-2T240M) is sometimes used. The merits of using the M-scope are: it is possible to obtain a good endoscopic view of the operation site using this scope and if the knife device cannot occasionally be smoothly operated, the problem will be solved because two channels are attached to this scope. Both scopes have a water jet system, which is very useful for keeping a good view of the site and for washing out mucus and blood, an indispensable function in treating bleeding by using hemostatic forceps.

Several knife devices have been developed by Japanese endoscopists, for example, the IT (insulated–tip) knife, Flex knife, Hook knife (Olympus Corporation, Tokyo, Japan) and Musectome (Pentax Ltd., Tokyo, Japan). These knife devices can be divided into two groups according to differences in how they cut. Both groups also have a variety of merits and drawbacks (Figure 3.1).

One group includes devices for cutting using a knife blade (IT knife and Mucosectome). The devices in this group can cut and dissect the submucosal layer of the lesion faster than those in the other group, although maneuvering with these knives is slightly difficult. The other group includes devices that cut

FIGURE 3.1. The Flex knife and IT knife. The tip of the Flex knife and the blade of the IT knife can be used to cut mucosa and exfoliate the gastric submucosa

with the tip of the knife (Flex and Hook knives). It is possible to cut and dissect the submucosal layer in as much detail as desired using the devices in this group, although this takes some time. It is important to be skilled in the use of one knife and to be able to make a good knife for operators.

Before marking around the lesion, indigo carmine dye should be sprayed to clearly demarcate the target lesion. Then, several spots are marked outside of the lesion using the tip of a Flex knife.

After a submucosal injection, a circumferential incision into the mucosa is made, mainly using a Flex knife or IT knife. It is necessary to prepare a transparent hood with the knife device and to image the strategy of treatment before the start of the incision and dissection. A transparent hood is essential for obtaining a better position and view of the dissection line and for performing the ESD safely. This hood, which is attached to the tip of the endoscope, is usually used to maintain a satisfactory view during treatment (Yamamoto *et al*., 2002). The strategy of an ESD differs according to the location of the lesion and the selection of knife devices.

When a lesion is found in the antrum of the stomach, the control of the scope and devices is easy during the performance of the ESD using any knife (Imagawa *et al*., 2006). The submucosal layer of the lesion in the antrum is thicker than lesions in other locations. In addition, it is expected for anatomical reasons that bleeding during the procedure would be rare.

First, an incision is made in the anal side of the lesion after an injection of glyceol. The purpose of this is to determine the goal of the dissection. Next, the oral side is cut using a Flex or IT knife to achieve a circumferential incision. A direct dissection of the submucosal layer is then carried out with a Flex knife, an IT knife, and a Mucosectome until a complete removal has been achieved. A submucosal dissection should be done parallel to the muscular layer using a transparent hood. Finally, the vessels in the artificial ulcer bed are coagulated by hemostatic forceps to prevent a hemorrhage after the procedure.

When a lesion is found at the upper or middle third of the stomach body, a Flex knife is mainly used in these situations: (Figure 3.2a–f). The anal side of the lesion is cut first in a reverse view using a Flex knife. This knife should splash and cut the mucosa toward the inside of the luminal side to avoid a perforation. When one-half of the incision is made, the subsequent incisions are made in a conventional

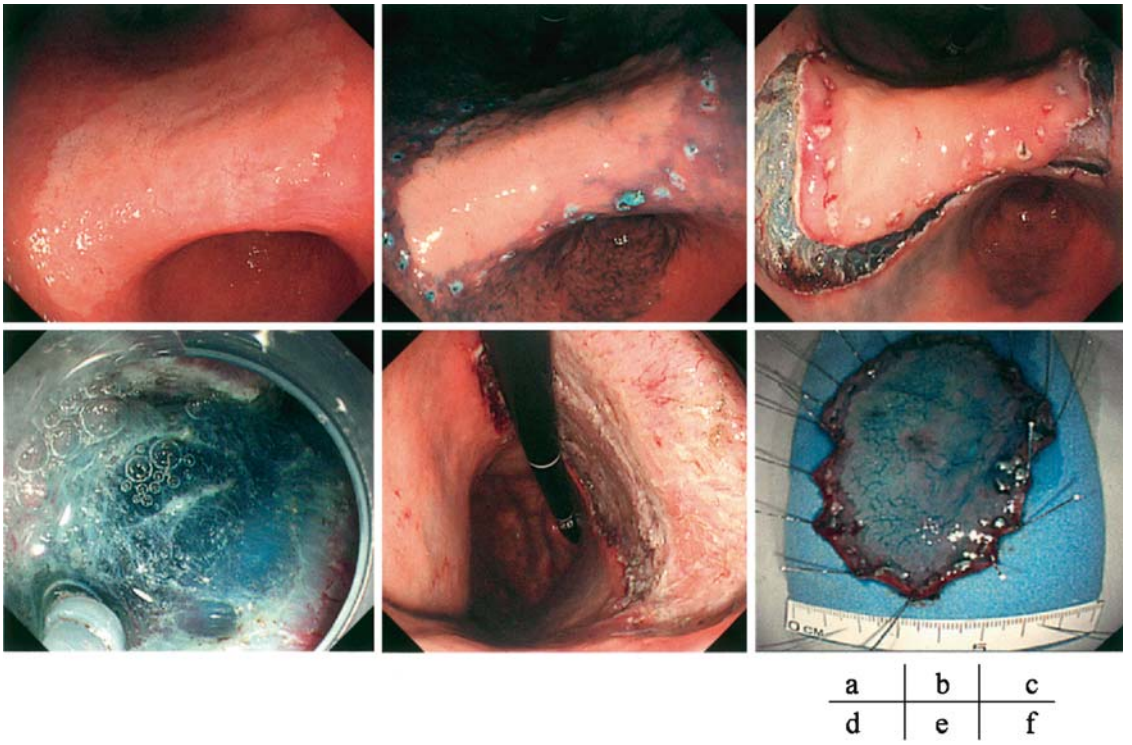

FIGURE 3.2 a. A flat elevated lesion was located at the lesser curvature of the middle body of the stomach. The size of the lesion was about 60 mm in diameter. b. After application of indigo carmine dye, the marking around the lesion was made using the tip of a Flex knife. c. About one-half of the incision was made after injection. d. A direct dissection of the submucosal layer was carried out using a Flex knife. e. Exfoliation was continued until a complete removal was achieved. f. The lesion was resected in one piece

view using a Flex knife. After that, a direct dissection is carried out using a Flex knife.

When a lesion is found at the upper or middle third of the stomach body, an IT knife is mainly used in these situations: The oral side of the lesion is cut with a conventional view at first using an IT knife. A circumferential incision is made at a time. After that, a direct dissection is carried out. When the dissection is difficult, an option is to use snare devices and another knife that looks like a Hook knife and Mucosectome according to the situation. Finally, the vessels in the artificial ulcer bed are coagulated by hemostatic forceps.

Setting of a High-Frequency Generator

A high-frequency generator (VIO 350, Erbe Elektromedizin Ltd., Tübingen, Germany) is used for marking, incision of the mucosa, and exfoliation of the submucosa. For marking around the lesion and the submucosal dissection using a Flex knife, the swift coagulation mode, 40 W, is selected. For the incision of the mucosa, we select the Endo-cut I mode (effect 2, duration 4, cut interval 3) when using a Flex knife or the Endo-cut Q mode (effect 2, duration 3, cut interval 2) when using an IT knife. Visible exposed vessels on the artificially created ulcer are coagulated with hemostatic

forceps using the soft coagulation mode (50–70 W).

Complications

Major complications of this method are perforation and bleeding. Perforation was reported in 4–5% of the cases, and we encountered it in 6.1% of the cases (Imagawa *et al*., 2006). In those patients in whom perforation occurred, the defect was immediately and successfully closed with hemoclips during the procedure and treated with administration of antibiotics. It is very important to use hemoclips to avoid urgent surgical treatment.

In contrast, there are two types of bleeding, depending on the time of occurrence. One is bleeding during resection; the other is bleeding after the procedure (which is a delayed bleeding). Bleeding during the procedure can be managed in all cases with hemostatic forceps (SDB2422; Pentax: Figure 3.3) and hemoclips with a water-jet system. Trimming the red vessels in the artificial ulcer bed after a complete resection can prevent delayed bleeding. Hemostatic forceps is a useful device for controlling bleeding, but it is necessary to understand how to use it. Hemostatic forceps with a water-jet system can be selected and used in any situation. Also, a water jet system supplies a continuous jet of water at high pressure, which easily and swiftly washes away any blood that is obstructing the visual field.

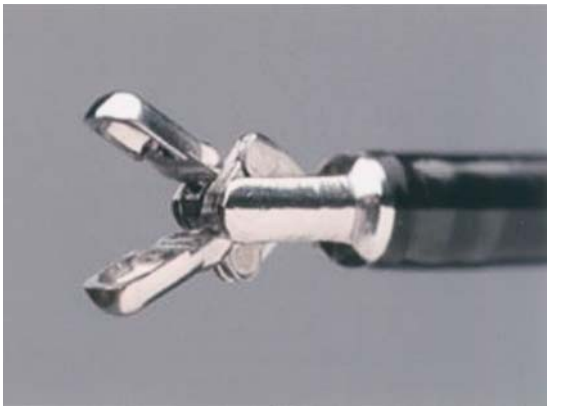

FIGURE 3.3. Hemostatic forceps. When bleeding occurred during the procedure, the bleeding vessels were grasped and coagulated via hemostatic forceps, after washing out the blood using a water-jet system

Esophageal and Colorectal Lesions

The difficulties of the endoscopic technique for esophageal lesions and colorectal lesions increase with the use of ESD. The problems associated with ESD for these lesions are that: (a) the walls of the esophagus and colon are thinner than that of the stomach; (b) the range of the operation area is narrow; (c) the scope is not steady (Onozato *et al*., 2007). It is necessary to have enough experience and knowledge to treat such lesions and to do so carefully. In conclusion, the methods of ESD are not sufficiently established for treating early esophageal cancer, including Barrett's neoplasia and colorectal cancer. Nonetheless, ESD for EGC has already been established. Further study of the training system for ESD is needed to make it known to the world outside of Japan.

REFERENCES

Fujishiro, M., Yahagi, N., Kashimura, K., Mizushima, Y., Oka, M., Matsuura, T., Enomoto, S., Kakushima, N., Imagawa, A., Kobayashi, K., Hashimoto, T., Iguchi, M., Shimizu, Y., Ichinose, M., and Omata, M. 2004. Different mixtures of sodium hyaluronate and their ability to create submucosal fluid cushions for endoscopic mucosal resection. *Endoscopy 36*: 584–589.

Gotoda, T., Yanagisawa, A., Sasako, M., Ono, H., Nakanishi, Y., Shimoda, T., and Kato, Y. 2000. Incidence of lymph node metastasis from early gastric cancer: estimation with a large number of cases at two large centers. *Gastric Cancer 3*: 219–225.

Imagawa, A., Okada, H., Kawahara, Y., Takenaka, R., Kato, J., Kawamoto, H., Fujiki, S., Takata, R., Yoshino, T., and Shiratori, Y. 2006. Endoscopic submucosal dissection for early gastric cancer: results and degrees of technical difficulty as well as success. *Endoscopy 38*: 987–990.

Onozato, Y., Kakizaki, S., Ishihara, H, Iizuka, H., Sohara, N., Okamura, S., Mori, M., and Itoh, H. 2007. Endoscopic submucosal dissection for rectal tumors. *Endoscopy 39*: 423–427.

Yamamoto, H., Kawata, H., Sunada, K., Satoh, K., Kaneko, Y., Ido, K., and Sugano, K. 2002. Success rate of curative endoscopic mucosal resection with circumferential mucosal incision assisted by submucosal injection of sodium hyaluronate. *Gastrointest. Endosc. 56*: 507–512.

4
Gastrointestinal Epithelial Neoplasms: Endoscopic Submucosal Dissection (Methodology)

Mitsuhiro Fujishiro

INTRODUCTION

Endoscopic resection can be theoretically applied to the localized neoplasms without lymph node metastases. However, presently the application is limited to small lesions. The reason is that the conventional endoscopic resection method, that is endoscopic mucosal resection (EMR) reported by Tada *et al.* (1993) and Inoue *et al*. (1993), has a limitation in the resected size. Endoscopic submucosal dissection (ESD) technique is a new endoscopic treatment using cutting devices, which removes the lesion by following three steps: injecting fluid into the submucosa to elevate the lesion from the muscle layer, precutting the surrounding mucosa of the lesion, and dissecting the connective tissue of the submucosa beneath the lesion. The major advantages of this technique in comparison with conventional EMR are: (1) the resected size and shape can be controlled, (2) *en bloc* resection is possible even in a large lesion, and (3) the lesions with ulcerative findings are also resectable. Using the ESD technique, we can resect a large or ulcerative gastrointestinal (GI) epithelial neoplasm endoscopically, which can lead to cure the target lesion without resection of the GI organ.

APPLICATION

From the results of large numbers of surgically treated cases, the malignant neoplasms without lymph node metastases are described in detail. It is reported by Tajima *et al*. (2000) for the esophagus, Gotoda *et al*. (2000) for the stomach, and Kitajima *et al*. (2004) for the colorectum that the malignant neoplasms (which are histologically diagnosed as follows without vessel infiltration) can be theoretically cured by endoscopic treatment.

Noninvasive Carcinoma in the GI Tract

Intramucosal Carcinoma

Esophagus: invasive squamous cell carcinoma into the lamina propria mucosae, or invasive squamous cell carcinoma into the muscularis mucosae, low histologic grade; in the case of adenocarcinoma, the criteria are the same as with the stomach.

Stomach: differentiated adenocarcinoma, irrespective of ulcer findings, ≤ 3 cm in

diameter, differentiated adenocarcinoma, without ulcer findings, >3 cm in diameter, or, undifferentiated adenocarcinoma, without ulcer findings, ≤ 2 cm in diameter.
Colorectum: differentiated adenocarcinoma.

Submucosal Carcinoma with Minute Submucosal Penetration

Esophagus: squamous cell carcinoma, low histologic grade, ≤ 200 μm below the muscularis mucosae; in the case of adenocarcinoma, the criteria are the same as with the stomach.
Stomach: differentiated adenocarcinoma, ≤500 μm below the muscularis mucosae, ≤3 cm in diameter.
Colorectum: differentiated adenocarcinoma, pedunculated type, limited to head invasion, or differentiated adenocarcinoma, non-pedunculated type, ≤1,000 μm below the muscularis mucosae.

Although the number is small, the duodenal carcinomas are considered to be cured as the same indication as with the gastric carcinomas.

However, another aspect of this protocol should be considered as an established treatment, which is technical aspect to obtain resected specimens as being histologically evaluable, because preoperative prediction of the fulfillment of the above criteria is not possible in all GI neoplasms. If multi-fragmental resection is performed, histological examination is difficult, and, furthermore, it was reported by Eguchi *et al*. (2003) and Tamura *et al*. (2004) that the local recurrent rate was higher than that of patients with *en bloc* resection. The indication of ESD, therefore, may be determined by each institution or each operator, according to the technical achievements, and the goal of indication after overcoming them is equal to the lesions that are preoperatively diagnosed as the node-negative malignant neoplasms.

ENDOSCOPIC SYSTEMS AND EQUIPMENT

Two types of endoscopes may be prepared. One is a slim single-channel endoscope with good flexibility, which is a main endoscope for ESD, and the other is a double-channel endoscope that is an auxiliary endoscope for difficult situations by a single-channel endoscope. It is preferable for the endoscopes to equip the water-jet system (e.g., GIF-Q260J, Olympus, Tokyo, Japan, EG-2931, Pentax, Tokyo, Japan) to wash out the blood or mucus of the target area from their tips. In the case of colorectal neoplasms, the application of the above upper GI endoscopes is preferable to a slim colonoscope, if they reach the target lesion considering maneuverability. The high-frequency electrosurgical unit is Erbotom ICC 200, or VIO 300D, ERBE Elektromedizin GmbH, Tübingen, Germany, which has a special kind of cutting current, that is in ENDOCUT mode.

Devices and solutions for ESD are listed below:

- Spraying tube for indigo carmine (stomach and intestine) or iodine (esophagus)
- 23-gauge injection needle for submucosal injection
- Hemostatic forceps (FD-410LR, Olympus, or, SDB2422, Pentax)
- Transparent soft attachment which fits to the tip of an endoscope (D201-11804, etc., Olympus) and/or small-caliber tip transparent (ST) hood (DH-15GR, 15CR, Fujinon Toshiba ES Systems, Tokyo, Japan) (Figure 4.1f)

Spraying tube for sucralfate reported by Fujishiro *et al*. (2002)
Rotatable endoscopic clipping device for hemostasis or perforation
Electrosurgical snare in case of snaring as the final step of resection
0.2% indigo carmine (stomach and intestine) or 1% iodine (esophagus) for chromoendoscopy
Submucosal injection solution

In our institution a 10% glycerin solution (Glyceol, Chugai pharmaceutical co. Tokyo Japan) with 0.0005% epinephrine and 0.005% indigo carmine is prepared for small distal gastric neoplasms without ulcer findings and a mixture of Glyceol and 1% 1,900 KDa hyaluronic acid preparation (Suvenyl, Chugai pharmaceutical co. Tokyo Japan) is prepared for complex or proximal gastric neoplasms and the neoplasms in the other GI organs. Mixing ratio of Glyceol and Suvenyl is 7:1 for complex or proximal gastric neoplasms and 3:1 for esophageal, duodenal and colorectal neoplasms (Fujishiro *et al*., 2006a). For the gastric neoplasms, it is reported by Gotoda (2005) that normal saline makes a sufficient submucosal fluid cushion when an IT knife is used as a cutting electrosurgical knife. A small amount of epinephrine is added to obtain vasoconstriction for hemostasis and indigo carmine to find out the seeping area of the submucosal injection solution as operators' preference.

One or more electrosurgical knife(-ves) among a needle knife, an IT knife, a flex knife, a hook knife, and a TT knife are needed.

The selection of electrosurgical knives (Figure 4.1a–e) depends on the operator's preference and expertise. The needle knife is the oldest and simplest knife that allows cutting sharply the tissue at the tip of the knife. However, when applied in the vertical direction from the wall plane, the knife can easily pass through the gut wall, which results in perforation. So, it is advisable to employ a transparent endoscopic hood at the same time, and to use hyaluronic acid solution as an injection solution. The IT-knife has a ceramic ball at the top of a needle

FIGURE 4.1. Devices for endoscopic submucosal dissection (ESD). (a) Needle knife (KD-1L-1, Olympus, Tokyo, Japan) ; (b): Insulation-tipped electrosurgical (IT) knife (KD-610L, Olympus, Tokyo, Japan) ; (c): Flex knife (KD-630L, Olympus, Tokyo, Japan) ; (d): Hook knife (KD-620LR, Olympus, Tokyo, Japan); (e): Triangle-tip (TT) knife (KD-640L, Olympus, Tokyo, Japan) ; (f) Small-caliber-tip transparent (ST) hood (DH-15GR, 15CR, Fujinon Toshiba ES Systems, Tokyo, Japan)

knife. This knife is designed to protect the tip so that cutting cannot be achieved at the tip but at the needle blade. The way to use it is to place the ceramic ball in the submucosal layer to hook the mucosa or the submucosal connective tissue that is intended to be cut, and then pulling the knife out. This is the only way to cut smoothly by using an IT-knife, so the knife sometimes has to be applied blindly, which may lead to complications such as bleeding and perforation. The flex-knife has a soft, thick, and looped tip of the knife, which acts well to prevent perforation. Furthermore, the tip of the outer sheath is rolled over 1 mm, which functions as a stopper to keep constant incised depth. The hook-knife has a bending part at a right angle on the top of a needle knife. The direction of the hook can be controlled via handle rotation, which should be kept parallel with the wall plane to prevent perforation. The TT-knife has a triangular shaped metal plate attached to the tip of a needle knife. Because the shape of the hook is triangular, there is no need to rotate the tip to hook the tissue intended to cut. But thermal damage of the tissue by the tip of a rather large triangle plate may occur, damaging the underlying muscle layer and precluding precise histological evaluation of the resected specimen.

PROCEDURE

To facilitate the understanding of the ESD procedure, schematic drawings of the procedure are shown in Figure 4.2 and representative cases are shown in Figure 4.3.

Marking Around the Lesion

After washing the gut wall with tapped water containing 0.01% dimethylpolysiloxane, 0.2% indigo carmine (stomach and intestine) or 1% iodine (esophagus) is sprayed to clarify border of the lesion. Circumferential markings are made by using a tip of the electrosurgical knife at 5 mm outside of the lesion with 2-mm intervals between each marking in soft coagulation mode. The tip is pressed softly onto the mucosa, and the electricity is turned on only for a second. For intestinal neoplasms markings are not made because the margins of the lesion are clearly identified and the gut wall is thin enough to be perforated by marking only.

Submucosal Injection

The solution mentioned above is injected into the submucosal layer just outside the markings where mucosal incision intends to be made at first. The volume of injection is about 2 ml in one time, and injection is repeated several times before starting mucosal incision until the targeted area is lifted enough. It is important to count the volume of injection loudly every 0.2 ml for the operator to find out that injection works effectively or not. Complete marginal cutting of the mucosa before submucosal dissection is not necessary, which means that mucosal incision and submucosal dissection are repeated several times before complete marginal cutting. After exposure of the submucosal layer, submucosal injection is applicable from the exposed submucosal layer to lift up the submucosal layer intended to be cut.

Mucosal Incision

After lifting the lesion, mucosal incision is started by using an electrosurgical knife the operator selected. The mucosa of outside the markings is incised circumferentially

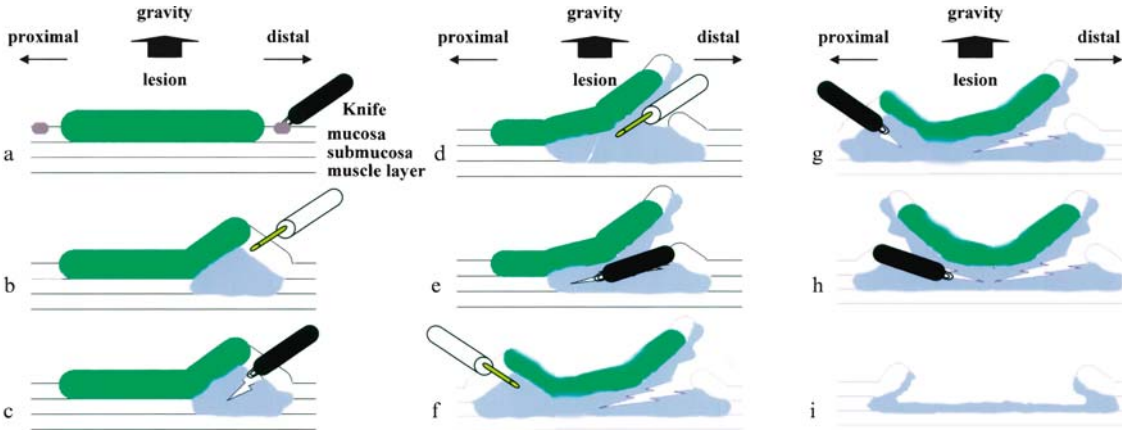

FIGURE 4.2. Schema of endoscopic submucosal dissection (ESD). (a) Marking; (b) Submucosal injection of the distal part; (c) Mucosal incision of the distal part; (d) Additional submucosal injection in the distal submucosal to facilitate submucosal dissection; (e) Submucosal dissection of the distal part; (f) Submucosal injection of the proximal part; (g) Mucosal incision of the proximal part; (h) Submucosal dissection of the proximal part; (i) Complete removal of the lesion

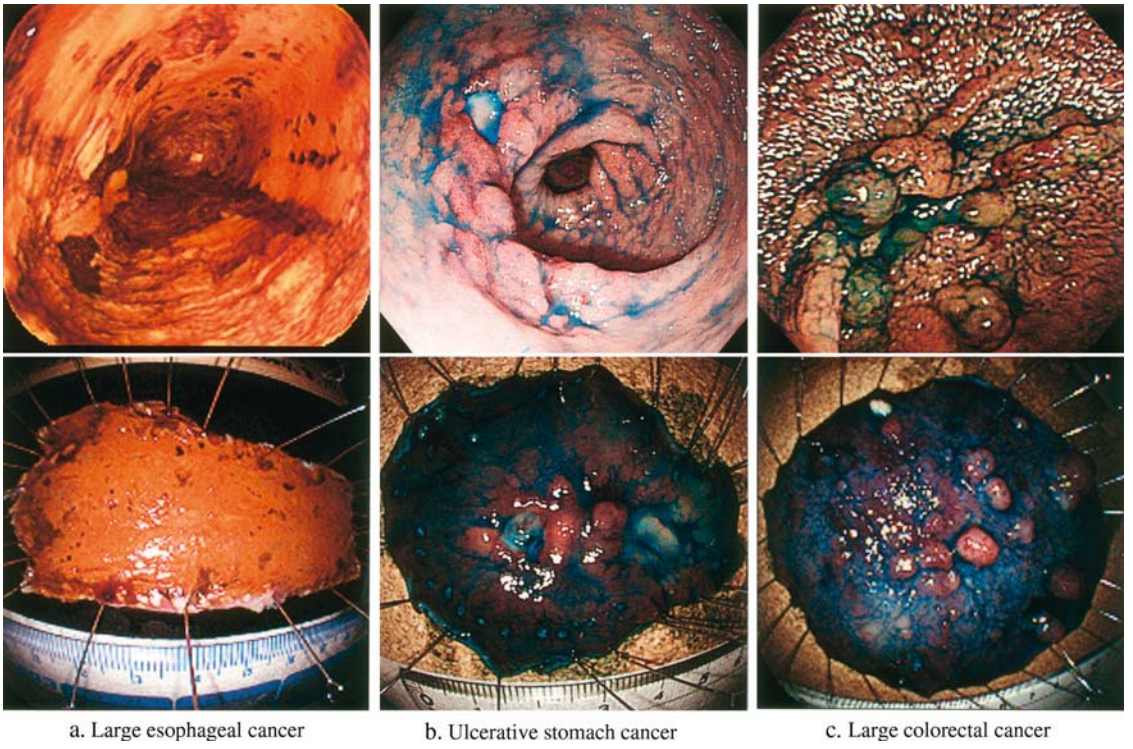

FIGURE 4.3. Representative cases of endoscopic submucosal dissection (ESD). (a) Wide-spread type esophageal carcinoma (chromoendoscopy and resected specimen); (b) Ulcerative gastric carcinoma (chromoendoscopy and resected specimen); (c) Large laterally spreading colorectal carcinoma (chromoendoscopy and resected specimen)

in ENDOCUT mode. If mucosal incision reaches below the muscularis mucosae, the submucosal layer dyed blue by indigo carmine comes in sight. If the blue submucosal layer does not appear, it means that the muscularis mucosae is cut incompletely. In the situation, the incising line is just traced again until the blue submucosal layer comes out. The starting point for cutting depends on the location of the lesion. Principally, we start cutting from a distal part from the endoscope. Retroflex position of the endoscope is usually used if possible when cutting a distal part, but cutting is done at the straight position in non-applicable situation of retroflex position. As the submucosal injection solution retaining in the submucosa comes down for the direction of the ground, it is better to start cutting from an opposite part of the ground as well as a distal part, or put the lesion on an opposite part of the ground if the patients' body positions are changeable.

Submucosal Dissection

Small lesions can be resected by an electrosurgical snare only after mucosal incision around the markings without submucosal dissection. However, large lesions, lesions with ulcer findings or lesions located in a tortuous area cannot be resected by an electrosurgical snare, which needs dissecting the submucosa completely. The electrosurgical knife the operator selected is also used for dissecting the submucosa. The knife is put slightly onto the connective tissue in the submucosal layer and the electricity is turned on intermittently for a short time to confirm the cutting tissue in forced coagulation mode. If the target to dissect cannot be seen directly at any way, a transparent attachment on the tip of the endoscope or an ST hood is very useful to stretch the connective tissue and make a good view field in the submucosa. Especially, in case of colorectal neoplasms, we consider gravity for proceeding submucosal dissection and may change the patients' body positions. The lesions should be positioned opposite to the ground because the detached parts of the specimen comes down and the connective tissue in the submucosa to dissect is stretched enough to dissect easily and safely. The injected solution in the submucosa pours out after mucosal incision gradually and submucosal cushion flattens down as time has passed. So it is also important to start dissecting the submucosa immediately from the incising part of the mucosa before marginal mucosal cutting.

Bleeding

Once the bleeding occurs, it takes a long time to achieve hemostasis and it is difficult to keep clear endoscopic views. So, instead of cutting blood vessels, it is important to treat them with coagulation without bleeding. For small vessels, which are smaller than the tip of the electrosurgical knife, the knife is usually enough to treat them without changing hemostatic devices. The tip is softly touched to the vessels, and they are coagulated in forced coagulation mode. For large vessels, hemostatic forceps should be used. The vessels are caught, pulled up a little to keep the forceps apart from the gut wall slightly, and coagulated in soft coagulation mode.

However, all vessels cannot be managed before bleeding. Once bleeding occurs, immediate hemostasis is necessary. Coagulation using the tip of the knife or the hemostatic forceps is the first choice

to achieve hemostasis. The power settings are the same with treating non-bleeding vessels. In order to identify the bleeding vessels, water-jet system is also very useful. If the bleeding cannot be managed using the hemostatic forceps after coagulation for several times, we unwillingly use endoscopic clips in order not to interfere the subsequent procedure.

After the total removal of the lesion, the visible vessels located in the post-procedure ulcer base are treated using hemostatic forceps in soft coagulation mode especially in case of the stomach. In the esophagus and the intestine, because thinner muscle layer may cause delayed perforation due to thermal damage and the rate of delayed bleeding is much lower than that in the stomach, only large vessels should be treated by hemostatic forceps. Or, hemoclips can be used to control visible vessels. And finally, 20 ml of sucralfate liquid are sprayed using the outer sheath of the rotatable endoscopic clip device for not only stomach, but also for other GI organs to confirm the achievement of hemostasis and coat the post-procedure ulcer base.

Perforation

From our experiences, the perforation experienced during ESD is very small and usually noticed as soon as it occurs. When perforation occurs, immediate closure by endoscopic clipping is necessary in order not to deteriorate the patients' condition. If tensional pneumoperitoneum is uncontrolled only by endoscopic clipping, combining with percutaneous transabdominal air deflation using 18-gauge elastic needle is very effective. Emergency surgical rescue is avoidable after successful closure of the perforations in the limited experience reported by Fujishiro *et al*. (2006b), but intensive managements with no oral intake, resting on bed, and, intravenous antibiotics for several days until symptoms become free and laboratory data improve are needed. When the perforation is closed and the patient's condition is not improved, continuation of the ESD procedure is permissible until completion of the resection.

Management After Endoscopic Submucosal Dissection

After ESD, patients are prohibited eating and drinking until the next day of ESD. The laboratory findings and chest and abdominal X-ray reveal unremarkable, then patients are permitted oral intake from soft foods. In case of the upper GI organs, follow-up endoscopies are performed within 1 week to check up post-procedure ulcer healing, and then discharge from the ward is determined. A proton pump inhibitor and sucralfate are administered until confirmation of healing of the post-procedure ulcers. In case of the colorectum, patients are discharged from the ward within 1 week without checking ulcer healing. All the patients with ESD principally undergo follow-up endoscopies 2 months after ESD to confirm the healing and excluding recurrence of the post-procedure ulcers.

FURTHER CONSIDERATIONS

Endoscopic submucosal dissection is a novel endoscopic treatment that makes it possible to perform *en bloc* resection even for complicated GI neoplasms and many lesions that used to require surgical treatment are now treated endoscopically. Endoscopic submucosal dissection brings many patients a great deal of benefit, but

it has been indicated that the technique needs some refinements before becoming a widely accepted technique. The major problem is that there are only a limited number of endoscopists who can perform ESD because of technical difficulty. Therefore, we should establish the efficient training system of ESD or develop new devices or innovations in order to change it to an easier technique. Without such refinements, endoscopic submucosal dissection carries a potential of complications such as hemorrhage and perforation, which hampers the widespread use of this marvelous technique.

REFERENCES

Eguchi, T., Gotoda T., Oda, I., Hamanaka, H., Hasuike, N., and Saito, D. 2003. Is endoscopic one-piece mucosal resection essential for early gastric cancer? *Dig. Endosc. 15*: 113–116.

Fujishiro, M., Yahagi, N., Oka, M., Enomoto, S., Yamamichi, N., Kakushima, N., Tateishi, A., Wada, T., Shimizu, Y., Ichinose, M., Kawabe, T., and Omata, M. 2002. Endoscopic spraying of sucralfate using the outer sheath of a clipping device. *Endoscopy 34*: 935.

Fujishiro, M., Yahagi, N., Nakamura, M., Kakushima, N., Kodashima, S., Ono, S., Kobayashi, K., Hashimoto, T., Yamamichi, N., Tateishi, A., Shimizu, Y., Oka, M., Ogura, K., Kawabe, T., Ichinose, M., and Omata, M. 2006a. Successful treatment outcomes of a novel endoscopic resection for gastrointestinal tumors- endoscopic submucosal dissection using a mixture of high-molecular-weight hyaluronic acid, glycerin, and sugar. *Gastrointest. Endosc. 63*: 243–249.

Fujishiro, M., Yahagi, N., Nakamura, M., Kakushima, N., Kodashima, S., Ono, S., Kobayashi, K., Hashimoto, T., Yamamichi, N., Tateishi, A., Shimizu, Y., Oka, M., Ogura, K., Kawabe, T., Ichinose, M., and Omata, M. 2006b. Successful nonsurgical management of perforation complicating endoscopic submucosal dissection of gastrointestinal epithelial neoplasms. *Endoscopy 38*: 1001–1006.

Gotoda, T. 2005. A large endoscopic resection by endoscopic submucosal dissection procedure for early gastric cancer. *Clin. Gastroenterol. Hepatol. 3*: S71–S73.

Gotoda, T., Yanagisawa, A., Sasako, M., Ono, H., Nakanishi, Y., Shimoda, T., and Kato, Y. 2000. Incidence of lymph node metastasis from early gastric cancer: estimation with a large number of cases at two large centers. *Gastric. Cancer 3*: 219–225.

Inoue, H., Takeshita, K., Hori, H., Muraoka, Y., Yoneshima, H., and Endo, M. 1993. Endoscopic mucosal resection with a cap-fitted panendoscope for esophagus, stomach, and colon mucosal lesions. *Gastrointest. Endosc. 39*: 58–62.

Kitajima, K., Fujimori, T., Fujii, S., Takeda, J., Ohkura, Y., Kawamata, H., Kumamoto, T., Ishiguro, S., Kato, Y., Shimoda, T., Iwashita, A., Ajioka, Y., Watanabe, H., Watanabe, T., Muto, T., and Nagasako, K. 2004. Correlations between lymph node metastasis and depth of submucosal invasion in submucosal invasive colorectal carcinoma: a Japanese collaborative study. *J. Gastroenterol. 39*: 534–543.

Tada, M., Murakami, A., Karita, M., Yanai, H., and Okita, K. 1993. Endoscopic resection of early gastric cancer. *Endoscopy 25*: 445–450.

Tajima, Y., Nakanishi, Y., Ochiai, A., Tachimori, Y., Kato, H., Watanabe, H., Yamaguchi, H., Yoshimura, K., Kusano, M., and Shimoda, T. 2000. Histopathologic findings predicting lymph node metastasis and prognosis of patients with superficial esophageal carcinoma: analysis of 240 surgically resected tumors. *Cancer 88*: 1285–1293.

Tamura, S., Nakajo, K., Yokoyama, Y., Ohkawauchi, K., Yamada, T., Higashidani, Y., Miyamoto, T., Ueta, H., and Onishi, S. 2004. Evaluation of endoscopic mucosal resection for laterally spreading rectal tumors. *Endoscopy 36*: 306–312.

5
Inoperable Abdomino-Pelvic Tumors: Treatment with Radio-Frequency Ablation and Surgical Debulking

Nathan W. Pearlman

INTRODUCTION

Standard resection of most abdominal and pelvic neoplasms entails removal of the tumor and a margin of normal, uninvolved, tissue. These goals come into conflict with operative safety or patient acceptance when the tumor abuts, or is adherent to vertebral bodies, upper sacrum, aorta, vena cave, superior mesenteric artery/vein, or upper sciatic nerve. While extended resections that include one or more of these structures have been performed in this setting, morbidity is significant and long-term benefit often limited. Most patients who require such an undertaking for tumor removal either refuse the procedure, or are deemed inoperable at the outset, and treated as such. Unfortunately, the palliation they receive from non-resectional therapy is also often quite limited.

Over the years, preoperative radiation or chemoradiation has often been employed in this situation in hopes of shrinking these neoplasms or separating them from critical structures enough to make them "operable". This rarely happens if the tumor is truly fixed due to critical structures at the outset. Even if sites of adherence are sterilized by radiation and converted to scar tissue, this cannot be assumed prior to operation. Experience shows that any abnormal or thickened tissue encountered at the edge of the tumor during surgery is potentially malignant and must be removed, again with a margin of normal tissue.

An alternative approach, first described by Cushing (1928) for extirpation of brain tumors, consists of stepwise removal of the lesion using a combination of electrosurgical thermal ablation and piecemeal debulking from the center outward ("excavation"), usually over several sittings. Similar treatment of small rectal cancers was described by Strauss *et al*. (1935). This general approach is still used for some brain tumors, and the electro-electrocautery is often replaced by ultrasonic or laser dissection (Harsh and Wilson, 1990). However, piecemeal electrofulguration of rectal cancer has, for the most part, been supplanted in recent years by resection, which has improved safety and better cure rates than in the past.

The electrosurgical units typically used for this type of thermal ablation in the past employed high voltage (500–3,000 V), low amperage (0.1–0.5 A) radiofrequency current (500–1,000 kHz), with an intermittent duty cycle (25%) of short duration (sec-

onds) (Buysse S., August 2005,Valleylab, Tyco Health Care, Boulder, CO, personal communication,). The devices were primarily designed for superficial coagulation or cutting, not deep tissue heating. If applied for more than a few seconds, energy transfer would shut down due to tissue dessication or charring around the electrode; thermal damage lateral to the electrode is usually < 1 cm. Thus, attempts to use these devices for ablation of tumors > 2–3 cm in diameter routinely failed due to inadequate tumor heating and/or coagulation of feeding vessels at any depth.

In 1989, a newer radiofrequency generator was introduced for treatment of bone tumors (Tillotson *et al*., 1989). The current was low voltage (generally 110 V), higher amperage (0.5–2.0 A), continuous (100% duty cycle), and of long duration (minutes) (Buysse S., August 2005, personal communication). There was much less tissue dessication/charring around the electrode, and deeper tissue heating/ablation, than with older electrosurgical units. Use of the device grew rapidly. Initially, the most common application was liver tumors (Decadt and Siriwardena, 2004; Gillams, 2005) but soon expanded to treatment of neoplasms in other sites, such as lung (Fernando *et al*., 2004; Belfiore *et al*., 2004), kidney (Zelkovic and Resnick, 2003), retroperitoneum (Abraham, *et al*., 2000), and pelvis (Ohhigashi *et al*., 2001). Suitable targets were treated by open surgery, laparoscopy, or percutaneous techniques, with ablated tissue left *in situ*. Over time, however, it was found that complete ablation of tumors over 4–5 cm was difficult with this approach (Abraham *et al*., 2000), and could lead to abscesses and/or damage to surrounding structures when treating lesions outside the liver (Ohhigashi *et al*., 2001; Zelkovic and Resnick, 2003; Rhim *et al*., 2004).

We felt that this obstacle to ablating larger extrahepatic neoplasms might be overcome if the ablated tissue is removed, and the radiofrequency probe reapplied, in a stepwise manner, i.e., the original "excavation" technique of Cushing. This approach seems preferable to repeated overlapping radiofrequency applications to an intact tumor and then attempting to remove it. The stepwise approach would theoretically facilitate more precise and predictable tissue ablation in the depths of the tumor, minimize retained necrotic tissue, and, hopefully, limit damage to the surrounding tissue. In fact, that is what generally occurred. In the sections that follow, our technique and initial results are reviewed.

TECHNIQUE

Lesions are approached through a laparotomy or generous incision in the perineum. When possible, temperature probes are placed at the periphery to protect adjacent tissue. Two different radiofrequency probes have been used; initially, the RITA Starburst™ expandible multitine array; in later years, the Valleylab Cool-Tip™ triple probe. Each device theoretically ablates up to 4–6 cm of tissue with 1 application according to the manufacturer, although we found results quite variable from patient to patient.

The probe is placed in the center of the tumor and heated to target temperature (RITA), or for the prescribed 12 min (Cool-Tip). The ablated tissue is then removed by piecemeal debulking or suction aspiration, depending on its consistency. Carcinomas

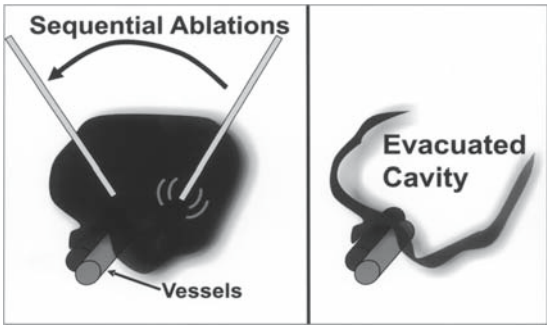

FIGURE 5.1. General approach to stepwise tumor debulking

generally remain quite firm after heating, and require piecemeal removal with a rongeur forceps or small osteotome. Some sarcomas are similar in this respect; however, most are liquefied by the radiofrequency current, and can be aspirated using an obstetric suction extraction device. Debulking is continued until bleeding. The radiofrequency probe is then reapplied and the ablate-curette/aspirate cycle repeated in a stepwise manner out to the tumor "capsule" (Figure 5.1). The "capsule" (hopefully sterilized) is stripped away from surrounding tissue if possible, or left *in situ* if adherent, and the tumor bed drained.

PATIENTS AND RESULTS

Between July, 2003, and October, 2006, we treated 26 patients: 17 males, 9 females; age range 28–84 years. Fifteen patients had fixed retroperitoneal or para-aortic tumor; 11 had bulky pelvic neoplasms. Nine lesions were primary, 17 were recurrent. Median size was 10 cm. All patients had prior treatment: 20 had received radiotherapy or chemoradiotherapy; 5 had chemotherapy alone; 1 patient had undergone repeated tumor embolization.

Tumor histology in 22 patients was either adenocarcinoma (11) or sarcoma (11). Two patients had squamous cancer, 1 had a recurrent adrenocortical carcinoma, and 1, a desmoid tumor. Patients were "unresectable" for a variety of reasons. In 9, the lesion was fixed to lumbar vertebrae or aorta. Seven patients had tumors adherent to the sacro-iliac joint or lateral bony pelvis (theoretically resectable); but refused hemi-pelvectomy. In 4, the neoplasm filled the pelvis, allowing no room for exposure. Three patients had cancers adherent to the proximal sacrum (S1, S2), 1 refused exenteration for radiation-induced sarcoma fixed to the prostate, and 1 had a desmoid tumor surrounding the superior mesenteric artery and vein. The final patient had a large malignancy involving stomach, left lobe of liver, and inferior vena cava.

Treatment outcome was defined as success if the target lesion was controlled for a minimum of 6 months. Failure was death from any cause within 3 months of surgery, or tumor progression in the treated field within 6 months. Using these criteria, 16 (61%) patients were a "success", and 11 (42%) remain free of disease at 8–48 months. An example is shown in Figures 5.2 and 5.3. Five patients initially considered a success relapsed after 6 months: 3 at local and distant sites; 2 at distant sites alone. Fourteen patients had significant pain (> 5 on scale of 10) prior to surgery; 7 had 60% or greater reduction in pain afterward. Ten patients (39%) were failures at the outset. One patient died within 30 days of surgery, and 3 others succumbed within 3 months, a treatment-related mortality of 16%. Six patients survived operation, but never achieved local control of their tumor, and died 5–9 months after surgery.

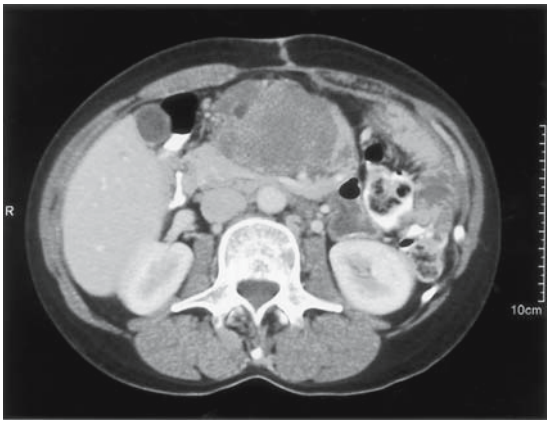

FIGURE 5.2. Abdominal CT scan: desmoid tumor is root of mesentry engulfing superior mesentric artery/vein.

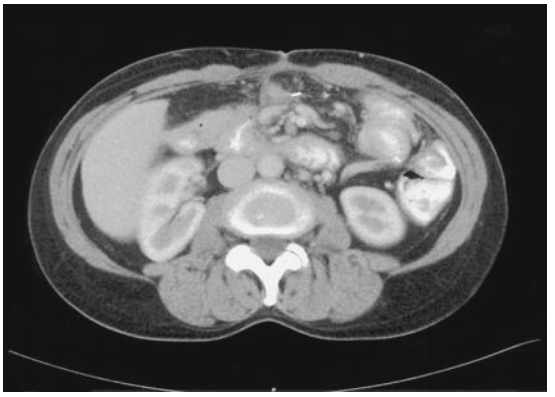

FIGURE 5.3. Same patient 6 months after combined RF ablation and debulking

Nonfatal morbidity was 16% (4 patients): osteoradionecrosis of the iliac wing (1); iliac arterial damage requiring a stent (1); nonhealing buttock incision (1); persistent retroperitoneal abscess cavity (1). Kaplan-Meier survival for all patients is presently 35% at 48 months (GraphPad Prism™, Version 4 for Windows, GraphPad Software, San Diego, CA).

In conclusion, our experience suggests that large and/or fixed extrahepatic tumors that would be difficult and/or impossible to treat with standard surgery or radiofrequency ablation alone, can often be addressed using both modalities together. Nevertheless, not all patients benefitted. In some, lesions abutting the aorta or vena cava could not adequately ablated, either as a result of these vessels acting as a heat sink, or our fear of injuring these with the radiofrequency probe. Conversely, in 2 other patients, bone and a major (iliac) artery were damaged by overheating. Thus, there is much to be learned with this approach, both in regard to technique and determination of the best candidates. The finding of 35% long-term survival is encouraging, but still early. It does suggest, however, that many patients with seemingly isolated bulky abdominal and/or pelvic neoplasms have no distant metastases at presentation. Thus, if their local disease can be controlled, a sizable percentage become long-term survivors.

REFERENCES

Abraham, J., Fojo, T., and Wood, B.J. 2000. Radiofrequency ablation of metastatic lesions in adrenocortical cancer. *Ann. Intern. Med 133*: 312–313.

Belfiore, G., Moggio, G., Tedeschi, E., Geco, M., Cioffi, R., Cincotti, F., and Rossi, R. 2004. CT-guided radiofrequency ablation: a potential complementary therapy for patients with-unresectable primary lung cancer - a preliminary report of 33 patients. *Am. J. Roent. 183*: 1003–1111.

Cushing, H. 1928. Electro-surgery as an aid to the removal of intracranial tumors. *Surg. Gynecol. Obstet. 47*: 751–784.

Decadt, B., and Siriwardena, A.K. 2004. Radiofrequency ablation of liver tumors: systematic review. *Lancet Oncol. 5*: 550–560.

Fernando, H.C., Hoyos, A.D., Litle, V., Belani, C.D., and Luketich, J.D. 2004. Radiofrequency ablation: identification of the ideal patient. *Clin. Lung Cancer 6*: 149–153.

Gillams. A. 2005. The use of radiofrequency in cancer. *Br. J. Cancer 92*: 1825–1829.

Harsh, G.R., and Wilson, C.B. 1990. Neuroepithelial tumors of the adult brain. In: Youmans J.R. (Ed.), *Neurological Surgery*, 3rd Edition. W.B. Saunders, Philadelphia, PA, pp. 3040–3136.

Ohhigashi, S., Nishio, T., Watanabe, F., and Matsusako, M. 2001. Experience with radiofrequency ablation in the treatment of pelvic recurrence of rectal cancer: report of 2 cases. *Dis Colon Rectum 44*: 741–745.

Rhim, H., Dodd, G.D., III, Chintapalli, K.N., Wood, B.J., Dupuy, D.E., Hvizda, J.L., Sewell, P.E., and Goldberg, S.N. 2004. Radiofrequency ablation of abdominal tumors: lessons learned from complications. *Radiographics 24*: 41–52.

Strauss, A.A., Strauss, S.F., Crawford, R.A., and Strauss, H.A. 1935. Surgical diathermy of carcinoma of the rectum. *JAMA 104*: 1480–1484.

Tillotson, C.L., Rosenberg, A.E., and Rosenthal, D.I. 1989. Controlled thermal injury of bone. Report of a percutaneous technique using radiofrequency electrode and generator. *Invest. Radiol. 24*: 888–892.

Zelkovic, P., and Resnick, M.I. 2003. Renal radiofrequency ablation: clinical status 2003. *Curr. Opinion Urol. 13*: 199–202.

6
Gastrointestinal Neuroendocrine Tumors: Diagnosis Using Gastrin Receptor Scintigraphy

Martin Gotthardt, Thomas M. Behr, and Martin Béhé

GASTROINTESTINAL NEUROENDOCRINE TUMORS

Gastrointestinal neuroendocrine tumors (NET) are mostly malignant tumors with a low incidence of 0.002–0.76 per 100,000 people per year. They are less malignant than adenocarcinomas of the gastrointestinal tract, most of them are highly differentiated, and they show slow growing patterns. Therefore, the term "carcinoid" was introduced by Oberndorfer in 1907 to distinguish this tumor entity from the more aggressive adenocarcinomas. Nowadays, to avoid confusion in the terminology, the nomenclature of NET should follow the WHO classification (Solcia *et al*., 2000). Older classifications, such as the well-known one from Williams and Sandler (1963) include tumors with different clinical and pathological features in the same group (such as "foregut") and, therefore, should not be used.

Though it was Oberndorfer who introduced the term "carcinoid" for NETs, he failed to detect their endocrine origin. It were Ciacco in 1906 and Gosset and Masson in 1914 who described that "carcinoids" arose from Kulchitzky's enterochromaffin cells in the glands of Lieberkühn. Although the neural crest has been believed to be the origin of the cells forming NET for a long time (Pearse, 1969), it seems to be more probable that the original ideas of Masson are correct and NET arise from endocrine cells of the gastrointestinal tract (van Eeden and Offerhaus, 2006).

Symptoms, Clinical Appearance, Therapy, and Prognosis

Many NET of the gastrointestinal tract are functionally inactive. Because of their slow growing pattern, symptoms often occur late in the course of the disease and often too late for curative therapy. Mechanical symptoms related to large liver metastases or gastrointestinal obstruction may lead to the diagnosis. Often, the primary tumor may be comparably small and only the (liver) metastases lead to the diagnosis. In case the tumors are functionally active, the symptoms are related to the kind of tumor and the hormones it produces. The carcinoid syndrome includes flushing, diarrhea, and bronchial obstruction which are caused by serotonin secretion. Other well-known syndromes are the Zollinger-Ellison syndrome caused by gastrin-producing

gastrinomas with peptic ulcera, reflux disease, and diarrhea or the Verner Morrison syndrome characterized by hypokalaemia and diarrhea caused by VIP (vasoactive intestinal polypeptide) secretion. These functionally active NET are often named after the hormones they produce, such as insulinoma, VIPoma, gastrinoma, glucagonoma etc. (Arnold, 2005). Although the patient may show impressive symptoms, the size of the tumors may be limited, which may complicate their detection by imaging modalities.

The therapy of NET includes many options. Surgery is the treatment of choice in patients with functionally active tumors as a curative approach. Palliative surgery should also be considered in functionally active metastatic tumors to reduce the symptoms. Symptom control or at least relief can also be obtained by pharmacological treatment (such as proton pump inhibitors in Zollinger Ellison syndrome). Octreotide may inhibit tumor growth as well as hypersecretion of peptide hormones causing symptoms. Also α-interferon may reduce tumor growth. Chemotherapy is indicated in patients with quickly-progressing metastatic disease (mostly Streptozocin, Doxorubicin, Cisplatinum, Etoposide, Dacarbazine), but seems to be of limited effect in NET of the small bowel and colon. Larger liver metastases may be treated by chemoembolization, radio frequency ablation, or radiosurgery. If the primary tumor has been resected and metastases are limited to the liver, these patients may in selected cases also be treated by liver transplantation. Peptide receptor radionuclide therapy (PRRT) with octreotide analogs labeled with ^{90}Y or ^{177}Lu is another option offering the advantage of much lesser side-effects in comparison to chemotherapy. However, in view of the comparably low numbers of patients, prospective randomized controlled clinical trials are missing so that there are no evidence-based guidelines for the use of these therapies. Therefore, treatment decisions will largely rely on personal experience of the treating physicians. Therapy should always follow an interdisciplinary approach.

Diagnostic Imaging Procedures

The diagnosis of a functional neuroendocrine tumor can usually be made based on the symptoms of the patient in conjunction with biochemical parameters. To localize the tumor, somatostatin receptor scintigraphy (SRS) is considered the central imaging procedure. SRS has a high sensitivity and specificity reaching up to 90% and 80%, respectively. In patients with functional NET of the pancreas, SRS should be combined with endoscopic ultrasound (EUS). Especially in gastrinomas, endoscopy will be necessary to examine the gastric mucosa and to exclude duodenal manifestation of the tumor. EUS is also able to detect small lesions in the pancreas down to 1–2 mm that may be missed by SRS or anatomical imaging modalities, such as magnetic resonance imaging (MRI) or computed tomography (CT). In the first work-up of pancreatic NET, CT and MRI should be performed after SRS and EUS but they are of value for the definition of the exact localization of lesions prior to invasive therapy or in the follow-up after therapy. It has also been shown that CT and MRI influence patient treatment in the same extent as SRS in patients with metastasized NET (Gotthardt *et al*., 2003b). In the case of insulinomas,

SRS shows only a low sensitivity because many insulinomas do not express the respective somatostatin receptor subtypes binding octreotide. This does not exclude positive scans in patients with insulinomas (which may be the case in up to 50%), but in most cases SRS will be false-negative. Therefore, in insulinoma SRS plays a minor role in comparison to other pancreatic NET. In non-functional NET of the gut, the imaging procedures to be used are identical with those for functional NET of the pancreas. In NET of the gut, SRS also plays a central role in the localization of the primary tumor. It should be combined with abdominal ultrasound (US) which is also very useful for the detection of liver and lymph node metastases. For further work-up of the patients, CT and MRI should be used dependent on the clinical situation. Especially in the case of negative SRS, CT scanning of thorax and abdomen is the imaging modality of choice. In NET of the colon and rectum, SRS may have a somewhat lower sensitivity. These tumors should then be imaged by CT (combined with an enteroclysma) and MRI. Algorithms for imaging of gastrointestinal NET have been defined by Ricke *et al*. (2001).

Potential Improvement of Scintigraphic Imaging of NET by Using Alternative Radiopeptides

In the diagnostic work-up of NET, SRS-negative tumors may form a considerable problem. In the case of insulinomas, the sensitivity of SRS lies clearly below 50%. Other NET or their metastases may also be SRS-negative. Therefore, alternative receptors for targeting of tumors with other peptides are warranted. Reubi and Waser (2003) have defined a number of alternative receptors that may have potential as targets for scintigraphic imaging. These include the GLP-1 (glucagon-like peptide-1) receptor and the CCK_2(cholecystokinin)/gastrin receptor. Indeed, insulinomas can be imaged by targeting the GLP-1 receptor (which is also an option for peptide receptor radiotherapy (PRRT)) (Gotthardt *et al*., 2006a; Wild *et al*., 2006; Wicki *et al*., 2007). For imaging of CCK2 receptors, recently a clinical study demonstrated that gastrin receptor scintigraphy (GRS) had an excellent sensitivity for the detection of metastatic medullary thyroid carcinoma (MTC) (Gotthardt *et al*., 2006b). Therefore, clinical targeting of other receptors than the somatostatin receptor is feasible and may be of additional value.

RADIOPEPTIDE SCANNING VERSUS ANATOMICAL IMAGING MODALITIES

Radiopeptide scanning is based on the principle of injection of a radiolabeled peptide which specifically targets a receptor overexpressed on a tumor. This radiopeptide is then taken up into and accumulates within the tumor cell while the unbound radiopeptide is cleared out of the body, preferably via the kidneys. In this way, high uptake into the target tissues can be achieved while the background activity is kept low. In addition to high target-to-background ratios, conventional nuclear medicine imaging as well as PET are very sensitive, allowing the detection of very small quantities of a radiopharmaceutical (in the range of

micrograms). Furthermore, an optimal radiopeptide will specifically accumulate only in the targeted tumor. It would therefore also be possible to differentiate between local recurrence and scar tissue which is a problem of CT and MRI scanning. Higher specificity is therefore a very important potential advantage of radiopeptide scanning over anatomical imaging. Unfortunately, this is not always true: octreotide is an example for a radiopeptide that accumulates in tumors as well as in inflammation/scar tissue because somatostatin receptors are also expressed on lymphocytes, activated leucocytes, and epitheloid cells (Gotthardt *et al*., 2004). A disadvantage of conventional nuclear medicine imaging is the comparably low resolution that can be achieved. In three-dimensional SPECT (single photon emission computed tomography) imaging, the spatial resolution of clinical scanners is limited to ~ 1 cm, which may result in a low sensitivity for small lesions. The use of higher-resolution systems leads to a decrease in physical sensitivity of the cameras requiring longer acquisition times, which is not always feasible in clinical practice. For older PET scanners, the spatial resolution is also limited to 8 – 10 mm. New systems with time-of-flight technique and the use of other new technologies are currently improving the spatial resolution to 2 – 4 mm for clinical scanners. Therefore, the disadvantage of lower spatial resolution will be much less important in the future. This will help to increase sensitivity of PET for very small lesions. Furthermore, these new scanners are also capable of whole-body scans in a shorter time of < 15 min which will further improve in the future.

RADIOLABELED PEPTIDES: DEVELOPMENT, ADVANTAGES, AND SHORTCOMINGS

The over-expression of proteins in pathological processes offers different possibilities for targeted diagnosis and therapy (Hutchinson, 2007; Suzuki *et al*., 2007). In the case of radiopeptide imaging, this is the case for several peptide receptors expressed on different tumors (Reubi, 2003). These receptors can be targeted with the respective ligand peptides which are used as Trojan Horses to deliver radioactivity for imaging and therapy or toxic substances to the cancer cells (Schally and Nagy, 2004). Radiometals can be coupled via chelators to the peptides whereas other nuclides may be attached via a covalent bond (Heppeler *et al*., 2000).

In the chemical part of the development of radiopeptides, problems such as complex or covalent binding stability have to be overcome whereas the biological aspects are related to metabolic stability, biological properties such as receptor affinity or biodistribution, which are more complicated. Naturally occurring peptides have a low stability in blood with half-lives in the range of minutes, and therefore need to be stabilized by replacing amino acids with other natural amino acids, D-configurated amino acids or artificial amino acids. Another possibility is to change the amide bond. However, it is crucial to preserve the biological properties such as binding affinity or internalization rate. The binding affinity should be in the nanomolar or better in the subnanomolar range.

Binding of a radionuclide to a peptide highly depends on chemical properties of

the radionuclides. Halogens may be bound covalently to peptides and proteins. At least for radioactive isotopes of iodine this is a disadvantage because they are attached in the ortho position of the hydroxy group on an aromatic ring (tyrosine). This structure is known from iodinated thyroid hormones which is why it is released from cells after internalization. Furthermore, the bound iodine may be cleaved by deiodinases (the same that are responsible for deiodination of thyroid hormones). This results in free iodine and high uptake of radioiodine in the thyroid while the target-to-background ratios become low. Most radiometal labeled compounds stay within the cells after receptor binding and internalization and are only slowly released. This so-called "residual labeling" leads to an increasing uptake in the cells with time. The reason is metabolic trapping of the radiometal-chelator complex within the target cell as there is no metabolic pathway for metabolization of these compounds. Recently, some strategies for residual radiodine labeling have also been developed.

The choice of the most suitable chelator for radiometals depends on the use of the compound. DTPA (diethylenetriaminepentaacetic acid) can be used as monofunctional or bifunctional chelator. Monofunctional DTPA is coupled as a dianhydride to free amines (lysine or N-terminal end) to the peptide. A carbonic acid side chain is used for coupling which lacks for the metal chelation. Therefore, the chelator stability is high for ^{111}In but not for other radiometals. This way of labeling is preferred for proof of principle experiments of newly developed peptides because the coupling of DTPA is easy and can be performed during a Merrifield peptide synthesis. Labeling with ^{111}In can be performed at room temperature achieving high specific activities. The bifunctional DTPA chelator has a side arm for coupling to the peptide and all of the carbonic acids arms will remain for the metal-chelator binding. This complex is more stable and may also be suitable for ^{90}Y, in addition to ^{111}In.

A very stable chelator for different radiometals is DOTA (1,4,7,10-Tetraazacyclododecane-1,4,7,10-tetraacetic acid) which is especially important for stable labeling for therapeutic applications. DOTA is coupled via a carbonic acid to a free amine of the peptide or protein. It can be labeled with ^{68}Ga, ^{90}Y, ^{111}In, or ^{177}Lu, etc. The disadvantage of DOTA is that it is necessary to heat it to 100°C during the labeling procedure which may destroy the peptide. Several other chelators like deferoxamine (DFO) for ^{68}Ga or NOTA (1,4,7-triazacyclononane-1,4,7-triacetic acid) for ^{64}Cu- can be used for labeling for PET applications. A good overview of the different coupling methods is given by Anderson and Welch (1999).

The advantage of peptides as compared to other proteins with a higher molecular weight (such as antibodies and antibody fragments) is a favorable pharmacokinetic behavior with rapid uptake into the target cells, fast clearance by the kidneys, and a low background in blood, liver, and other organs. An image with a good target to background ratio can be obtained within 30 min–24 h. Rapid clearance by the kidneys, however, also causes problems as the peptides are reabsorbed in the tubuli leading to high retention of the radiolabel in the kidney. Although this effect is of limited relevance in radiopeptide imaging, in peptide receptor radiotherapy it may cause considerable nephrotoxicity. This will be discussed in more detail later.

MINIGASTRIN FOR DETECTING METASTASIZED NEUROENDOCRINE TUMORS

Targeting of the CCK_2 receptor with radiolabeled minigastrin (^{111}In-DTPA-DGlu$_1$-minigastrin (MG)) has proven to add to the diagnosis of metastatic MTC (Gotthardt *et al*., 2006c). In direct comparison with other imaging modalities, gastrin receptor scintigraphy (GRS) together with CT imaging showed the highest tumor detection rate, better than MRI, US, and ^{18}F-FDG- PET. GRS may also be helpful in the detection of other NET. Therefore, a study has been conducted in patients with NET comparing GRS with the standard procedure in those patients, SRS (Gotthardt *et al*., 2006c).

Cholecystokinin 2 (CCK_2) Receptor Expression

CCK_2 receptors are overexpressed on MTC tumor cells (and also in cells of other tumors such as small-cell lung cancer, astrocytomas, neuroendocrine tumors of the gut, and others). Expression in healthy tissue is usually low (gallbladder, smooth muscle cells of the gut, pancreas, central nervous system). Only in the gastric mucosa, expression levels are high. In order to keep background activity low, a ligand specifically binding to CCK_2 receptors is favorable for imaging of MTC as additional binding to CCK_1 receptors would further increase uptake in organs physiologically expressing CCK_1 receptors. MG specifically binds to CCK_2 receptors and has therefore, apart from other favorable characteristics for imaging, been chosen as optimal compound for MTC imaging.

Labeling

A kit formulation was used for labeling. The kit was prepared by adding 250 µl of 20 µM DTPA-DGlu1-minigastrin in 0.5 M sodium acetate solution (pH 5.4) through a sterile filter into an elution flask under sterile conditions. The kit was then lyophilized and stored at −20°C until use. For reconstitution for patient studies, 250 MBq of $^{111}InCl_3$ in 500 µl 0.1 M HCl was added to the kit (Béhé *et al*., 2003). The radiochemical purity of the labelled minigastrin was always >95 % as evaluated by HPLC with a specific activity of 55.5 GBq/µmol.

Scanning Protocol

GRS with ^{111}In-DTPA-DGlu$_1$-minigastrin (MG) is basically performed in the same manner as SRS. Approximately, 180–250 MBq of the compound are injected intravenously. It is important to keep in mind that MG does exert the same effects as pentagastrin, which therefore also includes the same side effects: nausea, cough, an itchy "strange feeling" in chest and abdomen, and flush-like symptoms. Therefore, injection should be done slowly via a venous catheter. Usually, the side effects resolve within a few minutes. Whole-body scans are obtained 4 and 20–24 h after injection in anterior and posterior views using a gamma-camera equipped with a parallel-hole medium energy collimator. To guarantee for a sufficient count rate, the scanning speed is set below 10 cm/min. SPECT (single photon emission computed tomography) images should be obtained for higher sensitivity as well as in case of indeterminate findings. We suggest that 120 views should be obtained with 30 s per view.

Biodistribution of Minigastrin

Physiologically, ^{111}In-DTPA-DGlu$_1$-minigastrin accumulates in organs with CCK_2 receptor expression. The stomach has the highest level of CCK_2 receptor expression and is therefore the organ with the most prominent MG uptake, besides the kidneys. Though kidneys show only a low CCK_2 receptor expression, the compound is physiologically excreted via the kidney. A considerable part of MG is reabsorbed in the tubuli after glomerular filtration via the megalin/cubilin system (Gotthardt *et al*., 2007). As in tumor cells, the radiometal/chelator complex is retained in the tubuli leading to an even more pronounced uptake. Other organs with physiologic CCK_2 receptor expression are usually not visible on scans. Because MG is hydrophilic, it cannot cross the blood-brain barrier and does not accumulate in the central nervous system. In brain tumors that disturb the blood brain barrier (specific), uptake has been detected (Gotthardt *et al*., 2003a). Accumulation of activity in the guts of patients (as often detected in GRS) is most likely not caused by biliary secretion of the compound (as had been suggested) but by secretion from the gastric mucosa as in most patients, the gallbladder and liver are not visible. In addition to the organs mentioned above, in premenopausal women the breast tissue may also accumulate MG.

Clinical Imaging in Neuroendocrine Tumors

In a study with 60 patients suffering from NET, GRS was directly compared to SRS. CT and MRI served as reference to evaluate lesions negative in SRS while positive in GRS. From the patients included in the study, 3 had gastrinomas, 2 glucagonomas, 1 insulinoma, 3 paragangliomas, and 51 had carcinoid tumors (meaning other gastrointestinal NET independent of their functional status). In 6 of the 51 patients, the primary tumor was unknown. A tumor detection rate is given because the true sensitivity could only have been determined by histological evaluation which could not be obtained in these patients (due to the high number of lesions, no postmortem analyses). This had been replaced by verification of lesions by either CT/MRI or follow-up. The total number of detected sites of disease was 224, of which GRS detected 165 and SRS detected 184. The overall tumor detection rate was 73.7% for GRS and 82.1% for SRS. Although GRS performed not as good as SRS in respect to the tumor detection rate, from 11 patients with negative SRS scans, GRS was positive in 6 (54.5% of SRS-negative patients) (Figure 6.1). Furthermore, GRS was able to detect 18 additional sites of tumor involvement. Therefore, GRS detected tumor sites missed by SRS in 12 patients (20%). There was no significant correlation between the results of scintigraphy and the grade of tumor differentiation, but the authors found a weak inverse correlation of GRS and SRS both being positive and the rate of Ki-67 expression. No correlations between the performance of GRS or SRS and the localization of the primary tumor or the functional status of the NET could be demonstrated.

Because GRS detected additional tumor sites in 20% of all patients, half of which were negative in SRS, the authors concluded that GRS may provide additional information in patients with NET (especially if somatostatin uptake is missing). Furthermore, a possible advantage of GRS is that it can be performed in patients under

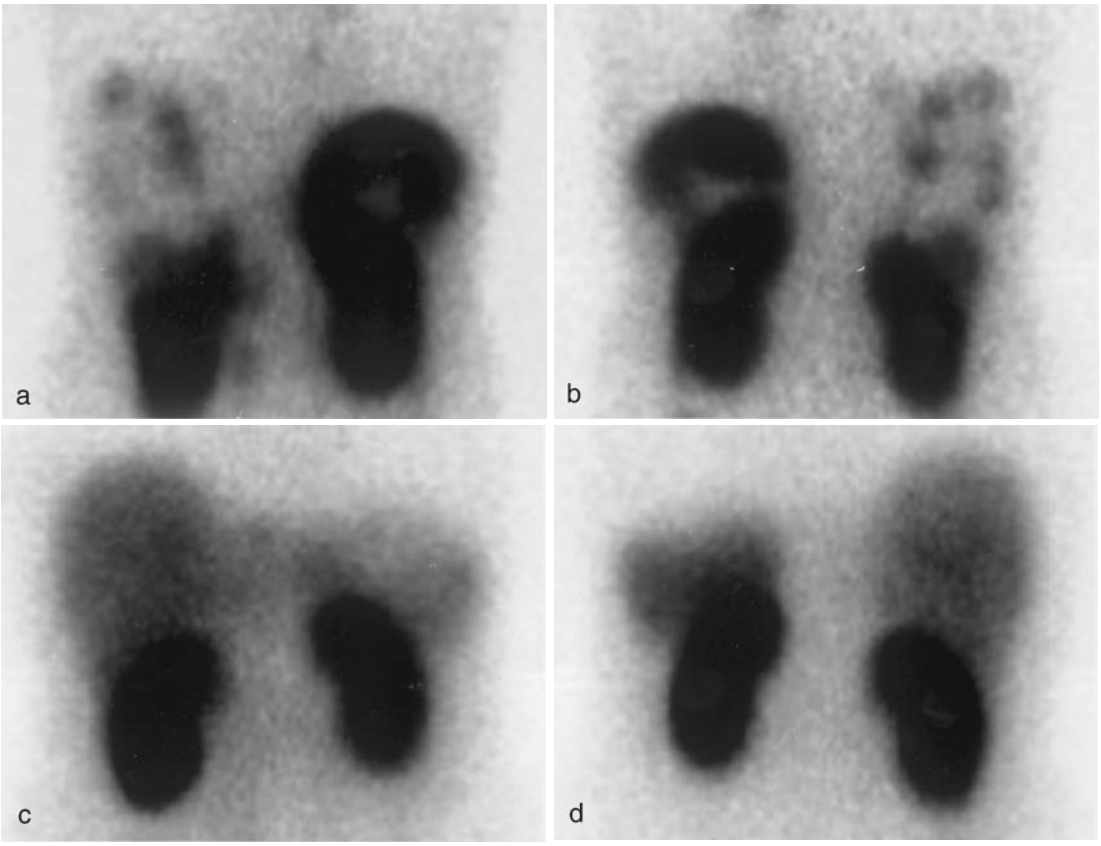

FIGURE 6.1. Patient with a metastasized NET of the ileum, details from 24 h planar scans. While GRS is positive (a, anterior view and b, posterior view) showing several lesions in the liver, SRS is negative (c, anterior view and d, posterior view). Note the uptake in the stomach in the left upper abdomen on GRS images while on the SRS images the spleen is visible. The kidneys are also visible

therapy with long-acting somatostatin analogs without restriction as Octreotide® is not known to interact with the CCK_2 receptor. Apart from imaging, an alternative to Octreotide® could also be helpful when exploring the possibilities for optimization of PRRT by choosing the peptide with more favorable tumor uptake, especially in patients showing low or missing Octreotide® uptake.

Interestingly, one patient who had been diagnosed as having a "bronchial carcinoid" was later found to have small cell lung cancer. In this patient, a high uptake of MG could be detected. GRS might thus also be of value in patients with SCLC where SRS does not perform well, although this has to be elucidated in future studies (Gotthardt *et al.*, 2006b). The overall conclusion of the authors was that GRS will not replace SRS but may be helpful in patients with negative or equivocal SRS and low uptake in SRS.

FUTURE PERSPECTIVES OF $DGLU_1$-MINIGASTRIN

In comparison to SPECT imaging, PET has a higher spatial resolution reaching

2–4 mm in the scanners of the newest generation. Furthermore, PET tracer uptake can easily be quantified. Therefore, one would expect that PET imaging has the potential to further increase sensitivity and accuracy of NET imaging. For targeting of the somatostatin receptor on other neuroendocrine tumors, an advantage of PET over SPECT imaging has been demonstrated (Buchmann *et al*., 2007). PET imaging for targeting of the CCK_2 receptor could be done with DOTA-DGlu$_1$-Minigastrin labeled with the positron emitter ^{68}Ga, a generator-derived emitter. The Ge/Ga generator is ideal for local radionuclide production. For labeling with ^{68}Ga, DTPA (used for labeling with ^{111}In) is not suitable due to a low stability of the chelate. Therefore, the chelator DOTA is required. Alternative radionuclides would include ^{89}Zr and ^{64}Cu, radionuclides with longer half-lives that can easily be shipped and are therefore suitable for local labeling. They again would require another chelator (desferral or NOTA).

For SPECT imaging, labeling with ^{99m}Tc instead of ^{111}In may increase the spatial resolution due to the more favorable gamma-energy of ^{99m}Tc. Therefore, a ^{99m}Tc-labeled MG derivative has been developed which showed promising results (Nock *et al*., 2005). Ongoing clinical studies with this compound will have to show its clinical potential.

REFERENCES

Anderson, C.J., and Welch, M.J. 1999. Radiometal-labeled agents (non-Technetium) for diagnostic imaging. *Chem. Rev. 99*: 2219–2234.

Arnold, R. 2005. Definition, historical aspects, classification, staging, prognosis and therapeutic options. *Best Pract. Res. Clin. Gastroenterol. 19*: 491–505.

Béhé, M., Becker, W., Gotthardt, M., Angerstein, C., and Behr, T.M. 2003. Improved kinetic stability of DTPA-D-Glu as compared with conventional monofunctional DTPA in chelating indium and yttrium: preclinical and initial clinical evaluation of radiometal labelled minigastrin derivatives. *Eur. J. Nucl. Med. Mol. Imag. 30*: 1140–1146.

Buchmann, I., Henze, M., Engelbrecht, S., Eisenhut, M., Runz, A., Schafer, M., Schilling, T., Haufe, S., Herrmann, T., and Haberkorn, U. 2007. Comparison of (68)Ga-DOTATOC PET and (111)In-DTPAOC (Octreoscan) SPECT in patients with neuroendocrine tumours. *Eur. J. Nucl. Med. Mol. Imag. 34*: 1617–1626.

Ciacco, C. 1906. Sur une nouvelle espèce cellulaire dans les glandes de Lieberkühn. *C. R. Soc. Biol. 1*: 76–78.

Gosset, A., and Masson, P. 1914. Tumeurs endocrines de l'appendice. *Presse Med. 22*: 237–240.

Gotthardt, M., Groß, M.W., Schipper, M.L., Henzel, M., Béhé, M.P., Schurrat, T., Pollum, H., Pfestrof, A., Schmidek, A., Heinis, J., Engenhart-Cabilic, R., and Behr, T.M. 2003a. Uptake of In-111-DTPA-D-Glu1-Minigastrin into malignant brain tumors: proof of specificity and results of the first 30 patients. *Eur. J. Nucl. Med. Mol. Imag. 30*: S237.

Gotthardt, M., Dirkmorfeld, L.M., Wied, M.U., Rinke, A., Béhé, M.P., Schlieck, A., Höffken, H., Joseph, K., Klose, K.J., Behr, T.M., and Arnold, R. 2003b. Influence of Somatostatin receptor scintigraphy and CT / MRI on the clinical management of patients with gastrointestinal neuroendocrine tumours: an analysis based on 188 patients. *Digestion 68*: 80–85.

Gotthardt, M., Boermann, O.C., Behr, T.M., Béhé, M.P., and Oyen, W.J.G. 2004. Development and clinical application of peptide-based radiopharmaceuticals. *Curr. Pharm. Design. 10*: 2951–2963.

Gotthardt, M., Lalyko, G., van Eerd-Vismale, J., Keil, B., Schurrat, T., Hower, M., Laverman, P., Behr, T.M., Boerman, O.C., Göke, B., and Béhé, M. 2006a. A new technique for in vivo imaging of specific GLP-1 binding sites: first results in small rodents. *Reg. Peptides 137*: 162–167.

Gotthardt, M., Behe, M.P., Beuter, D., Battmann, A., Bauhofer, A., Schurrat, T., Schipper, M., Pollum, H., Oyen, W.J.G., and Behr, T.M. 2006b. Improved tumour detection by gastrin receptor scintigraphy in patients with metasta-

sised medullary thyroid carcinoma. *Eur. J. Nucl. Med. Mol. Imag. 33*: 1273–1279.

Gotthardt, M., Béhé, M., Grass, J., Bauhofer, A., Rinke, A., Schipper, M.L., Kalinowski, M., Arnold, R., Oyen, W.J.G., and Behr, T.M. 2006c. Added value of gastrin receptor scintigraphy to somatostatin receptor scintigraphy in neuroendocrine tumors. *Endocr. Rel. Cancer 13*: 1203–1211.

Gotthardt, M., Eerd-Vismale, J., Oyen, W.J.G., de Jong, M., Zhang, H., Maecke, H.R., Behe, M., and Boerman, O. 2007. Indication for different mechanisms of kidney uptake of radio-labeled peptides. *J. Nucl. Med. 48*: 596–601.

Heppeler, A., Froidevaux, S., Eberle, A.N., and Maecke, H.R. 2000. Receptor targeting for tumor localisation and therapy with radiopeptides. *Curr. Med. Chem. 7*: 971–994.

Hutchinson, L. 2007. Targeted therapies: the answer to individualized treatment? *Nat. Clin. Pract. Oncol. 4*: 323.

Nock, B., Maina, T., Béhé, M., Nikolopoulou, A., Gotthardt, M., Schmitt, J.S., Behr, T.M., and Mäcke, H.R. 2005. CCK2/gastrin receptor-targeted tumor imaging with ^{99m}Tc-labeled minigastrin analogs. *J. Nucl. Med. 46*: 1727–1736.

Oberndorfer, S. 1907. Karzinoide Tumoren des Dünndarms. *Frankf. Z. Pathol. 1*: 426–429.

Pearse, A.G.E. 1969. The cytochemistry and ultrastructure of polypeptide hormone-producing cells of the APUD series and the embryologic, physiologic and pathologic implications of the concept. *J. Histochem. Cytochem. 17*: 303–313.

Reubi, J.C. 2003. Peptide receptors as molecular targets for cancer diagnosis and therapy. *Endocr. Rev. 24*: 389–427.

Reubi, J.C., and Waser, B. 2003. Concomitant expression of several peptide receptors in neuroendocrine tumours: molecular basis for in vivo multireceptor tumour targeting. *Eur. J. Nucl. Med. Mol. Imaging 30*: 781–793.

Ricke, J., Klose, K.J., Mignon, M., Oberg, K., and Wiedenmann, B. 2001. Standardisation of imaging in neuroendocrine tumours: results of a European delphi process. *Eur. J. Radiol. 37*: 8–17.

Schally, A.V., and Nagy, A. 2004. Chemotherapy targeted to cancers through tumoral hormone receptors. *Trends Endocrinol. Metab. 15*: 300–310.

Solcia, E., Heitz, P.U., Capella, C., and Klöppel, G. 2000. Endocrine tumors of the gastrointestinal tract. In: Solcia, E., Kloeppel, G., and Sobin, L.H. (eds). *Histological Typing of Endocrine Tumors. International Histological Classification of Tumors*. World Health Organization Pathology Panel, 2nd edn. Springer, Berlin: 61–68.

Suzuki, R., Rao, P., and Sasaguri, S. 2007. Current status and future of target-based therapeutics. *Curr. Cancer Drug Targets. 7*: 273–284.

van Eeden, S., and Offerhaus, G.J.A. 2006. Historical, current and future perspectives on gastrointestinal and pancreatic endocrine tumors. *Virchows Arch. 448*: 1–6.

Wicki, A., Wild, D., Storch, D., Seemeyer, C., Gotthardt, M., Béhé, M., Kneifel, S., Mihatsch, M., Reubi, J.C., Mäcke, H.R., and Christofori, G. 2007. A new therapeutic approach to insulinoma: [(Lys^{40}(Ahx-[^{111}In-DTPA])]-Exendin-4 is a highly efficient radiotherapeutic for glucagon-like-peptide-1 (GLP-1) receptor targeted therapy. *Clin. Cancer Res. 13*: 3696–3705.

Wild, D., Béhé, M., Wicki, A., Storch, D., Waser, B., Gotthardt, M., Keil, B., Christofori, G., Reubi, J.C., and Mäcke, H.R. 2006. Preclinical evaluation of [Lys^{40}(Ahx-[^{111}In-DTPA])]-Exendin-4, a very promising ligand for glucagon-like-peptide-1 (GLP-1) receptor targeting. *J. Nucl. Med. 47*: 2025–2033.

Williams, E.D., and Sandler, M. 1963. The classification of carcinoid tumours. *Lancet 1*: 238–239.

7
Distal Esophagus: Evaluation with 18F-FDG PET/CT Fusion Imaging

Domenico Rubello and Cristina Nanni

INTRODUCTION

Esophageal cancer is a malignant neoplastic disease characterized by a poor prognosis. In developed countries the incidence is 4–5/100,000 people, while a significant higher incidence is found in China, the Caspian region of Iran, and in South Africa (up to 100/100,000 people). Male individuals are affected two to four times more often than their female counterparts, and black men present the highest incidence of squamous cell carcinoma. The overall 5-year survival rate in patients amenable to definitive treatment ranges from 5% to 30%, although the occasional patient with very early disease may have a better chance of survival.

Several risk factors are associated with the development of esophageal cancer causing inflammation of the mucosa first, metaplasia, dispalsia, and then cancer. The strongest association was found with tobacco use, dietary habits (very spicy food), alcohol consumption, obesity, Barrett's esophagus due to chronic persistent gastroesophageal reflux disease (GERD), Plummer-Vinson syndrome, caustic injury, chronic achalasia, and tylosis.

Esophageal cancer may present with two histopathologic types, including more than 98% of all esophageal cancers: squamous cell carcinoma (frequently arising in the upper two third of the organ) and adenocarcinoma (commonly located in the distal esophagus). The remaining 2% of esophageal malignant lesions includes lymphomas, leiomyosarcoma, and neuroendocrine carcinoma.

Esophageal cancer has a very poor prognosis, and presently, surgery including esophagectomy and lymphadenectomy is the standard therapeutic approach, although it presents significant risks as intraoperative or peroperative mortality is 5%. Radiotherapy and chemotherapy can accompany surgery to improve the overall survival. Recently, neoadjuvant chemoradiotherapy has been employed to reduce the primary mass in otherwise inoperable patients, with promising results. This procedure improves patients' quality of life, but whether or not it improves the overall survival remains controversial.

The commonly used staging system for esophageal cancer is based on the evaluation of primary tumor characteristics, lymph nodes involvement, and presence of distant metastases (TNM stage system).

Prognosis usually depends on the stage at disease onset, and surgery is not recommended if distant metastasis is found. In this case palliative procedures may be required. Radiotherapy given as a single modality to relieve dysphagia or esophageal stents to relieve obstruction may be necessary, and are frequently used.

As for other malignant tumors, staging esophageal cancer at disease onset is a crucial point to subsequently choose the best therapeutic approach. Several classical diagnostic procedures are available to evaluate local invasion, lymph node involvement, and distant lesions (usually in the lungs, abdomen, or bones). Different combinations of barium esophagogram, upper endoscopy, whole body computed tomography, bone scan, and endoscopic ultrasonography are used to stage esophageal cancer and to assess disease relapse after therapy.

18-Fluorodeoxyglucose-Positron Emission Tomography/Computed Tomogaphy (18F-FDG-PET/CT)

In recent years 18F-Fluorodeoxyglucose-positron emission tomography (18F-FDG-PET) and 18F-FDG-PET/computed tomography (CT) are acquiring importance for oncological studies. Positron emission tomography is a molecular imaging technique based on the possibility to detect a positron emitter tracer biodistribution (in case of FDG the tracer is a glucose analog) over the whole body in order to visualize the metabolic activity of each organ and tissue, with a spatial resolution of 4.5 mm with the newest PET tomographs.

5.7 MBq/Kg of FDG is injected intravenously. To avoid the presence of hematic insulin that alters the tracer distribution, the patient is required to fast for at least 6 h before injection and not to take insulin or oral antidiabetic drugs. The optimal uptake time is 60 min. During that time the patient is hydrated and asked to void in order to avoid intense bladder activity. Finally, the patient undergoes the image acquisition procedure. Positron emission tomography is acquired for 4–5 min/bed position while the low-dose CT parameters are 120 kV and 80 mA. Positron emission tomography images are usually reconstructed with an iterative method (OSEM is the most common).

Fluorodeoxyglucose is a glucose analog and enters the cells via the membrane GLUT receptors proportionally to the glucose consumption. Once inside the cell, FDG is phosphorylated and trapped inside the cell. In fact, it cannot be metabolized and cannot exit the cell anymore. The result is that the cell is labeled proportionally to its glucose metabolism. This is very useful because malignant lesions have a high mitotic index and are characterized by increased metabolism (therefore, increased tracer uptake), which is an early neoplastic occurring change before morphological changes become detectable by conventional imaging methods (e.g., CT). It is possible, therefore, to identify malignant lesions at a very early stage, possibly changing patient management in a significant percentage of cases (15% in case of esophageal cancer), and to semi-quantify the metabolic activity of the lesion. Maximum Standardized Uptake Value (SUV max) is the most diffuse method to quantify the uptake of a lesion and gives an index of disease response to therapy or disease progression if measured before and after therapy.

Positron emission tomography has the disadvantage of an inaccuarate spatial localization of hypermetabolic findings. This is particularly important when PET is used to study anatomically complicated

systems as head and neck, abdomen, pelvis, and mediastinum. To improve PET accuracy in the localization of positive findings, hybrid PET/CT tomographs were implemented. Hybrid tomographs are able to coregister a whole body PET scan and a low-dose CT scan. Images are fused slice by slice superimposing PET to the anatomical map created from CT. Computed tomography scan is also used for attenuation correction purpose; thus, allowing an accurate calculation of quantitative parameters as SUV max.

Several studies in literature are aimed to the evaluation of the role of 18F-FDG-PET and 18F-FDG-PET/CT in the diagnostic work-up of esophageal cancer. Positron emission tomography is useful because it is a whole body scan, giving a complete overview of disease extension, and it allows an early detection of lymph nodes involvement and distant metastasis for the staging, and the assessment of therapy response for evaluating early disease relapse during the follow-up.

On the other hand, although PET/CT is very sensitive for the detection of primary mass (both adenocarcinoma and squamous cell carcinoma are clearly PET positive and have the same metabolic activity), the exact infiltration of esophageal wall cannot be evaluated by means of functional PET imaging because of the poor spatial resolution (~ 4–5 mm) compared to other techniques such us endoscopic ultrasonography. Nevertheless, 18F-FDG-PET/CT plays main role in the evaluation of nodes and distant metastasis in a single-step diagnostic procedure (Figs. 7.1–7.3).

In the case of nodes involvement, PET is considered more sensitive than CT because the diagnosis of positive lesions is based on a functional index (radiotracer uptake) instead of on morphological basis. In fact, small lymph nodes (negative at CT because they are smaller than 1 cm) show an increased tracer uptake and also are metastatic at histology. The same concept can be applied to the detection of distant metastasis. Positron emission tomography is always a whole body scan and explores all the tissues and organs, including bones at the same time and with the same accuracy. Other techniques must focus on a particular organ or apparatus and must be tailored on the pathology that is under evaluation. Furthermore, FDG is a positive indicator of cancer and the scan reading is somehow easier than other tomographic techniques.

18F-FDG-PET AND PET/CT IN ESOPHAGEAL CANCER

Positivity Criteria

18F-FDG-PET/CT is considered consistent with esophageal cancer when a focal area of increased tracer uptake is detected in correspondence to the esophageal wall on CT morphological map. Maximum Standardized Uptake Value indicates the presence of vital malignant tissue when it is higher that 2.0–2.5 according to international guidelines. Esophagitis due to GERD (or, rarely, due to previous radiotherapy on mediastinum) is frequently associated with esophageal cancer and can be misinterpreted. Inflammation, in fact, is the main cause of false-positivity in PET with 18F-FDG because it is a hypermetabolic process. Its uptake pattern, therefore, resembles cancer due to the increased metabolism (Figs. 7.1–7.3).

The only characteristic that differentiates esophageal inflammation from cancer is that

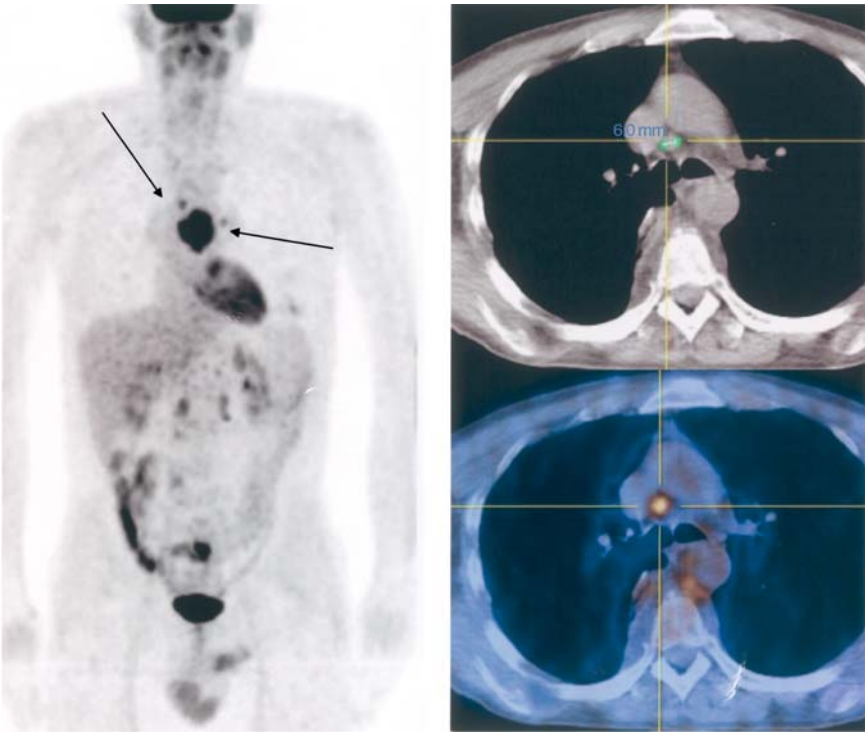

FIGURE 7.1. 18F-FDG-PET/CT evaluating a patient with esophageal cancer at diagnosis. MIP Image (left side – arrows) shows primary positive mass and two tiny mediastinal positive nodes. CT axial slice (right, upper image) shows a 6 mm carinal node, negative for neoplastic involvement according to CT criteria. The same lymph node shows increased metabolic activity at the correspondent PET/CT axial slice (right, lower image) and is therefore a positive finding (N+)

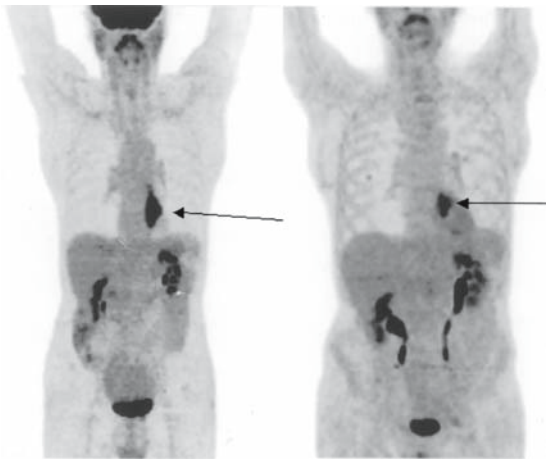

FIGURE 7.2. 18F-FDG-PET evaluating a patient with esophageal cancer before (left side image) and after (right side image) neoadjuvant chemotherapy. MIP images show primary positive mass (arrows) demonstrating a partial response after therapy (SUV max decreased from 12.6 to 8.4)

the former is usually diffuse and the latter is usually focal as suggested in the study of Rampin *et al*. (2005). These criteria are not strict and the extension of the uptake cannot be considered as a reliable method. FDG-PET is falsely negative only for lesions with a maximum diameter smaller than PET spatial resolution (4–5 mm) or for flat lesions with a thickness < 4–5 mm, growing parallel to the major axis of the esophagus. "In situ" carcinoma and severe displasia are, therefore, usually not detected.

Staging

18F-FDG PET/CT is a reliable and accurate method to stage esophageal carcinoma. Positron emission tomography is

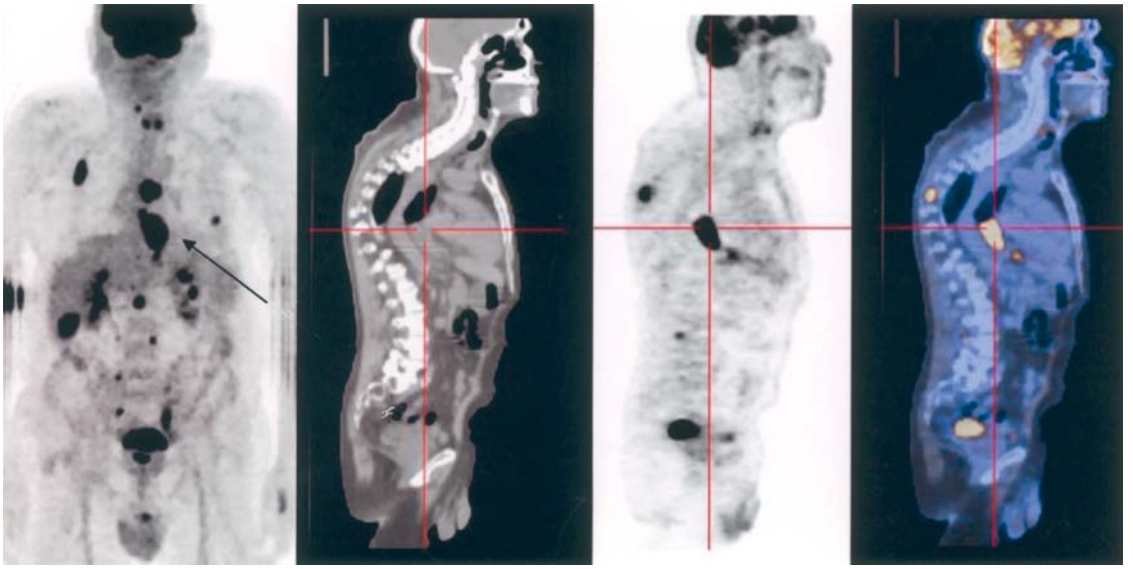

FIGURE 7.3. 18F-FDG-PET/CT (from the left to the right, MIP and sagittal CT, PET and PET/CT fusion images) evaluating a patient with esophageal cancer at diagnosis. PET shows positive primary mass (indicated by the arrow), mediastinal nodal involvement and several bone secondary lesions

sensitive for the detection of primary mass, even though it cannot accurately identify T due to the poor spatial resolution. Nodal metastases are detected with a sensitivity of ~ 80%. Abdominal and skeletal metastasis are detected with even higher sensitivity and specificity approaching 100%. Staging SUV max seems to be a prognostic index, according to some studies as that of van Westreenen *et al*. (2005). Forty patients with esophageal cancer were studied with 18F-FDG-PET for staging the disease and were divided into two groups. Group1 had a SUV max ≤ 6.7; group 2 had a SUV max > 6.7. The two groups presented a significant difference in the overall survival (613 ± 89 vs. 262 ± 47 days).

Disease Relapse

In patients operated for esophageal cancer, the presence of post-surgical fibrotic tissue causes difficulties in the interpretation of morphological tests as CT scan may not be easy to distinguish vital tissue (cancer relapse) from nonvital tissues (post-surgical scar) as they can have the same appearance. 18F-FDG-PET/CT is proved to have a high accuracy for the detection of early "*in loco*" cancer relapse.

Neoadjuvant Therapy Response

As indicated earlier, a significant number of patients are diagnosed with esophageal cancer in a late phase, when the disease is so extended that a surgical approach is useless or even dangerous. Recently, neoadjuvant chemo-radiotherapy has been proposed to reduce the primary mass in order to subsequently operate the patient. Neoadjuvant chemo-radiotherapy is known to obtain a high rate of response with a complete pathological response in ~10% of patients, but a significant modification of overall survival is not yet clearly demonstrated. 18F-FDG-PET/CT result is

proved to be correlated to the pathologic response concerning the variation of SUV max before and after therapy, and this is an accurate index to early and "*in vivo*" evaluate therapy response. Nevertheless, it is not clear if an early recognition of neoadjuvant therapy response is significantly correlated to a better prognosis. Despite that, Swisher *et al*. (2004) in their preliminary study found that after neoadjuvant chemoradiotherapy patients with SUV max ≤ 4 within the residual lesion had a significantly longer overall survival compared to patients with SUV max >4. 18F-FDG-PET is not routinely used for the follow-up and acquires importance only if equivocal findings at conventional imaging arise.

18F-FDG-PET/CT Versus Other Techniques

According to the classical diagnostic and staging work-up, if a patient presents with symptoms consistent with esophageal carcinoma, the first step usually consists of barium X-ray examination that may be performed before endoscopy. It can demonstrate the location of the tumor and the degree of tumor obstruction. The second and most important step is endoscopy, that provides tissue for diagnostic biopsy and brushings and for additional measurement of tumor size and determination of location. Once the diagnosis is done, the staging is performed through CT of the neck, chest, abdomen, and pelvis. Computed tomography is used to identify enlarged lymph nodes, metastasis to distant organs, and malignant fluid collections (pleural effusions, ascites) and may help in determining tumor surgical resectability, placement of radiation fields, and prognosis. More recently, endoscopic ultrasonography was used in association with CT. It gives information about detailed assessment of the intramural extent of tumor and the involvement of adjacent lymph nodes.

In this regard, for the evaluation of esophageal cancer 18F-FDG PET/CT is proved to have the same sensitivity as that of 18F-FDG PET alone (96%) but a significantly higher specificity (81% vs. 59%) and accuracy (90% vs. 83%). For staging the disease, PET is as accurate as CT and endoscopic ultrasonography, and these three methods showed similar sensitivity and specificity (82–86% and 60–67%, respectively).

This scenario significantly changes if these techniques are employed to evaluate response to neoadjuvant chemo-radiotherapy. Westerterp *et al*. (2005) analyzed 24 recent articles on esophageal cancer, and found that PET and endoscopic ultrasonography are equal and both are significantly more accurate than CT. The maximum joint values for sensitivity and specificity were 54% for CT, 86% for endoscopic ultrasonography, and 85% for FDG-PET. Accuracy of CT was significantly lower than that of FDG-PET ($p < 0.006$) and of endoscopic ultrasonography ($p < 0.003$). Instead, accuracy of FDG-PET and that of endoscopic ultrasonography was similar ($p = 0.839$). In all patients, CT was always feasible, whereas endoscopic ultrasonography was not feasible in 6% of the patients, and FDG PET was not feasible in < 1% of cases. The evaluation of disease relapse 18F-FDG-PET is more sensitive, specific, and accurate than CT (86% vs. 73%; $p = 0.0002$), but no specific studies have been published up till now on the additional value of PET/CT over PET for the evaluation of disease relapse.

PET/CT and Other Radiotracers

18F-FDG is not the only radiotracer feasible to study malignant tumors using a PET tomograph. 11C-Choline is the second radiotracer used in PET for clinical studies especially for the evaluation of prostate cancer, giving an index of cell membrane metabolism. According to literature, 11C-Choline is feasible to study esophageal cancer but, from preliminary studies, it has a significantly lower sensitivity, specificity, and accuracy for the detection of primary tumor and distant metastasis and is not feasible for studying liver and spleen due to their physiological high uptake. 11C-Choline PET seems to be more sensitive than 18F-FDG-PET in detecting nodal metastatic involvement and may be used to increase the accuracy of N evaluation. 18-F-Fluoro-thymidine (18F-FLT) is another radiotracer that was proposed for the evaluation of esophageal cancer. It is a direct marker of cell proliferation. 18F-FLT has a lower sensitivity compared to 18F-FDG-PET but gives a lower number of false-positive results. Various tracers are discussed in other chapters in these volumes.

REFERENCES

Rampin, L., Rubello, D., Nanni, C., and Fanti, S. 2005. Value of PET-CT fusion imaging in avoiding potential pitfalls in the interpretation of 18F-FDG accumulation in the distal esophagus. *Eur. J. Nucl. Med. Mol. Imag. 32*: 990–992.

Swisher, S.G., Erasmus, J., Maish, M., Correa, A.M., Macampilac, H., Ajani, J.A., Cox, J.D., Komaki, R.R., Hong, D., Lee, H.K., Putnam, J.B., Rice, D.C., Smythe, W.R., Thai, L., Vaporciyan, A.A., Walsh, G.L., Wu, T.T., and Roth, J.A. 2004. 2-Fluoro-2-deoxy-D-glucose positron emission tomography imaging is predictive of pathologic response and survival after preoperative chemoradiation in patients with esophageal carcinoma. *Cancer 15*: 1776–1785.

van Westreenen, H.L., Cobben, D.C.P., Jager, P.L., Van Dullemen, H.M., Wesseling, J., Elsinga, P.H., and Plukker, J.Th. 2005. Comparison of 18F-FLT PET and 18F-FDG PET in esophageal cancer. *J. Nucl. Med. 46*: 1321–1325.

Westerterp, M., van Westreenen, H.L., Reitsma, J.B., Hoekstra, O.S., Stoker, J., Fockens, P., Jager, P.L., van Eck-Smit, B.L.F., Plukker, J.T.M., van Lanschot, J.J.B., and Sloof, G.W. 2005. Esophageal cancer: CT, endoscopic US, and FDG PET for assessment of response to neoadjuvant therapy— systematic review. *Radiology 46*: 1321–1325.

8
Endoscopic Ultrasound and Staging of Esophageal Cancer

Kanwar Rupinder S. Gill and Timothy A. Woodward

OBJECTIVES

Accurate cancer staging allows the most favorable therapy and prognosis of a neoplastic process, and allows consistency when performing clinical trials for different stages of tumors. In the case of esophageal cancer, the available therapeutic options include resection, radiotherapy, chemotherapy, photodynamic therapy, and multimodal combination therapy. The most important para meter in determining the prognosis and optimal treatment is defining the anatomic extent of the cancer. Endoscopic ultrasound (EUS) is the most significant recent advance in gastrointestinal endoscopy. It provides close-proximity imaging of the esophageal wall and its adjacent structures and allows for accurate identification of the layers of the gastrointestinal wall, and is, therefore, uniquely suited to the local staging of esophageal cancer. Also, EUS has become a significant tool for the assessment of locoregional lymph nodes, and in some cases, distant organ metastases adjacent to luminal structures. EUS with the addition of fine needle aspiration (FNA) allows for minimally invasive access to these sites through a transesophageal or transgastric approach. The capability of performing FNA has greatly improved the accuracy and popularity of EUS for esophageal cancer staging. This review will outline the basic principals of the EUS-FNA technique, and its role in esophageal cancer staging and restaging after chemoradiotherapy, as well as the potential role of newer modalities such as endobronchial ultrasound (EBUS).

BASIC PRINCIPLES

Squamous cell cancer and adenocarcinoma account for the majority of esophageal cancers. The incidence of esophageal cancer has increased over the last 2 decades with adenocarcinoma of the distal esophagus having the highest rate of occurrence in the United States and Europe (Blot and McLaughlin, 1999; Pera *et al*., 1993). Survival of esophageal cancer patients depends on the anatomical extent of tumor. Treatment guidelines and prognosis are principally based on the degree of tumor invasion (T), the presence of nodal metastases (N) and/or distant metastases (M) as scored in the TNM classification system (Sobin *et al*., 2005). Tumors confined to

the esophageal wall are considered T1 or T2 disease, while those invading the adventitia or adjacent structures are considered T3 and T4, respectively. The N indicates the peritumoral nodal involvement, whereas the cervical and celiac lymph nodes, along with involvement of visceral organs, are considered M disease by some authors. The curative treatment is surgical resection; however, the 5 year survival rate is only, on average, 10% among patients with negative tumor margins on surgical resection (Eloubeidi *et al*., 2003; Enzinger and Mayer, 2003; Hulscher *et al*., 2002; Pera, 2000; Rouvelas *et al*., 2005). Furthermore, in patients selected for curative resection the surgical morbidity is quite high, with a mortality rate ranging between 4–10%. Unfortunately, many patients present with advanced stages may not be candidates for curative resection (Taylor, 1986). The esophagus lymphatics are just below the surface of the muscularis mucosa, so there is a high prevalence of lymph node metastases even at early T stage esophageal cancer. Tumor extending to the mucosa (T1m) and to the submucosa (T1sm) will demonstrate nodal metastasis ~ 5% and 25% of the time, respectively. The nodal involvement is much higher (40–50%) in tumors reaching muscularis mucosa (T2), and this reaches up to 80% in T3 and T4 disease (Rice *et al*., 2003; Sabik *et al*., 1995). Locoregional lymph node metastasis is one of the most important prognostic factors in predicting the survival and resectability (Kato *et al*., 2002). The accurate staging is very important to identify patients with T2 and T3 stage disease, who might be candidates for chemoradiation therapy before surgical therapy, and to avoid surgery in patients T4 lesions, i.e., patients with advanced disease involving vascular structures or adjacent organs, thus warranting palliative management (Rice *et al*., 2003). Thus, EUS is a valuable tool in staging of esophageal cancer. It can be used to evaluate the TNM staging at initial diagnoses and also to access for disease recurrence.

EQUIPMENT

Training in EUS-FNA techniques is available through advanced endoscopy fellowships, as well as short courses and tutorials, both of which can be supplemented with published literature, video materials, CD ROMs, and websites. Recognizing the variability in training, the American Society for Gastrointestinal Endoscopy has published minimum guidelines for competency in EUS, which include 150 supervised cases of which 75 should include FNA. The EUS application in assessing the anatomy of esophagus and application of FNA in the mediastinum is relatively simple. This is because the position of the scope is straight in the esophagus without particular angulation.

Echoendoscopes are available in two general formats, radially oriented transducers in which the image is oriented perpendicular in a “radial” format relative to the endoscope, and linearly oriented transducers that are oriented so the image is parallel with the endoscope. Mostly the assessment of esophageal cancer is done by radial echoendoscope; however, linear echoendoscopes are necessary to perform EUS-FNA because they allow visualization of the needle entering into the target lesion. Olympus, Pentax, and Toshiba currently manufacture linear echoendoscopes, which have small or standard accessory

FIGURE 8.1. Olympus linear EUS (left) and EBUS (right) scopes

channels (2.0–2.8 mm) and larger accessory channels (3.7 mm) capable of delivering needles and other therapeutic devices. All of the available linear echoendoscopes are capable of EUS-FNA (Figure 8.1). The echoendoscopes require attachment to a specific ultrasound processor, which cannot be used with other makes of echoendoscope. Each of the linear echoendoscopes is capable of oblique endoscopic viewing in addition to the ultrasound image. The endoscopic components (light source, air/water supply, image processor) plug into the standard endoscopic equipment for each manufacturer.

Needle systems designed for EUS-FNA are available from three different manufacturers (Olympus Co., GIP Mediglobe, Wilson-Cook Co.) in a wide variety of gauges (19–25 g, usually 22 g), with disposable and non-disposable handles. All needle systems are luer-locked to the accessory channel of the echoendoscope, and are advanced into the tissue with a piston-like handle. The needle is occluded with a stylet during passage through the GI tract wall to minimize contamination from pass-through structures. Expert cytopathology interpretation is essential to high quality EUS-FNA. When available, on-site interpretation during the procedure increases the accuracy and efficiency of EUS-FNA (Klapman *et al*., 2003).

PROCEDURE AND TUMOR INVASION (T), NODAL (N) AND DISTANT METASTASIS (M) CLASSIFICATION

After informed consent and sedation, the patient is incubated with the echoendoscope. EUS staging of esophageal cancer involve assessment of the primary tumor (T staging); assessment of the nodal and distant organ involvement (N and M) staging which may also involve performing FNA of lymph nodes. The examination can be performed initially with a radial echoendoscope and then with the linear echoendoscope for targeted EUS-FNA, if necessary.

The primary site of the tumor is examined for T staging followed by inspection of nodal involvement. The endoscopy guided high frequency transducers are utilized to examine the esophageal and parasophageal structures. Different ultrasound frequencies are utilized to evaluate the anatomical structures. At usual frequencies of 7.5 MHz, structures up to ~5 cm from the esophagus can be imaged. By increasing the frequencies to 20 MHz (Miniprobe) more detailed images can be obtained, but with a more limited field. Utilizing frequencies

of 7.5–12 MHz on standard echoendoscope, the esophagus appears as a five layer structure on EUS examination. The mucosa appears as first hyperechoic layer corresponding to superficial mucosa and second hypoechoic layer corresponding to deep mucosa. The third hyperechoic layer corresponds to submucosa. The fourth hypoechoic layer is muscularis propria (MP) followed by the fifth hyperechoic layer corresponding to adventitia. The visualization of the five esophageal layers gives detailed information as to the T staging. T1 tumors invade the mucosa (T1m) and submucosa (T1sm). Tumors invading MP, but not going through it are T2. Tumors expanding through MP and extending into the adventitia (manifesting endosonographically as pseudopodia) are T3 (Figure 8.2). Involvement of any adjacent organs is T4.

Lymph nodes are round or oval hypoechoic structures on EUS examination, which when identified at the peritumoral site, are classified as N1. When nodes are identified at cervical or celiac locations they may be classified as metastatic disease (M), depending upon their proximity to the primary tumor. The celiac nodes are inspected through posterior wall of stomach (Station 1). Accordingly, the liver is inspected through the duodenal bulb and lesser curve of the stomach. Examination of the esophagus and mediastinum with the radial echoendoscope is a simple pullback procedure. With the linear echoendoscope, the mediastinum is surveyed by first finding the descending aorta at the gastroesophageal junction, and then rotating 360° through the mediastinum until the aorta again comes into view. The instrument is withdrawn 2–3 cm and the maneuver repeated until the entire mediastinum has been inspected. Specific lymph node stations such as the subcarinal nodes can be found quickly by withdrawing the instrument to ~ 25–30 cm from the incisors. Color Doppler is not usually needed, as vascular structures are obvious because of their anechoic and large appearance.

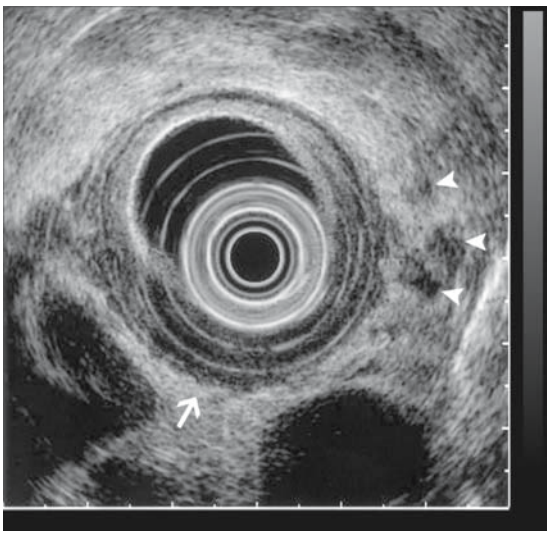

FIGURE 8.2. Esophageal cancer with tumor pseudopodia (arrow) extending through muscularis propria and peritumoral lumph nodes (arrowheads) consistent with T3, N1 stage

EUS-FNA is usually performed using a 22-gauge needle equipped with central stylet (Figure 8.3). The node is punctured under real time ultrasound guidance and the stylet withdrawn. The needle is then moved backwards and forwards within the node to acquire cellular material. In most cases, suction is not necessary to obtain an adequate specimen. The specimen is injected onto a slide for preparation by the endoscopist or specially trained cytology technicians. The slides are then interpreted by an on-site cytotechnician or pathologist. Three or four needle passes providing lymphocytes without malignant cells are usually sufficient to exclude malignancy in a particular node. The EUS can determine

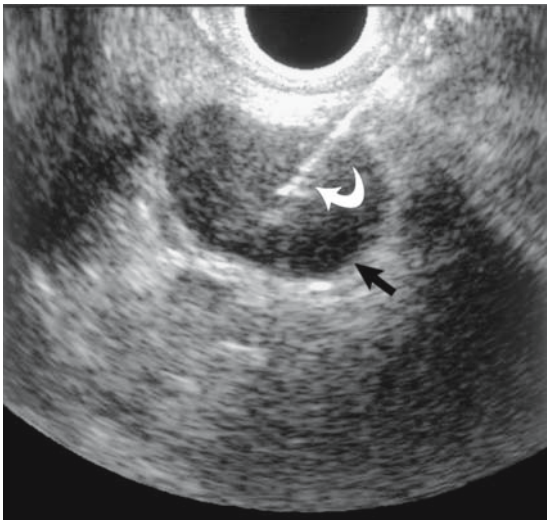

FIGURE 8.3. EUS-FNA of the Celiac lymph node (black arrow) using 22 gauge needle (white arrow)

the size, number, and echogenic features for suspicious metastatic involvement. Also, the EUS-FNA can be utilized in a safe manner for accurate staging.

ROLE OF ENDOSCOPIC ULTRASOUND-FINE NEEDLE ASPIRATION IN ESOPHAGEAL CANCER

Endoscopic Ultrasound in Assessing Primary Tumor (T Staging)

EUS is the most accurate method for T staging of the esophageal cancer (Mallery and Van Dam, 2000). Many studies have demonstrated the high accuracy of EUS compared to CT scan for T staging (Holden *et al*., 1996; Moorjani, *et al*., 2007; Rosch, 1995; Wakelin *et al*., 2002). A meta-analysis of 27 primary articles demonstrated the overall accuracy of EUS for T staging to be 89% (Rosch, 1995). The accuracy of the T staging with standard EUS (7.5–12 MHz) increases as the T stage progresses. The overall accuracy of EUS for the superficial (T1) tumors has been reported ~ 80% when compared to surgical staging (Hasegawa *et al*., 1996; Zuccaro Jr. *et al*., 2005). The staging accuracy for T3 increases to over 90% (Rice *et al*., 2003). The varying results displaying EUS accuracy likely represent the interobserver variation among endosonographers. The T1 staging may be improved by use of Miniprobe, as higher frequency (20 MHz) provides better delineation T1m and T1sm stages (Hasegawa *et al*., 1996; Murata *et al*., 1996; Shimoyama *et al*., 2006). This is particularly important as different T1 lesions can be effectively treated with photodynamic therapy (PDT) or endoscopic mucosal resection (EMR). The study by Hasegawa *et al*. (1996) reported an increase in accuracy with Miniprobe for differentiating T1 and T2 lesions to 92% from the 76% accuracy achieved with standard lower-frequency ultrasound endoscopes. Although Miniprobe has better accuracy for T staging, the N staging may be compromised given the limited depth of penetration into surrounding tissues (~3 cm) (Rosch and Classen, 1999). The combination of conventional EUS for T staging and Miniprobe for T staging has also been described by Shimoyama *et al*. (2006). In this study of 20 patients, Miniprobe had 100% accuracy in distinguishing between T1, T2, and T3 stages and 86% accuracy for differentiating T1m and T1sm.

A major problem encountered during EUS staging of esophageal cancer is advanced disease with esophageal strictures. A complete conventional EUS staging examination with scope tip diameters in

the 12- to 13-mm is prevented by luminal obstruction or stricture in ~30% of esophageal cancers (Botet *et al.*,1991; Fickling and Wallace, 2003). The studies evaluating the role of EUS in T staging for obstructive disease report varying accuracy depending methodology used. The earlier studies comparing EUS utility in determination of T stage for traversable verses nontraversable esophageal tumors reported accuracy of 84% versus 77%, respectively (Dittler and Siewert, 1993; Rosch and Classen, 1999). Similarly, only small differences were observed in another study comparing traversable verses non-traversable tumors (92% versus 87%, respectively). However, much lower accuracy was reported by Hordijk *et al.* (1993) in stenoses which could be traversed only with difficulty (46%) verses tumors which were easy to traversable (92%). The high accuracy of endosonography in nontraversable tumors may be due to the fact that most of these tumors represent advanced stage (T3 or T4). Stenotic tumors where passage of EUS scope is difficult, low focal distance between the ultrasonic transducer and tumor which hampers clear visualization of the wall layers, and tumor penetration depth have been suggested as causes of poor accuracy. To deal with this issue of decreased accuracy in advanced disease, alternative methods have been developed and proposed. These include (1) esophageal dilation prior to staging, (2) use of 7.9-mm nonoptical, wire guided echoendoscope, and (3) miniprobe examination. The esophageal dilation prior to using EUS has been utilized; however, earlier studies reported an esophageal perforation rate up to 24% (Lightdale and Kulkarni, 2005). This problem can be dealt with serial dilations over several days as demonstrated by Wallace *et al.* (2000). No complications were observed when 42 esophageal strictures were dilated in a serial, stepwise fashion using Savory-Gilliard dilators. This study also reported dilations of 14–16 mm which resulted in complete EUS-FNA staging of 87% of procedures compared with 36% with dilation to <14 mm ($p < 0.01$). Additional 19% (8/47) patients were diagnosed with advanced disease as a direct result of dilation of the malignant strictures. The 7.9-mm nonoptical, 7.5 MHz, echoendoscope have a steerable tip. These echoendoscopes are passed blindly over a stiff guidewire passing through the malignant stricture. Binmoeller *et al.* (1995) and Mallery *et al.* (1998) demonstrated that the nonoptical, echoendoscope could be passed in all of 87 and 18 patients, respectively, with malignant strictures. In both studies the complete T and N staging in all patients was achieved. In the study by Binmoeller *et al.* (1995), N staging was compromised in 15 patients because of inadequate visualization of the celiac axis region. The histopathologic correlation in 38 patients in this study who underwent surgery showed an excellent T stage accuracy rate of 89% (T2 = 80%, T3 = 95%, T4 = 87%); however, the N and M stage accuracies of 79% (N0 = 44%, N1 = 90%) and 91% (M0 = 94%, M1 = 75%), respectively. The third alternative of using Miniprobe examination is quite attractive as the small diameter allows the scope to pass tumor stenoses without dilation and also the high frequency can provide more accurate T staging than low-frequency probes. However, as described above, the miniprobes are limited by their range, and thus may be unable to fully image large tumors or regional lymph node involvement.

Endoscopic Ultrasound in Assessing Nodal Metastasis (N Staging)

Utilization of EUS for assessment of N stage is well documented in literature. EUS is superior to the CT scan for N staging (Vazquez-Sequeiros *et al*., 2003). The four EUS criteria suggestive of malignant lymph nodes include nodal width > 10 mm, round shape, smooth borders, and hypoechogenicity (Catalano *et al*., 1994; Tio *et al*., 1990). Among these criteria, hypoechogenicity and width of > 10 mm appear to be the most specific for malignancy (Bhutani *et al*., 1997; Catalano *et al*., 1994). Collectively, these four EUS features produced an additive effect in the prediction of malignant lymph node involvement; malignancy can be predicted with 80–100% accuracy when all four features are present. The presence off all four criteria are highly sensitive (80–100%). However, all of the four features are present only ~ 25% of the time. Also, given the subjective nature of these criteria the overall accuracy of conventional EUS in predicting N stage is ~ 79%, which is much less than for T staging (Kelly *et al*., 2001; Rosch, 1995).

Given the above limitations, multiple studies have evaluated the role of EUS-FNA in N staging (Wiersema *et al*., 1997; Giovannini *et al*., 1999). EUS-FNA provides cytologic confirmation of metastatic disease from accessible nodes as long as the primary tumor is not in the pathway of the aspiration needle. The application of EUS-FNA has further enhanced the accuracy of N staging to ~ 88–100% (Lightdale and Kulkarni, 2005). Of these studies, the largest study by Wiersema *et al*. (1997) involving 192 patients reported sensitivity, specificity, and accuracy for evaluation of malignant lymph nodes to be 92%, 93%, and 92%, respectively. However, a limitation remains for the assessment of peritumoral lymph nodes because of the potential contamination of needle passing through the main tumor. The most clinical useful information in EUS based staging is gained from the assessment of lymph nodes remote to the tumor, like celiac nodes (Eloubeidi *et al*., 2001). The finding of a malignant node in the celiac area is considered by some, M stage, and would be a sign of unresectability. Therefore, particular attention should be paid to celiac area during the EUS examination in staging esophageal cancer patients as it can impact patient management. Giovannini *et al*. (1999) demonstrated EUS-FNA sensitivity of 97% and specificity of 100% for detecting malignancy in enlarged celiac lymph nodes. More such studies are needed to reproduce the reported accuracy of EUS-FNA in celiac lymph node evaluation.

The bigger challenge in assessment of the celiac lymphadenopathy results from cases with advanced disease with luminal narrowing not permitting the examination of the celiac area. As described above, the use of serial dilation to use standard EUS-FNA examination or use of small diameter echoendoscopes such as nonoptical 7.9 mm and Miniprobe can be used without dilation. The disadvantage of both small diameter echoendoscopes is the lack of utilization of FNA. However, potential access for FNA by endosonographic evaluation might be available via the smaller diameter endobronchial ultrasound scope (see below).

To evaluate the added cost of EUS-FNA over standard EUS, a study by Vazquez-Sequeiros *et al*. (2003) compared the standard EUS features (hypoechoic, smooth border, round, or width > 5 mm) criteria for assessing malignant lymph

nodes to routine EUS-FNA. In this prospective study involving 141 patients, the modified EUS criteria (four standard plus EUS identified celiac lymph nodes, > five lymph nodes, or EUS T3 or T4 tumor) were found to have 100% sensitivity if > one modified criteria and specificity of 100% when > six modified criteria were present. The study predicted that utilizing the modified criteria approach routine EUS-FNA could have been avoided in 42% of patients. A new approach of utilizing endobronchial ultrasonography (EBUS)-FNA can be used to sample the suspicious lymph nodes in cervical region, which are in close proximity to the primary tumor where EUS-FNA cannot be possible (Noh *et al*., 2006).

Endoscopic Ultrasound in Assessing Distance Metastasis (M Staging)

The EUS can assess the metastatic disease in the organs in close proximity to the gastrointestinal track. The utility of EUS in the assessment of celiac nodes has been discussed above. The liver can be assessed for M disease and tissue diagnosis can also be obtained if hepatic metastases are identified. Besides these, EUS is limited in assessing the distant M disease. CT or MRI is the primary diagnostic tool in assessing the distant esophageal cancer metastasis and is usually recommended prior to the EUS examination. The sensitivity of CT scan for determining distant metastasis is ~ 90% compared to 70% with EUS (Botet *et al*., 1991). If metastatic disease is found with these modalities, then EUS may not be required. However, when CT is negative for M disease, the addition of EUS-FNA can be complimentary to assess M disease. The authors reported increase accuracy of combined CT and EUS-FNA of 86% compared to CT alone (64%), when the findings were compared to final surgical staging. The studies using PET scan in the preoperative assessment of M disease have reported increased sensitivity over CT (Kato *et al*., 2002). The combined accuracy of PET scan with EUS-FNA for staging is better than CT or EUS-FNA alone. A decision-analysis model study by Wallace *et al*. (2002) comparing different staging strategies concluded that PET + EUS-FNA was more effective than CT + EUS-FNA. Although slightly more expensive, PET + EUS-FNA offered the most quality-adjusted life years when compared to all other common staging modalities. The authors proposed PET/EUS-FNA as preferred over CT/EUS-FNA as initial strategy in esophageal cancer staging.

RESTAGING OF ESOPHAGEAL CANCER AFTER CHEMORADIATION

The use of neoadjuvant chemotherapy, radiotherapy, and the combined chemoradiationtherapy, is being increasingly used in conjunction with surgery in locally advanced (T3 and/or N1) esophageal cancer in an attempt to improve survival (Lightdale and Kulkarni, 2005). The neoadjuvant therapy goals are to reduce the size of the primary tumor, increase the rate of microscopic complete resection (R0), and eliminate micrometastatic disease (Ribeiro *et al*., 2006). In cases with preoperative chemoradiationtherapy, it is frequently

desirable to evaluate the response to treatment prior to recommending surgical resection. EUS-FNA in the setting of restaging of the esophageal cancer has demonstrated less accuracy as compared to TNM staging in non-chemoradiation setting (Lightdale and Kulkarni, 2005).

The overall accuracy of EUS for T staging after chemoradiation ranges from 27% to 82% when compared to histopathology. This is due to the fact that the identification of esophageal wall layers after chemotherapy is difficult because of significant fibrosis and edema, making distinction between postradiation changes and residual tumor difficult on EUS imaging (Lightdale and Kulkarni, 2005).This difficulty commonly leads to false-positive errors and overestimates T staging after chemoradiation. For the same reason, the assessment of early T stages (T1, T2) is more difficult as compared to advanced T stage tumors (T3) tumors. A recent study by Ribeiro *et al*. (2006) demonstrated EUS accuracy of 95% for T3 stage compared to only 26% accuracy for T1 and T2 stages. In summary, it appears that EUS has better restaging accuracy in nonresponders to chemotherapy than responders who had shrinkage in tumor size. Another less common error in this setting is the understaging (false-negatives) of lesions. That is, normal-appearing esophagus wall on EUS examination can have microscopic foci of cancer, which are detected in the postsurgical histopathologic specimen (Lightdale and Kulkarni, 2005). The aforementioned studies analyzing the clinical impact of T staging after chemoradiation also suggest that T staging may not impact the overall survival in patients (Agarwal *et al*., 2004). However, newer studies using measurement parameters of > 50% reduction in cross-sectional area of tumor, or decrease in tumor thickness post-chemoradiation have demonstrated better correlation in assessment of the treatment response, and predicting the overall survival after chemoradiation. In a study by Chak *et al*. (2000) patients who had > 50% reduction in the tumor area after multimodality therapy had a median survival of 17.6 months compared with 14.5 months in nonresponders ($p < 0.005$). Another study by Willis *et al*. (2002) demonstrated that EUS had a positive predictive value of 80% for pathologic tumor regression when reduction in cross-sectional area > 50% was considered. Similarly, studies using the pre- and post- chemoradiation percentage reduction of maximal tumor thickness by EUS also closely correlates with the pathological evaluation of treatment response. By defining patients with > 50% reduction of tumor maximum thickness after chemoradiation as responders, Ribeiro *et al*. (2006), reported a non-statistically significant but higher long-term survival (3-year survival 80% versus 61%).

Unlike T staging, the N staging is correlated well with patient survival after chemoradiation. Post-chemoradiation N1 stage has been reported to be the best predictor of survival (Ribeiro *et al*., 2006). The overall accuracy of EUS for nodal assessment has reported accuracy range of 38–71% (Lightdale and Kulkarni, 2005). This accuracy of EUS alone is limited in differentiating the malignant and chemoradiation related reactive nodes; however, EUS-FNA can be useful in this scenario. The PET scan is more accurate than EUS-FNA for nodal disease post-chemoradiation (Cerfolio *et al*., 2005).

ENDOSCOPIC ULTRASOUND-FINE-NEEDLE ASPIRATION MOLECULAR DIAGNOSIS OF ESOPHAGEAL CANCER

As in other tumors, EUS-FNA allows ready access to tissue at multiple time-points throughout the course of tumor progression and treatment. This access has opened up opportunities for translational research on esophagus cancer tissue. Pellise *et al*. (2004) have demonstrated the ability to assay for hypermethylated genes *(MGMT, p16 [INK4a],* and *p14* [ARF]) in lymph node aspirated of esophageal cancer patients. Hypermethylation analysis increased the sensitivity, although decreased the specificity of detecting micrometastatic disease. Other important areas for research include identifying markers predictive of response to specific chemoradiotherapeutic and biological agents, as well as markers for the detection of complete pathological response after chemoradiotherapy (and thus avoiding surgery if tumor-free).

COMPLICATIONS AND SAFETY

When performed by experienced endosono-graphers, EUS-FNA is a highly safe procedure. The major risk is of esophageal perforation in advanced disease. Although initial studies reported an unacceptable risk of up to 24% patients with malignant stricture, newer studies have reported no perforation when serial dilation are done prior to the EUS examination. A recent study by Mortensen *et al*. (2005) reported no increased mortality as a result of esophageal perforation from EUS. The other important safety precautions include careful visualization of the entire length of the needle as it passes into the target and use of color flow Doppler prior to FNA to visualize and avoid blood vessels in the needle path.

In conclusion, EUS-FNA requires a skilled endoscopist with specific experience and the necessary equipment, which is now becoming more available at many tertiary referral centers. Given that this is an operator-dependent technique, experience of the endosonographer correlates well with accuracy of staging (Fockens *et al*., 1996). EUS has proven its value in the initial staging of the esophageal cancer; however its value in restaging after chemoradiation therapy is not yet established. This may be improved with the new endoscopic techniques like three-dimensional EUS, which may allow better measurement of tumor volume to pre- and post- chemoradiation. Another challenge is the utilization of EUS–FNA in peritumoral lymph nodes where the tumor is in direct path of needle pass. The combined EUS/EBUS-FNA may have some role in future to accurately assess the nodal disease as the nodes can be approached through trachea.

EUS-FNA, like all sampling techniques, is subject to sampling error. Future molecular techniques may improve the FNA accuracy in case of micrometastasis.

REFERENCES

Agarwal, B., Swisher, S., Ajani, J., Kelly, K., Fanning, C., Komaki, R. R., Putnam, J. B., Jr., Abu-Hamda, E., Molke, K. L., Walsh, G. L., Correa, A. M., Ho, L., Liao, Z., Lynch, P. M., Rice, D. C., Smythe, W. R., Stevens, C. W., Vaporciyan, A. A., Yao, J., and Roth, J. A. 2004.

Endoscopic ultrasound after preoperative chemoradiation can help identify patients who benefit maximally after surgical esophageal resection. *Am. J. Gastroenterol. 99*: 1258–1266.

Bhutani, M. S., Hawes, R. H., and Hoffman, B. J. 1997. A comparison of the accuracy of echo features during endoscopic ultrasound (EUS) and EUS-guided fine-needle aspiration for diagnosis of malignant lymph node invasion. *Gastrointest. Endosc. 45*: 474–479.

Binmoeller, K. F., Seifert, H., Seitz, U., Izbicki, J. R., Kida, M., and Soehendra, N. 1995. Ultrasonic esophagoprobe for TNM staging of highly stenosing esophageal carcinoma. *Gastrointest. Endosc. 41*: 547–552.

Blot, W. J., and McLaughlin, J. K. 1999. The changing epidemiology of esophageal cancer. *Semin. Oncol. 26(Suppl 15)*: 2–8.

Botet, J. F., Lightdale, C. J., Zauber, A. G., Gerdes, H., Urmacher, C., and Brennan, M. F. 1991. Preoperative staging of esophageal cancer: comparison of endoscopic US and dynamic CT. *Radiology 181*: 419–425.

Catalano, M. F., Sivak, M. V., Jr., Rice, T., Gragg, L. A., and Van Dam, J. 1994. Endosonographic features predictive of lymph node metastasis. *Gastrointest. Endosc. 40*: 442–446.

Cerfolio, R. J., Bryant, A. S., Ohja, B., Bartolucci, A. A., and Eloubeidi, M. A. 2005. The accuracy of endoscopic ultrasonography with fine-needle aspiration, integrated positron emission tomography with computed tomography, and computed tomography in restaging patients with esophageal cancer after neoadjuvant chemoradiotherapy. *J. Thorac. Cardiovasc. Surg. 129*: 1232–1241.

Chak, A., Canto, M. I., Cooper, G. S., Isenberg, G., Willis, J., Levitan, N., Clayman, J., Forastiere, A., Heath, E., and Sivak, M. V., Jr. 2000. Endosonographic assessment of multimodality therapy predicts survival of esophageal carcinoma patients. *Cancer 88*: 1788–1795.

Dittler, H. J., and Siewert, J. R. 1993. Role of endoscopic ultrasonography in esophageal carcinoma. *Endoscopy. 25*: 156–161.

Eloubeidi, M. A., Wallace, M. B., Reed, C. E., Hadzijahic, N., Lewin, D. N., Van Velse, A., Leveen, M. B., Etemad, B., Matsuda, K., Patel, R. S., Hawes, R. H., and Hoffman, B. J. 2001. The utility of EUS and EUS-guided fine needle aspiration in detecting celiac lymph node metastasis in patients with esophageal cancer: a single-center experience. *Gastrointest. Endosc. 54*: 714–719.

Eloubeidi, M. A., Mason, A. C., Desmond, R. A., El-Serag, H. B. 2003. Temporal trends (1973–1997) in survival of patients with esophageal adenocarcinoma in the United States: a glimmer of hope? *Am. J. Gastroenterol. 98*: 1627–1633.

Enzinger, P. C., and Mayer, R. J. 2003. Esophageal cancer. *N. Engl. J. Med. 349*: 2241–2252.

Fickling, W. E., and Wallace, M. B. 2003. Endoscopic ultrasound and upper gastrointestinal disorders. *J. Clin. Gastroenterol. 36*: 103–110.

Fockens, P., Van den Brande, J. H., van Dullemen, H. M., van Lanschot, J. J., and Tytgat, G. N. 1996. Endosonographic T-staging of esophageal carcinoma: a learning curve. *Gastrointest. Endosc. 44*: 58–62.

Giovannini, M., Monges, G., Seitz, J. F., Moutardier, V., Bernardini, D., Thomas, P., Houvenaeghel, G., Delpero, J. R., Giudicelli, R., and Fuentes, P. 1999. Distant lymph node metastases in esophageal cancer: impact of endoscopic ultrasound-guided biopsy. *Endoscopy 31*: 536–540.

Hasegawa, N., Niwa, Y., Arisawa, T., Hase, S., Goto, H., and Hayakawa, T. 1996. Preoperative staging of superficial esophageal carcinoma: comparison of an ultrasound probe and standard endoscopic ultrasonography. *Gastrointest. Endosc. 44*: 388–393.

Holden, A., Mendelson, R., and Edmunds, S. 1996. Pre-operative staging of gastro-oesophageal junction carcinoma: comparison of endoscopic ultrasound and computed tomography. *Australas.Radiol. 40*: 206–212.

Hordijk, M. L., Zander, H., van Blankenstein, M., and Tilanus, H. W. 1993. Influence of tumor stenosis on the accuracy of endosonography in preoperative T staging of esophageal cancer. *Endoscopy 25*: 171–175.

Hulscher, J. B., van Sandick, J. W., de Boer, A. G., Wijnhoven, B. P., Tijssen, J. G., Fockens, P., Stalmeier, P. F., ten Kate, F. J., van Dekken, H., Obertop, H., Tilanus, H. W., and van Lanschot, J. J. 2002. Extended transthoracic resection compared with limited transhiatal resection for adenocarcinoma of the esophagus. *N. Engl. J. Med. 347*: 1662–1669.

Kato, H., Kuwano, H., Nakajima, M., Miyazaki, T., Yoshikawa, M., Ojima, H., Tsukada, K., Oriuchi, N., Inoue, T., and Endo, K. 2002. Comparison between positron emission tomography and computed tomography in the use of the assessment of esophageal carcinoma. *Cancer 94*: 921928.

Kelly, S., Harris, K. M., Berry, E., Hutton, J., Roderick, P., Cullingworth, J., Gathercole, L., and Smith, M. A. 2001. A systematic review of the staging performance of endoscopic ultrasound in gastro-oesophageal carcinoma. *Gut 49*: 534–539.

Klapman, J. B., Logrono, R., Dye, C. E., and Waxman, I. 2003. Clinical impact of on-site cytopathology interpretation on endoscopic ultrasound-guided fine needle aspiration. *Am. J. Gastroenterol. 98*: 1289–1294.

Lightdale, C. J., and Kulkarni, K. G. 2005. Role of endoscopic ultrasonography in the staging and follow-up of esophageal cancer. *J. Clin. Oncol. 23*: 4483–4489.

Mallery, S., and Van Dam, J. 2000. EUS in the evaluation of esophageal carcinoma. *Gastrointest. Endosc. 52(Suppl 6)*: S6–S11.

Mallery, S., Wallace, M., and Van Dam, J. 1998. Non-optical wire guided echoscope (esophagoprobe) markedly increases the rate of complete staging in patients with esophageal carcinoma. *Gastrointest. Endosc. 47*: AB 150.

Moorjani, N., Junemann-Ramirez, M., Judd, O., Fox, B., and Rahamim, J. S. 2007. Endoscopic ultrasound in oesophageal carcinoma: comparison with multislice computed tomography and importance in the clinical decision making process. *Minerva. Chir. 62*: 217–223.

Mortensen, M. B., Fristrup, C., Holm, F. S., Pless, T., Durup, J., Ainsworth, A. P., Nielsen, H. O., and Hovendal, C. 2005. Prospective evaluation of patient tolerability, satisfaction with patient information, and complications in endoscopic ultrasonography. *Endoscopy 37*: 146–153.

Murata, Y., Suzuki, S., Ohta, M., Mitsunaga, A., Hayashi, K., Yoshida, K., and Ide, H. 1996. Small ultrasonic probes for determination of the depth of superficial esophageal cancer. *Gastrointest. Endosc. 44*: 23–28.

Noh, K. W., Wallace, M. B., Pascual, J. M., Wolfsen, H. C., Raimondo, M., and Woodward, T. A. 2006. Fine-needle aspiration of peritumoral lymph nodes in esophageal cancer with endobronchial ultrasound. *Endoscopy. 38*: 953.

Pellise, M., Castells, A., Gines, A., Agrelo, R., Sole, M., Castellvi-Bel, S., Fernandez-Esparrach, G., Llach, J., Esteller, M., Bordas, J. M., and Pique, J. M. 2004. Detection of lymph node micrometastases by gene promoter hypermethylation in samples obtained by endosonography- guided fine-needle aspiration biopsy. *Clin. Cancer Res. 10*: 4444–4449.

Pera, M. 2000. Epidemiology of esophageal cancer, especially adenocarcinoma of the esophagus and esophagogastric junction. *Recent. Results. Cancer. Res. 155*: 1–14.

Pera, M., Cameron, A. J., Trastek, V. F., Carpenter, H. A., and Zinsmeister, A. R. 1993. Increasing incidence of adenocarcinoma of the esophagus and esophagogastric junction. *Gastroenterology 104*: 510–513.

Ribeiro, A., Franceschi, D., Parra, J., Livingstone, A., Lima, M., Hamilton-Nelson, K., and Ardalan, B. 2006. Endoscopic ultrasound restaging after neoadjuvant chemotherapy in esophageal cancer. *Am. J. Gastroenterol. 101*: 1216–1221.

Rice, T. W., Blackstone, E. H., Adelstein, D. J., Zuccaro, G., Jr., Vargo, J. J., Goldblum, J. R., Murthy, S. C., DeCamp, M. M., and Rybicki, L. A. 2003. Role of clinically determined depth of tumor invasion in the treatment of esophageal carcinoma. *J. Thorac. Cardiovasc. Surg. 125*: 1091–1102.

Rosch, T. 1995. Endosonographic staging of esophageal cancer: a review of literature results. *Gastrointest. Endosc. Clin. N. Am. 5*: 537–547.

Rosch, T., and Classen, M. 1999. Pitfalls in endosonographic imaging. In: Van Dam J., Sivak M., eds. *Gastrointestinal Endosonography*. UK: WB Saunders, 123.

Rouvelas, I., Zeng, W., Lindblad, M., Viklund, P., Ye, W., and Lagergren, J. 2005. Survival after surgery for oesophageal cancer: a population-based study. *Lancet Oncol. 6*: 864–870.

Sabik, J. F., Rice, T. W., Goldblum, J. R., Koka, A., Kirby, T. J., Medendorp, S. V., and Adelstein, D. J. 1995. Superficial esophageal carcinoma. *Ann. Thorac. Surg. 60*: 896–902.

Shimoyama, S., Imamura, K., Takeshita, Y., Tatsutomi, Y., Yoshikawa, A., Fujishiro, M., and Yahagi, N. 2006. The useful combination of a higher frequency miniprobe and endoscopic

submucosal dissection for the treatment of T1 esophageal cancer. *Surg. Endosc. 20*: 434–438.

Sobin, L. H. , Wittekind, Ch. , Hutter, R. , Greene, F. L. , and Klimpfinger, M. 2005. *TNM Atlas: Illustrated Guide to the TNM Classification of Malignant Tumours*, 5th ed. Livingston, NJ: Wiley.

Taylor, C. R. 1986. Carcinoma of the esophagus–current imaging options. *Am. J. Gastroenterol. 81*: 1013–1020.

Tio, T. L., Coene, P. P., den Hartog Jager, F. C., and Tytgat, G. N. 1990. Preoperative TNM classification of esophageal carcinoma by endosonography. *Hepatogastroenterology 37*: 376–381.

Vazquez-Sequeiros, E., Wiersema, M. J., Clain, J. E., Norton, I. D., Levy, M. J., Romero, Y., Salomao, D., Dierkhising, R., and Zinsmeister, A. R. 2003. Impact of lymph node staging on therapy of esophageal carcinoma. *Gastroenterology 125*: 1626–1635.

Wakelin, S. J., Deans, C., Crofts, T. J., Allan, P. L., Plevris, J. N., and Paterson-Brown, S. 2002. A comparison of computerised tomography, laparoscopic ultrasound and endoscopic ultrasound in the preoperative staging of oesophago-gastric carcinoma. *Eur. J. Radiol. 41*: 161–167.

Wallace, M. B., Hawes, R. H., Sahai, A. V., Van Velse, A., and Hoffman, B. J. 2000. Dilation of malignant esophageal stenosis to allow EUS guided fine-needle aspiration: safety and effect on patient management. *Gastrointest. Endosc. 51*: 309–313.

Wallace, M. B., Nietert, P. J., Earle, C., Krasna, M. J., Hawes, R. H., Hoffman, B. J., and Reed, C. E. 2002. An analysis of multiple staging management strategies for carcinoma of the esophagus: computed tomography, endoscopic ultrasound, positron emission tomography, and thoracoscopy/laparoscopy. *Ann. Thorac. Surg. 74*: 102610–102632.

Wiersema, M. J., Vilmann, P., Giovannini, M., Chang, K. J., and Wiersema, L. M. 1997. Endosonography-guided fine-needle aspiration biopsy: diagnostic accuracy and complication assessment. *Gastroenterology 112*: 1087–1095.

Willis, J., Cooper, G. S., Isenberg, G., Sivak, M. V., Jr., Levitan, N., Clayman, J., and Chak, A. 2002. Correlation of EUS measurement with pathologic assessment of neoadjuvant therapy response in esophageal carcinoma. *Gastrointest. Endosc. 55*: 655–661.

Zuccaro, G., Jr., Rice, T. W., Vargo, J. J., Goldblum, J. R., Rybicki, L. A., Dumot, J. A., Adelstein, D. J., Trolli, P. A., and Blackstone, E. H. 2005. Endoscopic ultrasound errors in esophageal cancer. *Am. J. Gastroenterol. 100*: 601–606.

9
Esophageal Cancer: Role of RNASEN Protein and microRNA in Prognosis

Hideyuki Ishiguro, Yoshiyuki Kuwabara, Nobuyoshi Sugito, and Yoshitaka Fujii

INTRODUCTION

Esophageal squamous cell carcinoma (ESCC) is one of the most lethal malignancies in Japan, with a 5-year survival rate of 20–30% after curative surgery (Isono *et al*., 1991). Even in early disease stages, we have experienced many patients developing local tumor recurrence or distant metastases within a short period after surgery.

MicroRNAs (miRNAs) are small noncoding RNAs thought to be involved in physiologic and developmental processes by negatively regulating the expression of target genes. The human genome contains up to 1,000 miRNA genes, which constitute ~1–5% of the expressed genes (Berezikov *et al*., 2005). The biological functions of miRNA are not yet fully understood, but it has been suggested that they play a role in the coordination of cell proliferation and cell death (Brennecke *et al*., 2003), apoptosis, fat metabolism (Xu *et al*., 2003), and cell differentiation (Chen, 2004; Dostie *et al*., 2003). This evidence appears to lend support to the notion that changes in miRNA are involved in the genesis and/or progression of various human cancers (Berezikov *et al*., 2005), revealing that miRNAs could act as potential oncogenes or repressors (Calin and Croce, 2006).

The mechanism of the maturation of microRNA is shown in Figure 9.1. The primary transcripts (pri-miRNA) are generated by polymerase II. The processing of pri-miRNAs in the nucleus is mediated by RNASEN, a RNase III endonuclease (Lee *et al*., 2003). RNASEN digests the pri-miRNA in the nuclease to release hairpin, precursor miRNA (pre-miRNA) (Lee *et al*., 2003). Specific RNA cleavage by RNASEN predetermines the mature miRNA sequence, and provides the substrate for subsequent processing events. The pre-miRNAs are transported to the cytoplasm from the nucleus by Exportin-5.

Once in the cytoplasm, a second RNase III endonuclease, Dicer, cleaves the pre-miRNA ~19 bp from the RNASEN cut site (Lee *et al*., 2003; Yi *et al*., 2003). Only one of the two strands is the mature miRNA. To control the translation of target mRNAs, mature miRNA finally enter the RNA-induced silence complex (RISC) (Hutvagner and Zamore, 2002).

We have previously reported that the higher expression levels of RNASEN detected in a significant fraction of ESCC are associated

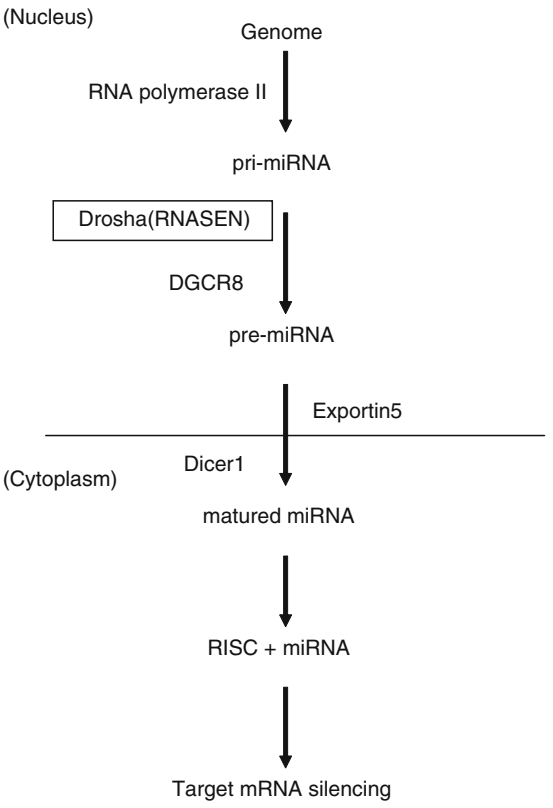

FIGURE 9.1. miRNA biogenesis and function

with shorter postoperative survival (Sugito *et al*., 2006). Overexpression of *RNASEN*, in addition to disease stage, was identified as a significant and independent prognostic factor for surgically treated ESCC patients (Sugito *et al*., 2006). We used TaqMan real-time reverse-transcription polymerase chain reaction (RT-PCR) and immunohistochemistry of RNASEN in these studies. The analysis of RNASEN expression with these methods will be useful for the diagnosis and treatment of the esophageal cancer.

REAL-TIME RT-PCR ANALYSIS USING TAQMAN PROBES

We performed real-time RT-PCR analysis using TaqMan probes (TaqMan® Gene Expression Assays) to examine the RNASEN expression in the esophageal cancer specimens.

A. Isolation of RNA from Tumor Samples and Reverse Transcription Reaction

1. Within 2–3 h after resection, pieces of tumor tissue were carefully selected for maximum tumor content. All samples were snap frozen in liquid nitrogen, followed by storage at −80°C until use.
2. Total RNA was extracted from the esophageal cancer tissues and from normal esophageal mucosa (as control) taken from a site as distant as possible from the tumor using Absolutely RNA™ RT-PCR Miniprep Kits (Stratagene, La Jolla, CA) according to the instruction manual. This kit is very easy and you can get high quality RNA.
3. Concentration of total RNA was adjusted to ~ 200 ng/ml using a spectrophotometer.
4. Reverse transcription was carried out at 42°C for 90 min and 95°C for 5 min, followed by incubation at 72°C for 15 min using 10 µg total RNA, random hexamer primers (Roche Applied Science, Alameda, CA) and Superscript II™ enzyme (Invitrogen, Carlsbad, CA).
5. cDNA with good quality was prepared and used to plot a standard curve (for example, RNA was extracted from cell lines).

B. Real-Time PCR Using TaqMan Probes

1. Real-time quantitative PCR amplification of the cDNA template after RT reaction, corresponding to 20 ng total RNA was performed using TaqMan® Universal PCR Master Mix (Applied Biosystems,

Foster City, CA, USA) in an ABI PRISM 7500 (Applied Biosystems).

2. RNASEN-specific TaqMan probes were designed from sequences in exons 11 (it can be ordered from Applied Biosystems. Assays-on-Demand Gene Expression system, RNASEN-assay ID: Hs00203008_m1, Applied Biosystems).
3. Expression levels were normalized against glyceraldehyde-3-phosphate dehydrogenase (GAPDH) (Applied Biosystems. Assays-on-Demand Gene Expression system, assay ID Hs99999905_m1, Applied Biosystems).
4. cDNA was prepared as control. The concentrations are the original concentration, 1/4, 1/16, 1/64, 1/128, and 1/256.
5. Mix gently, master mix 10 ul

Probe	1 ul
D.W	7 ul
cDNA	2 ul total 20 ul into 96 well plate (Figure 9.2)

6. Spin down 1,500 rpm 10–30 s.
7. Set into Taqman machine and click the start button to run the machine.
8. PCR conditions were 50°C for 2 min and 95°C for 10 min, followed by 40 cycles of 95°C for 15 s, 60°C for 1 min.
9. The window "The run completed successfully" is displayed in the end of the run.
10. Standard curve was made by control cDNA (Figure 9.3).
11. Data analysis.

Immunohistochemistry of RNASEN

RNASEN protein levels were closely correlated with mRNA expression quantified by TaqMan real-time RT-PCR.

Immunohistochemistry of RNASEN is shown in Figure 9.4. In the normal esophageal epithelium, RNASEN is abundant in the nuclei of basal and lower spinous layer cells. In esophageal cancer samples RNASEN was

	1	2	3	4	5	6	7	8	9	10	11	12
A	C1	C1/4	C1/16	C1/32	C1/128	C1/256	E96-1	E96-2	E96-3	E96-4	E96-5	E96-8
	→ Control						→ Sample					
B	E96-9	E97-1	E97-2	E97-3	E97-6	E97-7	E97-8	E97-9	E98-1	E98-3	E98-4	E98-5
C	E98-7	E98-8	E98-9	E98-11	E98-12	E98-13	E98-14	E98-15	E99-1	E99-2	E99-4	E99-5
D	E99-7	E99-9	E99-10	E99-11	E99-13	E99-14	E99-15	E99-16	E99-17	E99-18	E99-19	E99-20
E	E00-1	E00-2	E00-3	E00-4	E00-5	E00-6	E00-7	E00-8	E00-10	E00-11	E00-12	E00-13
F	E00-14	E00-15	E00-16	E01-1	E01-2	E01-3	E01-4	E01-5	E01-6	E01-7	E01-8	E01-9
G	E01-10	E01-11	E01-13	E01-14	E01-15	E01-16	E01-17	E01-18	E01-19	E01-20	E01-21	E01-22
H	E02-2	E02-4	E02-5	E02-6	E02-7	E02-8	E02-9	E02-10	E02-11			

FIGURE 9.2. The arrangement of RT-PCR in 96 well plate

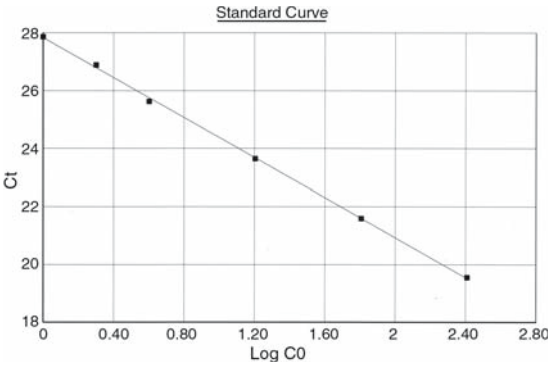

FIGURE 9.3. Standard curve of control cDNA

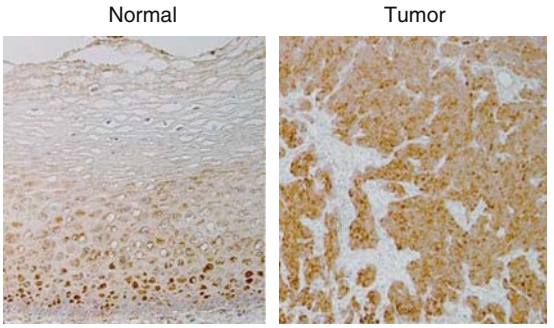

FIGURE 9.4. RNASEN staining of esophageal squamous cell carcinoma samples. Normal esophageal epithelium(left); RNASEN is expressed in basal and lower spinous layers. Tumor samples (right); strong staining was observed

strongly expressed in the nuclei and cytoplasm, and particularly strong staining was observed in the tumor periphery, where invasion to surrounding tissues is taking place. RNASEN staining was mainly seen in the nuclei of cell lines (Sugito *et al*., 2006).

1. For antigen unmasking, deparaffinized sections were boiled in citrate buffer (10 mM sodium citrate buffer, pH 6.0) before incubation with primary antibodies.
2. *RNASEN* protein levels were examined using rabbit polyclonal antibodies (ab12286) and mouse monoclonal antibodies (ab8191) (Abcam, Cambridge, UK). Antibody staining was performed using the DAKO EnVision system (DAKO EnVision labelled polymer, peroxidase).

Interestingly, expression of RNASEN, but not DGCR8 or DICER1, is correlated with poor prognosis in esophageal cancer. Our experiment using RNASEN siRNA supports the notion that the high RNASEN expression observed in our study might have a functional role in the development of esophageal cancers rather than being a mere surrogate marker (Sugito *et al*., 2006). Although the precise molecular mechanism of *RNASEN* up-regulation requires clarification, *RNASEN* is a good candidate molecular prognostic marker and a potential molecular target of the therapeutic reagents for the patients with this intractable disease.

Research on the molecular mechanisms leading to the oncogenesis and progression of the tumor has not been as widely applied in esophageal cancer as in the breast, lung, or colon cancer. The research of microRNA as the one described in this chapter may bring a major break-through in the diagnosis and future drug development for the esophageal cancer. How this microRNA is regulated is unknown and will be the focus of further study.

REFERENCES

Berezikov, E., Guryev, V., van de Belt, J., Wienholds, E., Plasterk, R. H., and Cuppen, E. 2005. Phylogenetic shadowing and computational identification of human microRNA genes. *Cell 120*: 21–24.

Brennecke, J., Hipfner, D. R., Stark, A., Russell, R. B., and Cohen, S. M. 2003. Bantam encodes a developmentally regulated microRNA that controls cell proliferation and regulates the

proapoptotic gene hid in Drosophila. *Cell 113*: 25–36.

Calin, G. A., and Croce, C. M. 2006. MicroRNA-cancer connection: the beginning of a new tale. *Cancer Res. 66*: 7390–7394.

Chen, X. 2004. A microRNA as a translational repressor of APETALA2 in Arabidopsis flower development. *Science 303*: 2022–2025.

Dostie, J., Mourelatos, Z., Yang, M., Sharma, A., and Dreyfuss, G. 2003. Numerous microRNPs in neuronal cells containing novel microRNAs. *RNA 9*: 180–186.

Hutvagner, G., and Zamore, P. D. 2002. A microRNA in a multiple-turnover RNAi enzyme complex. *Science 297*: 2056–2060.

Isono, K., Sato, H., and Nakayama, K. 1991. Results of a nationwide study on the three-field lymph node dissection of esophageal cancer. *Oncology 48*: 411–420.

Lee, Y., Ahn, C., Han, J., Choi, H., Kim, J., Yim, J., Lee, J., Provost, P., Radmark, O., Kim, S., and Kim, V. N. 2003. The nuclear RNase III Drosha initiates microRNA processing. *Nature 425*: 415–419.

Sugito, N., Ishiguro, H., Kuwabara, Y., Kimura, M., Mitsui, A., Kurehara, H., Ando, T., Mori, R., Takashima, N., Ogawa, R., and Fujii, Y. 2006. RNASEN regulates cell proliferation and affects survival in esophageal cancer patients. *Clin. Cancer Res. 12*: 7322–7328.

Xu, P., Vernooy, S. Y., Guo, M., and Hay, B. A. 2003. The Drosophila microRNA Mir-14 suppresses cell death and is required for normal fat metabolism. *Curr. Biol. 13*: 790–795.

Yi, R., Qin, Y., Macara, I. G., and Cullen, B. R. 2003. Exportin-5 mediates the nuclear export of pre-microRNAs and short hairpin RNAs. *Genes Dev. 17*: 3011–3016.

10
Esophageal Cancer: Initial Staging

Lana Y. Schumacher, Nicole B. Baril, and Sherry M. Wren

INTRODUCTION

The incidence of esophageal cancer is increasing. Worldwide it is the ninth most common malignancy and is endemic in many parts of the world, particularly in the developing countries. There were 14,550 new cases and 13,770 deaths from esophageal cancer in the United States in 2006. Esophageal cancer has two pathological subtypes: squamous cell carcinoma and adenocarcinoma. Squamous cell carcinoma is most common in geographic areas where esophageal cancer is endemic due to environmental or dietary factors. Squamous cell carcinoma occurs more frequently among men than women, and it is classically associated with alcohol and tobacco use. In addition, these patients often have a history of other squamous cell head and neck cancers. In the economically developed world adenocarcinoma is more common and its incidence is rapidly increasing. The reason for the substantial increase in the incidence of adenocarcinoma is multifactorial and may be due to an increasing frequency of gastroesophageal reflux disease (GERD) which currently affects up to 30% of the Western population. The majority of patients with adenocarcinoma also have evidence of Barrett's esophagus, a metaplastic change in the lining of the esophagus from normal squamous to columnar intestinal epithelium. Proper and accurate staging for esophageal cancer is essential because treatment modalities should be based not only on the staging information but also on the prognosis. Patients with metastatic disease should not undergo surgical resection. Therefore, there is a large emphasis on studying the most effective staging modalities which would allow patients to forgo expensive and invasive treatments which would offer no survival benefit in Stage IV (metastatic) disease.

PREOPERATIVE STAGING MODALITIES

The modern staging of carcinoma of the esophagus is based on the tumor/node/metastasis (TNM) classification developed by the American Joint Committee on Cancer (Table 10.1). While patient outcomes correlate with the initial clinical stage at diagnosis, survival is best correlated with the final pathologic stage. At present time in the United States nearly

half of the patients at time of diagnosis have cancer that extends beyond the locoregional confines of the primary tumor. Unfortunately, even in those patients with confined locoregional disease > 60% can undergo a curative resection. Pathologic examination reveals that the vast majority, up to 80%, of resected specimens harbor metastases in the regional lymph nodes. Thus, until a point in time where patients with earlier stage disease are found through surveillance or screening programs, clinicians currently are most often dealing with advanced-stage carcinoma in newly diagnosed patients.

An optimal staging modality would provide sensitive and specific information regarding each of the three TNM parameters, allowing individualized treatment based upon the specific cancer stage. While in the future molecular tumor information may also play a role in the initial evaluation of the patient, this is currently not available for clinical practice. Because at the present time there is no single staging modality that provides accurate information, most centers use a combination of screening tests. Currently, the most common noninvasive staging modalities include computed tomography (CT) of the chest and abdomen, for the evaluation of local tumor extent and distant metastases, and endoscopic ultrasound (EUS), for the evaluation of tumor depth and locoregional lymph node staging. Endoscopic ultrasound is an evolving technology providing high resolution images of the esophagus and surrounding tissues, but as is true of all US technologies, it is highly dependant upon the skill of the person performing the technique. With some of the limitations in CT and EUS, investigators looked to other modalities to try and increase the accuracy of the initial staging. There had been high hopes and support for the addition of positron emission tomography (PET), a physiological based imaging study, in cancer staging evaluations. 18F-fluorodeoxyglucose positron emission tomography (FDG-PET) can provide information regarding the functional activity of some malignant lesions rather than strictly anatomic information. PET scans also have limitations regarding lesions size and detectability and do not illuminate all cancers. Most recently there has been a fusion of PET with CT images which may improve each of these modalities. PET scans are also playing in increasing role not only in the staging of cancers but also to assess the response to neoadjuvant therapy. Lastly, investigators have examined the role of surgical staging with laparoscopy and thoracoscopy to try and increase detection of patients with metastatic disease. While these operative techniques are very sensitive and specific for detection of distant metastasis, they have the disadvantage of being invasive and their role in staging continues to be controversial (Buenaventura and Luketich, 2000).

An excellent online resource for up to date evidence based medicine guidelines which are frequently reviewed and updated is the National Comprehensive Cancer Network guidelines (Figure 10.1). In the 2007 guidelines the staging schema starts with a CT scan of the chest and abdomen. If there is no evidence of metastatic disease an EUS is then suggested with FNA of any suspicious regional or metastatic celiac lymph nodes. Lastly, if there is no evidence of metastatic disease with these imaging modalities a PET/CT should be performed (Ajani *et al*., 2006).

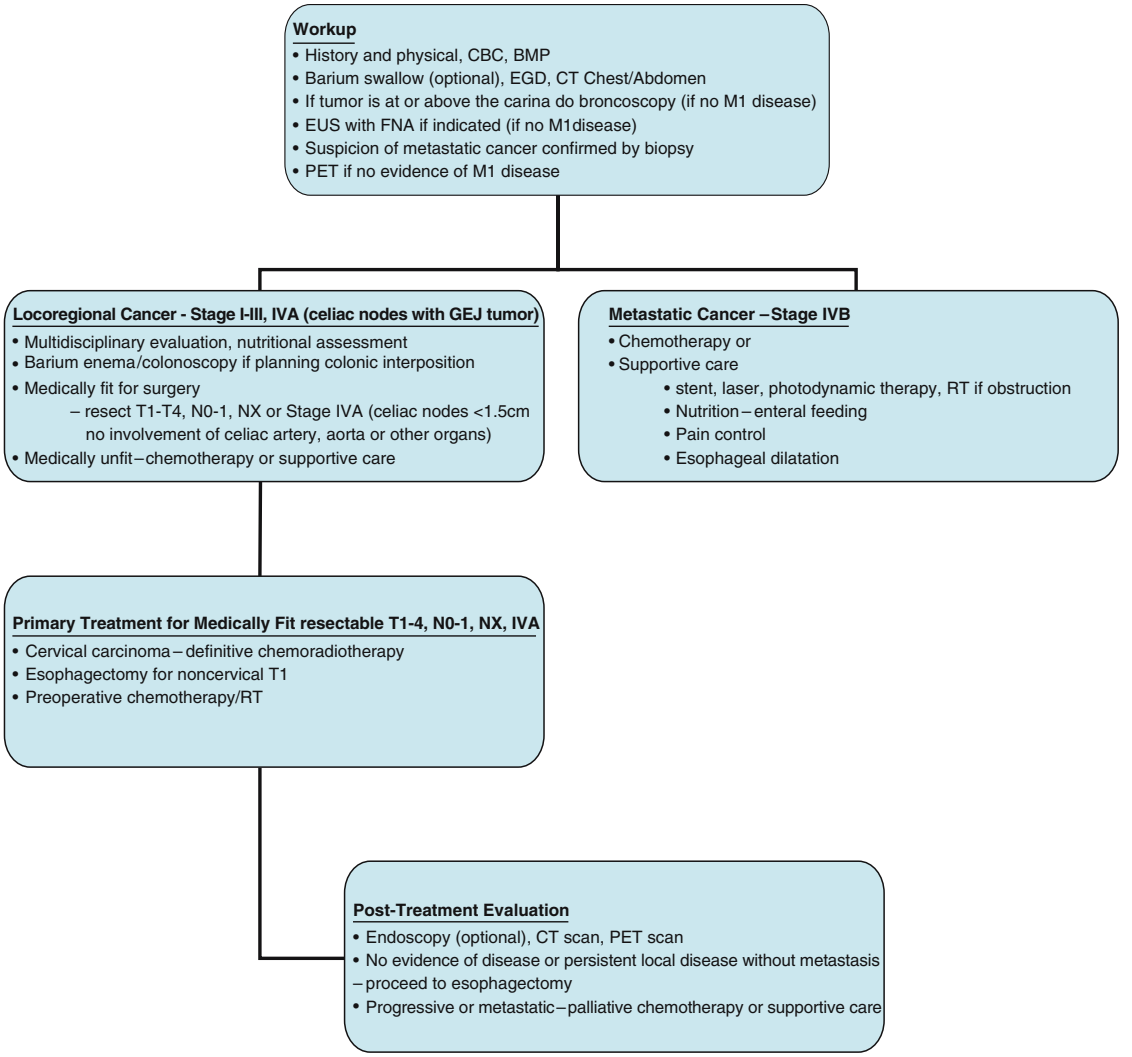

FIGURE 10.1. NCCN treatment algorithm esophageal cancer (V.1.2007)

PRIMARY TUMOR (T STAGE)

Primary tumor is evaluated by the depth of tumor invasion through the esophageal wall. At the present time endoscopic ultrasound (EUS) is the best modality for accurate T stage information. Endoscopic sonography can differentiate the individual layers of the esophageal wall and thereby visualize the depth of tumor penetration through the wall in real time. The normal esophagus has alternating five hyperechoic and hypoechoic layers as depicted by endoscopic sonography; esophageal cancers appear as hypoechoic masses that disrupt and invade through the layers. EUS has the limitation of being operator dependant and may be difficult in patients with large stenotic tumors where the endoscope cannot be passed through the tumor lumen thereby not getting the transducer into the region of interest. The overall

accuracy of endoscopic is reported to be between 85% and 90% (Kelly *et al*., 2001). The technique can suffer from both over and understaging for a variety as reasons such as peritumoral edema and if the tumor penetration is below the resolution of sonography. Even with its limitations comparative studies have consistently shown that EUS is superior to CT in assessing the depth of invasion (85% vs. 55%) (Vazquez-Sequeiros *et al*., 2003a).

As outlined in the NCCN guidelines, CT is recommended as the initial imaging study to exclude distant metastases, which is then followed by endoscopic sonography for local staging information. CT has significant limitations in its ability to accurately determine T stage because it cannot delineate the individual layers of the esophageal wall, and therefore cannot diagnose early stage lesions (Tis, T1, and T2). Unlike EUS, CT can only be used to define the primary tumor by showing the extent of esophageal wall involvement by tumor and its invasion of the peri-esophageal fat. CT can be highly suggestive of a T3 or T4 lesion if the tumor infiltrates into the peri-esophageal fat or mediastinal structures. Loss of fat planes between the tumor and the adjacent airway is not always a specific finding for tumor invasion, but can be highly suggestive of disease if it is focally associated with the tumor mass. It is vital to identify T4 disease because these patients are inoperable and may have other problems such as infiltration of the tumor into the tracheobronchial tree or aorta (Figure 10.2). Overall the reported accuracy of CT in diagnosing T3 or T4 disease ranges between 59% and 82% (Saunders *et al*., 1997).

The role of PET scan in determining T stage is more of a binary question of whether the tumor is present or not (Figure 10.3). The spatial resolution of PET is limited and therefore the sensitivity for identifying depth of invasion is also severely limited (Meltzer *et al*., 2000). PET can detect the presence of tumor with a sensitivity of 95% (Heeren *et al*., 2004). The use of PET can be difficult if the lesion is small because the scan depends on biological activity of the lesion.

FIGURE 10.2. CT scan with intravenous contrast demonstrating findings consistent with a locally advanced T4 esophageal cancer. Note loss of fat plane with the left main stem bronchus and thickened esophageal wall

REGIONAL LYMPH NODE (N STAGE)

Lymph node metastasis is one of the most important prognostic factors for esophageal cancer (Lerut *et al*., 2000). The probability of nodal spread increases with greater depths of tumor penetration (higher T stage) and is prognostic of worse outcomes. When tumors are limited to the mucosa

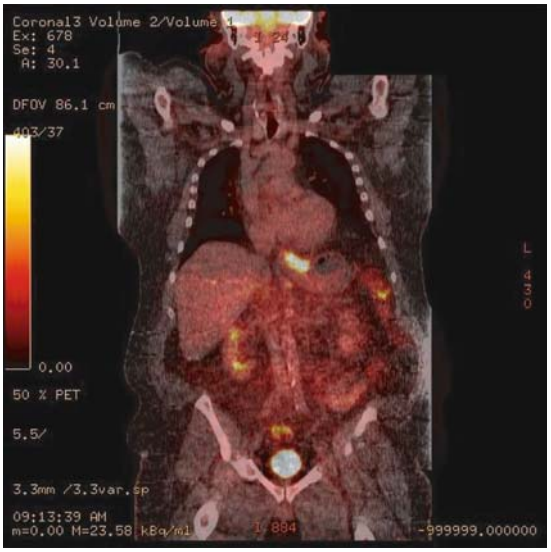

FIGURE 10.3. PET/CT coronal image demonstrates a distal esophageal cancer with no evidence of regional or metastatic spread. The image resolution does not allow for formal T staging

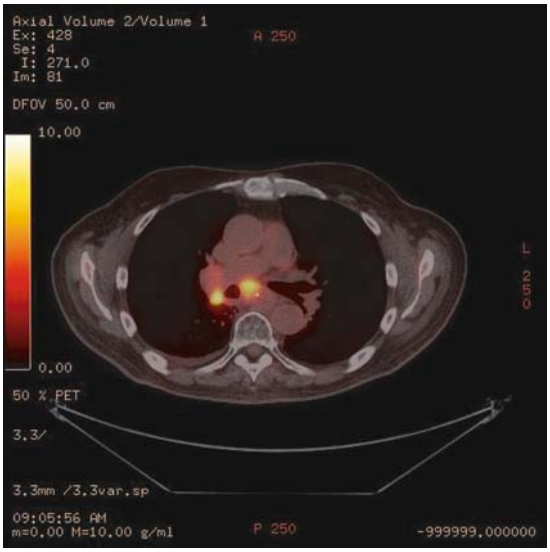

FIGURE 10.4. PET/CT demonstrating regional lymph node involvement in the right peribronchial region

(Tis), the likelihood of nodal disease is <1%, increasing to 50% when they are deeper than submucosal involvement by the primary tumor. The number and location of positive lymph nodes are also prognostic factors (Rizk *et al*., 2006). The lymphatic drainage pathway in the esophagus usually mirrors vascular inflow. In general, carcinomas of the upper esophagus drain to the cervical or upper mediastinal nodes, while those arising from the mid or lower esophagus spread to the lower mediastinal, celiac and/or perigastric nodes. Metastasis in the internal jugular, supraclavicular, paratracheal, hilar, subcarinal, paraaortic, and pericardial lymph nodes is considered to be metastatic but not regional disease. While some authors believe that celiac lymph nodes are regional lymph nodes for distal esophageal cancers and supraclavicular are regional for upper cancers, these nodal basins are generally considered metastatic disease.

Overall, CT and PET are not highly accurate for the evaluation of lymph nodes metastasis in esophageal cancer. Both CT and EUS criteria for positive lymph nodes are based on a size criterion; in general nodes that are >1 cm in short axis dimension are considered suspicious for metastatic disease. However, size is known to be an insensitive parameter for determining nodal spread because enlarged nodes can be from a benign hyperplasia, granulomatous disease, and small nodes can harbor metastatic deposits. PET scanning has no size criteria for positive nodes, for it is based on the presence of a detectable emission that can be spatially identified as a probable node (Figure 10.4).

CT has been the most widely used examination in the preoperative evaluation of patients with esophageal cancer. Most authors conclude that it is not a highly sensitive method for detection of metastasis to lymph nodes (Rankin *et al*., 1998).

Table 10.1. American Joint Committee on Cancer (AJCC) TNM Classification of carcinoma of the esophagus (6th edition)[a]

Primary tumor (T)	**Stage grouping**
TX Primary tumor cannot be assessed	Stage 0 Tis N0 M0
T0 No evidence of primary tumor	Stage I T1 N0 M0
Tis Carcinoma in situ	Stage IIA T2 N0 M0
T1 Tumor invades lamina propria or submucosa	T3 N0 M0
T2 Tumor invades muscularis propria	Stage IIB T1 N1 M0
T3 Tumor invades adventitia	T2 N1 M0
T4 Tumor invades adjacent structures	Stage III T3 N1 M0
	T4 Any N M0
	Stage IV Any T Any N M1
	Stage IVA Any T Any N M1a
	Stage IVB Any T Any N M1b
Regional lymph nodes (N)	
NX Regional lymph nodes cannot be assessed	
N0 No regional lymph node metastasis	
N1 Regional lymph node metastasis	
Distant metastasis (M)	
MX Distant metastasis cannot be assessed	
M0 No distant metastasis	
M1 Distant metastasis	
Tumors of the lower thoracic esophagus:	
M1a Metastasis in celiac lymph nodes	
M1b Other distant metastasis	
Tumors of the midthoracic esophagus:	
M1a Not applicable	
M1b Nonregional lymph nodes and/or other distant metastasis	
Tumors of the upper thoracic esophagus:	
M1a Metastasis in cervical nodes	
M1b Other distant metastasis	

[a] Used with permission of the American Joint Committee on Cancer (AJCC), Chicago, Illinois. The original and primary source for this information is the sixth edition (2002) published by Springer, New York. Any citation or quotation of this material must be credited to the AJCC as its primary source.

The inclusion of this information herein does not authorize any reuse or further distribution without the expressed written permission of Springer, New York on behalf of the AJCC.

The overall accuracy of CT for predicting regional lymphadenopathy ranges between 50% and 70%. The accuracy in predicting lymph node metastases in the abdomen is of the order of 85%. PET does not seem to perform much better with a reported overall accuracy for nodal staging between 48% and 90% (Kole *et al*., 1998; Flanagan *et al*., 1997; Yoon *et al*., 2003).

EUS appears to be more sensitive in evaluating lymph nodes and has improved the accuracy in identifying metastasis to regional lymph nodes when compared with CT scans. Overall, it has a reported sensitivity of 69%, specificity 76%, and accuracy of 72% (Heeren *et al*., 2004). In addition, EUS has the advantage of being able to confirm lymph node metastases by

FNA. The adjunct of fine needle aspiration (FNA) to EUS significantly increases the accuracy of identifying positive lymph nodes (87% compared to 74% with EUS alone), and EUS-FNA should be included as a tool in the preoperative staging algorithm (Vazquez-Sequeiros *et al*., 2003b). Combining endoscopic ultrasound and CT findings further improves accuracy for TNM staging up to 86% and therefore most recommend CT as the initial imaging study to exclude distant metastases followed by endoscopic sonography and FNA for the most accurate local staging information.

METASTATIC DISEASE (M STAGE)

Unfortunately, esophageal cancer patients commonly have distant metastasis at presentation. The most common sites of distant metastasis are to non-regional lymph nodes, liver, lung, bones, and adrenal glands. Typically, endoscopic ultrasound and CT of the chest and abdomen are performed to detect these metastases. CT is helpful in detecting metastases to the lungs, liver, adrenals, bones, and lymph nodes that EUS cannot evaluate. EUS can be useful in evaluating nodal metastasis in the celiac axis for which the sensitivity is low in CT (37–81%). The assessment of celiac axis lymph nodes is relevant especially with the rise of distal and gastroesophageal junction adenocarcinomas. Most surgeons believe that celiac lymph nodes should be classified as regional lymph nodes in distal esophageal tumors and EUS permits evaluation and biopsy of these lymph nodes. When EUS identifies celiac lymph nodes, FNA confirmed metastasis in 88% of cases (Reed *et al*. 1999). This assessment is essential for planning preoperative therapy.

The added benefit of using PET in staging for metastasis continues to be an ongoing debate. Most studies evaluating the impact of PET in the staging algorithm have been with retrospective case studies with a small number of patients. Because PET gives information of the functional activity of the tumor, it is speculated to be superior in detecting metastasis (Figure 10.5). In the results of many of these studies, PET has been reported to be more sensitive than CT in the detection of the primary tumor and distant metastatic disease. Furthermore, it has been consistently observed that PET appears to be more specific than CT in identifying distant metastatic disease. Many studies suggest that the addition of PET imaging to the staging algorithm improves the accuracy of preoperative staging and thus prevents inappropriate esophageal resection of up to 20% of patients who were initially deemed to be resectable (Flamen *et al*., 2000; Luketich *et al*., 1999; van Westreenen *et al*. 2005). Obtaining this accuracy is essential because the mortality and morbidity of an esophageal resection is high and it is important to minimize unnecessary operations. In order to help address this issue, a recent prospective multi-center trial Z0060 (ACOSOG) evaluated whether PET could detect metastatic disease that would preclude esophageal resection in patients initially believed to be surgical candidates after standard imaging using chest and abdominal CT and bone scinitgraphy. FDG-PET identified an additional 4.8% of patients with M1b disease after

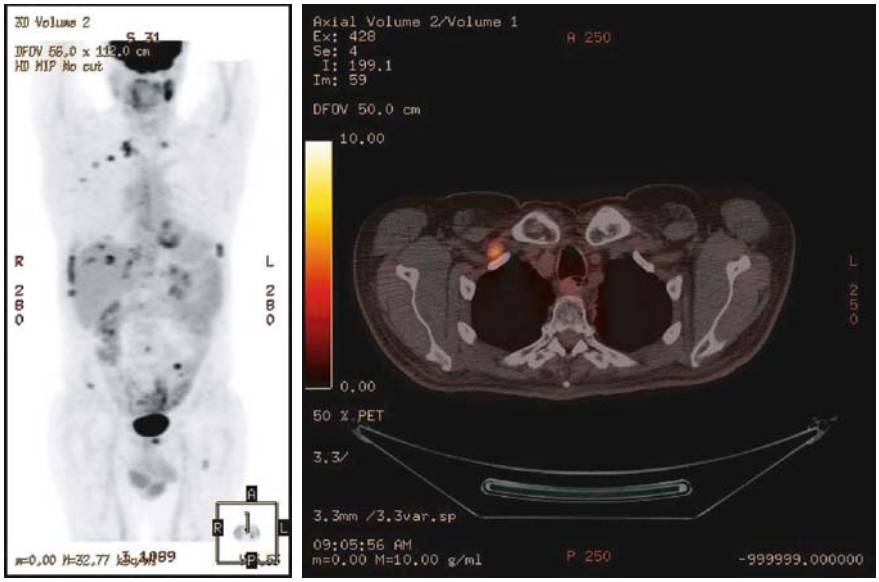

FIGURE 10.5 a. PET image of widely metastatic disease to multiple sites above and below the diaphragm. b. PET/CT image of metastatic disease to a left supraclavicular lymph node

standard clinical staging, as well as an extra 9.5% of patients with PET-detected metastasis without confirmatory biopsy, for an overall rate of 14.3%. This study was limited by not including EUS which has now become a standard modality in staging esophageal cancer. In addition, there was a delayed crossover of patients who were initially excluded due to receiving neoadjuvant treatment and later added to the cohort (Meyers *et al*., 2007).

PET scans seem to address bone metastasis better than other modalities. This is of significance because the incidence of bone metastasis in esophageal cancer is ~ 15% and again detecting this is crucial to preclude superfluous resection. When compared to CT, PET was clearly superior in the detection of boney metastasis (Wren *et al*., 2002). Studies comparing the use of PET to bone scintigraphy in evaluating the detection of bony metastasis demonstrated that PET was very accurate and PET also detected osteolytic metastases when bone scans had not. It is therefore recommended that when the findings for bone scintigraphy are negative, PET should be utilized for further evaluation (Kato *et al*., 2005).

Overall, PET scanning is accurate in the detection of metastasis and may help avoid unnecessary surgery in some patients. Moreover, PET scanning can also be implemented in the preoperative, post-treatment evaluation of patients undergoing neoadjuvant chemoradiation (this is discussed later in the chapter). The onus of using routine PET for staging for esophageal cancer however is confirming the positive findings. Without understanding the true rates of false-positivity in PET, more invasive procedures (such as thoracoscopic and laparoscopic evaluation) may need to be performed, thus resulting in more cost and morbidity.

THORACOSCOPIC AND LAPAROSCOPIC STAGING

The use of thoracoscopy and laparoscopy (TL and LS) as a staging modality for esophageal cancer has been added by some centers to improve the detection of lymph node positive disease and metastasis. These modalities have been shown to be safe with minimal morbidity and mortality. TL/LS staging identified patients who had positive lymph nodes which were occult on noninvasive tests as well as T4 lesions and pulmonary metastases. A multiinstitutional intergroup trial confirmed that TS/LS doubled the number of positive lymph nodes identified by conventional noninvasive staging (CT, EUS, and MRI). Furthermore, obtaining tissue samples has the added benefit of evaluating genetic markers for better prognostication of patients with esophageal cancer as well as potential treatment guided gene analysis (Krasna and Jiao 2000). Few centers currently use thoracoscopy/laparoscopy in the staging algorithm and the utility of these modalities is still being debated. With the advancements of EUS-FNA and PET, many feel that these surgical staging modalities add very little to the work-up, have added cost, and the risk of mortality and morbidity of general anesthesia and surgery (Wallace *et al*., 2002). Some have recommended using TS/LS if EUS-FNA is negative and if EUS-FNA is positive than no further work-up with TS/LS is needed; however, the ultimate role is yet to be determined.

RESTAGING AFTER NEOADJUVANT THERAPY

Concomitant chemoradiation therapy (CRT) followed by esophagectomy has been widely accepted for the treatment of locally advanced esophageal cancer despite conflicting results from randomized trials (Walsh *et al*., 1996). Approximately, 25% of esophageal cancer patients experience a pathologic complete response (pCR) to neoadjuvant chemoradiation therapy and about another 20% have a partial pathologic response. Because of the extensive use of preoperative CRT, there has been an emphasis to restage patients post treatment. EUS, CT, and FDG-PET imaging have all been used to try to predict pathologic responses, determine prognosis and help direct subsequent treatment decisions after neoadjuvant therapy. Of these modalities, PET appears to be the most accurate in determining pathologic response and prognosis after CRT. PET images can be analyzed both visually and quantitatively to determine the standardized uptake value (SUV). Many studies have been able to monitor a patient's metabolic response to therapy with SUVs. The decrease in SUV is a more accurate objective measurement than the change in tumor size measured by CT and EUS and better correlates to a complete response (Erasmus and Munden, 2007; Downey *et al*., 2003; Levine *et al*., 2006). Furthermore, pretreatment SUV values can help predict whether a patient will have a pathologic response. The accuracy of PET at determining non-responders was 75–76%. Moreover, survival can be predicted with the use of post-treatment PET SUV (Swisher *et al*., 2004).

CT and EUS have also been used to determine post-CRT responses and certain wall thickness and mass size respectively, have correlated with pathologic responses (CT wall thickness 13.3 vs. 15.3 mm $p = 0.04$, EUS mass size 0.7 vs. 1.7 cm $p = 0.01$).

The accuracy rates of CT and EUS were much lower, 62% and 68% vs. 75%, in comparison to PET (Swisher *et al*., 2004). Both EUS and CT have limitations for their use in restaging patients after therapy due to their inability to distinguish between inflammatory reaction and tumor necrosis and may actually overstage patients. EUS however, does have an added benefit of being able to repeat FNAs post therapy. Alternatively, the utilization of PET for downstaging has an advantage because it evaluates the metabolic activity of the tumor cells and thus can differentiate between cell necrosis and viability.

If PET can reliably identify CRT response then multimodality therapy could be tailored to individual patients to minimize treatment-related morbidity while maximizing therapeutic benefit. Based on post treatment SUVs, PET may also be helpful in predicting survival; however, more studies are need for validation. The difficulty still remains with the inability of any of these noninvasive modalities to confirm the absence of residual viable disease in the primary tumor, and esophagectomy should still remain as the main therapeutic option even when post-CRT imaging modalities are normal.

TREATMENT OVERVIEW

Treatment modalities for esophageal cancer include surgery, neoadjunvant chemotherapy and radiation therapy, photodynamic therapy, and palliative stenting/surgery (the details of which are beyond the scope of this chapter). Surgical management may include staging, resection with curative intent, and palliative techniques. Patients with limited disease progression and early stage tumors benefit from complete surgical resection. The intent of surgery should be to achieve an R0 resection, and palliative resections should be avoided in patients with clearly unresectable or advanced cancer who can be effectively palliated using nonsurgical modalities. Those with locally advanced disease have a poor prognosis in spite of aggressive attempts at resection. The 5-year survival after an R0 resection for locally advanced esophageal cancer is 15–20%, and the median survival after R0 resection is ~ 18 months with neoadjuvant therapy (Graham *et. al*., 2007; Urschel *et al*., 2002). Data from the National Cancer Data Base, describes the outcomes in 11,154 patients diagnosed in 1998 (Table 10.2) (http://www.cancer.org/). The data clearly show that for patients with carcinoma in situ and T1 lesions (those invading the lamina propria or submucosa) a significant proportion of these patients can be cured. Unfortunately, as the cancer stage progresses the survival rate drops substantially and at the present time the majority of patients are diagnosed at later stage diagnosis.

In conclusion, with the increasing incidence of esophageal cancer it is important that a complete preoperative staging workup is performed on each patient to avoid unnecessary procedures and morbidity. Non-invasive staging modalities continue

TABLE 10.2. National cancer data base: esophageal cancer.

Stage	Percent of patients (%)	5-year relative survival rate (%)
0	1	52
I	10	41
II	21	26
III	18	13
IV	26	3

to improve with advancements in technology. It is clear that a multi-modality evaluation is beneficial to guide patients to proper treatment and to determine prognosis. EUS has proven to be very sensitive and accurate for T and N stage evaluation and the adjunct of EUS-FNA notably increases its accuracy for staging. While costly and not always accessible to all centers, PET appears to be the most sensitive for diagnosing metastatic disease. PET also seems to be an applicable tool to reevaluate patients after neoadjuvant therapy and may be useful to determine those patients that are responding to their CRT. In the future, PET may be used to assess patients' overall survival based on their post-CRT SUVs. CT can also be utilized in evaluation for T, N, and M staging but should not be used as a single tool. If discrepancy exists between some of these studies, thoracoscopic and laparoscopic exploration is a worthwhile option for further staging work-up. Overall, many studies have validated the importance of accurate complete staging for esophageal cancer patients, and all three non-invasive staging modalities have proven benefit to this process. Accuracy rates will continue to increase as the expertise in technology evolves.

REFERENCES

Ajani, J., Bekaii-Saab, T., D'Amico, T.A., Fuchs, C., Gibson, M.K., Goldberg, M., Hayman, J.A., Ilson, D.H., Javle, M., Kelley, S., Kurtz, R.C., Locker, G.Y., Meropol, N.J., Minsky, B.D., Orringer, M.B., Osarogiagbon, R.U., Posey, J.A., Roth, J., Sasson, A.R., Swisher, S.G., Wood, D.E., and Yen, Y. 2006. Esophageal cancer clinical practice guidelines. *J. Natl. Compr. Canc. Netw. 4*: 328–347.

Buenaventura, P., and Luketich, J.D. 2000. Surgical staging of esophageal cancer. *Chest Surg. Clin. N. Am. 10*: 487–497.

Downey R.J., Akhurst, T., Ilson, D., Ginsberg, R., Bains, M.S., Gonen, M., Koong, H., Gollub, M., Minsky, B.D., Zakowski, M., Turnbull, A., Larson, S.M., and Rusch, V. 2003. Whole body 18FDG-PET and the response of esophageal cancer to induction therapy: results of a prospective trial. *J. Clin. Oncol. 21(3)*: 428–432.

Erasmus, J.J., and Munden, R.F. 2007. The role of integrated computed tomography positron-emission tomography in esophageal cancer: staging and assessment of therapeutic response. *Semin. Radiat. Oncol. 17*: 29–37.

Flamen, P., Lerut, A., Van Cutsem, E., De Wever, W., Peeters, M., Stroobants, S., Dupont, P., Bormans, G., Hiele, M., De Leyn, P., Van Raemdonck, D., Coosemans, W., Ectors, N., Haustermans, K., and Mortelmans, L. 2000.Utility of positron emission tomography for the staging of patients with potentially operable esophageal carcinoma. *J. Clin. Oncol. 18*: 3202–3210.

Flanagan, F.L., Dehdashti, F., Siegel, B.A., Trask, D.D., Sundaresan, S.R., Patterson, G.A., and Cooper, J.D. 1997. Staging of esophageal cancer with 18F-fluorodeoxyglucose positron emission tomography. *A.J.R. Am. J. Roentgenol. 168*: 417–424.

Graham, A.J., Shrive, F.M., Ghali, W.A., Manns, B.J., Grondin, S.C., Finley, R.J., and Clifton, J. 2007. Defining the optimal treatment of locally advanced esophageal cancer: a systematic review and decision analysis. *Ann. Thorac. Surg. 83*: 1257–1264.

Heeren, P.A., Jager, P.L., Bongaerts, F., van Dullemen, H., Sluiter, W., and Plukker, J.T. 2004. Detection of distant metastases in esophageal cancer with (18)F-FDG PET. *J. Nucl. Med. 45*: 980–987.

Kato, H., Miyazaki, T., Nakajima, M., Takita, J., Kimura, H., Faried, A., Sohda, M., Fukai, Y., Masuda, N., Fukuchi, M., Manda, R., Ojima, H., Tsukada, K., Kuwano, H., Oriuchi, N., and Endo, K. 2005. Comparison between whole-body positron emission tomography and bone scintigraphy in evaluating bony metastases of esophageal carcinomas. *Anticancer. Res. 25*: 4439–4444.

Kelly, S., Harris, K.M., Berry, E., Hutton, J., Roderick, P., Cullingworth, J., Gathercole, L., and Smith, M.A. 2001. A systematic review of the staging performance of endoscopic ultrasound in gastro-oesophageal carcinoma. *Gut. 49*: 534–539.

Kole, A.C., Plukker, J.T., Nieweg, O.E., and Vaalburg, W. 1998. Positron emission tomography for staging of oesophageal and gastroesophageal malignancy. *Br. J. Cancer 78*: 521–527.

Krasna, M.J., and Jiao, X. 2000. Thoracoscopic and laparoscopic staging for esophageal cancer. *Semin. Thorac. Cardiovasc. Surg. 12*: 186–194.

Lerut, T., Flamen, P., Ectors, N., Van Cutsem, E., Peeters, M., Hiele, M., De Wever, W., Coosemans, W., Decker, G., De Leyn, P., Deneffe, G., Van Raemdonck, D., and Mortelmans, L. 2000. Histopathologic validation of lymph node staging with FDG-PET scan in cancer of the esophagus and gastroesophageal junction: a prospective study based on primary surgery with extensive lymphadenectomy. *Ann. Surg. 232*: 743–752.

Levine, E.A., Farmer, M.R., Clark, P., Mishra, G., Ho, C., Geisinger, K.R., Melin, S.A., Lovato, J., Oaks, T., and Blackstock, A.W. 2006. Predictive value of 18-fluoro-deoxy-glucose-positron emission tomography (18F-FDG-PET) in the identification of responders to chemoradiation therapy for the treatment of locally advanced esophageal cancer. *Ann. Surg. 243*: 472–478.

Luketich, J.D., Friedman, D.M., Weigel, T.L., Meehan, M.A, Keenan, R.J., Townsend, D.W., and Meltzer, C.C. 1999. Evaluation of distant metastases in esophageal cancer: 100 consecutive positron emission tomography scans. *Ann. Thorac. Surg. 68*: 1133–1136.

Meltzer, C.C., Luketich, J.D., Friedman, D., Charron, M., Strollo, D., Meehan, M., Urso, G.K., Dachille, M.A., and Townsend, D.W. 2000. Whole-body FDG positron emission tomographic imaging for staging esophageal cancer comparison with computed tomography. *Clin. Nucl. Med. 25*: 882–887.

Meyers, B.F., Downey, R.J., Decker, P.A., Keenan, R.J., Siegel, B.A., Cerfolio, R.J., Landreneau, R.J., Reed, C.E., Balfe, D.M., Dehdashti, F., Ballman, K.V., Rusch, V.W., and Putnam, J.B., Jr. 2007. American College of Surgeons Oncology Group Z0060. The utility of positron emission tomography in staging of potentially operable carcinoma of the thoracic esophagus: results of the American College of Surgeons Oncology Group Z0060 trial. *J. Thorac. Cardiovasc. Surg. 133*: 738–745.

Rankin, S.C., Taylor, H., Cook, G.J., and Mason, R. 1998. Computed tomography and positron emission tomography in the pre-operative staging of esophageal carcinoma. *Clin. Radiol. 53*: 659–665.

Reed, C.E., Mishra, G., Sahai, A.V., Hoffman, B.J., and Hawes, R.H. 1999. Esophageal cancer staging: improved accuracy by endoscopic ultrasound of celiac lymph nodes. *Ann. Thorac. Surg. 67*: 319–321.

Rizk, N., Venkatraman, E., Park, B., Flores, R., Bains, M.S., and Rusch, V. 2006. American Joint Committee on Cancer staging system. The prognostic importance of the number of involved lymph nodes in esophageal cancer: implications for revisions of the American Joint Committee on Cancer staging system. *J. Thorac. Cardiovasc. Surg. 132*: 1374–1381.

Saunders, H.S., Wolfman, N.T., and Ott, D.J. 1997. Esophageal cancer. Radiologic staging. *Radiol. Clin. North. Am. 35*: 281–294.

Swisher, S.G., Maish, M., Erasmus, J.J., Correa, A.M., Ajani, J.A., Bresalier, R., Komaki, R., Macapinlac, H., Munden, R.F., Putnam, J.B., Rice, D., Smythe, W.R., Vaporciyan, A.A., Walsh. G.L., Wu, T.T., and Roth, J.A. 2004. Utility of PET, CT, and EUS to identify pathologic responders in esophageal cancer. *Ann. Thorac. Surg. 78*: 1152–1160.

Urschel, J.D., Vasan, H., and Blewett, C.J. 2002. A meta-analysis of randomized controlled trials that compared neoadjuvant chemotherapy and surgery to surgery alone for resectable esophageal cancer. *Am. J. Surg. 183*: 274–279.

Van Westreenen, H.L., Heeren, P.A., van Dullemen, H.M., van der Jagt, E.J., Jager, P.L., Groen, H., and Plukker, J.T. 2005. Positron emission tomography with F-18-fluorodeoxyglucose in a combined staging strategy of esophageal cancer prevents unnecessary surgical explorations. *J. Gastrointest. Surg. 9*: 54–61.

Vazquez-Sequeiros, E., Gines, A., and Wiersema, M.J. 2003a. Role of ultrasound-guided endoscopy in the evaluation of mediastinal lesions. *Med. Clin. Barc. 121*: 231–237.

Vazquez-Sequeiros, E., Wiersema, M.J., Clain, J.E., Norton, I.D., Levy, M.J., Romero, Y., Salomao, D., Dierkhising, R., and Zinsmeister, A.R. 2003b. Impact of lymph node staging on therapy of esophageal carcinoma. *Gastroenterology 125*: 1626–1635.

Walsh, T.N., Noonan, N., Hollywood, D., Kelly, A., Keeling, N., and Hennessy, T.P. 1996. A comparison

of multimodal therapy and surgery for esophageal adenocarcinoma. *N. Engl. J. Med. 335*: 462–467.

Wallace, M.B., Nietert, P.J., Earle, C., Krasna, M.J., Hawes, R.H., Hoffman, B.J, and Reed, C.E. 2002. An analysis of multiple staging management strategies for carcinoma of the esophagus: computed tomography, endoscopic ultrasound, positron emission tomography, and thoracoscopy/laparoscopy. *Ann. Thorac. Surg. 74*: 1026–1032.

Wren, S.M., Stijns, P., and Srinivas, S. 2002. Positron emission tomography in the initial staging of esophageal cancer. *Arch. Surg. 137*: 1001–1006.

Yoon, Y.C., Lee, K.S., Shim, Y.M., Kim, B.T., Kim, K., and Kim, T.S. 2003. Metastasis to regional lymph nodes in patients with esophageal squamous cell carcinoma: CT versus FDG PET for presurgical detection prospective study. *Radiology 227*: 764–770.

11
Automated Disease Classification of Colon and Gastric Histological Samples Based on Digital Microscopy and Advanced Image Analysis

Levente Ficsor and Bela Molnar

INTRODUCTION

The urgent need for the increase of histological diagnostic efficiency requires the support of automated, computerized prescreening systems. The ability of computers to render accurate diagnoses on cytopathologic specimens such as cervical Papanicolaou smears is well established and well documented since the early 1980s by Wittekind *et al*. (1983) and Stenkvist *et al*. (1987). For many reasons, automated analysis of histologic sections is profoundly more difficult than the automated analysis of cytopathologic preparations. Histologic sections may have complex architecture or high cellularity, whereas cytologic preparations have relatively simple architecture and relatively low cellularity. Furthermore, histologic sections are prone to artifacts such as chatter, folding, contamination, fragmentation, thermal injury, and crush-related injury. These artifacts represent noise that automated analysis must ignore during the final interpretation. Despite these obstacles, recent studies demonstrate highly effective automated analysis of histological sections, including the detection of cancer cells (Loukas *et al*., 2003). Most studies have focused on routinely-processed hematoxylin-and-eosin-stained sections. Usage of automated analysis has been successfully extrapolated to quantitative morphometry of immunostained sections in the setting of mammary carcinoma. Francis *et al*. (2000) introduced an analysis method for estimation of proliferating cell nuclear antigen (PCNA) in breast carcinoma that worked on single field of views with high accuracy. There are many frontiers regarding automated analysis that have yet to be explored. Many studies have concentrated on simple variables, such as the mere presence or absence of epithelium. In order for automated analysis to have maximal clinical utility, higher order functions such as precise architectural classification of glands and other epithelial structures, classification of cells into the proper type, fine nuclear and cytoplasmic detail, and even different types of stroma must be performed. This is because each pathologic diagnosis is rendered in part by assessing the architecture and cytology of epithelium, hematopoietic cells, stroma, and the presence or absence of infectious agents.

There is also a growing trend toward computerized automated analysis of histologic sections which is based on higher order functions as described above. Thompson *et al*. (1993) presented the knowledge-guided segmentation method that partitioned colorectal images to different histologic components where glands were recognized with 85% accuracy. The knowledge-guided method was adopted for prostate samples by Bartels *et al*. (1996) and was shown that measurement of progression or regression is possible by detecting and analyzing prostatic lesions. Hamilton *et al*. (1997) introduced an image texture analysis method to locate dysplastic fields in colorectal samples. The automatic identification of focal areas of colorectal dysplasia was based on co-occurrence matrix and optical density at low power microscopic images. The study also showed that the combination of automated localization at low magnification and knowledge-based image segmentation at high magnification creates an automated tool for supporting diagnostic decision making. Esgiar *et al*. (1998) presented a new solution for colon carcinoma identification based on geometric and texture analysis and achieved 90% accuracy in the classification. Four years later Esgiar *et al*. (2002) extended their measurements with fractal analysis which increased the accuracy to 95%.

All of the above mentioned studies showed good results but they have the same limitation in that these methods use single images and in this way they lack the knowledge of the whole slide. For this reason recent studies present automated histological analysis based on whole slide imaging. Petushi *et al*. (2006) introduced new grade-differentiating parameters for breast cancer by examining the whole digital slide, providing opportunity to pathologists to support their diagnosis by objective quantitative measurements.

Clearly, more sophisticated algorithms are required for automated analysis to address the issue of automated disease classification. Furthermore, these algorithms must incorporate large structures on large fields of view on an entire slide. For example, quantitative analysis of cells throughout an entire slide or for a specific region on a slide that harbors glands might help characterize different diseases. The recent advances in whole slide imaging and visualization support the development of dedicated organ specific algorithms that can be selectively applied on the entire specimen in low or high resolution depending on the analysis request. Whole slide imaging technology digitizes entire slides with high magnification and enables the selection and view of all available magnifications and even the complete slide in one view. Therefore, our aim was to develop efficient algorithms to detect and measure higher order architecture and nuclear and cellular alterations in parallel and determine whether these algorithms could be used by automated analysis to reliably diagnose gastric or colon mucosa as normal or diseased on digital slides in the environment of virtual microscopy.

MATERIALS AND METHODS

Samples

We retrospectively reviewed 5-micron-thick, hematoxylin-and-eosin-stained sections from 79 formalin-fixed, paraffin-embedded specimens from gastric biopsies

and 69 from colon biopsies. The 79 gastric specimens showed normal mucosa (14 specimens), gastritis (25 specimens, including 6 nonatrophic, 17 atrophic, 12 with intestinal metaplasia) and adenocarcinoma, all of the intestinal type (30 specimens). The initial review was made with conventional optical microscopy. Normal mucosa, gastritis, and adenocarcinoma were diagnosed according to standard morphologic criteria and Lauren's classification (1965) of adenocarcinoma. The 69 colon specimens included normal mucosa (24 specimens), aspecific colitis (11 specimens), colitis ulcerosa (25 specimens), and Crohn's disease (9 specimens).

Digitizing of Glass Slides

Automated analysis of histologic sections involves the detection of cells on the entire glass slide. Currently, only a few products are commercially available, which can digitize entire slides. We used the MIRAX Scan equipped with a 20X objective and a Sony DFW-X700 camera having 1024 × 768 resolution, sufficient for very sensitive algorithms used for cellular detection (the influence of resolution was studied by Belien *et al.* (1997)). The MIRAX Scan produces digital slides which can be examined in the MIRAX Viewer. This software is not only a simple viewer application but it is very powerful tool for research as well because its slide file format offers plug-in feasibility to store mask images and measured data. In this way our detection algorithms creates masks to cover the different structural shape. After the segmentation process finishes, the detection algorithms measure some parameters of the recognized objects. This flexibility provides more control than a simple screening machine, which examines only one field and discards the digital information. The MIRAX Viewer can also visualize results of detection algorithms as the masked and measured parameters. The MIRAX equipment is also capable of scanning fluorescent microscopy developed by Varga *et al.* (2004), which involves scanning fluorescent slides.

All specimens were scanned. The usual area of tissue from one section of each specimen was 5–6 mm^2, and the usual total number of cells was 30,000–40,000. Each specimen was reexamined using virtual microscopy, and these results were compared with the results obtained from optical microscopy as was done in a previous study.

Developer Tools

The algorithms for detection were written by the author in Microsoft Visual C++ 6.0, and they were run on a personal computer with an Intel Pentium 4, 3 GHz microprocessor with 512 MB of memory, operating under the environment of Microsoft Windows XP SP2.

Detection of Cells, Tissue Components, and Structures

Three algorithms were developed in our laboratory for the purpose of recognizing a given structure as either an individual epithelial or an interstitial cell (such as a fibroblast or inflammatory cell), a gland, or a component of superficial epithelium. The algorithms for the recognition of glands and of superficial epithelium are based on the results of cellular coordinates.

Cell Detection of Tissue Components and Measuring of Tissue Specific Parameters

The algorithm to detect an isolated cell works on single fields of view, converts the stored RGB images to HSV format, and applies a color-threshold on them (Laak *et al*., 2000). After these procedures, minor contaminants are eliminated by the morphological open operator. For the conversion to HSV format, the following formulas were used:

$$H = \arccos\left(\frac{(1.5R-0.5G-B)}{((R-G)^2+(R-B)(G-B))^{0.5}}\right),$$
$$S = 1-\frac{3a}{(R+G+B)}, \text{ and}$$
$$V = \frac{(R+G+B)}{3},$$

where R, G, B are one pixel's red, green, and blue components, and 'a' represents the lowest value from R, G, B (a = min (R, G, B)).

As a result of the previous steps we obtain a so-called mask image that contains the objects of the nucleus sized. The measured parameters are shown in Table 11.1. After the measurements, all the data (mask image and measured numerical parameters) are stored within the digital slide, and can be presented in the MIRAX Viewer.

Gland Detection

As we discussed previously, automated detection of architectural structures, such as glands, in histological sections is an underdeveloped area of digital image analysis. This is because traditional scanners and digitizers only analyze small fields rather than entire slides or entire specimens. Furthermore, architectural structures such as glands have attributes that are profoundly more complicated than those of individual cells. It is clear that detecting glands requires the entire slide to be analyzed, but analysis at high resolution is impractical because a virtual slide is built up from thousands of fields of view. One image from one field has 1,024 × 768 pixels, and one small biopsy slide has an average of 1,200 fields. This would require at least 2.6 GB of memory per slide. To facilitate the analysis, automated detection must predict the position of the glands prior to detection. This is done by creating a smaller (eightfold reduction in size, 64-fold reduction in memory) so-called preview image for the whole section which can show relevant areas of the slide for the gland recognition algorithm. The present concept in creating the preview image is based on cellular coordinates that help guide detection of cells. This image is created in three steps. In the first step two images are constructed. These images are known as cell-map and cell-web. Cell-map is a decimated schematic image of the sample where cells are represented by single spots. Cell-web is also created by using the position of the cell. It shows a very interesting sight of the sample indicating relationships of cells by drawing lines between them. The cell-web constructor (webbing) algorithm plays a critical role in the detection of glands. In the second step, the cell-map and cell-web are combined together and the open morphological operation is done on the resultant image. There are several spots on the final preview image, some of them represent glands, some of them are sample split, but most of them are only small cell-free areas. Determining which spots are really glands is done in two steps. In the first step, rough filtering is used. Rough filtering eliminates areas which are too small or too large. In the second phase further examination is

TABLE 11.1. Measured cellular and tissue related morphological parameters.

Measured parameters	Cell	Gland	Epith.	Tissue
Position (x,y)	+	+	−	−
Surface	+	+	−	+
Longest diameter	+	+	−	−
Shortest diameter	+	+	−	−
Perimeter	+	+	−	−
Shape factor	+	+	−	−
Elliptical shape factor	−	+	−	−
Surface and cell number (SpCN) ratio	−	+	−	−
Perimeter and cell number (PpCN) ratio	−	+	−	−
Length	−	−	+	−
Cell number within the object	−	+	+	+
Cells' average surface inside of the structure	−	+	+	−
SD of cells' surface inside of the structure	−	+	+	−
Cells' average perimeter	−	+	+	−
SD of cells' perimeter inside of the structure	−	+	+	−
Cells' average short-diameter	−	+	+	−
SD of cells' short-diameter inside of the structure	−	+	+	−
Cells' average long-diameter	−	+	+	−
SD of cells' long-diameter inside of the structure	−	+	+	−
Cells' average shape-factor	−	+	+	−
SD of cells' shape-factor inside of the structure	−	+	+	−
$\text{Bio/Gland Surf} = \frac{\text{Surface of the biopsy}}{\text{Total surface of the glands}}$	−	−	−	+
$\text{Bio/Gland CC} = \frac{\text{Total cell number of the biopsy}}{\text{Total cell number in the glands}}$	−	−	−	+
$\text{Bio/Epith Surf} = \frac{\text{Surface of the biopsy}}{\text{Total surface of the epithelia}}$	−	−	−	+
$\text{Bio/Epith CC} = \frac{\text{Total cell number of the biopsy}}{\text{Total cell number in the epithelia}}$	−	−	−	+
$\text{Bio/Int Surf} = \frac{\text{Surface of the biopsy}}{\text{Total surface of the interstital area}}$	−	−	−	+
$\text{Bio/Int Surf} = \frac{\text{Surface of the biopsy}}{\text{Total surface of the interstitial area}}$	−	−	−	+
$\text{Bio/Int CC} = \frac{\text{Total cell number of the biospy}}{\text{Total cell number of interstitial area}}$	−	−	−	+
$\text{Int Surf/CC} = \frac{\text{Surface of interstitial area}}{\text{Total cell number of interstitial area}}$	−	−	−	+
$\text{Bio Surf/CC} = \frac{\text{Surface of the biopsy}}{\text{Total cell number of the biopsy}}$	−	−	−	+
$\text{I/B} = \frac{\text{“Int Surf/CC”}}{\text{“Bio Surf/CC”}}$	−	−	−	+
I-B = “Int Surf/CC” − “Bio Surf/CC”	−	−	−	+

done on remaining areas by shape and cell number at the original resolution. After the recognition process measurements are done to get morphological data regarding glands. Figure 11.1 summarizes the second phase of gland detection.

Epithelium Detection

Epithelium detection has similar methodology as gland detection. It also needs a cell-web from the biopsy, but now we are interested in the contour of this web and not the texture. Therefore, the algo-

rithm first calculates the coordinates of the web's contour pixels which are examined as follows. Along this contour, cell-density is determined and all contour-pixels are signed as 'part of epithelial string' where the density is high. The result is several estimated epithelial strings. Only those strings are part of the real epithelial surface, which have a certain distance from the contour of the biopsy, which is equal to the cytoplasm thickness of the cell.

Feature Determination and Measurement

When one object (cell, gland, epithelial surface) is detected by one of the above algorithms it is measured for several morphometric parameters (Table 11.1). The parameters include: Shape factor = $4\pi S/P^2$, where S = the surface of the object; P = the perimeter of the object; and Elliptical shape factor = (perimeter of ideal ellipse)/(measured perimeter) = $2(\pi^2 ab+4(a–b)^2)^{0.5}$/(measured perimeter), where 'a' = long diameter and 'b' = short diameter. For the epithelial surface its length and cell number was determined. In addition, for the glands and the epithelial surface the average and the SD of the single cellular morphometric parameters were defined.

Determination of Tissue Cytometric Parameters

We find that the cellular, glandular, or epithelial surface morphometrical parameters themselves do not show significant information for the disease of a certain sample. For that reason we have developed tissue cytometric parameters (Table 11.1). For the tissue level characterization of the morphological alterations a dedicated parameter set was developed which describes the area ratio of the single tissue compartments to the entire biopsy. Furthermore, cell densities in the different tissue compartments were determined and compared.

Statistical Analysis

The 79 gastric and 69 colon independent samples were statistically analyzed by their measured morphometrical and tissue cytometric parameters. The examined parameters have skew distribution; therefore,

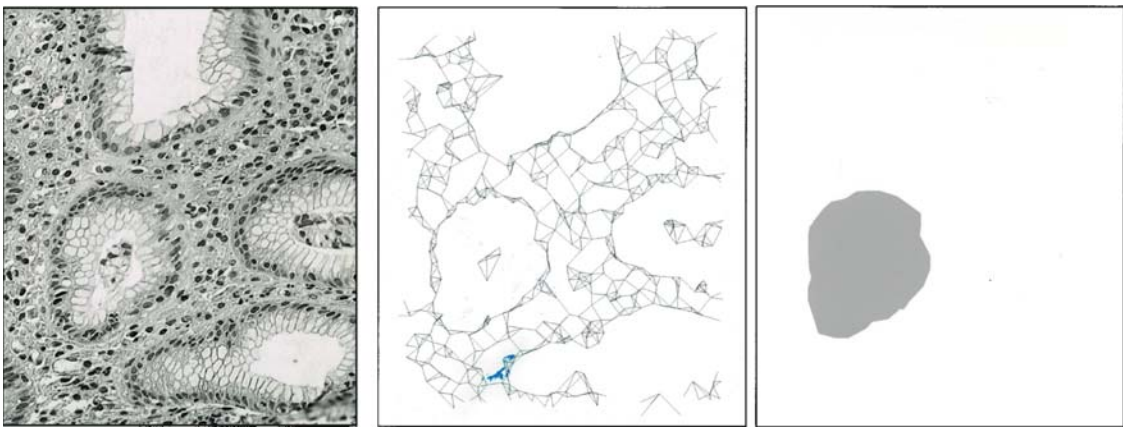

FIGURE 11.1. Process of gland detection: original image (left); cell-web (middle); detected shape of gland (right)

it is not allowed to analyze them by t-probe or ANOVA. We used Kruskall-Wallis nonparametric method to resolve which cytometric parameters show differences between the three major diagnostic groups, and Mann Whitney U test to examine parameters in pairs. Finally, linear discriminant analysis was applied to set up equations for classification The Statistica program package was used for the statistical analysis (Statsoft Inc., Tulsa, OK, USA, Statistica 7.1).

RESULTS

Gastric Samples

All 50 features were statistically analyzed by the methods described earlier. We found that measured morphometrical parameters on cells and epithelial surface do not show significant differences. But measured features of the gland are adequate for classifying disease groups. Two parameters have to be highlighted. Elliptical shape factor (normal 0.843 ± 0.066; gastritis 0.823 ± 0.072; carcinoma 0.808 ± 0.072) shows that glands in gastritis and carcinoma samples have less and less regular shape. Ratio of surface and cell number (SpCN) also shows significant differences between groups which can be easily confirmed by the human pathological observations that cell concentration is much higher in carcinoma glands than in the others (normal 114.9 ± 32.5; gastritis 112.1 ± 32.8; carcinoma 147.2 ± 45.2). We could find that higher structures' surface and cell number ratios, so called tissue cytometric features, have much higher importance in classifying gastric samples than simple morphometrical parameters. These ratios are based on the simple human observation that samples with gastritis have many more inflammatory cells in interstitial areas than do normal samples. The same holds for samples with adenocarcinoma, as these samples also have high numbers of cells in the interstitial areas. We found that all tissue cytometric parameters indicate differences among normal, gastritis, and carcinoma groups except "Bio Surf/CC" and "Bio/Epith Surf" (Table 11.2).

The Kruskall-Wallis test can show only that differences exist between groups with respect to certain parameters. Additional statistical analyses are required to study these differences in greater detail. We used the Mann-Whitney U test to determine the precise relationship between the diagnostic groups. The analysis showed that every group significantly differs from each other in five or more parameters (Table 11.2). The most significant differences were between the group of adenocarcinoma and the benign groups.

We found significant differences between diagnostic groups but our ultimate goal is to be able to distinguish whether each specimen is normal, gastritis, or adenocarcinoma. We used discriminant analysis to reach this goal. By using the result of discriminant analysis, we could classify the samples with 86% accuracy. Normal samples were classified with 64.3% accuracy, gastritis samples with 82.9%, and carcinoma samples with 100%.

We also examined whether there are significant differences among different kinds of gastritis samples (17 specimens were atrophy, 6 specimens were gastritis, 12 specimens were gastritis with intestinal metaplasia) by the measured morphometrical and tissue cytometric parameters. We could find that the detected morphometrical

Table 11.2. Descriptive statistics and significant differences among gastric diagnostic classes.

	Normal (1)	Gastritis (2)	Carcinoma (3)		Sign. Diff. between groups p < 0.01		
	Mean ± SD	Mean ± SD	Mean ± SD		1	1	2
Case number	14	35	30	Kruskal-Wallis test	2	3	3
Bio/Gland Surf	5.60 ± 2.53	6.88 ± 3.16	21.11 ± 16.30	p < 0.01		[b]	[c]
Bio/Gland CC	4.53 ± 1.52	9.85 ± 5.93	18.50 ± 7.57	p < 0.01	[a]	[b]	[c]
Bio/Epith Surf	30.42 ± 13.13	53.89 ± 77.00	100.70 ± 130.46	p = 0.08		[b]	[c]
Bio/Epith CC	22.28 ± 12.74	32.90 ± 33.49	78.67 ± 72.55	p = 0,01		[b]	[c]
Bio/Int Surf	1.36 ± 0.14	1.38 ± 0.32	1.02 ± 0.02	p < 0.01		[b]	[c]
Bio/Int CC	1.43 ± 0.12	1.23 ± 0.13	1.10 ± 0.05	p < 0.01	[a]	[b]	[c]
Int Surf/CC	169.55 ± 59.65	123.00 ± 29.51	178.66 ± 55.26	p < 0.01	[a]		[c]
Bio Surf/CC	158.93 ± 46.72	136.39 ± 34.71	166.33 ± 52.73	p = 0.11			[c]
I/B	1.06 ± 0.06	0.92 ± 0.17	1.08 ± 0.04	p < 0.01	[a]	[b]	[c]
GlandShape	0.84 ± 0.066	0.82 ± 0.07	0.81 ± 0.07	p < 0.01	[a]	[b]	[c]
SpCN	114.9 ± 32.5	112.1 ± 32.8	147.2 ± 45.2	p < 0.05		[b]	[c]

[a] There is significant difference between normal and gastritis
[b] There is significant difference between normal and carcinoma
[c] There is significant difference between gastritis and carcinoma

features of the object have no importance in differentiation of gastritis diseases. However, tissue cytometric parameters again have significance. First, we used the Mann-Whitney U test for statistical analysis, which showed only that the group of atrophy is different from gastritis samples and the samples with intestinal metaplasia. We could get similar results using discriminant analysis. Atrophy samples were classified with 94%, gastritis with 50%, and intestinal metaplasia with 66.7% accuracy which means that only atrophy samples can be classified reliably.

Colon Samples

The same statistical methods were applied for the colon samples as for the gastric ones and very similar results were found. We can emphasize the elliptical shape factor of crypts morphological parameter that showed significant differences (Table 11.3) among colon groups. The importance of cytometric features was also examined among the colon samples. As it was introduced for the gastric examination, Kruskal Wallis test was used to examine parameters and for further examination Mann-Whitney U test was used again to compare colon disease groups in pairs. Deeper investigations showed that the normal, aspecific colitis and colitis ulcerosa groups highly differ from each other but the Crohn's disease group does not show as many differences as the others (Table 11.3). It is emphasized that cytometric parameters have high significance in the differentiation of diseases. Almost every cytometric parameter showed significant difference between certain diseases. Discrepancy of a certain disease class can be calculated by summarizing the number of significant differences showed by any parameter against any group. The class of normal samples showed difference in

TABLE 11.3. Descriptive statistics and significant differences among colon diagnostic classes.

	Normal (1)	Aspecific Colitis (2)	Colitis ulcerosa (3)	Crohn's disease (4)		Sign. Diff. between groups p < 0.01					
	Mean ± SD	Mean ± SD	Mean ± SD	Mean ± SD		1	1	1	2	2	3
Case number	24	11	25	9	Kruskal-Wallis test	2	3	4	3	4	4
Bio/Gland Surf	7.48 ± 6.29	8.00 ± 4.90	9.86 ± 6.27	12.39 ± 12.55	p = 0.08		b				
Bio/Gland CC	5.00 ± 2.14	8.45 ± 5.89	11.84 ± 7.31	15.10 ± 15.73	p < 0.01			b		d	
Bio/Epith Surf	12.03 ± 4.63	16.17 ± 5.74	21.38 ±7.30	17.36 ± 7.56	p < 0.01	a		b		d	
Bio/Epith CC	8.55 ± 2.77	14.09 ± 4.06	24.37 ± 8.20	18.93 ± 8.25	p < 0,01	a		b	c	d	
Bio/Int Surf	1.39 ± 0.15	1.34 ± 0.18	1.23 ± 0.10	1.32 ± 0.12	p < 0.01			b			f
Bio/Int CC	1.57 ± 0.17	1.34 ± 0.16	1.19 ± 0.09	1.28 ± 0.11	p < 0.01	a		b	c	d	f
Int Surf/CC	189.65 ± 88.21	135.49 ± 14.90	111.53 ± 23.71	110.50 ± 10.19	p < 0.01	a		b	c	d	e
Bio Surf/CC	164.80 ± 61.38	135.2 ± 15.67	114.96 ± 22.77	114.49 ± 11.26	p < 0.01			b	c	d	e
I/B	1.13 ± 0.09	1.00 ± 0.03	0.97 ± 0.02	0.97 ± 0.03	p < 0.01	a		b	c	d	e
GlandShape	0.62 ± 0.01	0.59 ± 0.008	0.61 ± 0.01	0.60 ± 0.004	p < 0.01	a		b	c	d	e
SpCN	116.93 ± 12.95	139.14 ± 33.72	127.43 ± 25.45	123.25 ± 6.59	p = 0.25						

[a] Indicates there is significant difference between normal and aspecific colitis
[b] Indicates there is significant difference between normal and colitis ulcerosa
[c] Indicates there is significant difference between normal and Crohn's disease
[d] Indicates there is significant difference between aspecific colitis and colitis ulcerosa
[e] Indicates there is significant difference between aspecific colitis and Crohn's disease
[f] Indicates there is significant difference between colitis ulcerosa and Crohn's disease

22 events, the aspecific colitis class in 18 events, the colitis ulcerosa in 20, and the class of Crohn's disease only in 12 events (Table 11.3). These event numbers show that the group of normal is the most different from the others, and Crohn's disease is the last in this order. It is also evident from Table 11.3 that the weakest difference is between the group of colitis ulcerosa and Crohn's disease. Discriminant analysis showed the same results as above: normal samples were classified by 96% accuracy, aspecific colitis by 91%, colitis ulcerosa by 92%, and the group of Crohn's disease only by 56%; in the end, 88% overall accuracy was given. The scatterplot of the discriminant analysis shows clearly that Crohn's disease is very similar to colitis ulcerosa, but the significant discrepancies of the other groups are also obvious (Figure 11.2).

Results Visualized by Virtual Microscopy

As mentioned earlier, the results of the detection algorithms can be presented in the MIRAX Viewer software. With this software we can check the mask to see the accuracy of the detection and determine which obviously visible objects are detected and which are not (Figure 11.3). It can also visualize measured data on scatterplots and collect certain populations to gallery.

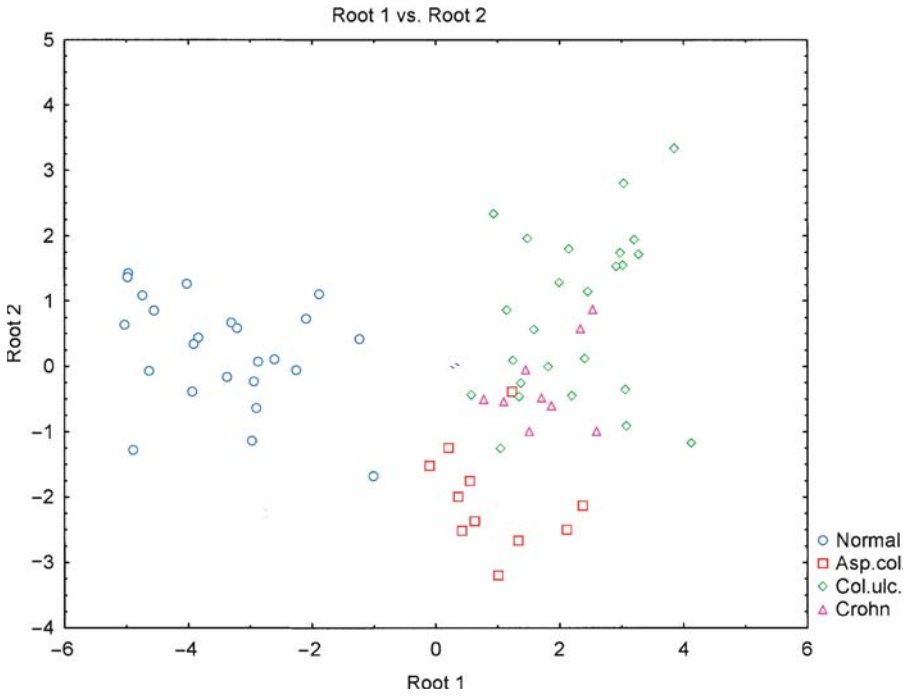

FIGURE 11.2. Scatterplot of discriminant analysis applied on colon samples

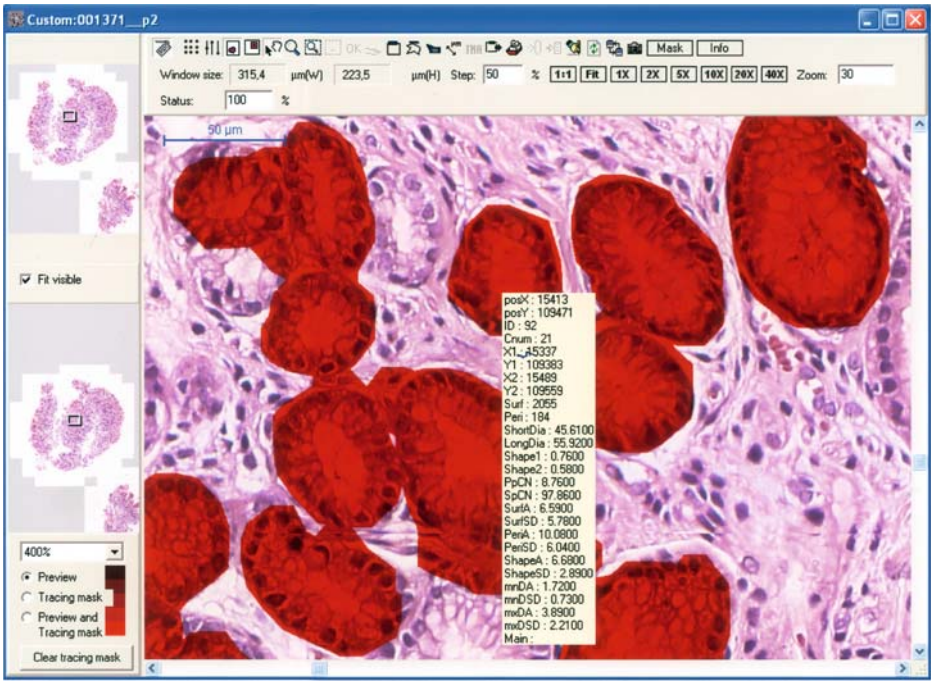

FIGURE 11.3. Detected glands in the MIRAX Viewer software: quick info box about measured parameters of a gland selected by the mouse pointer

DISCUSSION

The quantification of histologic parameters for automated quantification and classification is a longstanding problem. Early attempts were made on selected microscopic field of views. Depending on the selected problem, low or high resolution images could only be collected. A comprehensive analysis where architectural features could be seen at low and intermediate magnification (up to 200X) and cytologic features could be seen at high magnification (400X) could not be performed. Due to these limitations and working on single images instead, previous studies of image analysis concentrated on selected and specific problems of image analysis such as nuclear detection (Nedzved *et al*., 2000), detection of immunopositivity (Ruifrok, 1997), quantification of vascularisation (Loukas and Linney, 2004), mitotic counting (Belien *et al*., 1997) in high resolution.

Low resolution analysis of histologic architecture was attempted by Thompson *et al*. (1993) and Esgiar *et al*. (1998) for colonic carcinoma by different groups. An interesting approach of image analysis was introduced by Hamilton *et al*. (1997) for finding dysplastic fields in colorectal sections, using neural networks on a mosaic of pixilated images without any image analysis or image segmentation.

Digital slides offer a flexible platform for image analysis. Using this digital media the same specimen can be morphometrically quantified for architectural components in the 50–200 µm range, similar to the glands, surface, follicles, and for

cytologic components (nuclei, cytoplasm) in the 5–10 μm range. With this media the development of tissue specific parameters can be started. In our opinion in standardized environment where the thickness of sectioning, staining, and coverslipping is automated and standardized, morphometric and densitometric parameters of the sections must be comparable to each other.

We attempted to develop cell-specific and tissue-specific parameters to analyze specimens from gastric and colon biopsies. Specimens from gastric and colon biopsies are ideal for this purpose because they can be frequently obtained and thus provide a major load for the practice. As this study is a preliminary one, we did not include all of the available diagnostic groups. Important diagnostic criteria, such as *H. pylori* were not considered. We attempted to describe basic tissue-specific parameters and define the borders where additional alteration-related parameters are required.

In our study we showed that tissue cytometric parameters can distinguish major disease groups in gastric and colon samples. However, classification between gastritis subgroups would need study of additional features such as detection of goblet cells and parameters related to atrophy. The development of these parameters can be done parallel to features specific to carcinoma such as differentiation, dysplasia, and formation of gland. The study also showed that Crohn's disease needs further research to be able to eliminate it from colitis ulcerosa. For these types of analyses further intraepithelial, intraglandular analytical algorithms will be needed. In our analysis linear discriminant analysis was used which significantly reduced the necessary feature set for the automated analysis. With the incorporation of artificial intelligence learning techniques (neural networks), the discriminatory accuracy should be further increased.

Digital slides and Virtual microscopy opens new dimensions in histopathology which allows us to analyze whole specimens rather than only single field of view. The newly developed tissue cytometry features (as a product of virtual microscopy) are new milestones in histo/cytometry and are essential in the classification of gastric and colon samples. The study shows that there are strong differences among major gastric and colon disease groups, and that a high percentage of such cases can be correctly classified based on tissue and cellular parameters.

REFERENCES

Bartels, P.H., Thompson, D., and Montironi, R. 1996. Knowledge-based image analysis in the precursors of prostatic adenocarcinoma. *Eur. Urol. 30*: 234–242.

Belien, J.A.M., Baak, J.P.A., Diest, P.J., and Ginkel, AHM. 1997. Counting mitoses by image processing in Feulgen stained breast cancer sections: the influence of resolution. *Cytometry 28*:135–140

Esgiar, A.N., Naguib, R.N., Bennett, M.K., and Murray, A. 1998 Automated feature extraction and identification of colon carcinoma. *Anal. Quant. Cytol. Histol. 20*:297–301.

Esgiar, A.N., Naguib, R.N., Sharif, B.S., Bennett, M.K., and Murray A. 2002. Fractal analysis in the detection of colonic cancer images. *IEEE Trans. Inf. Technol. Biomed. 6*:54–58.

Francis, I.M., Adeyanju, M.O., George, S.S., Junaid, T.A., and Luthra U.K. 2000. Manual versus image analysis estimation of PCNA in breast carcinoma. *Anal. Quant. Cytol. Histol. 22*:11–16.

Hamilton, P.W., Bartels, P.H., Thompson, D., Anderson, N.H., Montironi, R., and Sloan, J.M. 1997. Automated location of dysplastic field in colorectal histology using image texture analysis. *J. Pathol. 182*:68–75.

Laak, J.A.W.M., Pahlplatz, M.M.M., Hanselaar, A.G.J.M., and Wilde, P.C.M. 2000. Hue-saturation-density (HSD) model for stain recognition in digital images from transmitted light microscopy. *Cytometry 39*:275–284.

Loukas, C.G., and Linney, A. 2004. A survex on histological image analysis-based assessment of three major biological factors influencing radiotherapy: proliferation, hypoxia and vasculature. *Comp. Meth. Progr. Biomed. 74*:183–199.

Loukas, C.G., Wilson, G.D., Vojnovic, B., and Linney, A. 2003. An image analysis-based approach for automated counting of cancer cell nuclei in tissue sections. *Cytometry 55A*:30–42.

Nedzved, A., Ablameyko, S., and Pitas I. 2000 Morphological segmentation of histology cell images. *Intern. Conf. Pattern Recog. 1*:1500–1504.

Petushi S., Garcia F., Haber M., Katsinis C., and Tozeren A. 2006. Large-scale computations on histology images reveal grade-differentiating parameters for breast cancer. *BMC Med. Imag. 6*:14.

Ruifrok, A.C. 1997. Quantification of immunohistochemical staining by color translation and automated thresholding. *Anal. Quant. Cytol. Histol. 19*:107–113.

Stenkvist, B., Bergström, R., Brinne, U., Hesselius, I., Kiviranta, A., Nordgren, H., Schnürer, L., Stendahl, U., Sténson, S., and Söderström, J., 1987. Automatic analysis of Papanicolaou smears by digital image processing. *Gynecol. Oncol. 27*:1–14.

Thompson, D., Bartels, P.H., Bartels, H.G., Hamilton, P.W., and Sloan, J.M. 1993. Knowledge-guided segmentation of colorectal histopathologic imagery. *Anal. Quant. Cytol. Histol. 15*:236–246.

Varga, V.S., Bocsi, J., Sipos, F., Csendes, G., Tulassay, Zs., and Molnar, B. 2004. Scanning fluorescent microscopy is an alternative for quantitative fluorescent cell analysis. *Cytometry 60A*:53–62.

Wittekind, D., Reinhardt, E.R., Kretschmer, V., and Zipfel, E. 1983. Influence of staining on fast automated cell segmentation, feature extraction and cell image analysis. *Anal. Quant. Cytol. 5*:55–60.

12
Early Gastric Cancer: Prediction of Metachronous Recurrence Using Endoscopic Submucosal Dissection (Methodology)

Hiroshi Yokozaki, Tadateru Hasuo, Shin-ya Satake, Yasuhiro Omori, Naoko Maeda, Korefumi Nakamura, and Shuho Semba

INTRODUCTION

Although gastric cancer remains the second most common malignancy worldwide, its incidence and mortality has fallen dramatically during the last 50 years. Correa (1992) reported that the consequences of early gastric cancer (EGC) are comparatively good. Endoscopic treatment of EGC is being widely applied and carries with it some improvement for their prognosis; therefore, it was reported by Nagano *et al*. (2005) that many patients have been able to avoid open–surgery and maintain better quality of life. For these reasons, endoscopic resection of EGC is now the standard therapy in Japan and has been increasingly accepted and regularly used in other countries. Recently, Ono *et al*. (2001) reported that an innovational technique for endoscopic submucosal dissection (ESD) has been developed for *en bloc* resection. Toyonaga *et al*. (2006) reported that ESD has also made it possible to give an accurate diagnosis by pathological examination of EGC. On the other hand, it was reported by Hamanaka and Gotoda (2005) that endoscopic treatment excises only gastric carcinoma tissues, which implies that patients are still at risk of developing metachronous cancer from the remnant mucosa of the stomach. Therefore, molecular diagnosis is required for the screening of patients expected to have metachronous gastric carcinoma.

It was proposed by Kinzler and Vogelstein (1996) that recent molecular biological studies have uncovered that there are at least two distinct genetic pathways for gastrointestinal carcinogenesis: the suppressor pathway and the mutator pathway. The suppressor pathway is caused by inactivation of tumor suppressor genes (e.g., *APC* and *p53*) and activation of oncogenes (e.g., K–*ras*) and the tumors demonstrate chromosomal instability; whereas in the mutator pathway, dysfunctions of the DNA mismatch repair (MMR) system is the profound abnormality that leads to the accumulation of nucleotide insertion/deletion mutation at the short repeat sequences in the genome, called microsatellites. The repeating unit comprising a microsatellite can be as short as one or two nucleotides. These regions of the genome tend to be polymorphic or variable among different

individuals. Altered length of microsatellites, called microsatellite instability (MSI), has been reported in DNA from the tumors of hereditary non–polyposis colorectal cancer (HNPCC) patients as a consequence of germline defect in the MMR system (Aaltonen *et al*., 1993; Ionov *et al*., 1993; Thibodeau *et al*., 1993). Importantly, genes with coding mononucleotide repeats including *transforming growth factor–beta type II receptor*, *insulin–like growth factor II receptor*, *BAX*, *E2F–4*, *hMSH3*, *hMSH6*, and *MBD4* have been found to be the targets of the MMR deficiencies. One of the important recent findings on the defects of MMR system in human cancer is that multiple primary cancers including stomach, colon, and gallbladder carcinomas arising in single case frequently display MSI (Horii *et al*., 1994; Yokozaki *et al*., 1999). This indicates the possibility for not only the existence of background abnormalities in some of the MMR genes in these patients but also the detection of MSI in a cancer may serve as a good molecular marker for the assessment of second cancer risk in the same patient.

In this chapter, we present the results and detailed methodology of our retrospective as well as prospective study designed to elucidate the significance of MSI as a molecular marker for the prediction of metachronous recurrence of gastric cancer treated endoscopically, especially with ESD.

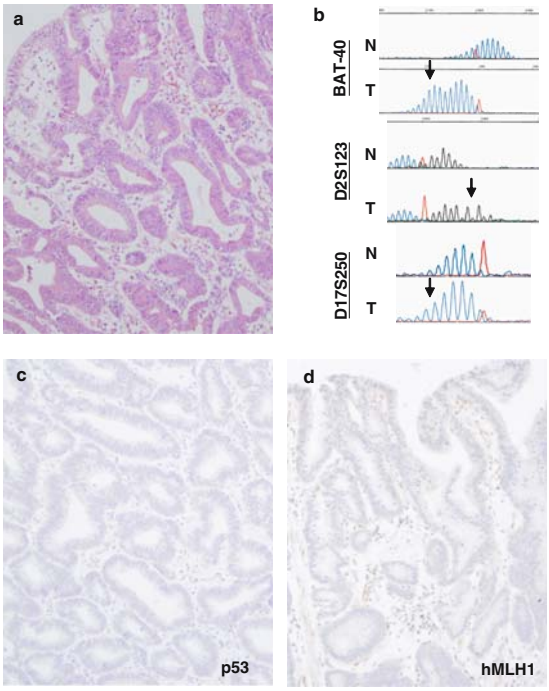

FIGURE 12.1. Representative EGC with MSI–H. (a) H&E stain of the tumor tissue demonstrating well–differentiated tubular adenocarcinoma. (b) Results of microsatellite analyses on BAT–40, D2S123 and D17S250. Arrows indicate MSI. N, normal gastric mucosa; T, tumor. (c) Cancer cells do not exhibit abnormal nuclear accumulation of p53 immunoreactivity. (d) Nuclear expression of hMLH1 is silenced in the cancer cells in comparison with that of surrounding lymphocytes

APPLICATION

Retrospective analysis of 596 patients with gastric tumor was conducted. Among them, 26 (4.4%) had gastric tumors with MSI–H (Figure 12.1). Table 12.1 summarizes comparisons of clinicopathological characters between patients with MSI–H and non–MSI–H tumors. Student's *t*–test showed a significant statistical difference between the mean age of MSI–H and non–MSI–H group ($P = 0.001$). Well–differentiated type or intestinal type cancers predominated within MSI–H group in comparison with their frequency in non–MSI–H group ($P = 0.0258$, Fisher's exact test). Surprisingly, 11 out of 26 (42.3%) patients with MSI–H tumors had additional tumor(s) within the stomach (10 cases) or colon (one case). On the other hand, only 16 of 570 individuals with non–MSI–H tumors revealed multiple

TABLE 12.1. Clinicopathological characters of cases with MSI–H gastric tumors.

	MSI–H (n = 26)	Non–MSI–H (n = 570)	*P*
Age (years)*	74 (14.0)	65 (11.5)	0.001[b]
M/F	16/10	401/169	0.3822[c]
Histological type[a] Well/Poorly	25/1	448/122	0.0258[c]
Number of cases with multiple tumors	11 (42.3%)	16 (2.8%)	<0.0001[c]

*Mean (SD)

[a]Well, well–differentiated type adenocarcinomas including papillary and tubular adenocarcinomas; Poorly, poorly differentiated type adenocarcinomas including poorly differentiated adenocarcinomas, signet ring cell carcinomas and mucinous adenocarcinomas

[b]Student's *t*–test ($t = 3.907310$, df = 594)

[c]Fisher's exact test

tumors. The two sided *P* value (< 0.0001) of Fisher's exact test suggested a very significant association between MSI–H tumors and existence of additional tumor.

Hasuo *et al*. (2007) performed a prospective analysis of 110 patients who had undergone curative resections for EGC with ESD from 2000 to 2004. Patients with hereditary cancer syndrome history, such as HNPCC, Li–Fraumeni syndrome, and familial adenomatous polyposis, and those who had hereditary diffuse gastric cancer, were excluded from this study. EGCs with MSI–H and MSI–L were detected in 9 (8%) and 16 (15%) of 110 cases, respectively. The patients examined were regularly followed and examined endoscopically to monitor for secondary metachronous tumors in the remnant stomach after ESD. Interestingly, patients with MSI–H EGCs had a tendency to develop secondary metachronous cancer in the remnant stomach after initial ESD (Figure 12.2), which was statistically higher than the non–MSI–H tumors ($P < 0.01$). These retrospective as well as prospective analyses clearly indicate the clinical usefulness of microsatellite analysis for predicting the potential risk of developing metachronous gastric cancer after curative resection with ESD.

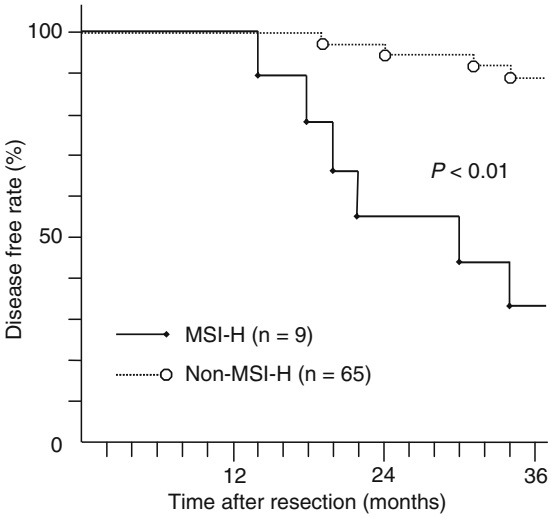

FIGURE 12.2. Overall disease–free curves of patients with EGCs in relation to the microsatellite status of the tumor. The 3–year disease free rate in the group of MSI–H tumors was 33% but was 94% in that of non–MSI–H ones ($P < 0.01$)

EQUIPMENT

Facilities for Processing Histopathological Specimens

The resected EGCs are extended on the rubber plate, fixed in 10% buffered formalin and step–cut (3 mm in width for each slice is recommended). Embedment in paraffin wax, sectioning and staining can

be performed in the conventional facilities for histopathology, available in any medical center with pathologist(s).

Thermal Cycler for Polymerase Chain Reaction (PCR)

Thermal cycler with hot bonnet attachment is useful for the overlay oil–free manipulation and can be used for routine PCR as well as programmable incubator for DNA extraction from the histological sections.

Automated DNA Sequencer with Fragment Analysis Software

Any kind of system providing DNA fragment analysis can be applied to microsatellite analysis. However, we prefer to use ABI PRISM 310 Genetic Analyzer (Applied Biosystems) with ABI Gene Scan software (Applied Biosystems).

PROCEDURE

DNA Extraction

For DNA extraction, the deparaffinized specimens were stained with hematoxylin and eosin (H&E). The tumor areas and corresponding non–neoplastic gastric mucosa were scraped using a sterile needle and placed in a microtube containing 20 μl of extraction buffer (Tris–HCl, pH 8.5; 1 mmol/l EDTA and 0.2 mg/ml proteinase K) and incubated at 55°C for 12 h. Proteinase K was inactivated by boiling for 5 min after inactivation and then the DNAs were used for polymerase chain reaction (PCR).

Microsatellite Assay

Nine microsatellite markers (BAT–25, BAT–26, BAT–40, BAT–RII, D1S191, D2S123, D5S346, D17S250, and D17S855) were analyzed according to the method by Li *et al*. (2005). The forward primers were fluorescein labeled with 6–FAM (D1S191, D17S250, BAT–26, and BAT–40), HEX (D17S855 and BAT–RII), VIC (D5S346) and TAMRA (D2S123 and BAT–25). PCR was performed in 15 μl reaction volumes containing 1 μl template DNA, 0.56 μmol/l of each primer, 74.7 μmol/l of dNTP, 4.5 mmol/l of $MgCl_2$, and 0.075 U of Ampli*Taq* Gold (Applied Biosystems, Foster City, CA, USA). After the initial *Taq* DNA polymerase activation step, the PCR amplification consisted of 45 cycles (94°C for 45 s, 55°C for 45 s, and 72°C for 45 s) followed by a final extension for 10 min at 72°C. PCR products were electrophoresed in ABI PRISM 310 Genetic Analyzer along with GeneScan–500 (ROX) molecular weight standard (Applied Biosystems). The size of the PCR product was analyzed using GeneScan software (Applied Biosystems). The status of MSI in each tumor was evaluated according to the criterion of Boland *et al*. (1998); MSI–H, if three or more out of nine microsatellite loci showed MSI; MSI–L, if one or two loci had MSI; MSS, if all the microsatellite loci examined were stable. Alleles were defined as the two highest peaks (tumor DNA alleles, T1, T2; normal DNA alleles, N1, N2) and a ratio of (T1/T2)/(N1/N2) of < 0.67 or > 1.50 was scored as a loss of heterozygosity (LOH) as defined by Wu *et al*. (2004).

Immunohistochemistry

Immunohistochemical analyses were carried out with monoclonal antibodies to p53 (DakoCytomation, Copenhagen, Denmark) and hMLH1 (BD Biosciences, San Diego, CA, USA). Dewaxed and

rehydrated specimens were autoclaved in citrate buffer for the antigen retrieval. Endogenous peroxidase activity and non-specific binding were blocked by 0.03% hydrogen peroxide in methanol and blocking reagent in LSAB2 kit (DakoCytomation), respectively. The slides were then incubated with the primary monoclonal antibody and incubated sequentially with a biotinylated secondary antibody, streptavidin, labeled with peroxidase and 3, 3'–diaminobenzidine. Slides were counterstained with Mayer's hematoxylin. Immunoreactivity of p53 and hMLH1 was graded as reported by Li *et al.* (2005): almost no positive cells; +, < 25% of the tumor cells showed positive immunoreactivity; ++, 25–50% of the tumor cells showed positive immunoreactivity; +++, > 50% of the tumor cells showed positive immunoreactivity.

FURTHER CONSIDERDATIONS

Close correlation of multiple gastric cancers with MSI of tumor DNA has been reported by several groups. Nakashima *et al*. (1995) examined a total of 30 gastric cancers developed in 14 Japanese patients with multiple cancers and reported that MSI in multiple gastric cancers was recognized in 11 (78.5%) out of 14 cases and in 16 (53.3%) out of 30 gastric cancers. Ohtani *et al*. (2000) and Yamashita *et al*. (2000) confirmed intimate association of MSI with multiple primary gastrointestinal cancers including gastric, colorectal or duodenal cancers. Interestingly, Yamashita *et al*. (2000) described that MSI–H was found often in patients with multiple cancers in the same organ, especially in multiple gastric cancer patients, while patients with multiple primary cancers in different organs had a tendency to show MSI–L or MSS phenotype. Miyoshi *et al*. (2001) examined MSI retrospectively in patients with multiple EGCs treated with endoscopic mucosal resetion (EMR) and found that MSI increased the frequency of synchronous as well as metachronous gastric cancer development. The problems of these earlier observations are following. (1) Researchers collected multiple EGC tissues with the intention of analyzing the relationship between MSI and synchronous and metachronous gastric cancer. (2) Gastric carcinoma tissues removed with EMR may possibly be related to local recurrence of carcinoma. The retrospective and prospective analysis presented in this chapter may be able to eliminate the possibility of intentional sample collection and local recurrence of gastric cancer as ESD is a more efficient method for curative resection of EGC and enables more accurate histopathological diagnosis than EMR. Together with previous reports, it could be concluded that MSI in tumor DNA may serve as a molecular marker for the prediction of multiple and metachronous gastric cancer.

Molecular mechanisms causing the MSI in the tumor DNA of gastric carcinomas has been elucidated. Fleisher *et al*. (1999) studied the prevalence of the hypermethylation of the *hMLH1* MMR gene promoter which was confirmed to be quite common in MSI–positive endometrial and colorectal cancers. Fleisher *et al*. (1999) reported that 14 (77.8%) of 18 MSI–H tumors showed *hMLH1* hypermethylation, whereas only 1 (2.6%) of 39 MSI–negative tumors demonstrated promoter methylation of the gene. Toyota *et al*. (2000) conducted a genome–wide analysis of the methylation status of 5' CpG islands of gastric cancer

DNA and demonstrated that approximately one–half of all gastric cancers have concordant methylation of multiple loci that seem to be methylated *de novo* during progression, and suggested a hypermethylator phenotype which leads to simultaneous inactivation of multiple genes including *hMLH1* and *p16*. Kang *et al*. (1999) confirmed the correlation of methylation of *hMLH1* promoter with lack of expression of the gene in sporadic gastric carcinomas with MSI. Sakata *et al*. (2002) reported the high frequency of *hMLH1* promoter hypermethylation in solitary as well as multiple gastric cancers with MSI. Moreover, they found methylation of the *hMLH1* promoter in 50% (6 out of 12) and 63% (5 out of 8) of non–cancerous gastric mucosa samples adjacent to, and in 33% (4 out of 12) and 40% (2 out of 5) of those obtained from distant portion of solitary and multiple gastric cancers with MSI. Interestingly, Semba *et al*. (1996) and Hamamoto *et al*. (2007) reported the existence of MSI–L in intestinal metaplasia, especially those surrounding gastric cancer with MSI.

These observations clearly demonstrate that epigenetic silencing of *hMLH1* by promoter hypermethylation is the main etiology of MSI in human gastric cancers. Therefore, frequent synchronous or metachronous carcinogenesis in the stomach with MSI tumor may attribute to the global hypermethylation of the mucosal genome in the affected individual. In other words, a hypothetical "carcinogenic field" may created by epigenetic alterations that may cause multiple tumorigenesis. Substantial evidences for this hypothesis have been reported. Maekita *et al*. (2006) indicated that *Helicobacter pylori* (HP) infection potently induced methylation of selected promoter to various degrees. Nakajima *et al*. (2006) demonstrated that methylation levels in gastric mucosae significantly increased in cases with a single gastric cancer and more in cases with multiple gastric cancers in HP negative individuals. Oue *et al*. (2006) also reported the methylation of promoter of several target genes in the corresponding noncancerous gastric mucosae of the cancers with frequent methylation of the genes. Detection of promoter methylation of specific genes in stomach biopsy may serve as a good biomarker for the risk assessment of cancer development in the future.

REFERENCES

Aaltonen, L. A., Peltomaki, P., Leach, F. S., Sistonen, P., Pylkkanen, L., Mecklin, J. P., Jarvinen, H., Powell, S. M., Jen, J., Hamilton, S. R., Petersen, G. M., Kinzler, K. W., Vogelstein, B., and de la Chapelle, A. 1993. Clues to the pathogenesis of familial colorectal cancer. *Science 260*: 812–816.

Boland, C. R., Thibodeau, S. N., Hamilton, S. R., Sidransky, D., Eshleman, J. R., Burt, R. W., Meltzer, S. J., Rodriguez-Bigas, M. A., Fodde, R., Ranzani, G. N., and Srivastava, S. 1998. A National Cancer Institute Workshop on Microsatellite Instability for cancer detection and familial predisposition: development of international criteria for the determination of microsatellite instability in colorectal cancer. *Cancer Res. 58*: 5248–5257.

Correa, P. 1992. International cancer epidemiology meetings. *Cancer Epidemiol. Biomarkers Prev. 1*: 245–247.

Fleisher, A. S., Esteller, M., Wang, S., Tamura, G., Suzuki, H., Yin, J., Zou, T. T., Abraham, J. M., Kong, D., Smolinski, K. N., Shi, Y. Q., Rhyu, M. G., Powell, S. M., James, S. P., Wilson, K. T., Herman, J. G., and Meltzer, S. J. 1999. Hypermethylation of the *hMLH1* gene promoter in human gastric cancers with microsatellite instability. *Cancer Res. 59*: 1090–1095.

Hamamoto, T., Yokozaki, H., Semba, S., Yasui, W., Yunotani, S., Miyazaki, K., and Tahara, E. 1997. Altered microsatellites in incomplete–type

intestinal metaplasia adjacent to primary gastric cancers. *J. Clin. Pathol. 50*: 841–846.

Hamanaka, H., and Gotoda, T. 2005. Endoscopic resection for early gastric cancer and future expectations. *Digest. Endos. 17*: 275–285.

Hasuo, T., Semba, S., Li, D., Omori, Y., Shirasaka, D., Aoyama, N., and Yokozaki, H. 2007. Assessment of microsatellite instability status for the prediction of metachronous recurrence after initial endoscopic submucosal dissection for early gastric cancer. *Br. J. Cancer 96*: 89–94.

Horii, A., Han, H. J., Shimada, M., Yanagisawa, A., Kato, Y., Ohta, H., Yasui, W., Tahara, E., and Nakamura, Y. 1994. Frequent replication errors at microsatellite loci in tumors of patients with multiple primary cancers. *Cancer Res. 54*: 3373–3375.

Ionov, Y., Peinado, M. A., Malkhosyan, S., Shibata, D., and Perucho, M. 1993. Ubiquitous somatic mutations in simple repeated sequences reveal a new mechanism for colonic carcinogenesis. *Nature 363*: 558–561.

Kang, G. H., Shim, Y. H., and Ro, J. Y. 1999. Correlation of methylation of the *hMLH1* promoter with lack of expression of hMLH1 in sporadic gastric carcinomas with replication error. *Lab. Invest. 79*: 903–909.

Kinzler, K. W., and Vogelstein, B. 1996. Lessons from hereditary colorectal cancer. *Cell 87*: 159–170.

Li, D., Semba, S., Wu, M., and Yokozaki, H. 2005. Molecular pathological subclassification of mucinous adenocarcinoma of the colorectum. *Pathol. Int. 55*: 766–774.

Maekita, T., Nakazawa, K., Mihara, M., Nakajima, T., Yanaoka, K., Iguchi, M., Arii, K., Kaneda, A., Tsukamoto, T., Tatematsu, M., Tamura, G., Saito, D., Sugimura, T., Ichinose, M., and Ushijima, T. 2006. High levels of aberrant DNA methylation in Helicobacter pylori–infected gastric mucosae and its possible association with gastric cancer risk. *Clin. Cancer Res. 12*: 989–995.

Miyoshi, E., Haruma, K., Hiyama, T., Tanaka, S., Yoshihara, M., Shimamoto, F., and Chayama, K. 2001. Microsatellite instability is a genetic marker for the development of multiple gastric cancers. *Int. J. Cancer 95*: 350–353.

Nagano, H., Ohyama, S., Fukunaga, T., Seto, Y., Fujisaki, J., Yamaguchi, T., Yamamoto, N., Kato, Y., and Yamaguchi, A. 2005. Indications for gastrectomy after incomplete EMR for early gastric cancer. *Gastric Cancer 8*: 149–154.

Nakajima, T., Maekita, T., Oda, I., Gotoda, T., Yamamoto, S., Umemura, S., Ichinose, M., Sugimura, T., Ushijima, T., and Saito, D. 2006. Higher methylation levels in gastric mucosae significantly correlate with higher risk of gastric cancers. *Cancer Epidemiol. Biomark. Prev. 15*: 2317–2321.

Nakashima, H., Honda, M., Inoue, H., Shibuta, K., Arinaga, S., Era, S., Ueo, H., Mori, M., and Akiyoshi, T. 1995. Microsatellite instability in multiple gastric cancers. *Int. J. Cancer 64*: 239–242.

Ohtani, H., Yashiro, M., Onoda, N., Nishioka, N., Kato, Y., Yamamoto, S., Fukushima, S., and Hirakawa-Ys Chung, K. 2000. Synchronous multiple primary gastrointestinal cancer exhibits frequent microsatellite instability. *Int. J. Cancer 86*: 678–683.

Ono, H., Kondo, H., Gotoda, T., Shirao, K., Yamaguchi, H., Saito, D., Hosokawa, K., Shimoda, T., and Yoshida, S. 2001. Endoscopic mucosal resection for treatment of early gastric cancer. *Gut 48*: 225–229.

Oue, N., Mitani, Y., Motoshita, J., Matsumura, S., Yoshida, K., Kuniyasu, H., Nakayama, H., and Yasui, W. 2006. Accumulation of DNA methylation is associated with tumor stage in gastric cancer. *Cancer 106*: 1250–1259.

Sakata, K., Tamura, G., Endoh, Y., Ohmura, K., Ogata, S., and Motoyama, T. 2002. Hypermethylation of the *hMLH1* gene promoter in solitary and multiple gastric cancers with microsatellite instability. *Br. J. Cancer 86*: 564–567.

Semba, S., Yokozaki, H., Yamamoto, S., Yasui, W., and Tahara, E. 1996. Microsatellite instability in precancerous lesions and adenocarcinomas of the stomach. *Cancer 77*: 1620–1627.

Thibodeau, S. N., Bren, G., and Schaid, D. 1993. Microsatellite instability in cancer of the proximal colon. *Science 260*: 816–819.

Toyonaga, T., Nishino, E., Hirooka, T., Ueda, C., and Noda, K. 2006. Intraoperative bleeding in endoscopic submucosal dissection in the stomach and stragegy for prevention and treatment. *Digest. Endosc. 18*: S123–S127.

Toyota, M., Ahuja, N., Suzuki, H., Itoh, F., Ohe Toyota, M., Imai, K., Baylin, S. B., and Issa, J. P. 1999. Aberrant methylation in gastric cancer

associated with the CpG island methylator phenotype. *Cancer Res. 59*: 5438–5442.

Wu, M., Semba, S., Li, D., and Yokozaki, H. 2004. Molecular pathological analysis of mucinous adenocarcinomas of the stomach. *Pathobiology 71*: 201–210.

Yamashita, K., Arimura, Y., Kurokawa, S., Itoh, F., Endo, T., Hirata, K., Imamura, A., Kondo, M., Sato, T., and Imai, K. 2000. Microsatellite instability in patients with multiple primary cancers of the gastrointestinal tract. *Gut 46*: 790–794.

Yokozaki, H., Semba, S., Fujimoto, J., and Tahara, E. 1999. Microsatellite instabilities in gastric cancer patients with multiple primary cancers. *Int. J. Oncol. 14*: 151–155.

13
Helicobacter pylori-Infected Neoplastic Gastric Epithelium: Expression of MUC2 as a Biomarker

Halagowder Devaraj, A. Anand Kumar, and Niranjali Devaraj

INTRODUCTION

Inductive and sequential transformation of gastric cancer has been an excellent model for experimental search on genetic alterations and marker definitions. The development of gastric cancer is unique wherein several etiological agents, either alone or in conjunction feed into few common prognostic pathways whose manifestations can be histologically staged or verified. Ninety percent of gastric cancer is sporadic involving nongenomic factors such as chronic infection with *Helicobacter pylori* and food habits, especially the intake of high-salt diets that, in common, initiates a chronic inflammation response. A link between the chronic inflammation and neoplastic transformation can be serially investigated in gastric cancers, and definitive boundaries can be laid between the reversible and nonreversible changes in the protoplasmic properties of the inducted cells. Intestinal metaplasia has long been considered as the intermediate stage, progression beyond which irreversibly commits the cells for neoplastic transformation. Several molecular biomarkers have been considered for defining the early diagnosis and prognosis of gastric cancer with much emphasis on mucins (MUCs) and its epitopes. In this chapter we will review the molecular shifts in the expression of biomarkers, including the evaluation of MUC2, during the progression of gastric cancer with emphasis on methodology and molecular basics for diagnosis.

MOLECULAR MECHANISM OF GASTRIC CANCER

The pathogenesis of gastric cancer represents a classic example of gene- environment interactions. A strong association seen between *H. pylori*, a class I carcinogen (WHO), and gastric adenocarcinoma suggests that bacterial factors and host responses play a vital role in initiation and progression of the disease. It was reported by Mandell *et al*. (2004) that the persistence of *H. pylori* infection sensitizes the pattern recognition receptors (Toll-like receptors or TLR) and cellular mediators of inflammation that result in chronic Th1 mediated inflammatory response. Besides, abrogation of T cell mediated response or a skewed response towards Th2 polarisation protects the C57BL/6 from *H. pylori* induced atrophy and cancer, suggesting

that chronic exposure to increased amount of proinflammatory cytokines, such as Interleukin-8 (IL-8), IL1β, tumor necrosis factor-α (TNF-α), and the inflammatory mediator NFκB represents the switch between the temporary inflammation process (healing process), chronic lesion, and gastric cancer.

Inflammatory cytokines activate several signaling cascades that feed into apoptotic and proliferative responses. In C57BL/6 mouse models, Cai *et al*. (2005) showed that infection with *H. pylori* causes a concomitant increase in apoptosis and proliferation resulting in the loss of parietal and chief cells (atrophy) that developed along the sequence of intestinal metaplasia (expression of mucus metaplastic cells), dysplasia and invasive carcinoma. Indeed, El-Omar *et al*. (2003) clearly showed that Th1 cytokines such as IL1β induce gastric secretion, inhibit acid secretion and promote apoptosis, and along with TNFα and INFγ upregulate Fas antigen on gastric mucosal cells leading to alterations in cell growth. However, subsequent adaptive changes in the Fas signaling appear to increase the proliferation of cells and maintain homeostasis. Though the imbalance in apoptotic and proliferation ratio could contribute to progression from premalignant to malignant conditions, the microenvironment that favors this outcome has not yet been clear. The expansion of proliferative zone throughout the gastric glands suggests that additional cell populations or recruitment of cells might contribute to the proliferation under these circumstances. In addition, sustained hypoxia within the acidic inflammatory environment induces angiogenic signals that promote neovascularisation with defective podocyte coverage on the endothelium.

Recruitment and activation of cell mediators of inflammation (macrophages and monocytes) to the site of gastric lesion release products of oxidative burst such as superoxide free radicals and nitric oxide that might exert an oncogenic effect through direct DNA and protein damage, inhibition of apoptosis, mutations in genes involved in cellular repair functions (such as P53), and promotion of angiogenesis. Loss of heterozygosity (LOH) that is seen frequently associated with gastric carcinomas is also mediated by inflammatory response. Erosion of gastric mucosa by the persistent inflammatory process exposes the fragile niche of gastric stem cells to the inflammatory assault. The compensatory proliferative response of the resident stem cells to the erosion of gastric mucosa fail to repair the lesion due to high incidence of apoptosis of the transit multiplying populations. The hallmark of persistent inflammation is, therefore, defined by Coussens and Werb. (2002) as rapid proliferation with concomitant cell loss by apoptosis that fails to repair the lesion. Van den Brink *et al*. (2002) reported that parietal cell loss during gastric atrophy and progression to metaplasia is associated with a reduction in the amount of numerous secreted signals such as sonic hedgehog (SHH), which modulate the growth and differentiation of gastric progenitors. Studies by Cai *et al*. (2005) further revealed that a combination of parietal cell loss and chronic inflammation is a necessary event for progression along the metaplasia-dysplasia-carcinoma pathway.

Persistence of multiplication signals remains the principle cause for genetic mutations in the dividing cell population. Gopal *et al*. (2007) and Sakakura *et al*. (2005) pointed out that the spectrum of

molecular pathogenesis involves activation of protooncogenes, suppression of tumor suppressor genes either by point mutation, or LOH (P53), and epigenetic suppression of gene expression (Runx genes). Down regulation of cell surface adhesion receptors (E-cadherins) and extracellular matrix proteins promotes proliferation and metastasis of gastric cancer cells.

Sustained proliferations of cancer cells require continuous growth hormone signaling. The epidermal growth factor (EGF) family, including EGF, TGFα, IGF II, and bFGF are commonly overexpressed in intestinal-type carcinoma. Similarly, up regulation of EGF receptor is highly documented in gastric cancer. It was reported by Tahara (2004) that though EGF signaling alone can contribute to proliferation of gastric cancer cells, the interplay between IL-1α, IL-6, and the EGF/receptor system acts to stimulate gastric cancer growth. Besides, Yang *et al*. (2005) reported that the neovascularisation of the gastric cancer tissue induced by VEGF and bFGF favors growth and metastasis. Furthermore, reactive stromal fibroblasts of the cancer secrete HGF/SF (hepatocyte growth factor/scatter factor) that functions in a paracrine manner as a morphogen or motogen.

CELL AND TISSUE SPECIFIC EXPRESSION OF MUCINS

Differential expression of mucins has been a common feature of different types of cancers whose patterns could be used to distinguish different carcinomas. The overlapping and heterogeneous patterns of MUC1, MUC2, and MUC5AC expression observed by Byrd *et al*. (1997) in many tumors, particularly those of gastrointestinal origin, necessitates a clear definition in the use of these markers in the routine immunohistochemical assessment of primary and secondary carcinomas. Besides, it requires a clear understanding of the pattern of mucin expression in normal regions as well.

Mucins often show a coordinated expression in tissues with cells expressing unique mucin types reflecting on their functional specialization. It was reported by Byrd *et al*. (1997) and Reis *et al*. (1999) that normal gastric mucosa expresses abundant gastric mucins MUC1, MUC5AC, and MUC6 and none of the intestinal mucins. Distribution of these mucins specially varies within the gastric epithelium. Expression of MUC1 is confined to the principal and parietal cells of the oxynthic region and foveolar epithelium and a few mucous gland cells of the antrum. MUC5AC, on the other hand, is seen in foveolar epithelium and mucous neck cells of both antrum and body regions. Expression of MUC6 is detected in the cytoplasm of the pyloric gland and mucous neck cells in the stomach. MUC2 and MUC3 are not detected in the normal mucosa.

Though intestinal mucins are not expressed in normal gastric tissues, it becomes necessary to appreciate their expressive pattern under altered environmental and pathologic conditions. It was observed by Mizoshita *et al*. (2007) that the distribution of intestinal epithelial cell markers, MUC2 is normally seen in the cytoplasm of goblet cells of the small intestine and colon, and Villin is detected in the luminal surfaces of the absorptive cells of small intestine and colon. Nuclear staining of Cdx2, the intestinal genes transcription factor, is detected only in the normal epithelial cells of the colon.

Quantitative and qualitative alterations of mucin expression have been frequently reported in gastric carcinomas. Though the mucin expression pattern of gastric carcinomas is heterogeneous, a definitive pattern emerges from several cohort studies. Ho *et al*. (1995) and Subramani *et al*. (2006) reported that the pattern of mucin expression in gastric carcinoma includes the expression of normal gastric mucins (MUC1, MUC5AC and MUC6) and de novo expression of the intestinal mucin MUC2 (Figures 13.1 and 13.2). Furthermore, Filipe *et al*. (1994), and

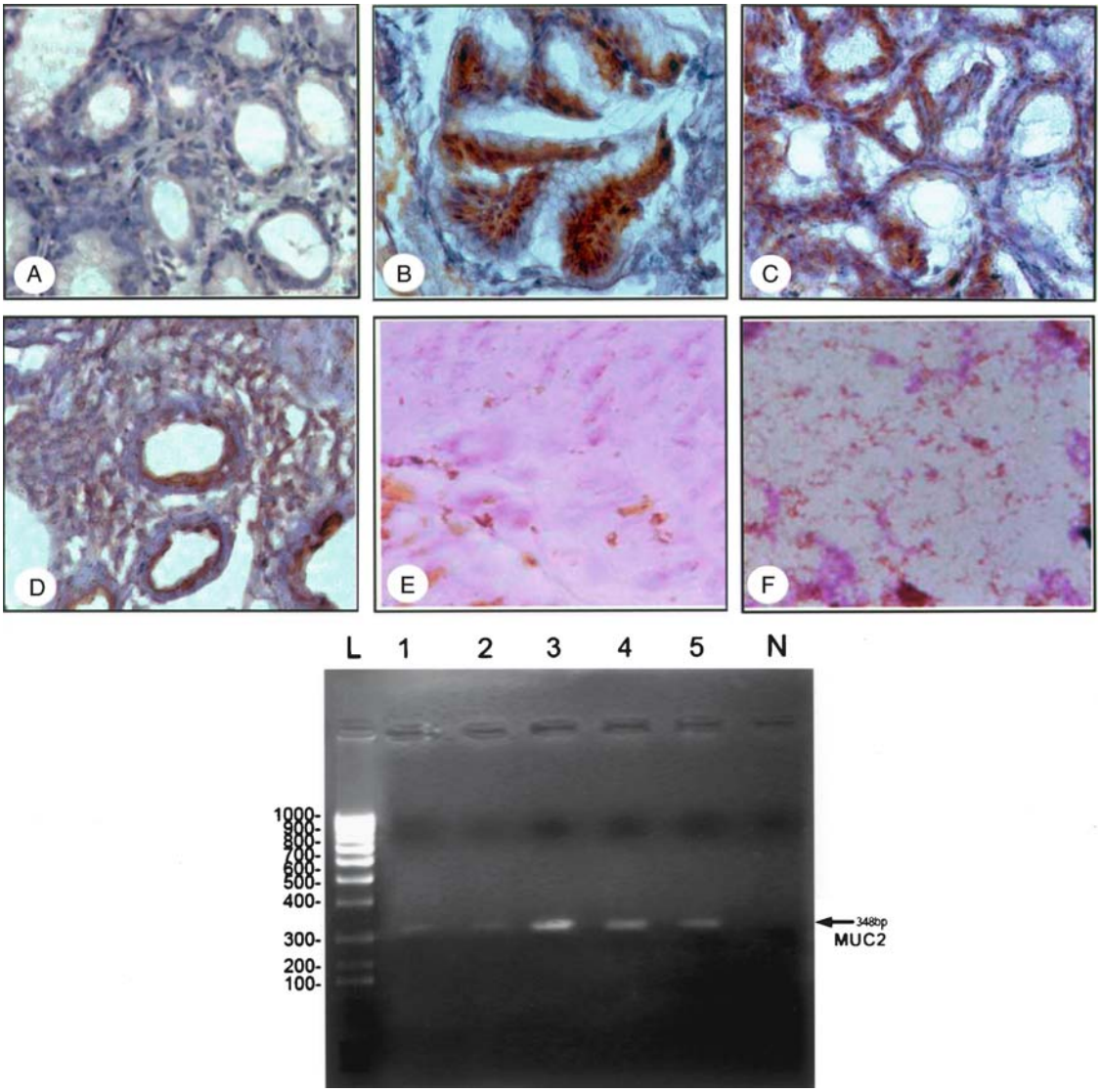

FIGURE 13.1. MUC2 expression in Human gastric epithelium. (A) Normal; (B) gastritis; (C) atrophic gastritis; (D) intestinal metaplasia; (E) dysplasia; (F) adenocarcinoma. (G) Agarose gel electrophoresis showing the expression of 348bp length of MUC2 mRNA in *H. pylori* infected pre-neoplastic and neoplastic human gastric epithelium. (Adopted from Subramani *et al*., 2006): Lane L: ladder (100 bp ladder); Lane 1: normal gastric epithelium; Lane 2: atrophic gastritis; Lane 3: intestinal metaplasia; Lane 4: dysplasia; Lane 5: adenocarcinoma; Lane N: negative control (without cDNA).

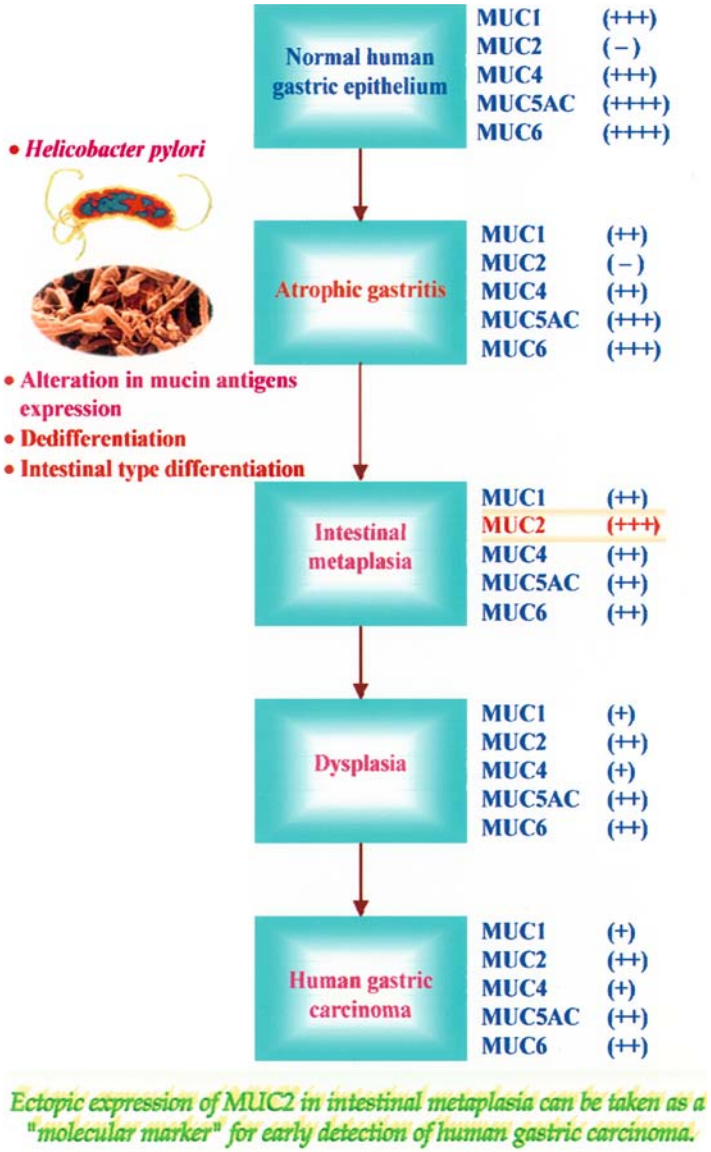

FIGURE 13.2. Expression profile of MUC1, MUC2, MUC4, MUC5AC, MUC6 in the progression of human gastric carcinoma. (Modified after Subramani *et al*., 2006.)

Reis *et al*. (1999, 2000) reported that the decrease in the expression of "gastric" mucins and a de novo expression of MUC2 could also be seen in the precancerous lesion of intestinal metaplasia. These observations suggest that the repertoire of mucins synthesized by gastric carcinoma cells is tightly associated with their differentiation program.

Laurén (1965) classified the major types of gastric carcinoma based on mucin expression as intestinal and diffused types. Histologically, the intestinal type is characterised by the presence of cohesive cells forming glandular and papillary structures and secrete acidic mucous (as seen in Alcian blue, pH 2.5/periodic acid Schiff staining) and the diffuse type of gastric

carcinoma is characterised by non-cohesive cells, the common presence of signet ring cells, and neutral mucous (stained by high iron diamine/Alcian blue (pH 2.5). Iniya *et al*. (2007) also reported such pattern of the mucin expression. The mixed type of gastric carcinoma has both of the above characteristics, and both acidic and neutral mucous. Interestingly, Parsonnet *et al*. (2005) reported that the prevalence of *H. pylori* in intestinal-type gastric cancer far exceeds the prevalence of *H. pylori* in diffuse type suggesting that *H. pylori* may be a cofactor in the development of intestinal-type gastric cancer. *H. pylori* infection appears to influence not only the progression of the disease but also the spatial and aberrant expression of mucins. Evaluation of aberrant expression of gland-type gastric mucins MUC6, MUC5, and MUC1 in the surface epithelium of *H. pylori*-infected patients by Byrd *et al*. (1997) revealed that MUC6 is limited to mucous glands of H.pylori-negative patients, whereas 72% of *H.pylori*-positive patients show MUC6 in surface mucous cells. In contrast, MUC5 mucin has been found in significantly fewer surface mucous cells of *H. pylori*-positive specimens. Reis *et al*. (2000) reported that unlike MUC5AC, which is significantly associated with diffuse type carcinomas and suggestive of "gastric" differentiation, the MUC6 is not associated with the histological type of the gastric carcinomas. Similarly, studies by Kamangar *et al*. (2006) on conditional logistic regression models to estimate the odds ratios (ORs) and 95% confidence intervals (CIs) for the association of *H. pylori* seropositivity revealed a strong association with the risk of noncardia gastric cancer and an inverse association with the risk of gastric cardia cancer. However, the trend seen with mucin expressions is similar, with a decrease in the normal gastric mucins MUC1, MUC5AC, and MUC6, and an increase in "aberrant" expression of MUC2 and MUC3 that defines the intestinal type of cancers.

Differential expression of mucins in carcinoma indicates the nature and type of cancer. For example, MUC1 is expressed in most of the cancers except adrenocortical and hepatocellular carcinomas. Expression of MUC2 is specific and confined to tumors of gastrointestinal origin. MUC5AC shows positive immunoreactivity in pancreatic ductal and endocervical adenocarcinomas. A MUC1+/MUC2−/MUC5AC− immunophenotype is observed in most breast, lung, kidney, bladder, endometrial, and ovarian carcinomas; MUC1+/MUC2−/MUC5AC+ is characteristic of pancreatic ductal adenocarcinomas and cholangiocarcinomas. These molecular phenotypes could be used to detect the metastatic populations in ectopic sites. Attempts have been already made to distinguish the breast cancer metastatic populations in the gastric tissues using mucin histochemical markers. Indeed, Yu *et al*. (2001) have used MUC1, MUC2, and MUC 5AC QC RT-PCR to detect the presence of exfoliated gastric cancer cells in metastatic pleural effusions with high degree of sensitivity and specificity.

MOLECULAR GENETIC ALTERATIONS AND MUCIN EXPRESSION AS INDICATORS OF MOLECULAR LESIONS

Mucin phenotypes reflect specific molecular genetic alterations that can be used to categorize the intramucosal neoplasias

and prognosis of gastric tumors. Since molecular genetic changes in general are responsible for the biological characteristics of neoplastic cells, it is likely that mucin phenotype would specify the genetic alterations and predict the behaviour of such cells. Fiocca *et al*. (2001) found that among differentiated-type adenocarcinomas of the stomach, those lesions that show higher frequency of *p53* gene mutations and extensive loss of heterozygosity (LOH) of cancer-related genes tend to differentiate into intestinal-type carcinomas. On the contrary, Sugai *et al*. (2004) found that diffuse-type carcinomas have infrequent *p53* gene mutations and a low frequency of LOH. These genetic profiles of differentiated-type adenocarcinomas of the stomach suggest that intestinal-type carcinomas are genetically distinct from diffuse-type carcinomas and originate and progress independently. Indeed, Mizoshita *et al*. (2007) reported that intestinal type cancers develop from intestinal metaplasia and assume differentiated phenotype, whereas gastric cancers develop from gastric proper.

Unlike gastric adenocarcinomas, which are positive for MUC5AC and/or HIK1083, intestinal-type adenocarcinomas (differentiated-type carcinomas) have a glandular structure, and subclassified into three groups based on their mucin phenotype: foveolar-, intestinal- and combined types. Endoh *et al*. (2000a, b) defined a foveolar-type cancer as a tumor having gastric foveolar epithelium morphologically with intracytoplasmic mucin of the gastric foveolar epithelium type (50% of neoplastic cells are positive for galactose oxidase-Schiff (GOS) stain or human gastric mucin), which roughly corresponds to gastric phenotype and derived from gastric proper epithelium. Intestinal phenotype is defined as a tumor with positive immunostaining with an MUC2 and/or a CD10 antibody (30% of neoplastic cells). MUC2 expression is seen within the cytoplasm around the nuclei, whereas CD10 staining was found along the brush border. The combined-type tumors show both foveolar and intestinal phenotypes (30% of neoplastic cells express both foveolar and intestinal type markers).

Foveolar-type tumors are prone to lose their glandular structure and progress to undifferentiated-type tumors and thus can be regarded as precursors of the undifferentiated-type tumors. Histopathologically such lesions are difficult to distinguish from regenerative or inflammatory changes in the foveolar epithelium, rather than the neoplastic lesion. Endoh *et al*. (2000a) found that such type of tumor often shows a low-grade cytologic atypia even in cases with overt invasion, but intramucosal tumorous elements are generally well preserved. Indeed, 75% of intramucosal foveolar-type tumors are classified as noninvasive neoplasia, low-grade especially when biopsy samples are taken superficially.

Frequent microsatellite instability (MSI), which represents mutations of short-tandem repeat sequences, is closely related to expression of the foveolar mucin phenotype. Kushima and Hattori (1993) reported that infrequent MSI and considerable *p53* mutations are seen in the tumors with a distinct intestinal cellular phenotype (the intestinal-type tumor). Studies on the gastric phenotypes of cancers revealed that the frequency of 3p allelic loss appears to be higher than that of other microsatellite markers, whereas 5q allelic loss is frequently

found in intestinal phenotype cancers. The genetic profiles of mixed phenotype cancers have two distinct genetic types: LOH and MSI types. In the former, 5q, 3p and 18q allelic losses are seen frequently in intramucosal carcinomas, wehereas 17p, 1p, and 9p allelic losses are associated with the development of submucosal carcinomas. MSI is significantly observed only in mixed phenotype cancers.

Epigenetic methylation-associated inactivation of the *hMLH1* mismatch repair gene is a potent trigger of MSI. Endoh *et al*. (2000a) reported that in foveolar-type tumors, the frequency of MSI is significantly higher in early lesions (mucosa and submucosa) than advanced lesions (subserosa and exposed beyond the subserosa). Similarly, the frequency of both MSI and hypermethylation of *hMLH1* is significantly higher in the foveolar type than in the intestinal-type tumors. Sukod *et al*. (2003) reported that generally the frequency of MSI in differentiated-type carcinomas is less in early (9–19%) than in advanced (27–38%) stages indicating that the MSI phenotype is a later event and secondarily accumulated during tumor progression. The high incidence of MSI in early foveolar-type tumors (71%) suggests that hypermethylation of *hMLH1* is an initial vital event that promotes tumorigenesis and distinguishes between foveolar-type phenotypic expression from the intestinal markers.

Based on the origin of stomach cancers from a progenitor cell specializing towards an endocrine or exocrine-cell lineage, Takenaka *et al*. (2007) classified stomach epithelial tumors into two major types: Exo-cell type (adenomas and carcinomas) and End-cell type [carcinoid tumors and endocrine cell carcinomas (ECC)]. Expression of MUC5AC and MUC6 are predominant in gastric Exo-cell phenotype, whereas MUC2 and villin are typical of the intestinal Exo-cell phenotype. Similarly, Otsuka *et al*. (2005) found that gastrin and somatostatin are markers for gastric End-cell phenotype, whereas GLP-1, GIP, and glicentin are typical of intestinal End-cell phenotype. Furthermore, Naritomi *et al*. (2003) opined that the presence of CgA, an End-cell differentiation marker in majority of gastric cancers suggest that cancer progressed from a common progenitor of Exo-cell and End-cell types. Stomach tumorous areas are, therefore, further classified as endocrine-gastric (e-G type) or endocrine-intestinal (e-I type), respectively, with at least one gastric or intestinal End-cell phenotype, and endocrine-gastric-and-intestinal mixed phenotype (e-GI type) when both gastric and intestinal markers are present. Those showing neither gastric nor intestinal phenotypic expression are grouped as endocrine-null type (e-N type). Besides, stomach tumorous areas positive for at least one gastric or intestinal Exo-cell marker are classified as gastric (G type) or intestinal (I type) phenotype, respectively. Those, which exhibited both phenotypes are classified as gastric-and-intestinal mixed (GI type), while those showing neither are grouped as null (N type).

CHARACTERISATION OF MUC2 EXPRESSION AND EARLY MOLECULAR DIAGNOSIS OF GASTRIC CANCER

Altered homeostasis between apoptotic and proliferative responses by the gastric epithelium in response to *H. pylori*

mediated chronic inflammation appear to initiate cellular and molecular variations that manifest in the form of ectopic expression of mucins and cellular phenotypes. Correa (1988) delineated these earliest changes that often progress in a predictable sequence and could be used for differential diagnosis. Though the Correa pathway of gastric adenocarcinoma sequence simplifies the identification of preneoplastic lesions, it is essentially a complex developmental signature, often complicated by the host response to the presence of *H. pylori*. Furthermore, extensive studies have indicated the convergences and preferences in the neoplastic transformation sequences that provide prognostic significance for gastric carcinogenesis. Indeed, gastric atrophy is sometimes considered as a better indicator of progression to gastric carcinoma than intestinal metaplasia though the latter is generally accepted as the precancerous intermediary stage that can be histologically verified easily.

Atrophic gastritis is frequently associated with the presence of antral-type mucosa at the site (termed antralization) of lesions. The prevalence of atrophic gastritis was higher in the presence of antralization than without antralization. The association between antralization at gastric body and fundus also appeared to be associated with atrophic gastritis and intestinal metaplasia of these sites. Scotiniotis *et al*. (2000) compared the alterations in the apoptotic (AI) and proliferation (PI) indices in antral epithelium from individuals negative for *H. pylori* (Hp), those with Hp-induced gastritis and those with Hp-induced gastritis with regions having gastric intestinal metaplasia, and revealed that apoptosis and proliferation significantly increased in Hp-positive (Hp(+)) patients compared to Hp-negative (Hp(−)) patients. Significantly, within the foci of intestinal metaplasia of Hp(+) patients apoptosis is markedly reduced compared with surrounding gastritis, whereas proliferation is not altered resulting in a lower AI/PI ratio in intestinal metaplasia than in surrounding gastritis. Hp-induced gastritis is thus associated with increased epithelial apoptosis and proliferation compared with uninfected controls. In intestinal metaplasia, proliferation remains increased but apoptosis reverts to normal levels and this perhaps contributes to Hp-associated gastric carcinogenesis, apoptosis, and proliferation.

Development of intestinal metaplasia as a pathological protective response to chronic inflammation is, though partially accepted, the implications for such a change is quite apparent as it is associated with substantial alterations in cell surface molecules that determine adhesive and functional attributes of the cells. Classically, Correa (1988) defined intestinal metaplasia as the replacement of original gastric glands with straight tubular crypts lined by alternating absorptive and goblet cells with inflammatory infiltrates in the lamina propria or simply the substitution of the gastric mucosa by an epithelium that resembles the intestinal mucosa. Filipe *et al*. (1994) showed that the glycosylation pattern in intestinal metaplasia differs from that of normal gastric mucosa. Accumulation of simple mucin-type carbohydrate antigens and abnormal expression of Lewis antigens, i.e., aberrant expression of Lewis a defines intestinal metaplasia of the human stomach. Nevertheless, the presence of these epitopes in normal gastric tissues

albeit colocalised with mucins limited their differential diagnostic importance.

Intestinal metaplasia is often subdivided to reflect the prognostic importance. Based on histopathological and histochemical studies, Filipe *et al*. (1994) identified three main types of intestinal metaplasia. (1) type I or complete type, that show mature absorptive cells, Paneth cells, and goblet cells, secrete sialomucins and correspond to the small intestine phenotype; and (2) the types II and III, which encompasses incomplete type, has columnar "intermediate" cells in various stages of differentiation and goblet cells secreting sialo and/or sulfomucins. Type II differs from type III intestinal metaplasia regarding the mucins produced by columnar cells: the neutral and acid sialomucins in type II and sulfomucins in type III. Concomitant with the histological classification, Matsukura *et al*. (1980) alternatively classified intestinal metaplasia into three types, reflecting on the marker enzymes they secrete. The complete type is associated with the intestinal marker enzymes sucrose α-D-glucohydrolase, α,α-trehalase, aminopeptidase-microsomal (APM), and alkaline phosphatase (ALP). This type of tissue contains goblet cells and Paneth's cells but not high-iron diamine (HID)-positive mucin staining with HID-alcian blue. The incomplete type is associated with sucrose α-D-glucohydrolase, APM, goblet cells, and HID-positive mucin but not with α,α- trehalase, ALP, or Paneth's cells. Gastric lesions often show a mixture of these two types and, therefore, intestinal metaplasia is divided based on the mucin expression as complete type only (class I), incomplete type only (class II), and a mixture of areas of the complete and incomplete types (class III). Though *H. pylori* infection is common in preneoplastic gastric lesions, the intestinal metaplasia of type III variant is predominant only in the mucosa that is associated with glandular and mixed (but not diffuse) early cancers. Similarly, in type I complete intestinal metaplasia, the levels of "gastric" mucins, MUC1, MUC5AC, and MUC6 are markedly decreased, though they are maintained in incomplete intestinal metaplasia (both type II and type III). Such apparent variations in the molecular phenotypes suggest that complete and incomplete intestinal metaplasia represent divergent differentiation programs, both starting from *H. pylori* gastritis. Filipe *et al*. (1994) suggested that the presence of nongastric, small intestine phenotype in complete type I intestinal metaplasia reflects a complete switch in the differentiation program, whereas the mixed gastric and intestinal phenotype of incomplete (type II and type III) shows an aberrant differentiation program with apparent absence of phenotypes observed in normal adult gastrointestinal epithelia. Given the increased risk of malignant transformation of the gastric mucosa from type III intestinal metaplasia, despite the apparent similarity of the mucin protein expression in both type II, it is plausible that incomplete type II intestinal metaplasia may represent a first step in the intestinal metaplasia pathway, which may evolve to complete intestinal metaplasia with loss of expression of the "gastric" mucins, MUC1, MUC5AC, and MUC6, or to incomplete type III intestinal metaplasia by further deregulation of mucin glycans processing with sulfation. In most of the cases only the type III variant with subsequent p53 gene alteration, and dysplasia ends in glandular cancer. In the

other pathway, diffuse cancer apparently arises directly from hyperplastic, sometimes atypical tissue.

Subtyping of intestinal metaplasia is useful for identifying individuals at high risk for gastric cancer. Reis *et al*. (1999) found that the relative risk of developing gastric cancer based on Cox's proportional hazards model was 2.14 for type II and 4.58 for type III, compared with type I. Such risk is especially increased for a subgroup of type III secreting sulphomucins in their goblet cells than those negative to sulphomucins (types I–II). Despite the advances and availability of plethora of cell surface markers for intestinal metaplasia characterization, requirement for a simple clinically oriented procedure that distinguishes one progressive premalignant lesion from the other is still lacking. Ectopic expression of MUC2 could be given as a marker for intestinal metaplasia but with apparent inconsistency in defining the potential lesions. It is, therefore, safe to look for a shift in mucin expression (increase in the expression of MUC2 and MUC3 and a decrease in MUC1, MUC5AC, and MUC6) as characteristic of intestinal metaplasia for a better prognostic evaluation. Detailed studies of expression of mucins in various types of intestinal metaplasia, however, suggest that there exist a subtle variation in the type and degree of mucin expressed in different cell types of intestinal metaplasia tissue. Based on these parameters, the immunodetection of intestinal metaplasia types can be safely defined as:

Type I Intestinal Metaplasia

Absence or markedly decreased levels of normal gastric mucins (MUC1, MUC5AC, and MUC6) and *de novo* expression of the MUC2 intestinal mucin in most goblet cells. No expression of MUC1 in goblet and columnar cells except for few superficial staining in columnar cells. No expression of MUC5AC and MUC6 either in the goblet or in the columnar cells except for rare MUC5AC immunoreactivity in a few superficial columnar cells.

Type II Intestinal Metaplasia

Recapitulation of normal expression of both MUC1 and MUC5AC in 75% of goblet and in columnar cells though MUC5AC is seen only in superficial metaplastic glands than in the deep parts. Reduced MUC6 expression in goblet and columnar cells. Fifty percent of the goblet cells and 25% of the columnar cells in all cases expresses MUC2. Mucin expression in type II intestinal metaplasia is thus characterised by maintenance or reexpression of MUC1 and MUC5AC mucins, decrease in the expression of the MUC6 gastric mucin, and a *de novo* expression of the intestinal mucin.

Type III Intestinal Metaplasia

Identical to that of type II intestinal metaplasia. Both MUC1 and MUC5AC expression are seen in 75% of the goblet and columnar cells. MUC5AC expression is evident in superficial part of the metaplastic glands. Reduced MUC6 expression and d*e novo* expression of MUC2 seen in 75% of goblet and, 25% of columnar cells.

Although cytological examination is the most informative laboratory procedure for diagnosis of intestinal metaplasia and gastric cancers, novel approaches are being employed to increase the efficiency and

reliability of diagnosis in both primary and secondary cancers. Yu *et al*. (2001) have used quantitative RT-PCR to identify malignant pleural effusions of gastric carcinoma with great accuracy. The advantage of such molecular techniques is that they are sensitive and screen multiple markers with consistency and reproducibility. The test sensitivity and specificity of quantitative RT-PCR ranged ~ 31–95% and 61–95%, respectively, with the accuracy at 65–85%. Similar approach albeit a modified one was also attempted to quantify the mucin transcripts in conjuctival samples using competitive PCR. Quantitative analysis of mucin transcripts using competing exogenous template allows us to determine the levels of mucin by densitometric analysis following electrophoresis using internal standards. Because epigenetic alterations control the MUC2 expression, Endoh *et al*. (2000a) resorted to specific techniques that identify methylated forms of alleles that could provide valuable information regarding the expression of genes. Methylation-specific polymerase chain reaction (MSP) distinguishes unmethylated from methylated alleles of a MUC2 gene based on sequence changes that are produced following bisulfite treatment of DNA, which converts unmethylated cytosines to uracils, while leaving methylated cytosines unaffected. Subsequent PCR using primers specific to sequences that correspond to either methylated or unmethylated DNA could identify the methylated pattern. Similarly, Reis *et al*. (2000) used Western blot methods to analyse the expression of antral and carcinoma mucins after being partially deglycosylated with trifluoromethanesulfonic acid (TFMSA).

Despite the recent advances in characterisation and diagnosis of intestinal metaplasia lesions and altered mucin expressions, it is a challenging issue to bring them as a routine clinical diagnostic tool. Immunohistochemistry is the best and efficient method for characterising such lesions and with the differential diagnosis involving a spectrum of mucin markers, it would provide invaluable prognostic indications with least imperfections or false-positivity. Nevertheless, considering the laborious nature of screening multiple mucin markers and the narrow definitions and margins of imperfections involved, it can be safely assumed that intestinal metaplasia with MUC2 ectopic expression is a prognostic marker for gastric carcinogenesis, which might evolve through incomplete type III grade.

MOLECULAR MECHANISM OF DIFFERENTIAL EXPRESSION OF MUC2

Though considered to be a protective mucin for intestinal epithelial surface, the regulatory mechanism of MUC2 mucin production in response to normal and pathological conditions is not completely understood. MUC2 is a secretory glycoprotein produced from intestinal goblet cells and is a major component of the intestinal epithelial mucus. *De novo* expression of MUC2 in gastric tissues is considered as a marker for IM and may have potential implications for the early diagnosis and prediction of tumor behavior.

MUC2 is clustered along with MUC5AC, MUC5B, and MUC6 on chromosome 11p15 that encodes for large secreted gel-forming mucins. They are frequently silenced in cancers due to epigenetic gene silencing in GC-rich structure of their pro-

moters. Studies by Vincent *et al*. (2007) have indicated that MUC2 gene is regulated by site-specific DNA methylation associated with establishment of a repressive histone code, whereas in MUC5B gene hypermethylation of its promoter is responsible for the silencing. Though they are clustered in the same region, the expression of *MUC5AC* is not frequently regulated by epigenetic mechanisms and the methylation of *MUC6* promoter is not correlated to its silencing, indicating that the molecular mechanisms regulating their expressions are not similar. Nevertheless, both *MUC2* and *MUC5B* epigenetic regulations are cell-specific, depended on differentiation status of the cell, and inhibited by activation by transcription factors that favor relaxed organisation of chromatin structure.

Transdifferentiation of the gastric mucosa to an intestinal phenotype requires alterations in the gene expression mediated by intestine-specific homeobox genes *Cdx-1* and *Cdx.2*. Aslam *et al*. (2001) reported that intestinal metaplasia and subset (intestinal-type) of gastric carcinomas show aberrant expression of Cdx-1 and/or Cdx-2 that play an important role in intestinal differentiation program, partially by upregulating *MUC2* expression at the transcriptional level. Studies on transgenic models suggest that they act as a transcription factor for several intestinal genes such as sucrase-isomaltase, lactase-phlorizin hydrolase, intestine phospholipaseA/lysophospholipase, and claudin-2. It appears that Cdx-2 is the principal regulator of MUC2 expression both in gastric and intestinal cancer cells, whereas Cdx-1 only transactivates *MUC2* in intestinal cells. Though CDX2 can initiate intestinal metaplasia transition in the gastric mucosa, Dang *et al*. (2006) reported that no significant differences in the proliferation of $CDX2^{-/-}$ cells compared to $CDX2^{+/+}$ cells were observed in *in vitro* or *in vivo* models, except for altered expression of genes involved in intestinal glandular differentiation and adhesion.

The promoter of *MUC2* contains putative binding sites for Cdx-1 or Cdx-2, which function as transcriptional regulators of *MUC2* expression. Studies by Lania *et al*. (1997) revealed that MUC2 expression is also regulated by Sp1 family of transcription factors, p53, lipopolysaccharides, epidermal growth factor, and by several cytokines. Ikeda *et al*. (2007) subsequently showed that cytokines including TNF-α can upregulate MUC2 in human gastric epithelial cells via signaling pathways, involving both NIK and PI3K/Akt, which converge at the common IKK/I-kappaB/NF-kappaB pathway. Pathogen-associated molecular patterns (PAMPs) can also upregulate CDX2 and MUC2 expression through TLR2 and TLR4 mediation involving nuclear factor-κB (NF-κB).

The ability of Sp1 factor in establishing the transcriptional competence of MUC2 is partially by preventing the methylation of CpG islands. Velcich *et al*. (1997) reported that the region surrounding the two Cdx-2 binding sites of MUC2 is GC-rich and binds Sp1. Patricia *et al*. (2003) observed that though the inhibition of Sp1 binding blocked the expression of *MUC2* in the HT29 adenocarcinoma cell line, it is not yet clear whether it is due to epigenetic repression or due to intrinsic transcriptional requirement. Several other transcription factors of the zinc finger family such as GATA-4/-5/-6 also have a cell-specific pattern of expression along with the gastrointestinal tract, and are

important factors in the differentiation of gastrointestinal cells. Synergistic activity between GATA and Cdx factors is already suggested for other intestine specific genes, and Cdx-2 and GATA-4/-5 factors are recently suggested to be associated with gastric carcinogenesis.

Transgenic experiments in mice that express Cdx2 provides the direct evidence for intestinal differentiation of gastric epithelium. Velcich *et al*. (1997) showed that CDX2 expression in transgenic mice resulted in a complete intestinalization of the gastric mucosa, development of goblet cells expressing acidic-type mucins, and formation of enterocyte-like cells expressing alkaline phosphatase and enteroendocrine type cells. The relationship between CDX2 expression and intestinal differentiation suggests that CDX2 may serve as a specific marker for epithelial neoplasms of the gastrointestinal tract.

In conclusion, mucin biomarkers have the potential to provide both sensitive and specific tests, which can be used in the screening, early diagnosis, staging, and surveillance of cancer. Given the diversity of gastric cancers, no one genetic marker is likely to be useful by itself. MUC2 ectopic expression in intestinal metaplastic condition comes very close to be an independent prognostic marker for gastric carcinogenesis. Nevertheless, its expression is more pronounced in intestinal type gastric cancers and to mucinous differentiation. Diffuse type cancer originates independently of intestinal type and does not involve intestinal metaplastic sequence. Diffuse type cancers express gastric mucins that are independent and exclusive of MUC2 expression. Besides, cell and tissue specific variations in the expression of mucin bound to inflict diagnostic contradictions especially when there is inconsistency in biopsy specimens. Considering that gastric carcinoma exhibit cellular diversity and clonal variations, and often with mixed types, it could be safely assumed that probing a biological specimen with a minimal set of both gastric and intestinal mucins would provide an excellent prognostic indication regarding the stage and development of cancer. Indeed, it would be the ideal signature for early diagnosis and conditions such as intestinal metaplasia.

Acknowledgements. We gratefully acknowledge LTMT, ICMR, CSIR and Special Assistance Program of UGC for funding the research programs. I thank Dr. V. Jayanthi, Department of Medical Gastroenterology, Stanley Medical College, Chennai for providing the samples for the work. Special thanks to Dr. V.P. Bhavanandan, Penn State University, Dr. Celso A. Reis, University of Porto and Dr. Sandra J. Gendler, Mayo Cilnic Scottsdale, Arizona, for providing the antibodies. I thank all my research scholars who have made the work possible.

REFERENCES

Aslam, F., Palumbo, L., Augenlicht, L.H., and Velcich, A. 2001. The Sp family of transcription factors in the regulation of the human and mouse *MUC2* gene promoters. *Cancer Res. 61*: 570–576.

Byrd, J.C., Yan, P., Sternberg, L., Yunker, C.K., Scheiman, J.M., and Bresalier, R.S. 1997. Aberrant expression of gland-type gastric mucin in the surface epithelium of *Helicobacter pylori*-infected patients. *Gastroenterology 113*: 455–464.

Cai, X., Carlson, J., Stoicov, C., Li, H., Wang, T.C., and Houghton, J. 2005. *Helicobacterfelis* eradication restores normal architecture and inhibits gastriccancer progression in C57BL/6 mice. *Gastroenterology 128*: 1937–1952.

Correa, P. 1988. A human model of gastric carcinogenesis. *Cancer Res. 48*: 3554–3560.

Coussens, L.M., and Werb, Z. 2002. Inflammation and cancer. *Nature 420*: 860–867.

Dang, L.H., Chen, F., Knock, S.A., Huang, E.H., Feng. J., Appelman, H.D., and Dang, D.T. 2006. CDX2 does not suppress tumorigenicity in the human gastric cancer cell line MKN45. *Oncogene 25*: 2048–2059.

El-Omar, E.M., Rabkin, C.S., Gammon, M.D., Vaughan, T.L., Risch, H.A., and Schoenberg, J.B. 2003. Increased risk of noncardia gastric cancer associated with proinflammatory cytokine gene polymorphisms. *Gastroenterology 124*: 1193–201.

Endoh, Y., Tamura, G., and Ajioka, Y. 2000a. Frequent hypermethylation of the hMLH1 gene promoter in differentiated-type tumors of the stomach with the gastric foveolar phenotype. *Am. J. Pathol. 157*: 717–722.

Endoh, Y., Sakata, K., and Tamura, G. 2000b. Cellular phenotypes of differentiated-type adenocarcinomas and precancerous lesions of the stomach are dependent on the genetic pathways. *J. Pathol. 191*: 257–263.

Filipe, M.I., Muños, N., Matko, I., Kato, I., Pompe–Kirn, V., Jutersek, A., Teuchmann, S., Benz, M., and Prijon, T. 1994. Intestinal metaplasia types and risk of gastric cancer. *Int. J. Cancer 57*: 324–329.

Fiocca, R., Luinetti, O., and Villani, L. 2001. Molecular mechanisms involved in the pathogenesis of gastric carcinoma: interactions between genetic alterations, cellular phenotype and cancer histotype. *Hepatogastroenterology 48*: 1523–1530.

Gopal, U., Jayanthi, V., Devaraj, N., and Devaraj, H. 2007. Interaction of MUC1 with β – catenin modulates the Wnt target gene cyclinD1 in H. pylori induced gastric cancer. *Mol. Calcinog. 46*: 807–817.

Ho, S.B., Shekels, L.L., Toribara, N.W., Kim, Y.S., Lyftogt, C., Cherwitz, D.L., and Niehans, G.A. 1995. Mucin gene expression in normal, preneoplastic, and neoplastic human gastric epithelium. *Cancer Res. 55*: 2681–2690.

Iniya, M., Duraibabu, S., and Devaraj, H. 2007. Mucin glycoarray in gastric and gall bladder epithelia. *J. Carcinog. 6*:10.

Ikeda, H., Motoko, S., Akria, I., Yasunori, S., Kenichi, H., Yoh, Z., Hideaki, K., and Yasuni, N., 2007. Interaction of Tol-like receptors with bacterial components induces expression of CDX2 and MUC2 in rat biliary epithelium in vivo and in culture. *Lab. Invest. 87*: 559–571.

Kamangar, F., Dawsey, S.M., Blaser, M.J., Perez-Perez, G.I., Pietinen, P., Newschaffer, C.J., Abnet, C.C., Albanes, D., Virtamo, J., and Taylor, P.R. 2006. Opposing risks of gastric cardia and noncardia gastric adenocarcinomas associated with *Helicobacterpylori* seropositivity. *J. Natl. Cancer Inst. 98*: 1445–1452.

Kushima, R., and Hattori, T. 1993. Histogenesis and characteristics of gastric-type adenocarcinomas in the stomach. *J. Cancer Res. Clin. Oncol. 120*: 103–111.

Lania, L., Majello, B., and De Luca, P. 1997. Transcriptional regulation by the SP family protein. *Int. J. Biochem. Cell Biol. 29*: 1313–1323.

Laurén, P. 1965. The two histological main types of gastric carcinoma: diffuse and so-called intestinal-type carcinoma. *Acta. Pathol. Microbiol, Scand. 64*: 31–49.

Mandell, L., Moran, A.P., Cocchiarella, A., Houghton, J., Taylor, N., and Fox, J.G. 2004. Intact Gram-negative *Helicobacterpylori*, *Helicobacter felis*, and *Helicobacter hepaticus* bacteria activate innate immunity via Toll-like receptor 2 but not Toll-like receptor 4. *Infect Immun. 72*: 6446–6454.

Matsukura, N., Suzuki, K., Kawachi, T., Aoyagi, M., Sugimura, T., Kitaoka, H., Numajiri, H., Shirota, A., Itabashi, M., and Hirota, T. 1980. Distribution of marker enzymes and mucin in intestinal metaplasia in human stomach and relation to complete and incomplete types of intestinal metaplasia to minute gastric carcinomas. *J. Natl. Cancer Inst. 65*: 231–240.

Mizoshita, T., Tsukamoto, T., Inada, K.-I., Hirano, N., Tajika, M., Nakamura, T., Ban, H., and Tatematsu, M. 2007. Loss of MUC2 expression correlates with progression along the adenoma-carcinoma sequence pathway as well as *de novo* carcinogenesis in the colon. *Histol. Histopathol. 22*: 251–260.

Naritomi, K., Futami, K., Arima, S., and Iwashita, A. 2003. Malignant potential regarding mucin phenotypes and endocrine cell differentiation in gastric adenocarcinoma. *Anticancer Res. 23*: 4411– 4422.

Otsuka, T., Tsukamoto, T., Mizoshita, T., Inada, K., Takenaka, Y., Kato, S., Yamamura, Y., Miki, K., and Tatematsu, M. 2005. Coexistence of gastric- and intestinal-type endocrine cells in gastric and intestinal mixed intestinal metaplasia of the human stomach. *Pathol. Int. 55*: 170–179.

Parsonnet, J., Vandersteen, D., Goates, J., Sibley, R.K., Pritikin, J., and Chang, Y. 2005. Helicobacterpylori infection in intestinal-and diffuse-type gastric adenocarcinomas. *J. Natl. Cancer Inst. 83*: 640–643.

Patrícia, M., Nicolas, J., Raquel, A., Marie-Paule, D., Jacinta, S., Elisabete, S., Pascal, P., Filipe, S.S., Celso, R., Debra, S., Isabelle, V.S., and Leonor, D., 2003. Human *MUC2 Mucin Gene Transcriptionally Regulated by Cdx Homeodomain* Proteins in Gastrointestinal Carcinoma Cell Lines. *J. Bio. Chem., 278*, 51549–51556.

Reis, C.A., David, L., Correa, P., Carneiro, F., de Bolo's, C., Garcia, E., Mandel, U., Clausen, H., and Sobrinho-Simo˜es, M. 1999. Intestinal metaplasia of human stomach displays distinct patterns of mucin (MUC1, MUC2, MUC5AC, and MUC6) expression. *Cancer Res. 59*: 1003–1007.

Reis, C.A., David, L., Carvalho, F., Mandel, U., de Bolós, C., Mirgorodskaya, E., Clausen, H., and Sobrinho-Simo˜es, M. 2000. Immunohistochemical study of the expression of MUC6 mucin and co-expression of other secreted mucins (MUC5ACand MUC2) in numan gastric varcinomas. *J. Histochem. Cytochem. 48*: 377–388.

Sakakura, C., Hagiwara, A., Miyagawa, K., Nakashima, S., Yoshikawa, T., Kin, S., Nakase, Y., Ito, K., Yamagishi, H., Yazumi, S., Chiba, T., and Ito, Y. 2005. Frequent downregulation of the runt domain transcription factors RUNX1, RUNX3 and their cofactor CBFB in gastric cancer. *Int. J. Cancer 113*: 221–228.

Scotiniotis, I.A., Rokkas, T., Furth, E.E., Rigas, B., and Shiff, S.J. 2000. Altered gastric epithelial cell kinetics in Helicobacterpylori-associated intestinal metaplasia: implications for gastric carcinogenesis. *Int. J. Cancer 85*: 192–200.

Subramani, D.B., Jayanthi, V., Devaraj, N., Reis, C.A., and Devaraj, H. 2006. Expression profile of mucins (MUC2, MUC5AC and MUC6) in *Helicobacter pylori* infected pre-neoplastic and neoplastic human-gastric epithelium. *Mol. Cancer 5*: 10.

Sugai, T., Habano, W., Uesugi, N., Jao, Y., Nakamura, S., Abe, K., Takagane, A., and Terashima, M. 2004. Three independent genetic profiles based on mucin expression in early differentiated-type gastric cancers—a new concept of genetic carcinogenesis of early differentiated-type adenocarcinomas. *Modern Pathol. 17*: 1223–1234.

Sukod, F., Kuroda, N., and Beothe, T. 2003. Deletion of chromosome 3p14.2-p25 involving the VHL and FHIT genes in conventional renal cell carcinoma. *Cancer Res. 63*: 455–457.

Tahara, E. 2004. Genetic pathways of two types of gastric cancer. *IARC Sci. Publ. 157*: 327–349.

Takenaka, Y.T., Tsukamoto, T., Mizoshita, N., Ogasawara, N., Hirano, T., Otsuka, H., Ban T. Nakamura, Yamamura, Y., Kaminishi, M., and Tatematsu, M. 2007. Gastric and intestinal phenotypic correlation between exocrine and endocrine components in human stomach tumors. *Histol. Histopathol. 22*: 273–284.

Velcich, A., Plaumbo, L., Selleri, L., Evans, G., and Augenlicht, L. 1997. Organization and regulatory aspects of the human intestinal mucin gene (MUC2) locus. *J. Biol. Chem. 272*: 7968–7976.

Vincent, A., Perrais, M., Desseyn, J.-L., Aubert, J.-P., Pigny, P., and Van seuningen, I. 2007. Epigenetic regulation (DNA methylation, histone modifications) of the 11p15 mucin genes (*MUC2*, *MUC5AC*, *MUC5B*, *MUC6*) in epithelial cancer cells *Oncogene* advance online publication - doi:10.1038/sj.onc.1210479.

Yang, F., Tuxhorn, J.A., Ressler, S.J., McAlhany, S.J., Dang, T.D., and Rowley, D.R. 2005. Stromal expression of connective tissue growth factor promotes angiogenesis and prostate cancer tumorigenesis. *Cancer Res. 65*: 8887–8895.

Yu, C., Shew, J., Liaw, Y., Kuo, S., Luh, K., and Yang, P. 2001. Application of mucin quantitative competitive reverse transcription polymerase chain reaction in assisting the diagnosis of malignant pleural effusion. *Am. J. Respir. Crit. Care Med. 164*: 1312–1318.

14
Gastric Cancer: Role of Intestinal Metaplasia by Histochemical Detection Using Biopsy Specimens

Akiko Shiotani, Ken Haruma, and David Y. Graham

INTRODUCTION

Intestinal metaplasia is a new metaplastic type of epithelium that replaces the surface, foveolar, and glandular epithelium of the stomach. Intestinal metaplasia is readily recognized histologically because of the presence of goblet cells which are not present in the normal gastric mucosa and is a response to injury and is a form of mucosal atrophy. Focal intestinal metaplasia can be seen as the damage site such as an acute or chronic ulcer; typically it represents the end stage of *Helicobacter pylori* (*H. pylori*) gastritis or autoimmune gastritis. Until recently, intestinal metaplasia was thought to be an important precancerous lesion along the multistep path to gastric carcinoma (Correa, 1992), but its role as a direct precursor has been challenged. However, the risk of developing gastric cancer is closely related to *H. pylori*-associated progressive gastric damage especially corpus atrophy (Graham and Shiotani, 2005; Shiotani *et al*., 2005; Uemura *et al*., 2001). It is likely that the type, location, and extent of intestinal metaplasia provide important information regarding cancer risk (Shiotani *et al*., 2005, 2006a).

DETECTION AND CLASSIFICATION OF INTESTINAL METAPLASIA

Since popularized by Morson (1955), intestinal metaplasia of the stomach has been a subject of interest both to pathologists and to endoscopists. Intestinal metaplasia is often present at the incisura angularis in patients with atrophic gastritis, and has been characterized by its morphology, pattern of histochemical staining, and glycoprotein expression. One of the most commonly used classifications of intestinal metaplasia in the stomach characterizes it according to the intestinal tissue that intestinal metaplasia closely mimics (e.g., small intestinal or complete and colonic or incomplete type). Another classification is based on the staining pattern of its mucins (type I equating with complete type and types II and III with incomplete type).

Detection of Intestinal Metasplasia

Alcian Blue/Periodic Acid-Schiff (PAS) Staining

Complete intestinal metaplasia is characterized by the presence of goblet cells

among the absorptive columnar cells on the surface and Paneth cells at the base of the pits (Figure 14.1). Normal foveolar and surface epithelial cells are intensely stained with periodic acid-Schiff (PAS) reagent indicating the presence of intracellular mucus. The foveolar and surface epithelial cells in complete intestinal metaplasia are replaced by absorptive cells that do not contain PAS positive mucosubstances and by goblet cells that contain acidic alcian blue positive mucus (Figure 14.1). The use of alcian blue markedly emphasizes the presence of the goblet cells. In incomplete intestinal metaplasia, the epithelium consists of a mixture of gastric surface mucous cells, goblet cells, and columnar cells, which are intermediate cells between intestinal and gastric surface mucous cells (Figure 14.2). Gastric surface mucous cells contain neutral mucin stained with alcian blue -PAS. The columnar cells contain a small amount of PAS positive mucus stained from blue-purple to purple-red depending on the content of acidic and neutral moieties. Iida *et al*. (1978) examined the columnar cells by electron microscopy and demonstrated that the columnar cells possess the properties of the both intestinal and the gastric foveolar epithelia (Figure 14.2b).

Alcian Blue/High Iron Diamine (HID) Staining

The mucin of goblet cell in complete intestinal metaplasia is stained with alcian blue but not with high iron diamine (HID). In the incomplete type some goblet cells are stained with alcian blue, and others contain granules giving a positive reaction with HID. Spicer and Duvenci (1964) reported that HID-positive cells in mouse submandibular and sublinguial glands incorporated radioactive sulfur consistent with the HID-positive mucin being sulfomucins. In contrast, HID-negative mucin are sialomucins and do not contain sulfated esters.

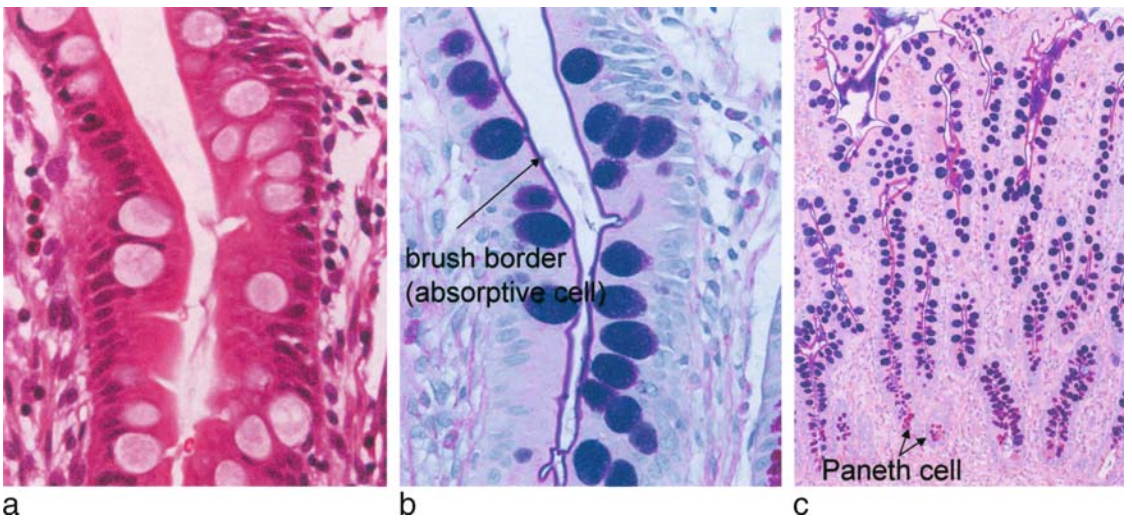

FIGURE 14.1. Hematoxylin-eosin (HE) and alcian blue (AB)/ periodic acid-Schiff (PAS) staining of complete intestinal metaplasia. Complete intestinal metaplasia is characterized by the presence of goblet cells among the absorptive columnar cells on the surface and Paneth cells at the base of the pits. (a) HE; (b) and (c) AB/PAS

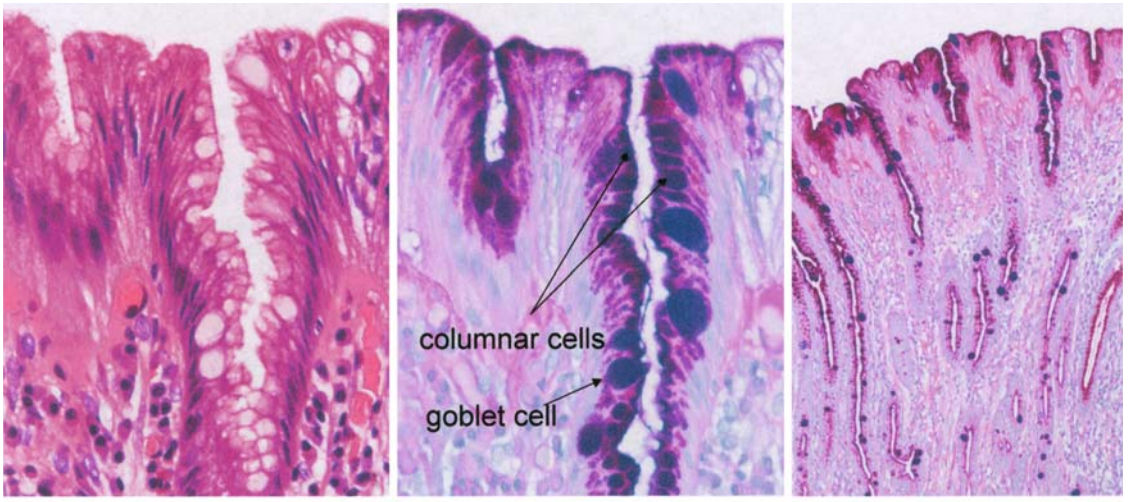

FIGURE 14.2. Hematoxylin-eosin (HE) and alcian blue (AB)/periodic acid-schiff (PAS) staining of incomplete intestinal metaplasia. Incomplete intestinal metaplasia consists of a mixture of gastric surface mucous cells, goblet cells, and columnar cells which are intermediate cells between intestinal and gastric surface mucous cells. (a) HE; (b) and (c) AB/PAS

MUC Staining

Mucins are heavily glycosylated (bottle-brush pattern) proteins that constitute the major component of the mucous protective layer for the surface of the mucosa. Twelve core proteins of human mucins have been described (MUC1, 2, 3, 4, 5AC, 5B, 6, 7, 8, 9, 11, 12) (Gendler and Spicer, 1995). MUC1, MUC5AC and MUC6 are found in the normal stomach. MUC2 is an intestinal phenotypic marker (Tanaka *et al*., 2005; Tatematsu *et al*., 2003; Tsukamoto *et al*., 2004). MUC5AC expression is typically found in foveolar epithelium and mucous neck cells of both the antrum and corpus, while MUC6 expression is present in pyloric glands of the antrum and the mucous cells of the neck zone of the corpus. MUC2 is found in areas of intestinal metaplasia and is expressed as vacuolar staining in most goblet cells (Figure 14.3b). Ota *et al*. (1998) described alterations of the expression pattern of mucins in the gastric surface mucous cells by *H. pylori* infection and reversible changes by eradication.

Classifications of Intestinal Metaplasia

One widely used classification was proposed by Filipe *et al*. (1988) in which intestinal metaplasia was classified into three types. Type I is the most common and consists of goblet cells secreting sialomucins, absorptive cells with brush borders, and Paneth cells. Types II and III are characterized by the presence of columnar cells and goblet cells secreting sialomucins and/or sulfomucins, with few Paneth cells. The difference between type II and type III is that the columnar cells secret sialomucins in type II and sulfomucins in type III (Filipe *et al*., 1988). It has been suggested that patients with type III intestinal metaplasia may have a higher risk for development of gastric cancer (Dinis-Ribeiro *et al*., 2004). El-Zimaity

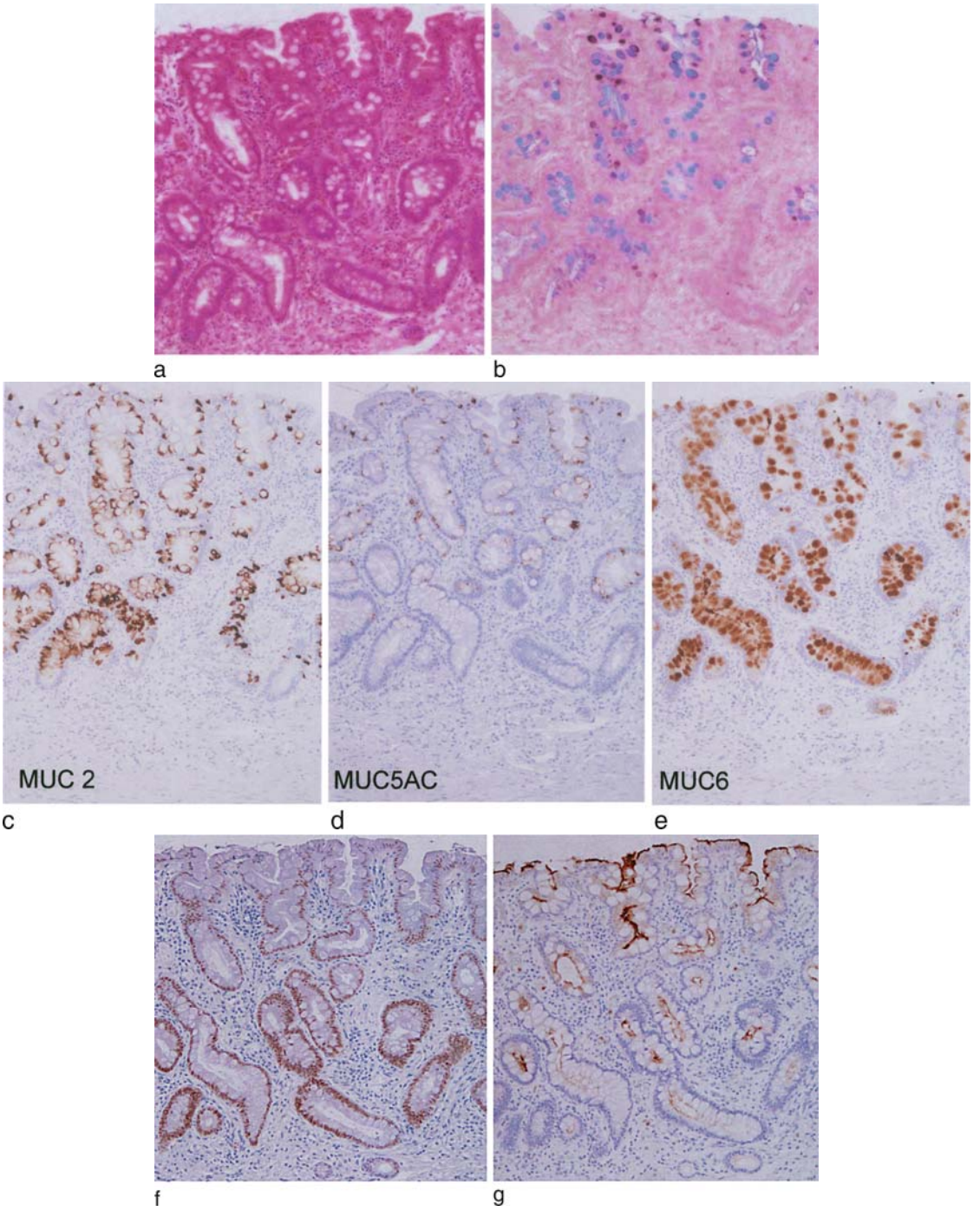

FIGURE 14.3. Hematoxylin-eosin (HE) and alcian blue (AB)/high iron diamine (HID) staining and MUC2, MUC5AC, MUC6, CDX2, and CD10 immunohistochemical staining of serial sections containing type III intestinal metaplasia taken from the non-cancerous mucosa of a patient with early gastric cancer. (a) HE staining; (b) AB–HID staining shows goblet cells and columnar cells stained in brown; (c) MUC2 is expressed as vacuolar staining in most goblet cells; (d) however MUC5AC is barely expressed; (e) MUC6 staining are detected in the goblet cells and in the columnar cells; (f) CDX2 is expressed in the nucleus of epithelial cells in areas of intestinal metaplasia; (g) CD10 staining can be seen along the brush border of the luminal surface of the epithelium

et al. (2002) performed detailed studies of the gastric mucosa in patients with gastric carcinoma and found that in all cases, patches of Type II and III intestinal metaplasia were intermingled and that type III was present in very small areas.

Intestinal metaplasia has also been classified based upon gastric and intestinal phenotypic markers (Tatematsu *et al*., 2003; Tsukamoto *et al*., 2004). This classification divides intestinal metaplasia into two major types; an intestinal type expressing only intestinal phenotypic markers including MUC2, vill in, and CD10 and a mixed gastric and intestinal (GI) type expressing intestinal and gastric phenotypic markers (MUC5AC and MUC6) (Figure 14.3). Villin is an actin-binding cytoskeletal protein and is essential for brush border formation in normal epithelial cells of small intestine, and CD10 is a brush border-associated neutral endopeptidase (Figure 14.3f).

RELATION OF MUC EXPRESSION AND TYPE OF INTESTINAL METAPLASIA

MUC5AC expression is the most common MUC expressed in type II and III intestinal metaplasia. Reis *et al*. (1999) and Silva *et al*. (2002) examined biopsy samples or surgical specimens taken from the gastric mucosa adjacent to carcinomas and reported that every case of the incomplete intestinal metaplasia expressed MUC1 and MUC5AC together with MUC2, both in goblet cells and in columnar cells (mixed GI type). Examination of the pyloric region of stomachs resected for gastric cancer has shown that the percentage of glands expressing MUC5AC was directly related to the type of intestinal metaplasia (e.g., 38% in type I, 78% in type II, and 91% in type III intestinal metaplasia) (Tanaka *et al*., 2005). These results are similar to our recent results evaluating the pattern of MUC expression in mucosal biopsy specimens obtained from the greater curvature of the antrum 3 cm proximal to the pylorus and at the mid-point of the lesser and greater curvature of the corpus (i.e., MUC5AC was detected in 46% of type I, 83% of type II, and 94% of type III intestinal metaplasia in the antrum and in 13% of type I, 57% of type II, and 90% of type III intestinal metaplasia in the corpus). The most incomplete IM (type II and III) preserving gastric mucin is considered to be GI mixed type, whereas complete type is considered to be type I, especially in the corpus lesser curve. MUC6 was less expressed in intestinal metaplasia than MUC5AC (46% of type II, 50% of type III intestinal metaplasia in the antrum) (Shiotani *et al*., 2006a).

GRADING ON INTESTINAL METAPLASIA USING BIOPSY SPECIMENS

In 1990, the Sydney classification of gastritis was proposed as a modification of the Whitehead system in order to update and standardize the morphological criteria for classification and grading of chronic gastritis in the *H. pylori* era. In 1994 the recommendations were modified by the addition of a biopsy specimen from the gastric angle and a change in the location of the antrum and corpus biopsies from the anterior and posterior walls to the greater and lesser curves of stomach. Five biopsy specimens are recommended to be taken from the antrum lesser and greater curve (both within 2–3 cm from

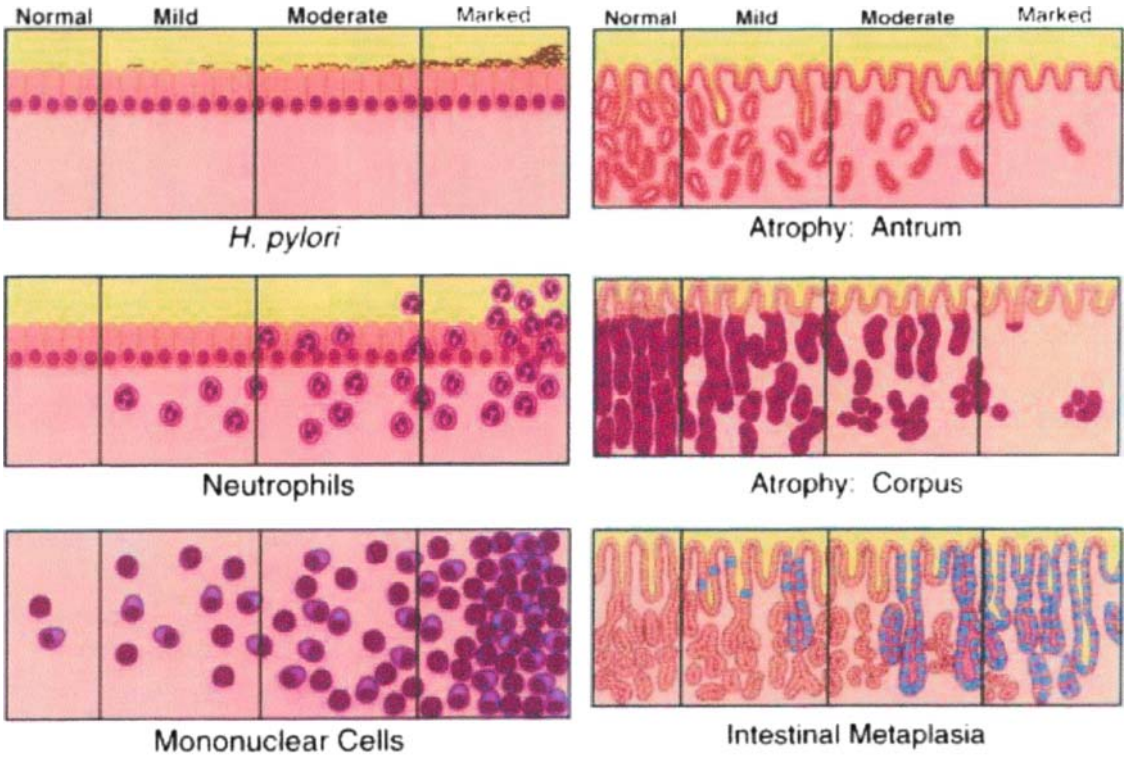

FIGURE 14.4. The visual analogue scale of the updated Sydney system

the pylorus), the corpus lesser curve (4 cm proximal to the angulus), the middle portion of the corpus greater curve (8 cm from the cardia) and the incisura angularis. Based on the success with grading of prostate carcinoma, a visual analogue scale was added to assist in grading morphological variables and guidelines for the application of the system were proposed (Figure 14.4) (Dixon *et al*., 1996). Probably the only feature of the Sydney system that is widely used today is the four point scale (0–3), and scoring is generally based on comparisons to the recommended visual analogue scale. After the Sydney system, there are few controversies regarding grading of inflammation or *H. pylori* density. However, the assessment and interpretation of atrophy and intestinal metaplasia have remained problematic, especially for clinicians.

ASSESSMENT OF ATROPHY

Atrophic gastritis, or gastric atrophy has been recognized since the 19th century. The term atrophic gastritis is applied to chronic gastritis with gland loss and a change in epithelial type. The most common causes are *H. pylori* infection and autoimmune gastritis. *H. pylori* infection is initially most severe in the antrum, and as time passes, the damage tends to progress into the gastric corpus. This change can be visualized as an advancing atrophic border which involves the lesser curve more rapidly than the greater curve (Graham and Shiotani, 2005; Kimura *et al*., 1996). The loss of the normal glandular components presents as one of two types of gastric mucosal metaplasia, pseudopyloric metaplasia and intestinal metaplasia.

Pseudopyloric metaplasia represents the replacement of parietal and chief cells in oxyntic glands by mucous-secreting cells of the type found in antral mucosa. These mucous-secreting cells are thought to arise from surviving mucous neck cells or stem cells in the damaged oxyntic glands.

Atrophy has proven difficult to identify in the antrum because the intense *H. pylori*-associated inflammation tends to separate glandular elements and make the mucosa appear atrophic. It has been suggested that it may not be possible to accurately access the presence of atrophy based on glandular loss in the antrum until after *H. pylori* eradication and subsidence of the inflammation. In the corpus, atrophy appears as pseudopyloric metaplasia in which the normal gastric mucosa is replaced by pyloric appearing mucosa. Thus, it is difficult or impossible for the pathologists to distinguish whether they are seeing atrophic corpus mucosa or antral mucosa unless they are confident from where the specimen was taken, and even then, the location should be confirmed by pepsinogen I (a marker of corpus tissue) and/or gastrin (a marker of antral tissue) staining. The presence of intestinal metaplasia is unequivocal evidence of atrophy and thus, most studies have focused on its presence as a surrogate for the extent and severity of atrophy.

PATHOGENESIS OF ATROPHIC GASTRITIS AND INTESTINAL METAPLASIA

The pathogenesis of atrophic gastritis is complex as it represents the end product of destructive and reparative processes which occur simultaneously. The presence of *H. pylori* infection alters the kinetic patterns of gastric glandular epithelium including gastric epithelial cell proliferation, induction of apoptosis, and DNA synthesis. Ierardi *et al*. (1997) have suggested that the development of intestinal metaplasia is associated with an impaired regulation of gastric epithelial proliferation with overexpression of the oncoprotein ras p21 being a maker.

Stomach consists of a large number of different microenvironments such that the host-bacterial interactions are likely to differ remarkably and simultaneously in the same stomach. The outcome will also depend on the virulence of the infecting organism, the genetic make-up of the host (e.g., responsiveness to inflammatory stimuli), and the presence or absence of damaging or protective elements in the diet (e.g., intake of salt vs. fresh fruits and vegetables). The end result is seen clinically as different patterns of gastritis (e.g., antral predominant vs. pangastritis) which have different clinical implications (i.e., duodenal ulcer and antral predominant gastritis and gastric cancer with atrophic pangastritis). Intestinal metaplasia is an end product of the process.

Tatematsu *et al*. (2003) and Tsukamoto *et al*. (2004) suggested that intestinal metaplasia may undergo a phenotype shift from mixed GI type to intestinal type. Their data are consistent with intestinalization progressing from mixed GI type to the intestinal type in both non-cancerous and cancerous tissues. However, our results suggest that intestinal type does not appear to follow mixed GI type. Mixed GI type of intestinal metaplasia seems to associate better with the severity of corpus atrophy and serum low levels of pepsinogen I/II ratios compared to intestinal type (Shiotani *et al*., 2006a).

GASTRIC CANCER AND INTESTINAL METAPLASIA

Intestinal-type gastric cancers are thought to evolve through a multistep process starting with superficial gastritis and progressing through atrophy with dysplasia preceding the appearance of carcinoma (Correa, 1992; Shiotani *et al*., 2005). The strong association of gastric cancer with gastric atrophy has been recognized for nearly a century and has been repeatedly confirmed. For example, Uemura *et al*. (2001) showed that the risk of developing cancer on follow-up was limited to those with *H. pylori* infection and the risk increased with increasing atrophy, especially involving the gastric corpus. There are many ways that the association between cancer risk and atrophy have been confirmed among those with *H. pylori* infections including noninvasive methods such as measuring serum pepsinogen I levels or pepsinogen I:II ratio, identification of hypo or achlorhydria by assessing acid secretion directly or indirectly as an increase in gastrin 17 (Shiotani *et al*., 2005). In the most severe atrophy, one expects very low pepsinogen I levels, elevated gastric 17 levels, and often the absence of *H. pylori* seropositivity reflecting the fact that *H. pylori* are no longer able to colonize in the stomach with extensive atrophy. Low pepsinogen levels or low acid secretion correlates well with histologic findings of atrophy and also with the extent and severity of intestinal metaplasia.

Tahara *et al*. (1994) proposed intestinal metaplasia as a possible precancerous lesion with a wide range of genetic changes including telomerase reduction, microsatellite instability, and mutation in *p53, APC*, and *k-ras*. It is currently thought that atrophy presents as a continuous or near continuous sheet with islands of intestinal metaplasia interspersed within the zone of atrophy. However, the role of intestinal metaplasia as a direct cancer precursor is unclear with the bulk of recent observations suggesting that it is not a direct precursor but rather is a marker for a mucosa predisposed to cancer development. Several Japanese studies suggest that cancer and intestinal metaplasia arise from different cell lineages in the proliferative cell zone at the neck region, which is also consistent with the opinion that intestinal metaplasia is a marker for increased risk and not a direct precursor lesion (Tatematsu *et al*., 2003). The study in animal models by Houghton *et al*. (2004) has suggested that gastric cancer may arise from bone marrow stem cells. In their study, bone marrow-derived cells homed to and repopulated the gastric mucosa in a *Helicobacter felis* infected mouse model of chronic infection. Bone marrow-derived cells might contribute to metaplasia and cancer (Houghton *et al*., 2004). Overall one must conclude that the pathogenesis of intestinal metaplasia and actual relationship to gastric cancer remains unclear such that additional studies are warranted to explore the relationship.

CDX2 EXPRESSION IN INTESTINAL METAPLASIA

The CDX proteins are intestine-specific transcription factors encoded by the *cdx1* and *cdx2* genes which are the mammalian homologues of the *Drosophilia* homeobox gene, *caudal* (Macdonald and Struhl, 1986). In adult mammals, the

expression of these genes is restricted to the epithelium of the gut from the duodenum to the large intestine, where they act as master regulators for intestinal development and differentiation (Silberg *et al*., 2000). CDX1 is predominantly expressed in the undifferentiated cells of the intestinal crypts, whereas CDX2 is mostly present in the villi or differentiated cell compartment of the small intestine (Silberg *et al*., 2000). In particular, the maintenance of intestinal differentiation appears to depend on the presence of CDX2. For example, loss of CDX2 expression leads to focal gastric differentiation in the colon (Beck *et al*., 1999). Aberrant expression of CDX2 in the upper gastrointestinal tract is thought to be a key event in the pathogenesis of Barrett's mucosa in the esophagus as well as in intestinal metaplasia in the stomach (Figure 14.3f) (Silberg *et al*., 2002). Aberrant expression of CDX2 correlates with the development of intestinal metaplasia and the expression of CDX2 as well as of MUC2 in isolated gastric glands, which is progressively up-regulated with intestinalization from the gastric type to the mixed GI type to the intestinal type (Tsukamoto *et al*., 2004).

The presence of CDX2 staining is likely a surrogate marker for the presence of intestinal metaplasia. We previously found that its expression at the corpus lesser curve was greater in patients with gastric cancer than in the controls, and that expression increased in relation to the atrophy score in the ascending order of those without intestinal metaplasia, complete intestinal metaplasia, and incomplete intestinal metaplasia (Shiotani *et al*., 2006b). CDX2 may be an essential signal for modulation to an intestinal metaplasia phenotype and might function by preventing the execution of the fundic gland differentiation pattern.

Little information is available concerning the factors (e.g., transcription factors) that cause altered differentiation of stem cells in the gastric epithelium. Runx3, a runt domain transcription factor, is a major growth regulator of gastric epithelial cells. Some gastric epithelial cells in the *Runx3−/−* mouse differentiate into intestinal-type cells expressing CDX2 (Fukamachi *et al*., 2004). *Sucrase-isomaltase, glucagon, carbonic anhydrase I, lactase*, and MUC2 have been suggested as candidates for CDX2-regulated target genes.

H. pylori-associated corpus inflammation is associated with suppression of parietal cell function (e.g., acid secretion is suppressed). Of interest, CDX2 expression in an intestinal cell line has been shown to be down-regulated under acidic conditions (Faller *et al*., 2004). Overall these data suggest that hypoacidity might allow stem cell differentiation in a particular direction to intestinal metaplasia and independently to cancer (Faller *et al*., 2004).

CDX2 in Gastric Cancer

The phenotypic expression of gastric cancer can be classified into gastric and intestinal epithelial cell types by immunohistochemistry using the same epithelial cell markers for intestinal metaplasia. CDX2 expression is associated with intestinal type gastric cancer, and it is expressed at the early stage of gastric carcinogenesis (Mizoshita *et al*., 2004). Mutoh *et al*. (2004) reported that gastric polyps developing from the intestinal metaplastic mucosa in *Cdx2*-transgenic mice consisted of intesti-

nal-type adenocarcinoma containing *p53* and *APC* gene mutations. The hypothesis that intestinal-type carcinomas arise in intestinalized mucosa, whereas diffuse–type cancers develop from the phenotypic gastric mucosa is based on morphological similarities. However, there are several contradictions. For example, the early stages of gastric cancers, independent of the histological type, are mainly gastric phenotype and the shift to intestinal phenotype occurs during tumor progression (Tatematsu *et al*., 2003). Mizoshita *et al*., (2004) divided gastric cancers into gastric (G-type), gastric intestinal mixed type (GI mixed type), intestinal type, and null type (N type). CDX2 expression was detected in the intestinal type region and in the N type regions. The GI mixed and intestinal types had significantly greater CDX2 expression than the N types ($p < 0.001$), while there was no CDX2 expression in the G type. The phenotype of gastric tumors is independent of phenotype of intestinal metaplasia existing in the background mucosa and seems to be determined by CDX2 expression.

Previous studies have suggested that *CDX2* is a tumor-suppressor gene with regard to colorectal carcinogenesis. CDX2 up-regulates transcription of p21/WAF1/CIP1, which plays a critical role in differentiation and tumor suppression and promotes intestinal differentiation as a cyclin-dependent kinase inhibitor leading to cell-cycle arrest (Bai *et al*., 2003). CDX2-positive expressing tumors show tendencies towards less invasiveness and fewer lymph node metastases and have a better outcome than the CDX2-negative tumors (Mizoshita *et al*., 2004). While the data are provocative, the actual role of CDX2 in gastric cancer remains unclear. It is also possible that CDX2 may have different roles depending on the cancer type.

HISTOLOGICAL MARKERS FOR INCREASED RISK FOR GASTRIC CANCER

The prevalence of intestinal metaplasia increases with age among *H. pylori*-infected individuals. Type I intestinal metaplasia is commonly found in random, particularly antral biopsies from patients with *H. pylori* infection. Because the detection of intestinal metaplasia in routinely obtained, endoscopic biopsy material is common. The finding of intestinal metaplasia by itself has not proven to be a suitable marker for identifying patients at increased risk of gastric cancer. Moreover, El-Zimaity *et al*. (2001) reported that biopsies taken repeatedly from predetermined sites showed that neither the presence nor the type of intestinal metaplasia was constant. However, the fact that intestinal metaplasia is found on multiple biopsy specimens taken from predetermined sites in the corpus suggests that intestinal metaplasia is widespread and is consistent with extensive and advanced corpus atrophy. For example, we obtained biopsy samples from the greater curve of the antrum 3 cm proximal to the pylorus as well as the midpoint of the greater and lesser curve of the corpus. The presence of intestinal metaplasia in the corpus, especially along the lesser curve, identified those at increased risk for gastric cancer, and as might be expected, the presence of intestinal metaplasia along the corpus greater curve was associated with the presence of multiple malignant lesions (Shiotani *et al*., 2005, 2006a).

Retrospective studies by Filipe *et al.* (1988) and Matsukura *et al.* (1980) have demonstrated that type III intestinal metaplasia can be detected in 75–90% of cases of intestinal type gastric cancer. Kabashima *et al.* (2000) studied the difference in phenotypic expression between multiple early gastric cancer (112 lesions) and solitary early cancer (53 lesions) from the files of gastric specimens which had been surgically resected. They reported that the incidence of mixed GI type of intestinal metaplasia in non-neoplastic mucosa within 5 mm from the margins of cancer cells was higher (75% vs. 40%) in the patients with multiple lesions than in the patients with a single lesion. Although type III intestinal metaplasia is frequently present in patients with gastric cancer, it is important to note that most of the studies on intestinal metaplasia as a risk marker have come from patients who already had gastric cancers, and thus little can be said regarding its predictive value. The same problem presents itself in regards to the role of altered mucin expression pattern in intestinal metaplasia.

Rokkas *et al.* (1991) followed up 26 patients with type III intestinal metaplasia by endoscopy and biopsy, and diagnosed early gastric cancer in 11 patients in 5 years. They concluded that early stage gastric cancer could be diagnosed with increasing frequency by endoscopic surveillance of patients with type III intestinal metaplasia. Filipe *et al.* (1994) followed up to 1,525 Slovenian patients with intestinal metaplasia (Type I n = 518 , Type II n = 197, Type III n = 275), patients with type III had a 2.7–5.8 times greater risk for the development gastric cancer compared with those with type I and II sulfomucin-negative intestinal metaplasia. Another recent cohort study of 144 patients by Dinis-Ribeiro *et al.* (2004) also demonstrated that patients with type III intestinal metaplasia may benefit from 6 to 12 monthly endoscopic examinations. In their study, 7% of patients with type II or III intestinal metaplasia at first biopsy progressed to high grade dysplasia, whereas no cases with atrophic gastritis or type I intestinal metaplasia progressed to high grade dysplasia during the first 3 years. It is likely that the presence of extensive type III intestinal metaplasia is actually indicative of extensive and advanced atrophy. However, these studies do not indicate the biopsy sites chosen, and whether diagnosis of its presence significantly adds more useful information compared to noninvasive testing (e.g., pepsinogen or gastrin levels) remains to be examined. Further large long-term prospective studies are needed to compare markers so as to establish the clinical utility of the classification of intestinal metaplasia using biopsy samples.

From the discussion above, it should be clear that there are both histological and biochemical methods of detecting and staging gastric mucosal atrophy. The presence of severe and extensive atrophy predicts cancer risk. The classification of intestinal metaplasia by histochemical detection using biopsy samples obtained from fixed points in the corpus may add additional information regarding risk. Recently, Rugge *et al.* (2007) introduced the Operative Link on Gastritis Assessment (OLGA)-staging system that takes account of the location and severity of atrophy. In 439 prospectively-enrolled, consecutive, dyspeptic outpatients who underwent endoscopy with standardized biopsy sampling according to the updated Sydney system, benign conditions consistently clustered in stages 0–II, whereas all neoplastic lesions clustered in

Table 14.1. The Operative Link on Gastritis Assessment (OLGA)-staging system.

		Corpus stages			
Atrophy		Absent	Mild	Moderate	Severe
Antrum stages	Absent	Stage 0	Stage I	Stage II	Stage II
	Mild	Stage I	Stage I	Stage II	Stage III
	Moderate	Stage II	Stage II	Stage III	Stage IV
	Severe	Stage III	Stage III	Stage IV	Stage IV

stages III–IV (Table 14.1). The OLGA-staging system may provide a risk estimate for developing gastric cancer. However, according to the previous studies, corpus atrophy or corpus gastritis seem to be more useful risk markers for gastric cancer compared to antral gastritis or atrophy (Shiotani *et al*., 2006b; Uemura *et al*., 2001). Prospective multicenter studies are needed to validate this new staging system in different epidemiological contexts.

ERADICATION OF *H. PYLORI* AND FUTURE STUDIES

Patients with corpus gastritis and reduced acid secretion often experience an increase in acid secretion after eradication, presumably due to the removal of the postulated inhibitory factors and possibly improvement in parietal cell number. Wong *et al*. (2004) conducted a prospective randomized placebo-control eradication study on prevention of gastric cancer in a region of high prevalence in China after 7.5 years of follow-up. They reported a beneficial effect from eradication only in the subgroup of patients without atrophy, intestinal metaplasia, or dysplasia, suggesting that the benefit of *H. pylori* eradication diminishes once intestinal metaplasia is present (Wong *et al*., 2004).

As noted above, the data are consistent with the cancer risk proportional to the severity of corpus atrophy. The fact that in some patients corpus function may partially recover, as reflected in a return or increase in acid secretion and a fall in serum gastrin levels, suggests that the simple presence of atrophy may be a course measure of risk. We speculate that the degree of improvement in function probably correlates inversely with the actual baseline risk and the subsequent risk. Although the current data do not support the notion that *H. pylori* eradication results in disappearance of intestinal metaplasia, we recently showed a decrease in the expression of CDX2 in the corpus mucosa after *H. pylori* eradication of subjects at high risk for gastric cancer (Shiotani *et al*., 2007). Of interest, the improvement in CDX2 expression in the corpus was limited to the atrophic mucosa without incomplete intestinal metaplasia which was unchanged following *H. pylori* eradication.

As for future studies, there is a need to examine improvements in acid secretion, pepsinogen levels, serum gastrin levels, or CDX2 expression as prognostic markers. One might suspect that continued inflammation after eradication in areas of extensive corpus incomplete intestinal metaplasia may identify patients lacking favorable biochemical responses or changes in CDX2 expression and having

higher residual risks of gastric cancer. Long term follow-up studies after eradication are required to address these questions and to identify the patients suitable for a program of targeted surveillance following population as a cancer prevention strategy for high risk populations (e.g., Japan, Korea, China) (Graham and Shiotani, 2005).

Acknowledgement. Photomicrographs (Figures 14.1, 14.2) were kindly provided by Professor Hiroyoshi Ota, Shinshu University.

REFERENCES

Bai, Y.Q., Miyake, S., Iwai, T. and Yuasa, Y. 2003. CDX2, a homeobox transcription factor, upregulates transcription of the p21/WAF1/CIP1 gene. *Oncogene 22*: 7942–7949.

Beck, F., Chawengsaksophak, K., Waring, P., Playford, R.J. and Furness, J.B. 1999. Reprogramming of intestinal differentiation and intercalary regeneration in Cdx2 mutant mice. *Proc. Natl. Acad. Sci. U S A 96*: 7318–7323.

Correa, P. 1992. Human gastric carcinogenesis: a multistep and multifactorial process–First American Cancer Society Award Lecture on Cancer Epidemiology and Prevention. *Cancer Res. 52*: 6735–6740.

Dinis-Ribeiro, M., Lopes, C., da Costa-Pereira, A., Guilherme, M., Barbosa, J., Lomba-Viana, H., Silva, R. and Moreira-Dias, L. 2004. A follow up model for patients with atrophic chronic gastritis and intestinal metaplasia. *J. Clin. Pathol. 57*: 177–182.

Dixon, M.F., Genta, R.M., Yardley, J.H. and Correa, P. 1996. Classification and grading of gastritis. The updated Sydney System. International Workshop on the Histopathology of Gastritis, Houston 1994. *Am. J. Surg. Pathol. 20*: 1161–1181.

El-Zimaity, H.M., Ramchatesingh, J., Saeed, M.A. and Graham, D.Y. 2001. Gastric intestinal metaplasia: subtypes and natural history. *J. Clin. Pathol. 54*: 679–683.

El-Zimaity, H.M., Ota, H., Graham, D.Y., Akamatsu, T. and Katsuyama, T. 2002. Patterns of gastric atrophy in intestinal type gastric carcinoma. *Cancer 94*: 1428–1436.

Faller, G., Dimmler, A., Rau, T., Spaderna, S., Hlubek, F., Jung, A., Kirchner, T. and Brabletz, T. 2004. Evidence for acid-induced loss of Cdx2 expression in duodenal gastric metaplasia. *J. Pathol. 203*: 904–908.

Filipe, M.I., Munoz, N., Matko, I., Kato, I., Pompe-Kirn, V., Jutersek, A., Teuchmann, S., Benz, M. and Prijon, T. 1994. Intestinal metaplasia types and the risk of gastric cancer: a cohort study in Slovenia. *Int. J. Cancer 57*: 324–329.

Filipe, M.I., Barbatis, C., Sandey, A. and Ma, J. 1988. Expression of intestinal mucin antigens in the gastric epithelium and its relationship with malignancy. *Hum. Pathol. 19*: 19–26.

Fukamachi, H., Ito, K. and Ito, Y. 2004. Runx3−/− gastric epithelial cells differentiate into intestinal type cells. *Biochem. Biophys. Res. Commun. 321*: 58–64.

Gendler, S.J. and Spicer, A.P. 1995. Epithelial mucin genes. *Annu. Rev. Physiol. 57*: 607–634.

Graham, D.Y. and Shiotani, A. 2005. The time to eradicate gastric cancer is now. *Gut 54*: 735–738.

Houghton, J., Stoicov, C., Nomura, S., Rogers, A.B., Carlson, J., Li, H., Cai, X., Fox, J.G., Goldenring, J.R. and Wang, T.C. 2004. Gastric cancer originating from bone marrow-derived cells. *Science 306*: 1568–1571.

Ierardi, E., Francavilla, R. and Panella, C. 1997. Effect of *Helicobacter pylori* eradication on intestinal metaplasia and gastric epithelium proliferation. *Ital. J. Gastroenterol. Hepatol. 29*: 470–475.

Iida, F., Murata, F. and Nagata, T. 1978. Histochemical studies of mucosubstances in metaplastic epithelium of the stomach, with special reference to the development of intestinal metaplasia. *Histochemistry 56*: 229–237.

Kabashima, A., Yao, T., Sugimachi, K. and Tsuneyoshi, M. 2000. Gastric or intestinal phenotypic expression in the carcinomas and background mucosa of multiple early gastric carcinomas. *Histopathology 37*: 513–522.

Kimura, K., Satoh, K., Ido, K., Taniguchi, Y., Takimoto, T. and Takemoto, T. 1996. Gastritis in the Japanese stomach. *Scand. J. Gastroenterol. Suppl. 214*: 17–20.

Macdonald, P.M. and Struhl, G. 1986. A molecular gradient in early Drosophila embryos and its

role in specifying the body pattern. *Nature 324*: 537–545.

Matsukura, N., Suzuki, K., Kawachi, T., Aoyagi, M., Sugimura, T., Kitaoka, H., Numajiri, H., Shirota, A., Itabashi, M. and Hirota, T. 1980. Distribution of marker enzymes and mucin in intestinal metaplasia in human stomach and relation to complete and incomplete types of intestinal metaplasia to minute gastric carcinomas. *J. Natl. Cancer Inst. 65*: 231–240.

Mizoshita, T., Inada, K., Tsukamoto, T., Nozaki, K., Joh, T., Itoh, M., Yamamura, Y., Ushijima, T., Nakamura, S. and Tatematsu, M. 2004. Expression of the intestine-specific transcription factors, Cdx1 and Cdx2, correlates shift to an intestinal phenotype in gastric cancer cells. *J. Cancer Res. Clin. Oncol. 130*: 29–36.

Morson, B.C. 1955. Intestinal metaplasia of the gastric mucosa. *Br. J. Cancer 9*: 365–376.

Mutoh, H., Sakurai, S., Satoh, K., Tamada, K., Kita, H., Osawa, H., Tomiyama, T., Sato, Y., Yamamoto, H., Isoda, N., Yoshida, T., Ido, K. and Sugano, K. 2004. Development of gastric carcinoma from intestinal metaplasia in Cdx2-transgenic mice. *Cancer Res. 64*: 7740–7747.

Ota, H., Nakayama, J., Momose, M., Hayama, M., Akamatsu, T., Katsuyama, T., Graham, D.Y. and Genta, R.M. 1998. Helicobacter pylori infection produces reversible glycosylation changes to gastric mucins. *Virchows Arch. 433*: 419–426.

Reis, C.A., David, L., Correa, P., Carneiro, F., de Bolos, C., Garcia, E., Mandel, U., Clausen, H. and Sobrinho-Simoes, M. 1999. Intestinal metaplasia of human stomach displays distinct patterns of mucin (MUC1, MUC2, MUC5AC, and MUC6) expression. *Cancer Res. 59*: 1003–1007.

Rokkas, T., Filipe, M.I. and Sladen, G.E. 1991. Detection of an increased incidence of early gastric cancer in patients with intestinal metaplasia type III who are closely followed up. *Gut 32*: 1110–1113.

Rugge, M., Meggio, A., Pennelli, G., Piscioli, F., Giacomelli, L., De Pretis, G. and Graham, D.Y. 2007. Gastritis staging in clinical practice: the OLGA staging system. *Gut 56*: 631–636.

Shiotani, A., Iishi, H., Uedo, N., Kumamoto, M., Nakae, Y., Ishiguro, S., Tatsuta, M. and Graham, D.Y. 2005. Histologic and serum risk markers for noncardia early gastric cancer. *Int. J. Cancer 115*: 463–469.

Shiotani, A., Haruma, K., Uedo, N., Iishi, H., Ishihara, R., Tatsuta, M., Kumamoto, M., Nakae, Y., Ishiguro, S. and Graham, D.Y. 2006a. Histological risk markers for non-cardia early gastric cancer: pattern of mucin expression and gastric cancer. *Virchows Arch. 449*: 652–659.

Shiotani, A., Iishi, H., Uedo, N., Ishihara, R., Ishiguro, S., Tatsuta, M., Nakae, Y., Kumamoto, M., Hinoi, T. and Merchant, J.L. 2006b. Helicobacter pylori-induced atrophic gastritis progressing to gastric cancer exhibits sonic hedgehog loss and aberrant CDX2 expression. *Aliment. Pharmacol. Ther. 24 Suppl. 4*: 71–80.

Shiotani, A., Uedo, N., Iishi, H., Tatsuta, M., Ishiguro, S., Nakae, Y., Kamada, T., Haruma, K. and Merchant, J.L. 2007. Re-expression of sonic hedgehog and reduction of CDX2 after Helicobacter pylori eradication prior to incomplete intestinal metaplasia. *Int. J. Cancer* 121:1182–1189.

Silberg, D.G., Swain, G.P., Suh, E.R. and Traber, P.G. 2000. Cdx1 and cdx2 expression during intestinal development. *Gastroenterology 119*: 961–971.

Silberg, D.G., Sullivan, J., Kang, E., Swain, G.P., Moffett, J., Sund, N.J., Sackett, S.D. and Kaestner, K.H. 2002. Cdx2 ectopic expression induces gastric intestinal metaplasia in transgenic mice. *Gastroenterology 122*: 689–696.

Silva, E., Teixeira, A., David, L., Carneiro, F., Reis, C.A., Sobrinho-Simoes, J., Serpa, J., Veerman, E., Bolscher, J. and Sobrinho-Simões, M. (2002) Mucins as key molecules for the classification of intestinal metaplasia of the stomach. *Virchows Arch. 440*: 311–317.

Spicer, S.S. and Duvenci, J. 1964. Histochemical characteristics of mucopolysaccharides in salivary and exorbital lacrimal glands. *Anat. Rec. 149*: 333–357.

Tahara, E., Kuniyasu, H., Yasui, W. and Yokozaki, H. 1994. Gene alterations in intestinal metaplasia and gastric cancer. *Eur. J. Gastroenterol. Hepatol. 6 Suppl. 1*: S97–S102.

Tanaka, H., Tsukamoto, T., Mizoshita, T., Inada, K., Ogasawara, N., Cao, X., Kato, S., Joh, T. and Tatematsu, M. 2005. Expression of small intestinal and colonic phenotypes in complete intestinal metaplasia of the human stomach. *Virchows Arch. 447*: 806–815.

Tatematsu, M., Tsukamoto, T. and Inada, K. 2003. Stem cells and gastric cancer: role of gastric and intestinal mixed intestinal metaplasia. *Cancer Sci. 94*: 135–141.

Tsukamoto, T., Inada, K., Tanaka, H., Mizoshita, T., Mihara, M., Ushijima, T., Yamamura, Y., Nakamura, S. and Tatematsu, M. 2004. Down-regulation of a gastric transcription factor, Sox2, and ectopic expression of intestinal homeobox genes, Cdx1 and Cdx2: inverse correlation during progression from gastric/intestinal-mixed to complete intestinal metaplasia. *J. Cancer Res. Clin. Oncol. 130*: 135–145.

Uemura, N., Okamoto, S., Yamamoto, S., Matsumura, N., Yamaguchi, S., Yamakido, M., Taniyama, K., Sasaki, N. and Schlemper, R.J. 2001. Helicobacter pylori infection and the development of gastric cancer. *N. Engl. J. Med. 345*: 784–789.

Wong, B.C., Lam, S.K., Wong, W.M., Chen, J.S., Zheng, T.T., Feng, R.E., Lai, K.C., Hu, W.H., Yuen, S.T., Leung, S.Y., Fong, D.Y., Ho, J. and Ching, C.K. 2004. *Helicobacter pylori* eradication to prevent gastric cancer in a high-risk region of China: a randomized controlled trial. *JAMA 291*: 187–194.

15
Gastric Cancer: Antitumor Activity of RUNX3

Zhihai Peng and Keping Xie

INTRODUCTION

Although the incidence of gastric cancer declined in the West from the 1940s to the 1980s, it remains a major public health problem throughout the world (Parkin *et al*., 2005). In Asia and parts of South America in particular, gastric cancer is the most common epithelial malignancy and leading cause of cancer-related deaths. Moreover, gastric cancer remains the second most frequently diagnosed malignancy worldwide and the cause of 12% of all cancer-related deaths each year (Parkin *et al*., 2005; Zheng *et al*., 2004). Advances in the treatment of this disease are likely to come from a fuller understanding of its biology and behavior. The aggressive nature of human metastatic gastric carcinoma is related to mutations of various oncogenes and tumor suppressor genes and abnormalities of several growth factors and their receptors (Ushijima and Sasako, 2004). These mutations and abnormalities affect the downstream signal transduction pathways involved in the control of cell growth and differentiation. Specifically, they confer a tremendous survival and growth advantage to gastric cancer cells. Studies have indicated the role of several tumor suppressor genes in gastric cancer development and progression, including the E-cadherin/*CDH1* gene, *TP53*, *p16* (Ushijima and Sasako, 2004), and, recently, runt-related (*RUNX*) genes (Li *et al*., 2002).

The Runt family of transcription factors consists of three members – RUNX1, RUNX2, and RUNX3 – that play important roles in both normal developmental processes and carcinogenesis (Lund and van Lohuizen, 2002). The *RUNX1* locus, which is required for definitive hematopoiesis (Yokomizo *et al*., 2001), is the most frequent target of chromosome translocations in leukemia (Look, 1997). *RUNX2*, which is essential for osteogenesis (Ducy *et al*., 1997), is mutated in the human disease cleidocranial dysplasia (Lee *et al*., 1997; Mundlos *et al*., 1997), an autosomal dominant bone disorder. *RUNX3* is necessary for suppression of cell proliferation in the gastric epithelium (Li *et al*., 2002), neurogenesis of the dorsal root ganglia (Levanon *et al*., 2002), and T-cell differentiation (Woolf *et al*., 2003). Primary gastric cancer specimens have significantly lower levels of *RUNX3* expression when compared with that in normal gastric tissues because of a combination of a hemizygous deletion and

hypermethylation of the *RUNX3* promoter region (Li *et al*., 2002). Furthermore, the gastric epithelium of *RUNX3* knockout mice exhibits hyperplasia, a reduced rate of apoptosis, and reduced sensitivity to transforming growth factor (TGF)-β1, which suggests that the tumor suppressor activity of *RUNX3* operates downstream of the TGF-β signaling pathway.

RUNX3 AS A GASTRIC CANCER SUPPRESSOR

Two groups previously produced Runx3 knockout mouse strains that exhibited comparable defects: one involving neurogenesis and the other involving thymopoiesis (Li *et al*., 2002; Levanon *et al*., 2002). Surprisingly, researchers observed a stomach defect pertaining to gastric cancer in one of the strains but not in the other. Authors assessed this discrepancy and proposed several solutions for reconciling it (Levanon *et al*., 2003; Coffman, 2003). Recent studies further challenged the hypothesis that RUNX3 acts as a tumor suppressor gene in gastric cancer cases (Carvalho *et al*., 2005; Friedrich *et al*., 2006). However, many lines of evidence indicate that RUNX3 plays a critical role in gastric cancer development and progression.

Clinical evidence. Researchers have studied a potential connection between *RUNX3* and gastric cancer using human gastric cancer cell lines and primary human gastric tumors. Of 46 primary human gastric cancer specimens, 30% displayed hemizygosity of *RUNX3*. However, intragenic mutation in the remaining allele was very rare. Instead, about 45–60% of the primary human gastric tumors exhibited reduced *RUNX3* expression accompanied by hypermethylation of the CpG island located in the proximal (p2) promoter region (Li *et al*., 2002; Waki *et al*., 2003). We recently determined the level of RUNX3 expression in gastric cancer cells and primary gastric cancer specimens and the impact of alteration of this expression of this protein on gastric cancer biology and clinical outcome (Wei *et al*., 2005). We found that RUNX3 protein expression in 86 gastric tumors was lost or substantially decreased as compared with that in normal gastric mucosa ($P < 0.0001$) and that this loss or reduced expression was significantly associated with inferior survival durations ($P = 0.0005$). Using a Cox proportional hazards model, we found that RUNX3 expression independently predicted increased survival durations ($P = 0.036$). Moreover, various human gastric cancer cell lines exhibited loss of or drastic decreases in RUNX3 expression.

Experimental evidence. *RUNX3* is expressed in the gastrointestinal organs of the developing embryo and throughout adulthood in mice. A study of targeted inactivation of *Runx3/* in mice revealed in more detail the role that this gene plays in gut development (Li *et al*., 2002). First, the gastric epithelium of *Runx3*$^{-/-}$ mice displayed hyperplasia resulting from an increase in cell proliferation and a reduced rate of apoptosis. Second, glandular stomach epithelial cell lines obtained from *Runx3*$^{-/-}$ mice on a *p53*$^{-/-}$ background were tumorigenic in nude mice, whereas the same cell lines obtained from *Runx3*$^{+/+}$ mice on a *p53*$^{-/-}$ background were not. This indicates that *Runx3* keeps cell proliferation under control, which is a typical feature of tumor suppressors.

Using a chemical carcinogenesis murine model of gastric cancer, Guo *et al*. (2002)

found that *RUNX3* was inactivated by DNA methylation in *N*-methyla-*N*-nitrosourea-treated mice that had gastric cancer. In contrast, exogenous expression of *RUNX3* in the gastric epithelial cells obtained from the mice inhibited their growth in soft agar. Although the mechanism by which *N*-methyla-*N*-nitrosourea induces gastric carcinoma remains unknown, *Runx3* apparently is one of the major targets of this carcinogen, because this study found that CpG islands in the *Runx1* and *Runx2* promoter regions were not methylated.

Interestingly, researchers found one incidence of a mutation in *RUNX3* in 119 human gastric tumors (Li *et al*., 2002). This was a single-nucleotide transition within the conserved Runt domain that converted arginine 122 to cysteine (R122C). Moreover, when researchers in another study transfected gastric cancer cells with *RUNX3* followed by drug selection, only small numbers of G418-resistant foci formed, whereas cells transfected with *RUNX3-R122C* produced numbers of foci similar to those in control cells transfected with a vector only (Guo *et al*., 2002). Also, a tumorigenesis assay using nude mice revealed that *RUNX3* significantly suppressed gastric tumor growth and that the R122C point mutation of the *RUNX3* gene found in a patient with gastric cancer abolished this antitumor ability (Li *et al*., 2002). The identification of this loss-of-function mutation of *RUNX3* in a primary gastric tumor specimen significantly supports the notion that this gene can act as a tumor suppressor. Recently, investigators found that suberoylanilide hydroxamic acid, a member of highly potent histone deacetylase inhibitors, causes growth arrest, differentiation, and apoptosis of tumor cells (Huang *et al*., 2007). The tumor-suppressive activities of these inhibitors include upregulation of RUNX3 expression by suberoylanilide hydroxamic acid.

Mechanistic evidence. Researchers have proposed a few underlying mechanisms of reduced RUNX3 expression. For example, Waki *et al*. (2003) initially reported that 70% of the gastric cancer cell lines they studied exhibited RUNX3 promoter hypermethylation and that 45% and 8% of the neoplastic and corresponding non-neoplastic gastric epithelial tissue samples studied, respectively, had RUNX3 promoter methylation, suggesting that RUNX3 methylation is mostly gastric cancer-specific. Many laboratories immediately confirmed these initial findings in gastric cancer (Homma *et al*., 2006) and many other tumor types, including human lung cancer (Yanada *et al*., 2005).

In addition to the deregulation of mechanisms that control *RUNX3* gene expression, a mechanism that controls nuclear translocation of RUNX3 protein is impaired frequently in gastric cancer and contributes to gastric carcinogenesis. A study found that in normal gastric mucosa, RUNX3 was expressed most strongly in the nuclei of chief cells as well as in surface epithelial cells (Ito *et al*., 2005). The investigators found that in chief cells, a significant portion of RUNX3 protein was located in the cytoplasm, whereas 44% of cases of gastric cancer did not exhibit detectable levels of RUNX3 protein expression, 38% showed exclusive cytoplasmic localization of RUNX3, and only 18% showed nuclear localization of RUNX3. In the cytoplasm, RUNX3 is inactive as a suppressor of cancer cells. Therefore, RUNX3 is inactive in 82% of gastric cancer cases as a result of either gene silencing or protein mislocalization to the cytoplasm.

RUNX3 is a target of the acetyltransferase activity of p300. The p300-dependent acetylation of three lysine residues protects RUNX3 from ubiquitin ligase Smurf-mediated degradation. This acetylation is upregulated by the TGF-β signaling pathway and downregulated by histone deacetylase activity. Therefore, the level of RUNX3 protein expression is controlled by competitive acetylation and deacetylation of the three lysine residues, revealing a new mechanism for the posttranslational regulation of RUNX3 expression (Jin *et al*., 2004).

Finally, the chromosome locus 1p36, which harbors *RUNX3*, is among the most frequently affected chromosomal regions in various types of common cancers, including gastric cancer (Weith *et al*., 1996). Furthermore, introduction of a normal human chromosome locus 1p36 into colon carcinoma cells markedly suppresses their tumorigenicity (Tanaka *et al*., 1993). Therefore, *RUNX3* may be inactivated by the loss of heterozygosity. Examining the inactivation of *RUNX3* to determine whether it is also associated with other types of cancers that are related to 1p36 deletion would be particularly interesting. Taken collectively, the existing clinical, experimental, and mechanistic evidence indicates that *RUNX3* acts as a tumor suppressor of gastric cancer, and that its inactivation plays an important role in human gastric cancer development and progression.

MECHANISMS UNDERLYING THE TUMOR SUPPRESSOR ACTIVITY OF *RUNX3*

The increased proliferation and decreased apoptosis of *Runx3*$^{-/-}$ gastric epithelial cells are accompanied by reduced sensitivity to TGF-β1, as studies have shown that TGF-β1-induced inhibition of proliferation was only modestly affected in *Runx3*$^{-/-}$ gastric epithelial cells, whereas TGF-β1-induced apoptosis was significantly impaired in these cells (Schuster and Krieglstein, 2002). These results indicate that the tumor suppressor activity of *RUNX3* is associated with the TGF-β signaling pathway and that loss of functional RUNX3 may impair the tumor suppressor activity of this pathway as manifested by aberrant cell proliferation and apoptosis. A large amount of research is clearly needed to understand the full potential of *RUNX3* as a tumor suppressor as well as the underlying mechanisms of this gene.

Regulation of cell growth. RUNX3 is expressed by gastric epithelial cells throughout development. Researchers found that mice whose *Runx3* gene had been knocked out died soon after birth (Fukamachi and Ito, 2004). In these knockout mice, gastric epithelia exhibited hyperplasia, and epithelial apoptosis was suppressed. Analysis of the epithelial cells using a primary culture system suggested that this was caused by reduced sensitivity of *Runx3*$^{-/-}$ gastric epithelial cells to the growth-inhibiting and apoptosis-inducing activities of TGF-β. Exogenous expression of RUNX3 in cells that did not express the endogenous gene inhibited the growth of tumor cells both *in vivo* and *in vitro*. In addition, RUNX3 is required for TGF-β-dependent induction of p21 expression in stomach epithelial cells, and overexpression of RUNX3 potentiates TGF-β-dependent induction of endogenous p21 expression. In cooperation with Smads, RUNX3 synergistically activates the p21 promoter. Furthermore, investigators found that areas in murine and human

gastric epithelium in which RUNX3 was expressed coincided with those in which p21 was expressed (Chi *et al*., 2005). These results suggest that the tumor suppressor activity of RUNX3 is at least partly associated with its ability to induce p21 expression. Our study showed that enforced restoration of RUNX3 expression led to downregulation of cyclin D1 but upregulation of p27, Caspase 3, Caspase 7, and Caspase 8 expression; cell cycle arrest; and apoptosis *in vitro*, which was consistent with dramatic attenuation of tumor growth and abrogation of metastasis in animal models (Wei *et al*., 2005).

Regulation of apoptosis. Generally, RUNX3 is believed to regulate apoptosis via the TGF-β1 signaling pathway. Recent findings showed that the physical interaction of RUNX3 and FoxO3a/FKHRL1 on the Bim promoter activated transcription of Bim (Yamamura *et al*., 2006). RUNX3 cooperates with FoxO3a/FKHRL1 to participate in the induction of apoptosis by activating Bim and may play an important role in tumor suppression in gastric cancer. Furthermore, authors reported that in Runx3$^{-/-}$ mouse gastric epithelium, expression of Bim was downregulated, and the level of apoptosis was reduced to the same extent as that in Bim$^{-/-}$ gastric epithelium (Yano *et al*., 2006; Vogiatzi *et al*., 2006). These results demonstrate that RUNX3 is responsible for transcriptional upregulation of Bim expression in TGF-β-induced apoptosis. Also, overexpression of Runx3 may sensitize gastric cancer cells to chemotherapeutic drugs by downregulating expression of Bcl-2, MDR-1, and MRP-1 at the transcriptional level (Guo *et al*., 2005).

Regulation of cell differentiation. A study found that some Runx3$^{-/-}$ mouse gastric epithelial cells could differentiate into intestinal-type cells that expressed Cdx2, a transcription factor that has been shown to induce intestinal metaplasia in transgenic mice (Fukamachi *et al*., 2004). The researchers did not find differentiation of intestinal-type cells in cultures of Runx3$^{+/+}$ gastric epithelial cells. These results suggest that gastric epithelial cells can differentiate into intestinal-type cells, probably because of expression of Cdx2 in them when the function of Runx3 is impaired. These results imply a close relationship between loss of function of Runx3, formation of intestinal metaplasia, and development of gastric cancer. Also, this study showed that when subcutaneously implanted into nude mice, Runx3$^{-/-}$ gastric epithelial cells formed tumors in which some cells differentiated into intestinal-type cells. Clonal analysis showed that gastric epithelial cells transdifferentiated into intestinal-type cells in the tumors. Considering that gastric epithelial differentiation is very stable and that intestinal-type cells never differentiate in the murine stomach, the fact that gastric epithelial cells transdifferentiate into intestinal-type cells is remarkable. Therefore, Runx3 plays a very important role in the control of growth, specification, and differentiation of gastric epithelial cells (Fukamachi, 2006, Nakase et al., 2005).

Regulation of angiogenesis and meta-stasis. The results of one study, indicate that silencing of RUNX3 may affect the expression of important genes involved in various aspects of metastasis, including cell adhesion, proliferation, and apoptosis and promotion of the peritoneal metastasis of gastric cancer (Sakakura *et al*., 2005). Also, we found both clinical and mechanistic evidence that RUNX3 negatively regulated gastric

cancer angiogenesis and metastasis (Peng *et al*., 2006). Specifically, we found that loss of RUNX3 expression directly correlated with increased VEGF expression and tumor angiogenesis. We also found for the first time that restoration of RUNX3 expression dramatically suppressed the angiogenic potential of human gastric cancer cells, which correlated with downregulation of VEGF expression via promoter repression *in vitro* and attenuation of tumorigenicity and abrogation of metastasis in animal models. Therefore, our study provides a novel molecular mechanism for the antitumor activity of RUNX3, further underscores the importance of RUNX3 in gastric cancer development and progression, and provides a better understanding of the molecular basis for aberrant RUNX3 signaling pathways, which may help in designing effective therapeutic modalities to control gastric cancer growth and metastasis.

MATERIALS

1. Formalin-fixed, paraffin-embedded primary gastric adenocarcinoma specimens and normal gastric tissue specimens
2. Xylene
3. Ethanol
4. Distilled H_2O (dH_2O)
5. Phosphate-buffered saline (PBS): 100 mg of anhydrous calcium chloride, 200 mg of potassium chloride, 200 mg of monobasic potassium phosphate, 100 mg of magnesium chloride 6 H_20, 8 g of sodium chloride, and 2.16 g of dibasic sodium phosphate 7 H_2O; bring volume to 1 l with dH_2O, adjust pH to 7.5
6. 50 mM Tris buffer: 0.6 g of Tris(hydro xymethyl)aminomethane in 100 ml of dH_2O; adjust pH to 7.6 using HCl
7. 10 mM sodium citrate buffer: add 2.94 g of sodium citrate to 1 l of dH_2O, adjust pH to 6.0
8. Trypsin (Invitrogen Corporation, Carlsbad, CA)
9. Three percent H_2O_2 in methanol: add 9 ml of 30% H_2O_2 to 92 ml of methanol
10. Blocking solution: 5% bovine serum albumin and 5% normal horse serum (Jackson ImmunoResearch Laboratories, Inc., West Grove, PA) in PBS
11. Primary antibody: a polyclonal rabbit antibody against human RUNX3 (Active Motif, Carlsbad, CA)
12. Secondary antibody: peroxidase-conjugated anti-rabbit IgG (Jackson Immuno Research Laboratories, Inc.)
13. 3,3-Diaminobenzidine tetrahydrochloride (DAB) solution: dissolve 50 mg of DAB (Sigma Chemical Co., St. Louis, MO) in 99.5 ml of PBS and add 0.5 ml of 30% H_2O_2; use immediately because solution is good for only 20 min
14. Hematoxylin (Biogenex Laboratories, San Ramon, CA)
15. Universal mount (Research Genetics, Huntsville, AL)

METHODS

Tissue Slide Preparation

1. Cut standard sections (5 µm thick) of tissue specimens and mount them on glass slides.
2. Air-dry the slides overnight at room temperature.

Deparaffinization

1. Heat the slides at 60°C for 30 min.

2. Incubate the slides in xylene for 6 min at room temperature. Repeat this step once.

Rehydration

1. Rinse the slides with 100% ethanol (ETOH) twice for 2 min each.
2. Rinse the slides with 95% ETOH twice for 1 min each.
3. Rinse the slides with 80% ETOH for 1 min.
4. Rinse the slides with 50% ETOH for 1 min.
5. Rinse the slides with PBS twice for 2 min each.

Antigen Retrieval

1. Immerse the slides in 10 mM sodium citrate buffer (pH 6.0).
2. Heat the slides in a microwave oven for 1 min at high power followed by 19 min at medium power.
3. Cool the slides for 20 min after antigen unmasking.

Tissue Digestion

1. Incubate sections with 0.025% trypsin in 50 mM Tris buffer (pH 7.6) for 5 min at 37°C.
2. Rinse slides with PBS three times for 2 min each and continue the immunostaining.

Immunostaining Procedure

1. Use a paper towel to wipe around the tissue on each slide.
2. Draw a circle with a Pap pen around the tissue on each slide.
3. Place all slides in a humidified chamber (care must be taken to prevent tissue from drying out).
4. Quench endogenous peroxidase by placing slides in 3% H_2O_2 methanol for 15 min.
5. Rinse the slides with PBS three times for 5 min each.
6. Incubate each slide with 300 µ*l* of blocking solution for 1 h at room temperature.
7. Remove blocking solution and add 200 µl of diluted primary antibody (diluted 1:200 in blocking solution) to each slide. Incubate the slides overnight at 4°C.
8. Rinse as described in step 2.
9. Incubate each slide with 300 µl of blocking solution for 1 h at room temperature.
10. Remove blocking solution and add diluted secondary antibody (anti-rabbit IgG, 1:500 diluted in blocking solution). Incubate the slides with the antibody for 2 h.
11. Rinse as described in step 2.
12. Add 150 µl of DAB solution to each slide. At this point, the slides may be examined under a bright-field microscope to monitor the staining quality. Positive staining is indicated by a reddish-brown precipitate in the nucleus.
13. As soon as the section turns brown, immerse slides in dH_2O.
14. Rinse the slides with dH_2O three times for 5 min each.
15. Counterstain slides with hematoxylin for 10 s.
16. Rinse the slides briefly with dH_2O.
17. Rinse the slides with PBS for 1 min.
18. Rinse the slides with dH_2O two times for 5 min each.
19. Mount the slides using Universal mount and place on a hot plate (65°C) for 30 min to dry the slides.

20. The slides are now ready for final examination under a bright-field microscope.

Specimen Analysis

1. The sections were examined by a pathologist who was blinded to the clinical characteristics of the patients.
2. The intensity of staining for RUNX3 was evaluated using a digital image analysis system (Sony 3CD color video camera; Sony, Tokyo, Japan) and a personal computer equipped with the Optimas Image Analysis software program (Optimas Corp., Bothell, WA).
3. Intranuclear staining of tumor cells was considered to indicate the presence of constitutively activated Stat3.

Immunohistochemical staining results were classified into three groups depending on the percentage of cells with cytoplasm and/or nuclei positive for RUNX3 as follows: negative (< 10%), weakly positive (10–24%), and strongly positive (≥ 25%). Specifically, if < 10% of the tumor cells showed a staining pattern, the slide was classified as negative. When the percentage of RUNX3-positive tumor cells was 10–25%, the slide was classified as weakly positive. When the percentage of RUNX3-positive tumor cells was 25% or higher, the slide was classified as strongly positive.

REFERENCES

Carvalho, R., Milne, A.N., Polak, M., Corver, W.E., Offerhaus, G.J., and Weterman, M.A. 2005. Exclusion of RUNX3 as a tumour-suppressor gene in early-onset gastric carcinomas. *Oncogene* 24: 8252–8258.

Chi, X.Z., Yang, J.O., Lee, K.Y., Ito, K., Sakakura, C., Li, Q.L., Kim, H.R., Cha, E.J., Lee, Y.H., Kaneda, A., Ushijima, T., Kim, W.J., Ito, Y., and Bae, S.C. 2005. RUNX3 suppresses gastric epithelial cell growth by inducing p21(WAF1/Cip1) expression in cooperation with transforming growth factor {beta}-activated SMAD. *Mol. Cell. Biol*. 25: 8097–8107.

Coffman, J.A. 2003. Runx transcription factors and the developmental balance between cell proliferation and differentiation. *Cell Biol. Int*. 27: 315–324.

Ducy, P., Zhang, R., Geoffroy, V., Ridall, A.L., and Karsenty, G. 1997. Osf2/Cbfa1: a transcriptional activator of osteoblast differentiation. *Cell* 89: 747–754.

Friedrich, M.J., Rad, R., Langer, R., Voland, P., Hoefler, H., Schmid, R.M., Prinz, C., and Gerhard, M. 2006. Lack of RUNX3 regulation in human gastric cancer. *J. Pathol*. 210: 141–146.

Fukamachi, H. 2006. Runx3 controls growth and differentiation of gastric epithelial cells in mammals. *Dev. Growth Differ*. 48: 1–13.

Fukamachi, H., and Ito, K. 2004. Growth regulation of gastric epithelial cells by Runx3. *Oncogene* 23: 4330–4335.

Fukamachi, H., Ito, K., and Ito, Y. 2004. Runx3−/− gastric epithelial cells differentiate into intestinal type cells. *Biochem. Biophys. Res. Commun*. 321: 58–64.

Guo, W.H., Weng, L.Q., Ito, K., Chen, L.F., Nakanishi, H., Tatematsu, M., and Ito, Y. 2002. Inhibition of growth of mouse gastric cancer cells by Runx3, a novel tumor suppressor. *Oncogene* 21: 8351–8355.

Guo, C., Ding, Y.L., Sun, L., Lin, T., Song, Y., Sun, L., and Fan, D. 2005. Tumor suppressor gene Runx3 sensitizes gastric cancer cells to chemotherapeutic drugs by downregulating Bcl-2, MDR-1 and MRP-1. *Int. J. Cancer* 116:155–160.

Homma, N., Tamura, G., Honda, T., Matsumoto, Y., Nishizuka, S., Kawata, S., and Motoyama, T. 2006. Spreading of methylation within RUNX3 CpG island in gastric cancer. *Cancer Sci*. 97: 51–56.

Huang, C., Ida, H., Ito, K., Zhang, H., and Ito, Y. 2007. Contribution of reactivated RUNX3 to inhibition of gastric cancer cell growth following suberoylanilide hydroxamic acid (vorinostat) treatment. *Biochem. Pharmacol*. 73: 990–1000.

Ito, K., Liu, Q., Salto-Tellez, M., Yano, T., Tada, K., Ida, H., Huang, C., Shah, N., Inoue, M., Rajnakova, A., Hiong, K.C., Peh, B.K., Han, H.C., Ito, T., Teh, M., Yeoh, K.G., and Ito, Y. 2005. RUNX3,

a novel tumor suppressor, is frequently inactivated in gastric cancer by protein mislocalization. *Cancer Res*. 65: 7743–7750.

Jin, Y.H., Jeon, E.J., Li, Q.L., Lee, Y.H., Choi, J.K., Kim, W.J., Lee, K.Y., and Bae, S.C. 2004. Transforming growth factor-beta stimulates p300-dependent RUNX3 acetylation, which inhibits ubiquitination-mediated degradation. *J. Biol. Chem*. 279: 29409–29417.

Lee, B., Thirunavukkarasu, K., Zhou, L., Pastore, L., Baldini, A., Hecht, J., Geoffroy, V., Ducy, P., and Karsenty, G. 1997. Missense mutations abolishing DNA binding of the osteoblast-specific transcription factor OSF2/CBFA1 in cleidocranial dysplasia. *Nat. Genet*. 16: 307–310.

Levanon, D., Bettoun, D., Harris-Cerruti, C., Woolf, E., Negreanu, V., Eilam, R., Bernstein, Y., Goldenberg, D., Xiao, C., Fliegauf, M., Kremer, E., Otto, F., Brenner, O., Lev-Tov, A., and Groner, Y. 2002. The Runx3 transcription factor regulates development and survival of TrkC dorsal root ganglia neurons. *EMBO J*. 21: 3454–3463.

Levanon, D., Brenner, O., Otto, F., and Groner, Y. 2003. Runx3 knockouts and stomach cancer. *EMBO Rep*. 4:560–564.

Li, Q.L., Ito, K., Sakakura, C., Fukamachi, H., Inoue, K., Chi, X.Z., Lee, K.Y., Nomura, S., Lee, C.W., Han, S.B., Kim, H.M., Kim, W.J., Yamamoto, H., Yamashita, N., Yano, T., Ikeda, T., Itohara, S., Inazawa, J., Abe, T., Hagiwara, A., Yamagishi, H., Ooe, A., Kaneda, A., Sugimura, T., Ushijima, T., Bae, S.C., and Ito, Y. 2002. Causal relationship between the loss of RUNX3 expression and gastric cancer. *Cell* 109: 113–124.

Look, A.T. 1997. Oncogenic transcription factors in the human acute leukemias. *Science* 278: 1059–1064.

Lund, A.H., and van Lohuizen, M. 2002. RUNX: a trilogy of cancer genes. *Cancer Cell* 1: 213–215.

Mundlos, S., Otto, F., Mundlos, C., Mulliken, J.B., Aylsworth, A.S., Albright, S., Lindhout, D., Cole, W.G., Henn, W., Knoll, J.H., Owen, M.J., Mertelsmann, R., Zabel, B.U., and Olsen, B.R. 1997. Mutations involving the transcription factor CBFA1 cause cleidocranial dysplasia. *Cell* 89: 773–779.

Nakase, Y., Sakakura, C., Miyagawa, K., Kin, S., Fukuda, K., Yanagisawa, A., Koide, K., Morofuji, N., Hosokawa, Y., Shimomura, K., Katsura, K., Hagiwara, A., Yamagishi, H., Ito, K., and Ito, Y. 2005. Frequent loss of RUNX3 gene expression in remnant stomach cancer and adjacent mucosa with special reference to topography. Br. J. *Cancer* 92: 562–569.

Parkin, D.M., Bray, F., Ferlay, J., and Pisani, P. 2005. Global cancer statistics, 2002. CA. *Cancer J. Clin*. 55:74–108.

Peng, Z., Wei, D., Wang, L., Tang, H., Zhang, J., Le, X., Jia, Z., Li, Q., and Xie, K. 2006. RUNX3 inhibits the expression of vascular endothelial growth factor and reduced the angiogenesis, growth and metastasis of human gastric cancer. *Clin. Cancer Res*. 12: 6386–6394.

Sakakura, C., Hasegawa, K., Miyagawa, K., Nakashima, S., Yoshikawa, T., Kin, S., Nakase, Y., Yazumi, S., Yamagishi, H., Okanoue, T., Chiba, T., and Hagiwara, A. 2005. Possible involvement of RUNX3 silencing in the peritoneal metastases of gastric cancers. *Clin. Cancer Res*. 11: 6479–6488.

Schuster, N., and Krieglstein, K. 2002. Mechanisms of TGF-beta-mediated apoptosis. *Cell Tissue Res*. 307: 1–14.

Tanaka, K., Yanoshita, R., Konishi, M., Oshimura, M., Maeda, Y., Mori, T., and Miyaki, M. 1993. Suppression of tumourigenicity in human colon carcinoma cells by introduction of normal chromosome 1p36 region. *Oncogene* 8: 2253–2258.

Ushijima, T., and Sasako, M. 2004. Focus on gastric cancer. *Cancer Cell* 5:121–125.

Vogiatzi, P., De Falco, G., Claudio, P.P., and Giordano, A. 2006. How does the human RUNX3 gene induce apoptosis in gastric cancer? Latest data, reflections and reactions. *Cancer Biol. Ther*. 5: 37157–37164.

Waki, T., Tamura, G., Sato, M., Terashima, M., Nishizuka, S., and Motoyama, T. 2003. Promoter methylation status of DAP-kinase and RUNX3 genes in neoplastic and non-neoplastic gastric epithelia. *Cancer Sci*. 94: 360–364.

Wei, D., Gong, W., Oh, S.C., Li, Q., Kim, W.D., Wang, L., Le, X., Yao, J., Wu, T.T., Huang, S., and Xie, K. 2005. Loss of RUNX3 expression significantly impacts the clinical outcome of gastric cancer patients and its restoration causes drastic suppression of tumor growth and metastasis. *Cancer Res*. 65: 4809–4816.

Weith, A., Brodeur, G.M., Bruns, G.A., Matise, T.C., Mischke, D., Nizetic, D., Seldin, M.F., van

Roy, N., and Vance, J. 1996. Report of the second international workshop on human chromosome 1 mapping 1995. Cytogenet. *Cell Genet*. 72: 114–144.

Woolf, E., Xiao, C., Fainaru, O., Lotem, J., Rosen, D., Negreanu, V., Bernstein, Y., Goldenberg, D., Brenner, O., Berke, G., Levanon, D., and Groner, Y. 2003. Runx3 and Runx1 are required for CD8 T cell development during thymopoiesis. *Proc. Natl. Acad. Sci.* U. S. A. 100: 7731–7736.

Yamamura, Y., Lee, W.L., Inoue, K., Ida, H., and Ito, Y. 2006. RUNX3 cooperates with FoxO3a to induce apoptosis in gastric cancer cells. *J. Biol. Chem*. 281: 5267–5276.

Yanada, M., Yaoi, T., Shimada, J., Sakakura, C., Nishimura, M., Ito, K., Terauchi, K., Nishiyama, K., Itoh, K., and Fushiki, S. 2005. Frequent hemizygous deletion at 1p36 and hypermethylation downregulate RUNX3 expression in human lung cancer cell lines. *Oncol. Rep*. 14: 817–822.

Yano, T., Ito, K., Fukamachi, H., Chi, X.Z., Wee, H.J., Inoue, K., Ida, H., Bouillet, P., Strasser, A., Bae, S.C., and Ito, Y. 2006. The RUNX3 tumor suppressor upregulates Bim in gastric epithelial cells undergoing transforming growth factor beta-induced apoptosis. *Mol. Cell. Biol*. 26: 4474–4488.

Yokomizo, T., Ogawa, M., Osato, M., Kanno, T., Yoshida, H., Fujimoto, T., Fraser, S., Nishikawa, S., Okada, H., Satake, M., Noda, T., Nishikawa, S., and Ito, Y. 2001. Requirement of Runx1/AML1/PEBP2alphaB for the generation of haematopoietic cells from endothelial cells. *Genes Cells* 6: 13–23.

Zheng, L., Wang, L., Ajani, J., and Xie, K. 2004. Molecular basis of gastric cancer development and progression. *Gastric Cancer* 7: 61–77.

16
Early Gastric Cancer: Laparoscopic Gastrectomy (Methodology)

Seigo Kitano, Kazuhiro Yasuda, and Norio Shiraishi

INTRODUCTION

Gastric cancer is one of the leading causes of cancer-related deaths worldwide (Roder, 2002; Brennan, 2005). In Asian countries, up to 60% of all gastric cancers are now diagnosed as early gastric cancers because of widespread mass screening and improved diagnostic instruments (Tsubono and Hisamichi, 2000; Japanese Gastric Cancer Association Registration Committee, 2006). Most early gastric cancers are cured by surgery, and it is important to improve the short-term quality of life of these patients after surgery.

During the last 2 decades, laparoscopic surgery has undergone rapid development and has been applied to a variety of gastrointestinal diseases because of its minimal invasiveness (Siu *et al*., 2002; Draaisma *et al*., 2006). We first performed laparoscopy-assisted Billroth I gastrectomy for cancer in 1991 and reported our experience in 1994 (Kitano *et al*., 1994). Many studies have shown that laparoscopic gastrectomy is feasible and safe for early gastric cancer (Kitano *et al*., 2002), and that, in comparison to open gastrectomy, it provides a better short-term postsurgical outcome, including less pain, quicker recovery of gastrointestinal function, preserved postoperative respiratory function, decreased inflammatory and immune responses, and shorter hospital stay (Huscher *et al*., 2005). Moreover, a recent multicenter study of a large patient series showed that laparoscopic gastrectomy for early gastric cancer provides the same oncological curability as open gastrectomy (Kitano *et al*., 2007). Laparoscopic gastrectomy has become an acceptable alternative in the treatment of gastric cancer, and its use is increasing worldwide (Carboni et al., 2005). This report describes the current status, indications, and technical details of laparoscopic gastrectomy for early gastric cancer.

CURRENT STATUS OF LAPAROSCOPIC GASTRECTOMY FOR CANCER IN JAPAN

The Japan Society of Endoscopic Surgery (JSES) conducts a nationwide survey regarding endoscopic surgery every 2 years. The eighth survey was conducted in 2006. Questionnaires were sent to the 2,619 facilities of which the members of JSES

belonged to, and responses were received from 1,373 facilities (52.4%).

According to the eighth nationwide survey, a total of 12,626 laparoscopic surgeries were performed for gastric cancer during the period of 1991 through 2005. These included 9,063 laparoscopy-assisted distal gastrectomies (LADGs), 1,844 laparoscopic local resections, 496 laparoscopy-assisted total gastrectomies (LATGs), 433 laparoscopy-assisted proximal gastrectomies (LAPGs), 416 laparoscopic intragastric mucosal resections, and 374 other laparoscopic surgeries. LADG is the procedure most frequently used to treat gastric cancer and the number of LADGs has increased rapidly. Moreover, the number of advanced and complicated laparoscopic gastric surgeries such as LATG and LAPG have increased gradually with the development of new laparoscopic surgery instruments and techniques.

Laparoscopic lymph node dissections performed in the 9,063 LADGs consisted of 5,405 D1+α dissections (No. 7 nodes), 2,506 D1+β dissections (no. 7, 8, 9 nodes), and 1,153 D2 dissections. The numbers and groups of dissected lymph nodes were defined according to the Japanese Classification of Gastric Carcinoma. D1+α lymph node dissection includes removal of perigastric lymph nodes and lymph nodes at the base of the left gastric artery (no. 7), D1+β dissection includes removal of lymph nodes along the common hepatic artery (no. 8), around the celiac artery (no. 9). In addition to D1+α dissection, D2 dissection includes removal of lymph nodes along the splenic artery, in the hepatodudenal ligament, and along the superior mesenteric vein, in addition to D1+β dissection. In 2005, up to 14.6% (2,631/18,070) of all gastric cancers treated surgically or endoscopically were treated by laparoscopic surgery. The rates of intra- and postoperative complications after LADG were 1.9% and 9.0%, respectively, and the rate of conversion to open surgery was 1.3%.

INDICATIONS FOR LAPAROSCOPIC GASTRECTOMY FOR EARLY GASTRIC CANCER

The Clinical Guidelines for the Treatment of Gastric Cancer published by the Japanese Gastric Cancer Association (JGCA) provide detailed treatment strategies based on preoperative determination of the depth of wall invasion and status of lymph node metastasis (JGCA, 2004). When endoscopic treatment, such as endoscopic mucosal resection or endoscopic submucosal dissection cannot be performed, early gastric cancer is managed by laparoscopic surgery. The recommended degrees of lymph node dissection are as follows: (1) D1+α for mucosal cancer with ulceration, poorly differentiated mucosal cancer, or submucosal cancer measuring ≤ 1.5 cm in diameter, (2) D1+β for submucosal cancer measuring > 1.5 cm in diameter, and mucosal cancer measuring 4 cm or less in diameter and without ulceration, and (3) D2 for submucosal cancer with lymph node metastasis.

LAPAROSCOPY-ASSISTED DISTAL GASTRECTOMY

Patient Positioning and Operating Room Setup

The patient under general anesthesia is placed in a slight 10° reverse Trendelenburg

position, and the legs are abducted on flat padded boards. The laparoscopic and video units are positioned at the left side of the patient's head. The surgical nurse's table is placed on the patient's right side, at his right foot. The surgeon stands between the patient's abducted legs, and the camera operator stands on the patient's right side. The first assistant is on the patient's left and the second assistant on the right.

Equipment

The following equipment and instruments are recommended for LADG.

- Laparoscopic unit
- A 30° laparoscope
- One Hasson trocar
- Three 10 mm trocars
- One 5 mm trocars
- Three fenestrated grasping forceps
- Maryland dissection forceps
- One 10 mm clip applicator
- One "snake" retractor
- One 5 mm suction and irrigation tube for laparoscopic application
- Ultrasonic shears
- Vessel sealing system if available
- Wound protector and retractor
- Linear stapler

Port Placement

One Hasson's trocar, three 10 mm trocars, and one 5 mm trocar are used. Initially, the Hasson's trocar is inserted at the inferior margin of the umbilicus in an open manner. Pneumoperitoneum at 10 mm Hg is created, and the camera is inserted into the abdomen. The left-sided surgical trocar (surgeon's right hand) is placed above and to the left of the umbilicus, roughly one-third of the distance to the left subcostal margin, and the right-sided surgical trocar (surgeon's left hand) is placed above and to the right of the umbilicus (Figure 16.1). A third 10-mm left lateral subcostal trocar (first assistant) is placed for the purpose of exposure. A 5-mm right lateral subcostal trocar (second assistant) allows retraction of the liver.

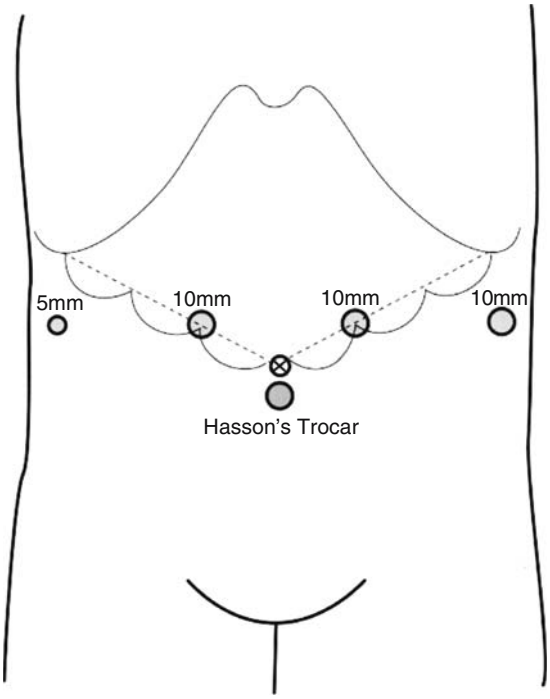

FIGURE 16.1. Port placement

Surgical Procedure

Technical principles of LADG include the following: (1) dissection of the greater omentum and division of the gastroepiploic vessels, (2) dissection of the lesser omentum and division of the right gastric vessels, (3) division of the left gastric vessels and dissection of the right paracardial lymph nodes, (4) dissection of the extragastric lymph nodes, (5) mini-laparotomy and division of the stomach, and (6) reconstruction.

Dissection of the Greater Omentum and Division of the Gastroepiploic Vessels

The greater omentum is opened and divided approximately 3 cm from the gastroepiploic arcade along the greater curvature with the use of ultrasonic shears. By retracting the stomach upward with the first assistant's grasping forceps, it is easier to identify the gastroepiploic vessels. Dissection is carried out around the gastrosplenic ligament, and the left gastroepiploic vessels are exposed and divided with the use of ultrasonic coagulating shears. At this time, the greater curvature of the stomach is cleared of fat for subsequent anastomosis. Division of the gastrocolic ligament is then advanced distally toward the pylorus. The infrapyloric lymph nodes are dissected, and the right gastroepiploic vessels are controlled by clipping and divided at their origin. It is important to carefully expose the inferior plane of the pancreas head to identify the origins of the right gastroepiploic vessels.

Dissection of the Lesser Omentum and Division of the Right Gastric Vessels

The liver is lifted with a "snake" retractor. The lesser omentum is opened and then dissected between the hepatoduodenal ligament and the abdominal esophagus. The right gastric vessels are carefully isolated, allowing dissection of the suprapyloric lymph nodes, and are divided at their origins with the use of ultrasonic shears. When Roux-en Y reconstruction is planned, the first portion of the duodenum is divided at this time with a linear stapling device.

Division of the Left Gastric Vessels and Dissection of the Right Paracardial Lymph Nodes

The peritoneum along the anterior border of the right crus is incised to the esophageal hiatus. The left gastric vessels are isolated and divided at their origin with double clips, allowing dissection of the lymph nodes along the left gastric artery (Figure 16.2). To dissect the right paracardial lymph nodes, the upper third of the lesser curvature of the stomach is skeletonized with the use of ultrasonic shears.

Dissection of the Extragastric Lymph Nodes

When D1+β or D2 lymph node dissection is planned, additional lymph node dissection is performed. Exposure of the common hepatic artery, splenic artery, and celiac artery is facilitated by caudal retraction of the pancreas. With the use of ultrasonic shears, lymph nodes along the common hepatic artery are dissected up to the celiac axis, and the lymph nodes along the splenic artery are dissected.

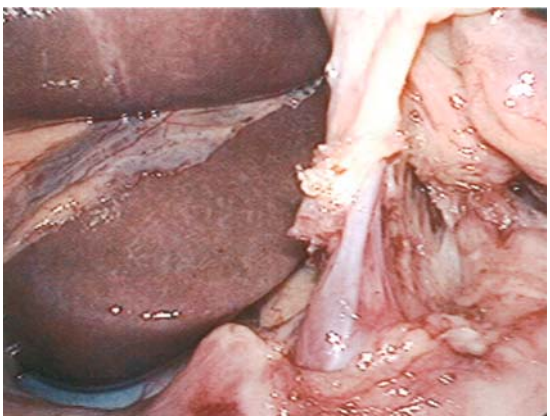

FIGURE 16.2. Isolation of the left gastric vein

Mini-Laparotomy and Division of the Stomach

When Billroth I reconstruction is selected, a 5 cm long mini-laparotomy is made at the upper abdomen and 2 cm to the right of the midline. If Roux-en Y reconstruction is planned, a mini-laparotomy is made on the upper midline. The wound is protected with a wound-sealing device, and the fully mobilized stomach is exteriorized through this opening. The distal two-thirds of the stomach is resected with a linear stapler.

Reconstruction

For Billroth I reconstruction, a hand-sewn gastroduodenostomy is created through the mini-laparotomy. For Roux-en Y reconstruction (Figure 16.3), gastrojejunostomy and jejunostomy are created through the mini-laparotomy. These procedures are carried out as functional end-to-end anastomoes, with linear staplers. The abdomen is then irrigated, and the hemostasis is checked. A closed-suction drain is placed in the subhepatic space. Finally, the wounds are cleaned with saline and closed.

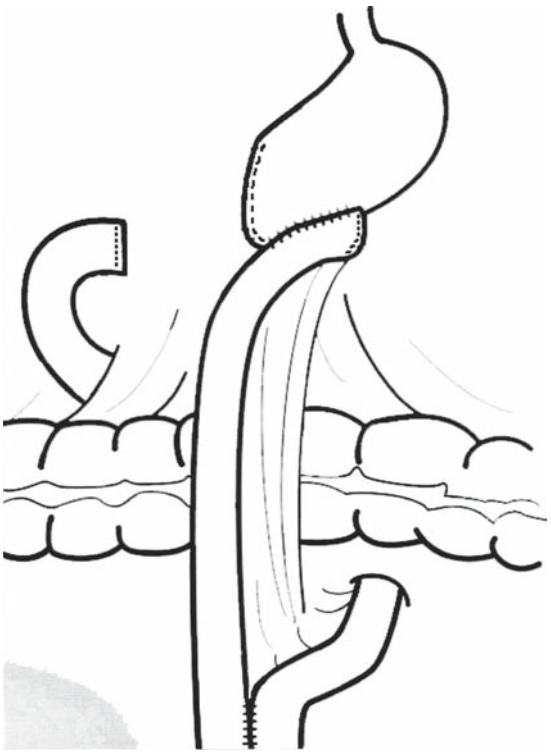

FIGURE 16.3. Roux-en Y reconstruction

LAPAROSCOPY-ASSISTED PROXIMAL GASTRECTOMY

In 1999, we described laparoscopy-assisted proximal gastrectomy followed by gastric tube reconstruction for early gastric cancer (Kitano *et al*., 1999). Previous studies showed that open proximal gastrectomy with gastric tube reconstruction is simple and safe (Adachi *et al*., 1999) and that it provides earlier recovery and better performance status than those provided by total gastrectomy with Roux-en Y reconstruction or proximal gastrectomy with jejunal interposition (Shiraishi *et al*., 2002).

Early proximal gastric cancers confined to the mucosa or submucosa are associated with lymph node-negative status in most patients, and metastatic nodes are limited to the perigastric nodes of the upper part of the stomach (Kitamura *et al*., 1997; de Manzoni *et al*., 1998). Therefore, LAPG is applied to early proximal gastric cancer. Patient positioning, operating room setup, and port placement are the same as for LADG.

Surgical Procedure

Technical principles of LAPG include the following: (1) mobilization of the upper half of the greater curvature of the stomach, (2) dissection of the lesser curvature and division of the left gastric vessels, (3) mobilization of the upper portion of

the stomach and division of the lower esophagus, (4) mini-laparotomy and division of the proximal stomach, and (5) gastric tube reconstruction.

Mobilization of the Upper Half of the Greater Curvature of the Stomach

The greater omentum is opened and divided approximately 3 cm lateral to the gastroepiploic arcade along the greater curvature. To free the greater curvature of the upper stomach, gastrosplenic and gastrophrenic ligaments are dissected, and short gastric vessels are divided with the use of ultrasonic shears or a vessel sealing system. For gastric tube reconstruction, it is necessary to preserve the right gastroepiploic vessels and gastroepiploic arcade.

Mobilization of the Upper Portion of the Stomach and Division of the Left Gastric Vessels

The left lobe of the liver is lifted with a "snake" retractor. The lesser omentum is then opened and divided from the esophagus to the region of the lower antrum. The left gastric vessels are doubly clipped and divided at their origins. The peritoneum of the right crus is incised and dissected in the anterior to posterior direction, and complete dissection of the left crus, gastric fundus, and the vagal nerve is performed, allowing circumferential mobilization of the abdominal part of the esophagus. The abdominal esophagus is transected with a laparoscopic linear stapler.

Mini-Laparotomy and Division of the Proximal Stomach

A 5-cm mini-laparotomy is created in the upper midline, and the mobilized stomach is pulled out of the peritoneal cavity. To form a gastric tube 15 cm long and 4 cm wide, the stomach is transected between two points of the distal three-fourths of the lesser curvature and one-half of the greater curvature with the use of linear staplers (Figure 16.4).

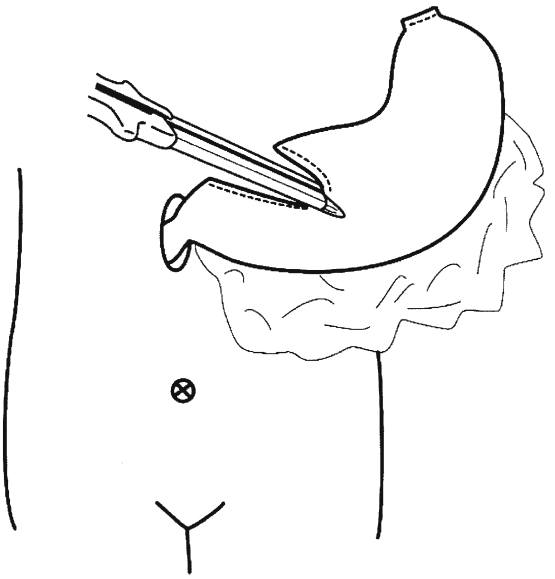

FIGURE 16.4. Making a gastric tube with linear staplers

Gastric Tube Reconstruction

Esophagogastrostomy is achieved using a circular stapler through mini-laparotomy (Figure 16.5). The lower esophagus is anastomosed to the posterior wall of the gastric tube. Simultaneous resection of the proximal stomach and closure of the stapler introduction site of the gastric tube with a linear stapler is carried out (Figure 16.6). Pyloroplasty is not performed. The integrity of the anastomosis is tested by indigogarmine injection via a nasogastric tube. After the abdomen is irrigated and hemostasis is confirmed, a closed-suction drain is placed in the subhepatic space. The wounds are cleaned with saline and closed. Postoperative roentgenography should show no stenosis of the anastomosis and good passage through the gastric tube.

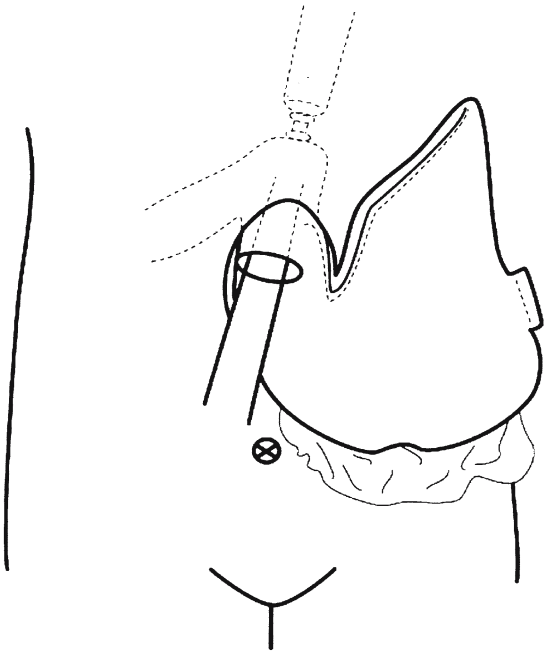

FIGURE 16.5. Performing esophagogastrostomy with a circular stapler through mini-laparotomy

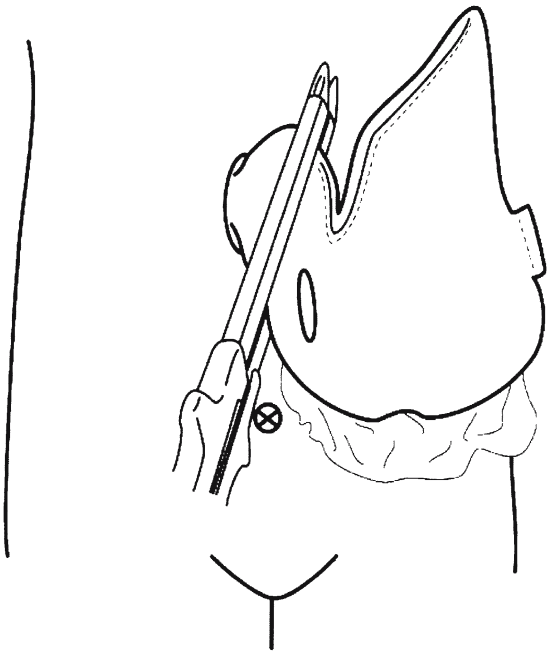

FIGURE 16.6. Resection of the proximal stomach and closure of the stapler introduction site of the gastric tube

In summary, with the establishment of laparoscopic gastrectomy techniques, the operation time and morbidity of this procedure have been reduced (Shiraishi *et al*., 2006). Laparoscopic gastrectomy has become the best treatment option for patients with early gastric cancer (Kitano and Shiraishi, 2005). To determine the future role of laparoscopic surgery in the treatment of gastric cancer, including cases of advanced cancer, a large prospective randomized trial of laparoscopic versus open gastrectomy should be performed.

REFERENCES

Adachi, Y., Inoue, T., Hagino, Y., Shiraishi, N., Shimoda, K., and Kitano, S. 1999. Surgical results of proximal gastrectomy for early-stage gastric cancer: jejunal interposition and gastric tube reconstruction. *Gastric Cancer 2*: 40–45.

Brennan M.F. 2005. Current status of surgery for gastric cancer: a review. *Gastric Cancer 8*: 64–70.

Carboni, F., Lepiane, P., Santoro, R., Mancini, P., Lorusso, R., and Santoro, E. 2005. Laparoscopic surgery for gastric cancer: preliminary experience. *Gastric Cancer 8*: 75–77.

de Manzoni, G., Morgagni, P., Roviello, F., Di Leo, A., Saragoni, L., Marrelli, D., Guglielmi, A., Carli, A., Folli, S., and Cordiano, C. 1998. Nodal abdominal spread in adenocarcinoma of the cardia: results of a multicenter prospective study. *Gastric Cancer 1*: 146–151.

Draaisma, W.A., Rijnhart-de, Jong, H.G., Broeders, I.A., Smout, A.J., Furnee, E.J., and Gooszen, H.G. 2006. Five-year subjective and objective results of laparoscopic and conventional Nissen fundoplication: a randomized trial. *Ann. Surg. 244*: 34–41.

Huscher, C.G.S., Mingoli, A., Sgarzini, G., Sansonetti, A., Paola, MD., Recher, A., and Ponzano, C. 2005. Laparoscopic versus open subtotal gastrectomy for distal gastric cancer: five-year results of a randomized prospective trial. *Ann. Surg. 241*: 232–237.

Japanese Gastric Cancer Association Registration Committee, Maruyama, K., Kaminishi, M., Hayashi, K., Isobe, Y., Honda, I., Katai, H., Arai, K., Kodera, Y., and Nashimoto, A. 2006. Gastric cancer treated in 1991 in Japan: data analysis of nationwide registry. *Gastric Cancer 9*: 51–66.

Japanese Gastric Cancer Association. 2004. Guidelines for the treatment of gastric cancer, 2nd edition [in Japanese]. Tokyo. Kanehara-shuppan.

Kitamura, K., Yamaguchi, T., Nishida, S., Yamamoto, K., Ichikawa, D., Okamoto, K., Taniguchi, H., Hagiwara, A., Sawai, K., and Takahashi, T. 1997. The operative indications for proximal gastrectomy in patients with gastric cancer in the upper third of the stomach. *Surg. Today 27*: 993–998.

Kitano, S., Iso, Y., Moriyama, M., and Sugimachi, K. 1994. Laparoscopy-assisted Billroth I gastrectomy. *Surg. Laparosc. Endosc. 4*: 146–148.

Kitano, S., Adachi, Y., Shiraishi, N., Suematsu, T., and Bando, T. 1999. Laparoscopic-assisted proximal gastrectomy for early gastric carcinomas. *Surg. Today 29*: 389–391.

Kitano, S., and Shiraishi, N. 2005. Minimally invasive surgery for gastric tumors. *Surg. Clin. N. Am. 85*: 151–164.

Kitano, S., Shiraishi, N., Fujii, K., Yasuda, K., Inomata, M., and Adachi, Y. 2002. A randomized controlled trail comparing open vs laparoscopy-assisted distal gastrectomy for the treatment of early gastric cancer: an interim report. *Surgery 131*: S306–S311.

Kitano, S., Shiraishi, N., Uyama, I., Sugihara, K., and Tanigawa, N., Japanese Laparoscopic Surgery Study Group. 2007. A multicenter study on oncologic outcome of laparoscopic gastrectomy for early cancer in Japan. *Ann. Surg. 245*: 68–72.

Roder, D.M. 2002. The epidemiology of gastric cancer. *Gastric Cancer 5* (Suppl 1): 5–11.

Shiraishi, N., Adachi, Y., Kitano, S., Kakisako, K., Inomata, M., and Yasuda, K. 2002. Clinical outcome of proximal versus total gastrectomy for proximal gastric cancer. *World J. Surg. 26*: 1150–1154.

Shiraishi, N., Yasuda, K., and Kitano, S., 2006. Laparoscopic gastrectomy with lymph node dissection for gastric cancer. *Gastric Cancer 9*: 167–176.

Siu, W.T., Leong, H.T., Law, B.K., Chau, C.H., Li, A.C., Fung, K.H., Tai, Y.P., and Li, M.K. 2002. Laparoscopic repair for perforated peptic ulcer: a randomized controlled trial. *Ann. Surg. 235*: 313–219.

Tsubono, Y., and Hisamichi, S. 2000. Screening for gastric cancer in Japan. *Gastric Cancer 3*: 9–18.

17
Gastric Cancer: Overexpression of Hypoxia-Inducible Factor 1 as a Prognostic Factor

Yoshihiro Kakeji, Eiji Oki, Noriaki Sadanaga, Masaru Morita, and Yoshihiko Maehara

INTRODUCTION

Despite a worldwide decline in incidence, gastric cancer remains the fourth most common cancer and the second most frequent cause of death from cancer, accounting for 10.4% of cancer deaths worldwide (Parkin, 2004). Though the prognosis of resectable gastric cancer remains fair, the treatment of advanced or recurrent gastric cancer is still far from satisfactory. Currently, the only curative treatment for gastric cancer is a surgical resection of the primary tumor with an appropriate lymphadenectomy because the disease is considered to be resistant to chemotherapy and radiotherapy (Griffiths *et al*., 2005). Patients with early gastric cancer are in the minority and the disease typically presents at an advanced stage, which often precludes a curative surgical resection. Even in patients who have an apparently curative resection, approximately, a quarter of all individuals tend to progress and develop either recurrent or metastatic disease.

The process of tumor progression (i.e., proliferation, local invasion, and distant metastasis) is characterized by rapid cellular growth accompanied by alterations of the microenvironment of the tumor cells (Vaupel, 2004). To a large extent, the alterations in the cellular microenvironment are due to an inadequate oxygen (O_2) supply and the resultant hypoxia or even anoxia. Hypoxia is defined as a loss of oxygen in tissues and is widespread in solid tumors due to the ability of the tumor to outgrow the existing vasculature (Kimbro and Simons, 2006). The oxygen tension in normal tissues has a mean of ~ 7% oxygen; in tumors, the mean oxygen tension is 1.5% (Vaupel, 2004).

Lethal clones of human cancer have the ability to adapt to the hypoxic environments in primary or metastatic sites. Tumor cells must survive by adapting to a low pO_2 or by increasing vascularization, or both. To grow beyond a diameter of 1 mm, newly developing tumors must form their own vascular network and blood supply, which they accomplish either by incorporating preexisting host vessels or by forming new microvessels through the influence of tumor angiogenesis factors (Folkman, 1990). Many gene products are involved in tumor neoangiogenesis. One of the most investigated and 'drugable' targets is vascular endothelial growth factor (VEGF), which is secreted by hypoxic

tumor cells. In addition to increased vascularization, hypoxia initiates multiple cellular responses, such as erythropoiesis, matrix metabolism, glucose metabolism, cell proliferation, and apoptosis (Ke and Costa, 2006). These adaptive changes contribute to alterations leading to increased survival phenotype with clinical aggressiveness. Tumor hypoxia tends to result in a poorer prognosis at diagnosis in several types of cancers. In turn, these hypoxic adaptations make the tumors more difficult to treat and confer increased resistance to death from chemotherapy and radiotherapy.

This report is a focused review of what has been learned regarding a pivotal gene in the cancer biology of hypoxic adaptation and angiogenesis: the hypoxia inducible factor 1 (HIF-1) complex. This review will concentrate on gastrointestinal tract oncology. New data on HIF-1 signaling, the potential for targeted therapies, and the selective investigational HIF-1α inhibiting small molecules will also be discussed.

HYPOXIA INDUCIBLE FACTOR-1

Cellular recognition of hypoxia, i.e., decreased oxygen tension, and an appropriate response to meet this kind of stress is predominantly facilitated by the transcription factor known as HIF (Zhou *et al*., 2006). HIF-1 is a heterodimer composed of one of the three alpha subunits (HIF-1α, HIF-2α, or HIF-3α) and one HIF-1β subunit. HIF-1β is also known to be an aryl hydrocarbon nuclear translocator (ARNT). The HIF-1β subunit is constitutively expressed independent of cellular hypoxia, whereas the expression and activity of the HIF-1α subunit are precisely regulated by the cellular O_2 concentration. Under normoxia, HIF-1α is usually unstable and virtually undetectable. HIF-1α is regulated post-transcriptionally in normoxia by ubiquitination and interaction with the von Hippel-Lindau tumor suppressor protein (pVHL) and then degraded by the 26S proteasome (Maxwell *et al*., 1999). Small changes in the oxygen supply affect enzyme activity, making the system well suited to function as an oxygen sensor. When cells are hypoxic, HIF-1α hydroxylation and pVHL association are lowered and steady-state HIF-1α protein levels rise. HIF-1α protein with its nuclear localization sequence is then translocated to the nucleus; in this process, it forms heterodimers with HIF-1β, and the HIF-1α complex binds to the hypoxic responsive elements (HREs) upstream of the hypoxic-regulated genes where it acts as a transcription factor (Kaelin, 2002).

HIF-1α Signaling Pathway

HIF-1β is activated by both oncogenes and the loss of tumor suppressor gene function. One of the oncogene pathways modulating and influencing HIF-1α regulation is the Harvey rat sarcomal viral oncogene homology/extracellular signal-regulated kinase (*RAS*/ERK) pathway (Lim *et al*., 2004). *RAS* effects the VEGF expression through HIF-1α, which is mediated through tyrosine kinase signaling. Murine leukemia viral oncogene homolog 1/Map/ERK Kinase-1/extracellular signal-regulated kinase (*Raf*/MEK1/ERK), a pathway shared with AKT (Chun *et al*., 2003) (Figure 17.1). Another oncogene that has been shown to induce VEGF through HIF-1α signaling via activation of the protein tyrosine kinase, is c-*Src*, and/or

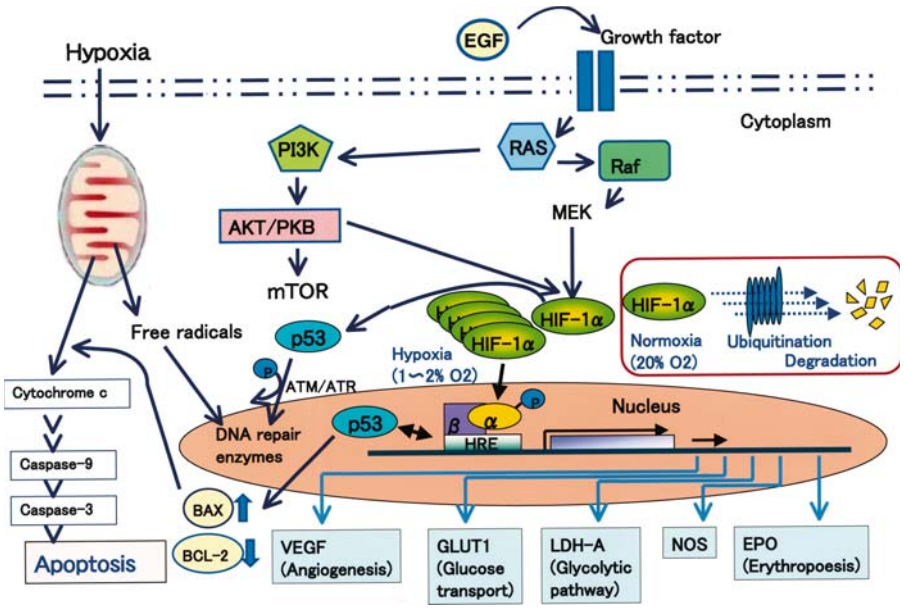

FIGURE 17.1. Under hypoxic conditions, HIF-1α is phosphorylated and stabilized through a complex multi-responsive series of different oncogenic signalling pathways originating from RAS to either phosphatidylinositol 3-OH kinase (PI3K)/AKT or RAF/MEK pathway. In turn, HIF-1α dimerizes with HIF-1α/ARNT, translocates to the nucleus, and interacts with transcription factors to activate transcription. HIF-1α activates genes which promote angiogenesis, glucose transport, glycolytic pathway, and erythropoiesis. HIF-1 also interacts with the tumor suppressor p53 to promote p53-dependent apoptosis

its downstream mediator phosphatidylinositol 3-kinase (PI3K). *Src* and PI3K activation appear to increase the expression and the stability of HIF-1α; therefore, increasing the VEGF levels (Karni, 2002). HIF-1α physically associates with STAT3, CBP/p300, and Redox effector factor 1/apurinic/apyrimidinic endonuclease (Ref-1/APE) (Gray *et al*., 2005).

The loss of *VHL* tumor suppressor gene creates upregulation of HIF-1α in renal carcinoma (Zagzag *et al*., 2005), and mutations and the allelic loss of the phosphatase and tensin homolog (*PTEN*) tumor suppressor gene activate HIF-1α through increased downstream signaling from AKT-1 (Zundel *et al*., 2000).

Although hypoxia is the main regulator of HIF-1α, there is emerging evidence that it is stabilized by several non-oxygen dependent mechanisms. Various tumor specific genetic alterations involving oncogenes (*PAS* and *MYC*) and tumor suppressor genes (*p53*, *PTEN* and *VHL*) have been associated with HIF-1α stabilization (Semenza, 2002). Cytokines, such as insulin, insulin-like growth factor (IGF), epidermal growth factor (EGF), and interleukin-1 stimulate receptor tyrosine kinases which also influence HIF-1α levels.

HIF-1α Regulated Products

Approximately, 100 HIF-1 downstream genes with varying functions have been identified (Ke and Costa, 2006). HIF-1 binds to a 50-base pair *cis*-acting HRE located in their enhancer and promoter regions and activates the expression of these genes.

Glucose Metabolism

In the expanding tumor mass, which is generally characterized by a limited O_2 supply and a high glucose consumption rate, anaerobic glycolysis can become the predominant pathway of adenosine triphosphate (ATP) generation (Wenger, 2002). Under conditions of a low oxygen supply, the expression of glycolytic enzymes and glucose transporters 1 and 3 (GLU1, GLU3) are upregulated, which switch the glucose metabolism pathway away from the oxygen-dependent tricarboxylic acid (TCA) cycle to the oxygen-independent glycolysis (Seagroves *et al*., 2001).

Angiogenesis

Vascular endothelial cell growth factor (VEGF) is the most potent endothelial-specific mitogen, and it directly participates in angiogenesis by recruiting endothelial cells into hypoxic and avascular area and stimulates their proliferation (Neufeld *et al*., 1999). HIF-1 not only mediates angiogenesis by induction of VEGF, but also influences the tumor blood flow by more complex mechanisms involving target genes that play a role in vessel tone, such as, nitric oxide synthase (NOS2), heme oxygenease 1, endothelin 1 (ET1), adrenomedullin (ADM), and the α_{1B}-adrenergic receptor (Ke and Costa, 2006). Moreover, hypoxia induces genes involved in matrix metabolism and vessel maturation such as matrix metalloproteinases (MMPs), plasminogen activator receptors and inhibitors (PAIs), and collagen prolyl hydroxylase (Ke and Costa, 2006).

Cell Proliferation

Hypoxia and HIF-1 induce growth factors, such as insulin-like growth factor-2 (IGF2) and transforming growth factor-β (TGF- β) (Krishnamachary *et al*., 2003). Cytokines and growth factors as well as hypoxia in some cell types can activate the MAPK and PI3K signaling pathways, which promote cell proliferation as well as contribute to HIF-1 activity. This leads to increased HIF-1 transcriptional activity of target genes, including those encoding IGF2 and TGF- β; thereby, contributing to autocrine-signaling pathways that are crucial for cancer progression (Semenza, 2003).

Apoptosis

Cell adaptation to hypoxia leads not only to cell proliferation/survival but also to cell death in some circumstances. The expression of HIF-1α and HIF-1β is significantly correlated with apoptosis and the proapoptotic factors, such as caspase-3, Fas, and Fas ligand (Volm and Koomagi, 2000). Moreover, hypoxia depresses the antiapoptotic protein Bcl-2, whereas the proapoptotic protein Bcl-2/adenovirus EIB 19-kDa interacting protein 3 (BNip3) and its homolog Nip3-like protein X (NIX) are upregulated in a HIF-dependent manner (Bruick, 2000). Some genes involved in cell cycle control, such as *p53* and *p21*, are also found to be HIF-dependent, and *p53* has been implicated in regulating hypoxia-induced apoptosis through the induction of apoptosis-related genes such as *Bax*, *NOXA*, *PUMA*, and *PERP* (Schuler and Green, 2001).

HIF-1α in Tumor

An overexpression of HIF-1α and HIF-2α was found in various human cancers, probably as a consequence of intratumoral hypoxia or genetic alteration (Talks *et al*., 2000). Immunohistochemical analyses

demonstrated detectable levels of HIF-1α protein in benign tumors, with elevated levels in primary malignant tumors, and a marked amount in tumor metastases. In contrast, it is absent in normal tissues (Harris, 2002). In addition, the injection of HIF-1α (or HIF-1β) positive and deficient cells into immunocompromised mice revealed that HIF-1α is a positive tumorigenesis factor (Maxwell *et al*., 1997). It seems that HIF-1α overexpression confers selective advantages to tumor cells. A correlation between HIF-1 overexpression and patient mortality, poor prognosis, or treatment resistance has also been noted in many studies (Semenza, 2003).

HIF-1α in Gastric Cancer

HIF-1α is not generally expressed in normal gastric mucosa. HIF-1α, VEGF, and IGF-2 expression patterns were examined immunohistochemically in 126 specimens of gastric carcinoma (Mizokami *et al*., 2006a). The expression of HIF-1α in gastric carcinomas was frequently detected at the invading edge of the tumor margin and at the periphery of necrotic regions within the tumor mass. Of the gastric carcinoma specimens from 126 patients, 49 (38.9%) were positive for HIF-1α immunoreactivity. HIF-1α expression was positively correlated with tumor size ($P < 0.005$) and with depth of invasion ($P = 0.018$) and was more frequent in cases of tumors with lymphatic invasion and undifferentiated adenocarcinomas. The expression of HIF-1α, VGEF, and IGF-2 proteins was observed in serial sections of several specimens. The intratumor microvessel density (MVD), determined using anti-CD34 antibodies, was significantly higher in tumors from HIF-1α positive patients than in HIF-1α negative sections. In gastric carcinoma, HIF-1α seems to induce VEGF and this event leads to the formation of vascular networks which supply oxygen and nutrients. The 5-year survival rate was 58.4% for HIF-1α positive patients and 81.5% for HIF-1α negative patients ($P = 0.009$). HIF-1α expression is an independent prognostic factor in gastric carcinoma ($P = 0.032$). Griffiths *et al*. (2007) recently reported the investigation of United Kingdom population containing 97 gastro-esophageal junction tumors and 80 noncardia gastric cancers. Their result suggested that HIF-1α was involved in gastric carcinogenesis and disease progression, but was only a weak prognostic factor for survival.

The expression of HIF-1α and p53 proteins was also investigated in 216 specimens of primary gastric cancer (Sumiyoshi *et al*., 2006). HIF-1α(+)/p53(+) tumors showed an undifferentiated type, an infiltrative growth appearance, and an invasive lymphatic involvement more frequently in comparison to HIF-1α(−)/p53(−) tumors. HIF-1α(+)/p53(+) tumors also had more lymph node metastasis in comparison to HIF-1α(−)/p53(−) tumors. When stratified for HIF-1α and p53 positivity, the patients who were p53-negative and HIF-1a-negative had the most favorable prognosis, whereas patients who were p53-positive and HIF-1α-positive had the worst prognosis ($P = 0.0018$) (Figure 17.2). Using a multivariate Cox regression analysis, the depth of invasion, lymph node metastasis, and HIF-1α positivity were all found to be independent prognostic factors in patients with gastric cancer.

Determining the relative hypoxic fraction of a solid tumor is of clinical relevance. Many studies have shown that the greater the hypoxic fraction, the worse

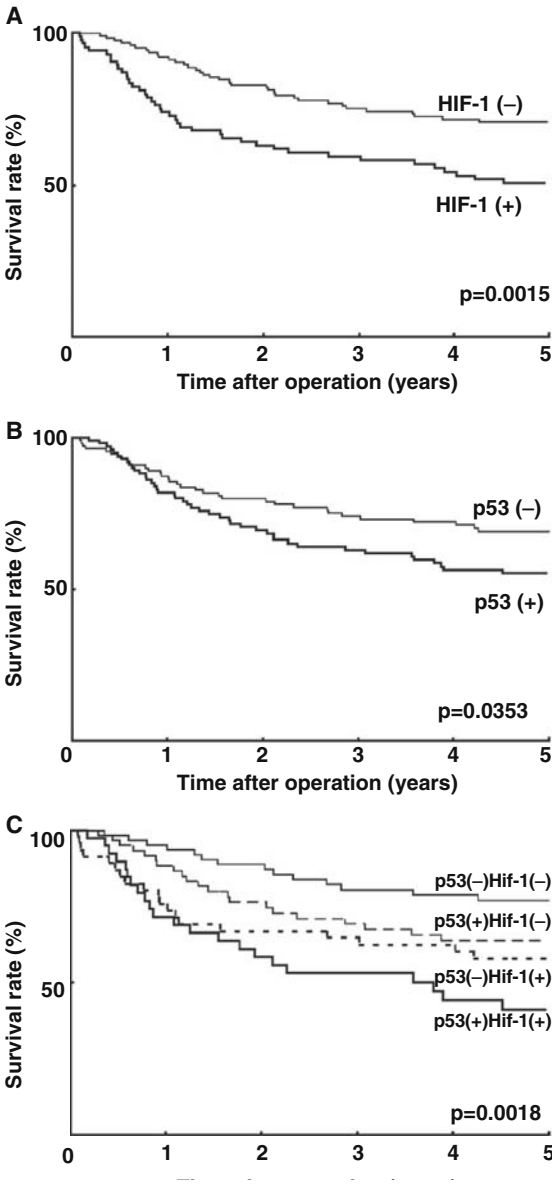

FIGURE 17.2. Survival curves for patients with gastric cancer, in relation to HIF-1α and p53 expressions. a, patients with HIF-1a-positive tumors (n = 85) had a shorter survival time than did those with HIF-1a-negative tumors (n = 131, P = 0.0015). b, patients with p53-positive tumors (n = 102) had a shorter survival time than did those with p53-negative tumors (n = 114, P = 0.0353). c, there was a significant difference among groups stratified to HIF-1a/p53 expressions (P = 0.0018).The patients with HIF-1α(+)/p53(+) tumors had the worst prognosis. (Reproduced with permission of Sumiyoshi *et al*., 2006.)

the prognosis for the patient (Hockel and Vaupel, 2003). The reasons behind this are multifaceted but, for simplicity, can be divided into two categories. First, cells that adapt to a hypoxic environment have a growth advantage and are therefore more aggressive. Secondly, hypoxic cells are more resistant to both chemotherapy and radiotherapy (Hammond and Giaccia, 2006). A loss of p53 is actively selected during in tumor development and mutant p53 is observed in tumor sections (Figure 17.3). In brief, HIF-1 has been described as mediating the accumulation of p53 in response to hypoxia, although p53 inhibits HIF-1α stabilization (Chen *et al*., 2003). Furthermore, the loss of HIF-1á-dependent *p21* expression results decreased apoptosis, increased cell survival, and more aggressive tumors (Mizokami *et al*. 2006b). *p21* mediates cell cycle arrest and is one of the downstream genes targeted by HIF-1. It seems that HIF-1α overexpression confers selective advantages to tumor cells. A correlation between HIF-1 overexpression and patient mortality, poor prognosis, or treatment resistance has been noted in many studies (Semenza, 2003).

HIF Targeted Therapeutics

Overexpression of either HIF-1 negatively affects patient prognosis. What remains to be seen is where these findings will lead cancer therapy. More recently, there have also been exciting developments in the search for efficacious HIF-1 inhibitors (Kimbro and Simons, 2006). The small molecule YC-1 3-(5'-hydroxy-methyl-2'-furyl) -1-benzylindazole) was also shown to reduce HIF-1 levels and gastric tumor xenograft growth (Yeo *et al*., 2003). A disruption of microtubule polymerization

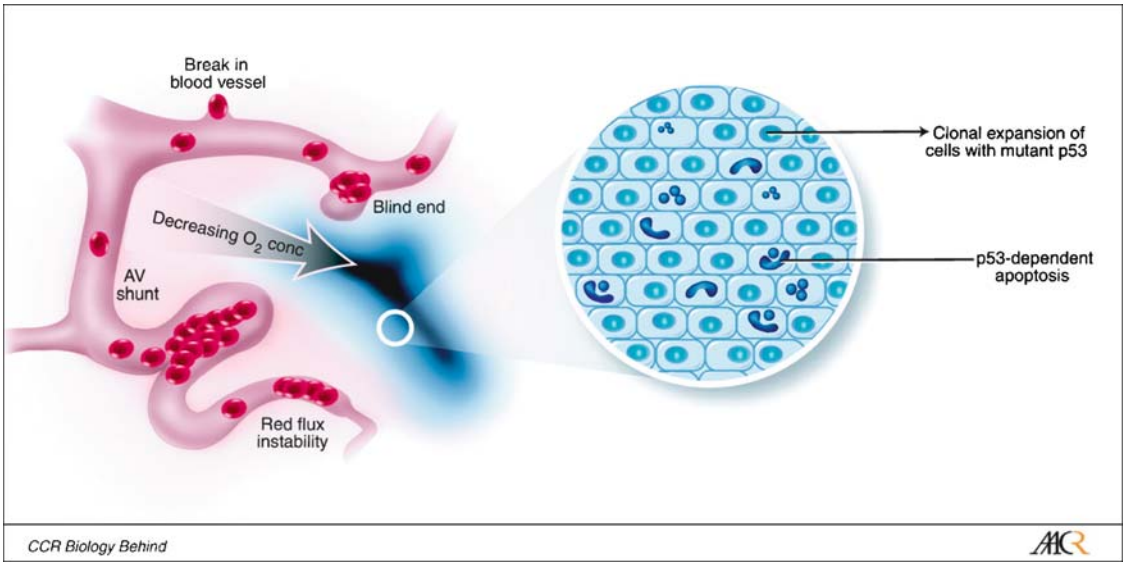

FIGURE 17.3. Regions of hypoxia form within solid tumors as a result of the inefficient and disorganized vasculature. Hypoxic regions represent a gradient of oxygen concentrations, the highest being nearest the vessels and the lowest being the furthest away. In the most hypoxic regions, p53 is stabilized and induces apoptosis. A selection pressure therefore exists to loose p53 and allows the clonal expansion of cells. These cells are also resistant to chemotherapy and radiotherapy, both of which require an efficient blood supply. (Reproduced with permission of Hammond and Giaccia, 2006.)

by 2-methoxyoestradiol (2ME2) has also been shown to result in decreased HIF-1α levels and decreased VEGF mRNA expression in cultured cells (Mabjeesh *et al.*, 2003). Disruption of HIF-1α upstream signaling by attacking *RAS*-related proteins has also been reported (Delmas *et al.*, 2003). Another upstream approach to inhibit HIF-1α in normoxic tumors utilizes the anti-epidermal growth factor receptor monoclonal antibody cetuximab (C225; Erbitux), which has been approved for the treatment of metastatic colorectal cancer. This monoclonal antibody has been known to inhibit VEGF secretion *in vitro* and *in vivo*. Studies show that cetuximab reduces HIF-1α in epidermoid carcinoma cells under both normoxic and hypoxic conditions. This inhibition occurs through the RAS pathway and confirms that VEGF secretion can be modulated by signal transduction inhibition of HIF-1α protein translation (Luwor *et al.*, 2005). In addition to monoclonal antibodies, compounds that share a 2,2-dimethylbenzopyran structural motif have been shown to inhibit hypoxia-induced transcription activity. Small molecule 103D5R markedly decreased HIF-1α protein levels induced by hypoxia or cobaltous ions in a dose- and time-dependent manner. 103D5R was shown to inhibit the phosphorylation of Akt, Erk1/2, and stress-activated protein kinase/c-jun-NH(2)-kinase, is also worthy of continued investigation of the drug as an HIF-1α inhibitor (Tan *et al.*, 2005). A selective proteasome inhibitor bortezomib (Velcade) has been shown to disrupt the transcriptional activity of HIF-1α via specific effects on the COOH-terminal

activation domain (Kaluz *et al*., 2006). Nonsteroidal anti-inflammatory drugs (NSAIDs), which have been shown to reduce the risk of gastric cancer, can also decrease the expression of HIF-1α (Griffiths *et al*., 2005).

Hypoxia is a common characteristic of the microenvironment in advanced solid tumors that has lead to the epigenetic and genetic adaptation of clones, a diminished therapeutic response, and increased invasiveness and metastasis. The oxygen-sensitive transcriptional activator, HIF-1 is a master regulator of tumor cell adaptation to hypoxic stress. Hypoxia can initiate cell demise by apoptosis/necrosis, while also preventing cell death by provoking adaptive responses that, in turn, facilitate cell proliferation or angiogenesis, thus contributing to tumor progression. In gastric cancer, HIF-1α expression is correlated with diagnostic and prognostic indicators for early relapse and metastatic disease, thus making HIF-1α a potential prognostic biomarker in proteomic assessments of gastric cancer. Understanding the mechanisms by which HIF-1 affects the expression and/or function of other oncogenic or tumor suppressor pathways will help to elucidate precisely how HIF-1 induces cell death and the manner in which cells can overcome such signals. The targeted inhibition of HIF-1α has been shown to inhibit the growth of gastric tumors in animals. An increased understanding of hypoxia and the HIF-1α pathways may therefore hold the key to a greater individualization of therapy and new treatments for patients with gastric cancer.

REFERENCES

Bruick, R.K. 2000. Expression of the gene encoding the proapoptotic Nip3 protein is induced by hypoxia. *Proc. Natl. Acad. Sci. U.S.A. 97*: 9082–9087.

Chen, D., Li, M., Luo, J., and Gu, W. 2003. Direct interactions between HIF-1α and Mdm2 modulate p53 function. *J. Biol. Chem. 278*: 13595–13598.

Chun, Y.S., Lee, K.H., Choi, E., Bae, S.Y., Yeo, E.J., Huang, L.E., Kim, M.S., and Park, J.W. 2003. Phorbol ester stimulates the nonhypoxic induction of a novel hypoxia-inducible factor 1alpha isoform: implications for tumor promotion. *Cancer Res. 63*: 8700–8707.

Delmas, C., End, D., Rochaix, P., Favre, G., Toulas, C., and Cohen-Jonathan, E. 2003. The farnesyltransferase inhibitor R115777 reduces hypoxia and matrix metalloproteinase 2 expression in human glioma xenograft. *Clin. Cancer Res. 9*: 6062–6068.

Folkman, J. 1990. What is the evidence that tumors are angiogenesis dependent? *J. Natl. Cancer Inst. 82*: 4–6.

Gray, M.J., Zhang, J., Ellis, L.M., Semenza, G.L., Evans, D.B., Watowich, S.S., and Gallick, G.E. 2005. HIF-1alpha, STAT3, CBP/p300 and Ref-1/APE are components of a transcriptional complex that regulates Src-dependent hypoxia-induced expression of VEGF in pancreatic and prostate carcinomas. *Oncogene 24*: 3110–3120.

Griffiths, E.A., Pritchard, S.A., Welch, I.M., Price, P.M., and West, C.M. 2005. Is the hypoxia-inducible factor pathway important in gastric cancer? *Eur. J. Cancer 41*: 2792–2805.

Griffiths, E.A., Pritchard, S.A., Valentine, H.R., Whitchelo, N., Bishop, P.W., Ebert, M.P., Price, P.M., Welch, I.M., and West, C.M. 2007. Hypoxia-inducible factor-1alpha expression in the gastric carcinogenesis sequence and its prognostic role in gastric and gastro-oesophageal adenocarcinomas. *Br. J. Cancer 96*: 95–103.

Hammond, E.M., and Giaccia, A.J. 2006. Hypoxia-inducible factor-1 and p53: friends, acquaintances, or strangers? *Clin. Cancer Res. 12*: 5007–5009.

Harris, A.L. 2002. Hypoxia—a key regulatory factor in tumour growth. *Nat. Rev. Cancer 2*: 38–47.

Hockel, M., and Vaupel, P. 2003. Oxygenation of cervix cancers: impact of clinical and pathological parameters. *Adv. Exp. Med. Biol. 510*: 31–35.

Kaelin, Jr., W.G. 2002. How oxygen makes its presence felt. *Genes Devel. 16*: 1441–1445.

Kaluz, S., Kaluzova, M., and Stanbridge, E.J. 2006. Proteasomal inhibition attenuates transcriptional activity of hypoxia-inducible factor 1 (HIF-1) via specific effect on the HIF-1alpha C-terminal activation domain. *Mol. Cell. Biol. 26*: 5895–5907.

Karni, R., Dor, Y., Keshet, E., Meyuhas, O., and Levitzki, A. 2002. Activated pp60c-Src leads to elevated hypoxia-inducible factor (HIF)-1alpha expression under normoxia. *J. Biol. Chem. 277*: 42919–42925.

Ke, Q., and Costa, M. 2006. Hypoxia-inducible factor-1 (HIF-1). *Mol. Pharm. 70*: 1469–1480.

Kimbro, K.S., and Simons, J.W. 2006. Hypoxia-inducible factor-1 in human breast and prostate cancer. *Endocr. Relat. Cancer 13*: 739–749.

Krishnamachary, B., Berg-Dixon, S., Kelly, B., Agani, F., Feldser, D., Ferreira, G., Iyer, N., LaRusch, J., Pak, B., Taghavi, P., and Semenza, G.L. 2003. Regulation of colon carcinoma cell invasion by hypoxia-inducible factor 1. *Cancer Res. 63*: 1138–1143.

Lim, J.H., Lee, E.S., You, H.J., Lee, J.W., Park, J.W., and Chun, Y.S. 2004. Ras-dependent induction of HIF-1alpha785 via the Raf/MEK/ERK pathway: a novel mechanism of Rasmediated tumor promotion. *Oncogene 23*: 9427–9431.

Luwor, R.B., Lu, Y., Li, X., Mendelsohn, J., and Fan, Z. 2005. The antiepidermal growth factor receptor monoclonal antibody cetuximab/C225 reduces hypoxia-inducible factor-1 alpha, leading to transcriptional inhibition of vascular endothelial growth factor expression. *Oncogene 24*: 4433–4441.

Mabjeesh, N.J., Escuin, D., LaVallee, T.M., Pribluda, V.S., Swartz, G.M., Johnson, M.S., Willard, M.T., Zhong, H., Simons, J.W., and Giannakakou, P. 2003. 2ME2 inhibits tumor growth and angiogenesis by disrupting microtubules and dysregulating HIF. *Cancer Cell 3*: 363–375.

Maxwell, P.H., Dachs, G.U., Gleadle, J.M., Nicholls, L.G., Harris, A.L., Stratford, I.J., Hankinson, O., Pugh, C.W., and Ratcliffe, P.J. 1997. Hypoxia-inducible factor-1 modulates gene expression in solid tumors and influences both angiogenesis and tumor growth. *Proc. Natl. Acad. Sci. U.S.A. 94*: 8104–8109.

Maxwell, P.H., Wiesener, M.S., Chang, G.-W., Clifford, S.C., Vaux, E.C., Cockman, M.E., Wykoff, C.C., Pugh, C.W., Maher, E.R., and Ratcliffe, P.J. 1999. The tumour suppressor protein VHL targets hypoxia-inducible factors for oxygen-dependent proteolysis. *Nature 399*: 271–275.

Mizokami, K., Kakeji, Y., Oda, S., Irie, K., Yonemura, T., Konishi, F., and Maehara, Y. 2006a. Clinicopathologic significance of hypoxia-inducible factor 1 alpha overexpression in gastric carcinomas. *J. Surg. Oncol. 94*: 149–154.

Mizokami, K., Kakeji, Y., Oda, S., and Maehara, Y. 2006b. Relationship of hypoxia-inducible factor 1á and p21WAF1/CIP1 expression to cell apoptosis and clinical outcome in patients with gastric cancer. *World. J. Surg. Oncol. 4*: 94.

Neufeld, G., Cohen, T., Gengrinovitch, S., and Poltorak, Z. 1999. Vascular endothelial growth factor (VEGF) and its receptors. *FASEB J. 13*: 9–22.

Parkin, D.M. 2004. International variation. *Oncogene 23*: 6329–6340.

Schuler, M., and Green, D.R. 2001. Mechanisms of p53-dependent apoptosis. *Biochem. Soc. Trans. 29*: 684–688.

Seagroves, T.N., Ryan, H.E., Lu, H., Wouters, B.G., Knapp, M., Thibault, P., Laderoute, K., and Johnson, R.S. 2001. Transcription factor HIF-1 is a necessary mediator of the pasteur effect in mammalian cells. *Mol. Cell. Biol. 21*: 3436–3444.

Semenza, G.L. 2002. HIF-1 and tumor progression: pathophysiology and therapeutics. *Trends Mol. Med. 8*: S62–S67.

Semenza, G.L. 2003. Targeting HIF-1 for cancer therapy. *Nat. Rev. Cancer 3*: 721–732.

Sumiyoshi, Y., Kakeji, Y., Egashira, A., Mizokami, K., Orita, H., and Maehara, Y. 2006. Overexpression of hypoxia-inducible factor 1α and p53 is a marker for an unfavorable prognosis in gastric cancer. *Clin. Cancer Res. 12*: 5112–5117.

Talks, K.L., Turley, H., Gatter, K.C., Maxwell, P.H., Pugh, C.W., Ratcliffe, P.J., and Harris, A.L. 2000. The expression and distribution of the hypoxia-inducible factors HIF-1alpha and HIF-2alpha in normal human tissues, cancers, and tumor-associated macrophages. *Am. J. Pathol. 157*: 411–421.

Tan, C., de Noronha, R.G., Roecker, A.J., Pyrzynska, B., Khwaja, F., Zhang, Z., Zhang, H., Teng, Q., Nicholson, A.C., Giannakakou, P., Zhou, W., Olson, J.J., Pereira, M., M., Nicolaou, K.C., and Van Meir, E.G. 2005. Identification of a novel small-molecule inhibitor of the hypoxia-inducible factor 1 pathway. *Cancer Res. 65*: 605–612.

Vaupel, P. 2004. The role of hypoxia-induced factors in tumor progression. *Oncologist 9*: 10–17.

Volm, M., and Koomagi, R. 2000. Hypoxia-inducible factor (HIF-1) and its relationship to apoptosis and proliferation in lung cancer. *Anticancer Res. 20*: 1527–1533.

Wenger, R.H. 2002. Cellular adaptation to hypoxia: O_2-sensing protein hydroxylases, hypoxia-inducible transcription factors, and O_2-regulated gene expression. *FASEB J. 16*: 1151–1162.

Yeo, E.J., Chun, Y.S., Cho, Y.S., Kim, J., Lee, J.C., Kim, M.S., and Park, J.W. 2003. YC-1: a potential anticancer drug targeting hypoxia-inducible factor 1. *J. Natl. Cancer Inst. 95*: 516–525.

Zagzag, D., Krishnamachary, B., Yee, H., Okuyama, H., Chiriboga, L., Ali, M.A., Melamed, J., and Semenza, G.L. 2005. Stromal cell-derived factor-1alpha and CXCR4 expression in hemangioblastoma and clear cell-renal cell carcinoma: von Hippel-Lindau loss-of-function induces expression of a ligand and its receptor. *Cancer Res. 65*: 6178–6188.

Zhou, J., Schmid, T., Schnitzer, S., and Brune, B. 2006. Tumor hypoxia and cancer progression. *Cancer Lett. 237*: 10–21.

Zundel, W., Schindler, C., Haas-Kogan, D., Koong, A., Kaper, F., Chen, E., Gottschalk, A.R., Ryan, H.E., Johnson, R.S., Jefferson, A.B. Stokoe, D., and Giaccia, A.J. 2000. Loss of PTEN facilitates HIF-1-mediated gene expression. *Genes Devel. 14*: 391–396.

18
Pancreatic Cancer: Hepatoma-Derived Growth Factor as a Prognostic Factor

Yasuhiko Tomita, Hirokazu Uyama, and Hideji Nakamura

HEPATOMA-DERIVED GROWTH FACTOR MOLECULE

Hepatoma-derived growth factor (HDGF) is a heparin-binding protein purified from the conditioned medium of the human well-differentiated hepatocellular carcinoma (HCC) cell line, HuH-7, which can proliferate autonomously in a serum-free chemically-defined medium (Nakamura *et al*., 1989, 1994). Hepatoma-derived growth factor is highly expressed in several cancer cells (Nakamura *et al*., 1994, 2002; Mori *et al*., 2004; Lepourcelet *et al*., 2005). This growth factor is also more highly expressed in various fetal organs than in adult organs (Oliver and Al-Awqati, 1998; Everett *et al*., 2000; Enomoto *et al*., 2002). In the fetus, HDGF was abundantly expressed in the liver, heart, kidney, lungs, and gut. Thus, HDGF is one of the developmentally regulated genes which is abundantly expressed in cancer cells.

Hepatoma-derived growth factor is an acidic 26 kDa protein consisting of 230 amino acids, and does not have a hydrophobic signal sequence in its N-terminus, and is a major member of HDGF family proteins which consists of HDGF and five HDGF-related proteins (HRP). The N-terminal region of HDGF is highly conserved among the other five HDGF-related proteins (HRP) (Izumoto *et al*., 1997; Dietz *et al*., 2002). This region is called *hath* (homologous to the amino terminus of HDGF) region. Hepatoma-derived growth factor family members are characterized based on whether they contain the *hath* region and nuclear localization signals (NLS) in their gene-specific regions and are targeting the nucleus (Nakamura and Hada, 2004). A member of HDGF family proteins, lens epithelial cell-derived growth factor (LEDGF), is identical to p54/72, which is an RNA-binding protein and transcriptional cofactor for regulating general transcriptional factors. *Hath* region, which is well-conserved in the HDGF family proteins contains the PWWP domain (Qiu *et al*., 2002). Hepatoma-derived growth factor contains two NLS in the molecule. The first functional NLS1 resides in the *hath* region of the N-terminal region and the second NLS2 in gene-specific regions of the C-terminal region of the HDGF molecule (Kishima *et al*., 2002a). Hepatoma-derived growth factor can traffic to the nucleus using these NLSs, especially the NLS2 in its gene-specific region (Everett *et al*., 2001;

Kishima *et al*., 2002a). Hepatoma-derived growth factor was dominantly localized in the nucleus, rather than the cytoplasm. The ability for trafficking to the nucleus is essential to display growth stimulating activity in HDGF-over-expressed cells. In particular, the gene-specific region of HDGF, at least the bipartite NLS sequence and both the N-and C-terminal neighboring portions, is essential for the mitogenic activity. Hepatoma-derived growth factor is a unique factor that is categorized in the nuclear targeting growth factors.

In contrast, exogenously supplied HDGF stimulates the proliferation of fibroblasts, endothelial cells, vascular smooth muscle cells, pulmonary epithelial cells and hepatocytes, as well as HCC, lung cancer and colon cancer cells. Hepatoma-derived growth factor has a high affinity for the glycosaminoglycans heparin and heparan sulphate (Dietz *et al*., 2002; Sue *et al*., 2004). A possible receptor-binding site is estimated to reside at amino acid residues 81–100 within the *hath* region (Abouzied *et al*., 2005). Exogenous HDGF stimulates the Erk phosphorylation in endothelial cells (Everett *et al*., 2004). Hepatoma-derived growth factor exerts its proliferating activity via two different pathways; (1) via a putative plasma membrane-located HDGF receptor for which signaling depends on the *hath* region, especially amino acid residues 81–100, resulting in MAP kinase activation, and (2) via targeting to the nucleus by NLS.

Role in Carcinogenesis and Cancer Progression

HDGF is expressed more abundantly in various cancers including that of the liver, lung, stomach, esophagus, colon and pancreas than in non-malignant tissues. HDGF significantly stimulates the proliferation of HCC, lung cancer and colon cancer cells.

The Fatty Liver Shionogi (FLS) mouse is an inbred strain that develops spontaneous fatty liver without obesity, resulting in HCC development in about 45% in 52 weeks and 90% at 72 weeks after birth in male mice. In the liver of FLS mice, HDGF expression has already increased at an early stage before the tumors develop microscopically in the liver (Yoshida *et al*., 2003). By differential subtractive chain reaction from strong anchorage-independent growth to its negative HCC cells, HDGF was cloned as one of the genes related to anchorage-independency (Huang *et al*., 2004). Furthermore, HDGF expression is dramatically increased in human colorectal cancers, especially in tumors proficient in DNA mismatch repair, and HDGF expression in fetal intestine explants inhibits maturation, suggesting a significant and important role in epithelial differentiation (Lepourcelet *et al*., 2005). Conversely, down regulation of HDGF by use of HDGF-siRNA has a minimal effect on the anchorage-dependent growth but significantly reduces anchorage-independent growth of non-small cell lung cancer (NSCLC) cells in soft agar (Zhang *et al*., 2006). The HDGF-over-expressing NIH3T3 cells generate sarcomatous tumors in nude mice, but do not show significant anchorage-independent growth in soft agar assay. However, HDGF-over-expressing NIH3T3 cells develop more small colonies in soft agar than parent or neomycin-resistant cells (Okuda *et al*., 2003). Thus, these findings suggest that HDGF is an oncogenic protein which plays a role in cancer development.

Hepatoma-derived growth factor protein is abundantly expressed in various human cancer cell lines, including pancreatic cell lines (Uyama *et al*., 2006). The HDGF-over-expressing hepatoma cell line HepG2 proliferates more rapidly and produces larger tumors, showing more rapid growth, in nude mice than neomycin-resistant cells *in vivo*. Recombinant HDGF stimulates the growth of HCC and colon cancer cells, while antisense HDGF oligonucleotides or polyclonal anti-HDGF antibody suppresses their growth (Nakamura *et al*., 2002; Kishima *et al*., 2002b). Exogenously supplied HDGF promotes the proliferation of bronchial squamous cell carcinoma cell line, A549 cells, knock-down expression of HDGF by small interfering RNA (siRNA) in NSCLC cells significantly show more slow growth, less colony formation in soft agar and lesser *in vitro* invasion activity (Mori *et al*., 2004; Zhang *et al*., 2006). By proteomic differential display analysis and mass spectrometry, HDGF is down-regulated in regressive cancer cells as compared with that in inflammatory cell-promoting progressive cells of the murine fibrosarcoma cell line (Hayashi *et al*., 2005). The higher expression of HDGF showed more malignant potential for cancer progression.

Hepatoma-derived growth factor is intrinsically related to angiogenesis and vasculogenesis. HDGF expression was induced in the regenerating process of vascular vessels in wound repair, and is highly expressed in the fetal stage of the cardiovascular system (Everett *et al*., 2000). Additionally, HDGF is a candidate endothelial growth factor for involvement in glomerulus formation (Oliver and Al-Awqati, 1998). Tumors developed from HDGF-over-expressing NIH3T3 cells inoculated in nude mice were macroscopically red-colored and were histologically rich in vasculature. Hepatoma-derived growth factor stimulated the proliferation and tubule formation of human umbilical vein endothelial cells (Okuda *et al*., 2003). Using chick chorioallantoic membrane (CAM) as a biological assay for angiogenesis, recombinant HDGF stimulated blood vessel formation, and stimulated cellular reorganization within the CAM from a loose network into a more compact, linear alignment reminiscent of tube formation (Everett *et al*., 2004). Furthermore, HDGF induces a potent angiogenic factor, vascular endothelial growth factor (VEGF) gene expression. Hepatoma-derived growth factor shows potent angiogenic activity via its own direct stimulation of the proliferation of endothelial cells and vascular smooth muscle cells, and through the induction of VEGF in the nucleus. The growth stimulating activity of HDGF is more potent *in vivo* than *in vitro,* and must be brought on by both the direct cell growth activity and its angiogenic activity. Hepatoma-derived growth factor is a potent angiogenic factor.

IMMUNOHISTOCHEMICAL AND ANALYTICAL METHODS

Materials

1. Rabbit polyclonal antibody raised against C-terminal amino acids (amino acids 231–240) of the human HDGF.
2. Dulbecco's phosphate-buffered saline without magnesium and calcium – Tween 20 (PBS-T): 200 mg potassium chloride, 200 mg monobasic potassium phosphate, 8 g sodium chloride, and

2.9 g dibasic sodium phosphate $\cdot 12H_2O$, bring vol to 1 l with deionized distilled water, pH 7.4. Add 0.1 ml Tween 20 and mix well.

3. Fixative: 10% formalin in distilled water.
4. 10 mM citric acid buffer (pH 6.0): 294.10 g Trisodium citrate $\cdot 2H_2O$, bring vol to 1 l with deionized distilled water to prepare 1 M trisodium citrate. 210.14 g Citric acid $\cdot H_2O$, bring vol to 1 l with deionized distilled water to prepare 1 M citric acid. Add 5 ml of 1 M trisodium citrate and 0.8 ml of 1 M citric acid to 494.2 ml of deionized distilled water to prepare 10 mM citric acid pH 6.0.
5. Methanol containing 0.2% hydrogen peroxydase: 9 ml of 31% hydrogen peroxydase in 150 ml methanol.
6. Blocking serum (goat serum) diluted at 1/50 in PBS-T.
7. Primary antibody (rabbit polyclonal anti-HDGF antibody) diluted at 1/5,000 in PBS-T.
8. Secondary antibody (biotinylated goat polyclonal anti-rabbit antibody) diluted at 1/100 in PBS-T.
9. Avidin-biotin-complex solution: Add 20 µl of VECTASTAIN Elite REAGENT A and B to 1 ml PBS-T. Mix well and stand more than 30 min.
10. 3,3′-Diaminobenzidine, tetrahydrochloride (DAB) solution: 75 mg of DAB powder in 150 ml PBS-T. Stir well. Add 1 ml of 31% hydrogen peroxydase to 150 ml of DAB solution.

Method

1. Samples are fixed in 10% formalin, dehydrated, and embedded in paraffin.
2. Cut the paraffin block at 4 µm thickness and mount sections on poly-L-Lysine-coated glass slides.
3. Deparaffinize the slide in xylene three times for 15 min and in 100% ethanol three times for 5 min.
4. Immerse the slide in PBS-T.
5. For antigen retrieval, heat the slide in 10 mM citrate buffer (pH 6.0) for 15 min using microwave at 600 W.
6. Rinse the slide three times in PBS-T for 5 min.
7. Immerse the slide in methanol containing 0.2% hydrogen peroxidase for 20 min to block the endogenous peroxidase activity at room temperature.
8. Rinse the slide three times in PBS-T for 10 min.
9. Incubate the slides with 2% goat serum in PBS-T for 30 min in a humidity chamber at room temperature to block the non-specific binding of the primary antibody.
10. Lightly tap off excess serum from each slide, then apply anti-HDGF primary antibody diluted in PBS-T. Incubate the slides overnight in a humidity chamber at 4°C.
11. Rinse the slide three times in PBS-T for 5 min.
12. Prepare Avidin-biotin-complex solution.
13. Incubate the slides with secondary antibody diluted in PBS-T for 30 min in a humidity chamber at 37°C.
14. Rinse the slide three times in PBS-T for 5 min.
15. Incubate the slides with Avidin-biotin-complex solution for 45 min in a humidity chamber at 37°C.
16. Rinse the slide three times in PBS-T for 5 min.
17. Prepare DAB solution.
18. Immerse the slide in DAB solution for 1 min.
19. Wash the slide in distilled water five times.

20. Immerse the slide in methyl green for 10 min.
21. Wash the slide in distilled water five times.
22. Dehydrate with 100% ethanol three times for 5 min, and xylene three times for 5 min, then mount with mounting medium.

EVALUATION OF HEPATOMA-DERIVED GROWTH FACTOR EXPRESSION IN PANCREATIC DUCTAL CANCER

Observe the slide under light microscope. Epithelial cells of the pancreatic ducts in the non-neoplastic lesion consistently show weakly positive HDGF staining both for the nucleus and cytoplasm. Cancer cells showing stronger staining than the noncancerous ducts can be regarded as positive. Carefully examine the positivity ratio of all the cancer cells in the slide for both the nucleus and the cytoplasm. HDGF labeling index (LI) can be determined as follows: samples with less than 90% of cancer cells showing positive staining are regarded as HDGF LI Level 1, and those with more than 90% as Level 2. Determine the HDGF LI separately for the nucleus and the cytoplasm.

PROGNOSTIC SIGNIFICANCE OF HDGF IN PANCREATIC DUCTAL CANCER AND OTHER CANCERS

Rate of Level 2 HDGF LI in pancreatic ductal cancer is 54% and 56% for the nucleus and the cytoplasm, respectively (Uyama *et al*., 2006). Nuclear HDGF LI is an independent prognostic factor of pancreatic ductal cancer. Patients with Level 2 HDGF LI show a poorer 5-year survival rate than those with Level 1. No significant difference is observed in the cytoplasmic HDGF expression. Besides pancreatic ductal cancer, HDGF is a prognsostic factor of HCC (Hu *et al*., 2003; Yoshida *et al*., 2006), lung cancer (Ren *et al*., 2004; Iwasaki *et al*., 2005), gastric cancer (Yamamoto *et al*., 2006) and esophageal cancer (Yamamoto *et al*., 2007).

Hepatoma-derived growth factor is a unique nuclear targeted growth factor, which is expressed abundantly in cancer cells and promotes their malignant potential. HDGF generates tumors and promotes their growth *in vivo* via its mitogenic activity and angiogenic activity deriving from both its own direct angiogenic activity and the induction of VEGF. Multivariate analysis of the relationship of HDGF expression and overall survival in patients with pancreatic cancer confirms that HDGF expression, as determined by immunohistochemistry, can be used as a new prognosticator for pancreatic ductal cancer. Additionally, radiosensitive esophageal cancers show higher expression of HDGF than radioresistant ones, suggesting that HDGF may be a biomarker for radiosensitivity for cancer cells (Matsuyama *et al*., 2001). Future studies should focus on HDGF in pancreatic ductal cancers and the relationship between HDGF expression and chemotherapy sensitivity and/or radiosensitivity. Although further study is still needed to clarify the role of HDGF in the malignant behavior of pancreatic ductal cancer, HDGF may serve as a potential target for drug design regulating the carcinogenesis and cancer progression.

REFERENCES

Abouzied, M.M., El-Tahir, H.M., Prenner, L., Haberlein, H., Gieselmann, V., and Franken, S. 2005. Hepatoma-derived growth factor. Significance of amino acid residues 81-100 in cell surface interaction and proliferative activity. *J. Biol. Chem. 280*: 10945–10954.

Dietz, F., Franken, S., Yoshida, K., Nakamura, H., Kappler, J., and Gieselmann, V. 2002. The family of hepatoma-derived growth factor proteins: characterization of a new member HRP-4 and classification of its subfamilies. *Biochem. J. 366*: 491–500.

Enomoto, H., Yoshida, K., Kishima, Y., Kinoshita, T., Yamamoto, M., Everett, A.D., Miyajima, A., and Nakamura, H. 2002. Hepatoma-derived growth factor is highly expressed in developing liver and promotes fetal hepatocyte proliferation. *Hepatology 36*: 1519–1527.

Everett, A.D., Lobe, D.R., Matsumura, M.E., Nakamura, H., and McNamara, C.A. 2000. Hepatoma-derived growth factor stimulates smooth muscle cell growth and is expressed in vascular development. *J. Clin. Invest. 105*: 567–575.

Everett, A.D., Stoops, T., and McNamara, C.A. 2001. Nuclear targeting is required for hepatoma-derived growth factor-stimulated mitogenesis in vascular smooth muscle cells. *J. Biol. Chem. 276*: 37564–37568.

Everett, A.D., Narron, J.V., Stoops, T., Nakamura, H., and Tucker, A. 2004. Hepatoma-derived growth factor is a pulmonary endothelial cell-expressed angiogenic factor. *Am. J. Physiol., Lung Cell. Mol. Physiol. 286*: L1194–L1201.

Hayashi, E., Kuramatsu, Y., Okada, F., Fujimoto, M., Zhang, X., Kobayashi, M., Iizuka, N., Ueyama, Y., and Nakamura, K. 2005. Proteomic profiling for cancer progression: differential display analysis for the expression of intracellular proteins between regressive and progressive cancer cell lines. *Proteomics 5*: 1024–1032.

Hu, T.H., Huang, C.C., Liu, L.F., Lin, S.Y., Chang, H.W., Changchien, C.S., Lee, C.M., Chuang, J.H., and Tai, M.H. 2003. Expression of hepatoma-derived growth factor in hepatocellular carcinoma. *Cancer 98*: 1444–1456.

Huang, J.S., Chao, C.C., Su, T.L., Yeh, S.H., Chen, D.S., Chen, C.T., Chen, P.J., and Jou, Y.S. 2004. Diverse cellular transformation capability of overexpressed genes in human hepatocellular carcinoma. *Biochem. Biophys. Res. Commun. 315*: 950–958.

Iwasaki, T., Nakagawa, K., Nakamura, H., Takada, T., Matsui, K., and Kawahara, K. 2005. Hepatoma-derived growth factor as a prognostic marker in completely resected non-small-cell lung cancer. *Oncol. Rep. 13*: 1075–1080.

Izumoto, Y., Kuroda, T., Harada, H., Kishimoto, T., and Nakamura, H. 1997. Hepatoma-derived growth factor belongs to a gene family in mice showing significant homology in the amino terminus. *Biochem. Biophys. Res. Commun. 238*: 26–32.

Kishima, Y., Yamamoto, H., Izumoto, Y., Yoshida, K., Enomoto, H., Yamamoto, M., Kuroda, T., Ito, H., Yoshizaki, K., and Nakamura, H. 2002a. Hepatoma-derived growth factor stimulates cell growth after translocation to the nucleus by nuclear localization signals. *J. Biol. Chem. 277*: 10315–10322.

Kishima, Y., Yoshida, K., Enomoto, H., Yamamoto, M., Kuroda, T., Okuda, Y., Uyama, H., and Nakamura, H. 2002b. Antisense oligonucleotides of hepatoma-derived growth factor (HDGF) suppress the proliferation of hepatoma cells. *Hepatogastroenterology 49*: 1639–1644.

Lepourcelet M., Tou L., Cai L., Sawada J., Lazar A.J.F., Glickman J.N., Williamson J.A., Everett A.D., Redston M., Fox E.A., Nakatani Y., and Shivdasani R.A. 2005. Insights into development mechanisms and cancers in the mammalian intesitine derived from serial analysis of gene expression and study of the hepatoma-derived growth factor (HDGF). *Development 132*: 415–427.

Matsuyama, A., Inoue, H., Shibuta, K., Tanaka, Y., Barbnard, G.F., Sugimachi, K., and Mori, M. 2001. Hepatoma-derived growth factor is associated with reduced sensitivity to irradiation in esophageal cancer. *Cancer Res. 61*: 5714–5717.

Mori, M., Morishita, H., Nakamura, H., Matsuoka, H., Yoshida, K., Kishima, Y., Zhou, Z., Kida, H., Funakoshi, T., Goya, S., Yoshida, M., Kumagai, T., Tachibana, I., Yamamoto, Y., Kawase, I., and Hayashi, S. 2004. Hepatoma-derived growth factor is involved in lung remodeling by stimulating epithelial growth. *Am. J. Respir. Cell Mol. Biol. 30*: 459–469.

Nakamura, H., and Hada, T. 2004. Hepatoma-derived growth factor in ontogeny and tumorigenesis. *Recent Res. Devel. Biophys. Biochem. 4*: 17–27.

Nakamura, H., Kambe, H., Egawa, T., Kimura, Y., Ito, H., Hayashi, E., Yamamoto, H., Sato, J., and Kishimoto, S. 1989. Partial purification and characterization of hepatoma-derived growth factor. *Clin. Chim. Acta 183*: 273–284.

Nakamura, H., Izumoto, Y., Kambe, H., Kuroda, T., Mori, T., Kawamura, K., Yamamoto, H., and Kishimoto, T. 1994. Molecular cloning of complementary DNA for a novel human hepatoma-derived growth factor. *J. Biol. Chem. 269*: 25143–25149.

Nakamura, H., Yoshida, K., Ikegame, K., Kishima, Y., Uyama, H., and Enomoto, H. 2002. Antibodies against hepatoma-derived growth factor and mucosal repair in ulcerative colitis. *J. Gastroenterol. 37 [Suppl 14]*: 8–14.

Okuda, Y., Nakamura, H., Yoshida, K., Enomoto, H., Uyama, H., Hirotani, T., Funamoto, M., Ito, H., Everett, A.D., Hada, T., and Kawase, I. 2003. Hepatoma-derived growth factor induces tumorigenesis in vivo through both direct angiogenic activity and induction of vascular endothelial growth factor. *Cancer Sci. 94*: 1034–1041.

Oliver, J.A., and Al-Awqati, Q. 1998. An endothelial growth factor involved in rat renal development. *J. Clin. Invest. 102*: 1208–1219.

Qiu, C., Sawada, K., Zhang, X., and Cheng, X. 2002. The PWWP domain of mammalian DNA methyltransferase Dnmt3b defines a new family of DNA-binding folds. *Nat. Struct. Biol. 9*: 217–224.

Ren, H., Tang, X., Lee, J.J., Feng, L., Everett, A.D., Hong, W.K., Khuri, F.R., and Mao, L. 2004. Expression of hepatoma-derived growth factor is a strong prognostic predictor for patients with early-stage non-small cell lung cancer. *J. Clin. Oncol. 22*: 3230–3237.

Sue, S.C., Chen, J.Y., Lee, S.C., Wu, W.G., and Huang, T.H. 2004. Solution structure and heparin interaction of human hepatoma-derived growth factor. *J. Mol. Biol. 343*: 1365–1377.

Uyama, H., Tomita, Y., Nakamura, H., Nakamori, S., Zhang, B., Hoshida, Y., Enomoto, H., Okuda, Y., Sakon, M., Aozasa, K., Kawase, I., Hayashi, N., and Monden, M. 2006. Hepatoma-derived growth factor is a novel prognostic factor for patients with pancreatic cancer. *Clin. Cancer Res. 12*: 6043–6048.

Yamamoto, S., Yasuhiko, T., Hoshida, Y., Takiguchi, S., Fujiwara, Y., Yasuda, T., Doki, Y., Yoshida, K., Aozasa, K., Nakamura, H., and Monden, M. 2006. Expression of hepatoma-derived growth factor is correlated with lymph node metastasis and prognosis of gastric carcinoma. *Clin. Cancer Res. 12*: 117–122.

Yamamoto, S., Tomita, Y., Hoshida, Y., Morii, E., Yasuda, T., Doki, Y., Aozasa, K., Uyama, H., Nakamura, H., and Monden, M. 2007. Expression level of hepatoma-derived growth factor correlates with tumor recurrence of esophageal carcinoma. *Ann. Surg. Oncol. 14*:2141–2149.

Yoshida, K., Nakamura, H., Okuda, Y., Enomoto, H., Kishima, Y., Uyama, H., Ito, H., Hirasawa, T., Inagaki, S., and Kawase, I. 2003. Expression of hepatoma-derived growth factor in hepatocarcinogenesis. *J. Gastroenterol. Hepatol. 18*: 1293–1301.

Yoshida, K., Tomita, T., Okuda, Y., Yamamoto, S., Enomoto, H., Uyama, H., Ito, H., Hoshida, Y., Aozasa, S., Nagano, H., Sakon, M., Kawase, I., Monden, M., and Nakamura, H. 2006. Hepatoma-derived growth factor is a novel prognostic factor for hepatocellular carcinoma. *Ann. Surg. Oncol. 13*: 159–167.

Zhang, J., Ren, H., Yuan, P., Lang, W., Zhang, L., and Mao, L. 2006. Down-regulation of hepatoma-derived growth factor inhibits anchorage-independent growth and invasion of non-small cell lung cancer cells. *Cancer Res. 66*: 18–23.

19
Pancreatic Cancer: 18F-Fluorodeoxyglucose Positron Emission Tomography as a Prognostic Parameter

Tatsuya Higashi

INTRODUCTION

Patients with pancreatic cancer are known for their poor survival; this caner is the cause of death of ~ 21,100–28,600 patients, and is the sixth and fourth leading cause of cancer death each year in Japan and in the United States, respectively (National Cancer Center, 2001; National Cancer Institute, 1999). At the time of diagnosis after the appearance of symptoms, ~ 80% of patients have an advanced stage that is not suitable for curative operation. The 5-year survival rate of patients with unresectable or metastatic pancreatic cancer is only 0–5%, at the same time the 5-year survival rate of patients who have undergone curative resection is only ~ 10–25%. The incidence of pancreatic cancer in Japan has increased 1.5-fold over the past 3 decades; on the other hand, incidence and mortality rates are identical even now. Although systemic treatment procedures, including operation, chemotherapy, and radiation, are necessary to improve this poor therapeutic outcome, there has been no established treatment method with improved prognosis so far (Oya, 2004).

Tumor imaging using fluorine-18 fluorodeoxyglucose (FDG) positron emission tomography (PET) has been established as a useful clinical tool in a variety of cancers, including pancreatic cancer. As already mentioned in other chapters in this volume, FDG-PET has shown its excellent diagnostic ability as a pretreatment evaluation of pancreatic cancer. As a predictor of prognosis, however, we have only limited information on this subject. Regarding this clinical background, it is better to look at this issue assuming that prognosis of pancreatic cancer is mainly regulated by the invasiveness or aggressiveness of cancer itself, but not influenced by selection of patient management. In this chapter, the following three subjects will be discussed; (1) predicting malignant potential or aggressiveness by pretherapeutic FDG-PET, (2) improving accuracy of clinical staging by pretherapeutic FDG-PET, and (3) monitoring therapeutic effect by pre- and post-therapeutic FDG-PET.

PREDICTING MALIGNANT POTENTIAL OR AGGRESSIVENESS

Recently, the survival-prediction of cancer patients by means of quantitative

evaluation of FDG uptake has become an important topic in the field of PET oncology. Many studies evaluating the relationship between FDG uptake and prognosis have been reported for a variety of cancers, including non-small-cell lung cancer, head and neck cancer, and malignant lymphoma (Higashi K. *et al*., 2002; Jeong *et al*., 2002; Minn *et al*., 1997). These studies have shown positive relationship between poor prognosis and high FDG uptake in the primary tumor before treatment. As for the results of multivariate analysis are concerned, most studies demonstrated that a specific threshold standardized uptake value (SUV) provides prognostic information independent of the clinical stage and lesion size, while other studies showed that clinical stage and other factors were independent predictors of survival, but SUV was not (Minn *et al*., 1997). One study showed that there was difference in the prognostic value of FDG uptake between squamous cell carcinoma and adenocarcinoma of the lung (Jeong *et al*., 2002). Thus, it seems that there are different tendencies in the prognostic value of FDG uptake between each malignancy or each pathological type or each reporting institute.

As for prognostic pretreatment evaluation of pancreatic cancer using FDG-PET, to the best of our knowledge, there have been only five studies at four institutions reported so far. Nakata *et al*. (1997, 2001) reported consecutive two studies with 14 and 37 patients concerning the predictability of SUVs achieved before treatment for the prognosis of patients with pancreatic cancer. They reported that a group with SUV of 3.0 or smaller had a longer survival period than the other group with SUV of 3.0 or higher when SUV = 3.0 as the cut-off value is a median SUV of total cases. These two studies have patient number < 37, therefore, statistical significance is not strong. Their multivariate analysis showed a positive significance for SUV ($p < 0.05$), but did not show a significant value in any factors of TNM in UICC '97 staging (T: $p = 0.874$, N: $p = 0.363$ and M: $p = 0.214$). Zimny *et al*. (2000) also reported a similar tendency of prognostic difference, although the cut-off value (SUV = 6.0) was different. Their cut-off value (SUV = 6.0) seems to be a median SUV of total cases. They also performed multivariate analysis with positive significance for SUV ($p < 0.05$), while their multivariate analysis did not show significant values in UICC '87 and '97 staging ($p = 0.109$ and 0.76). Thus, in these three studies it was concluded that a group with a specific threshold SUV or smaller had a longer survival period than the other group with higher SUV when the cut-off value is a median SUV of total cases, although the difference in clinical staging did not show any influence on patient survival.

Sperti *et al*. (2003) reported a similar tendency of prognostic difference using the different cut-off value (SUV = 4.0). Their cut-off value (SUV = 4.0) was also a median SUV of total cases. However, their multivariate analysis revealed that SUV ($p = 0.005$) and UICC 1997 tumor staging ($p = 0.001$) are the only independent predictors of survival. They also separated the patients into three groups according to treatment methods; resection (n = 16), bypass (n = 22), and palliative therapy (n = 22), and found that in each group median survival time of low SUV patients was longer than that of high SUV patients ($p = 0.006$, 0.043, 0.082, respectively).

On the other hand, the report from our university differs from their findings. Lyshchik *et al*. (2005) evaluated 65 pancreatic cancer patients using dual-phase FDG-PET and calculated the retention index (RI) by dividing the difference between SUV2 (SUV at 2 h after injection of FDG) and SUV1 (SUV at 1 h after injection of FDG) by SUV1. In our data, multivariate analysis revealed only three factors that had an independent association with longer patient survival: female gender ($p < 0.01$), TNM stage I-III ($p < 0.05$), and higher RI ($p < 0.01$) (Figure 19.1). In the single-variate analysis, SUV1 and SUV2 showed positive correlation with clinical TNM staging ($p = 0.01$ and 0.01, respectively), but did not show any

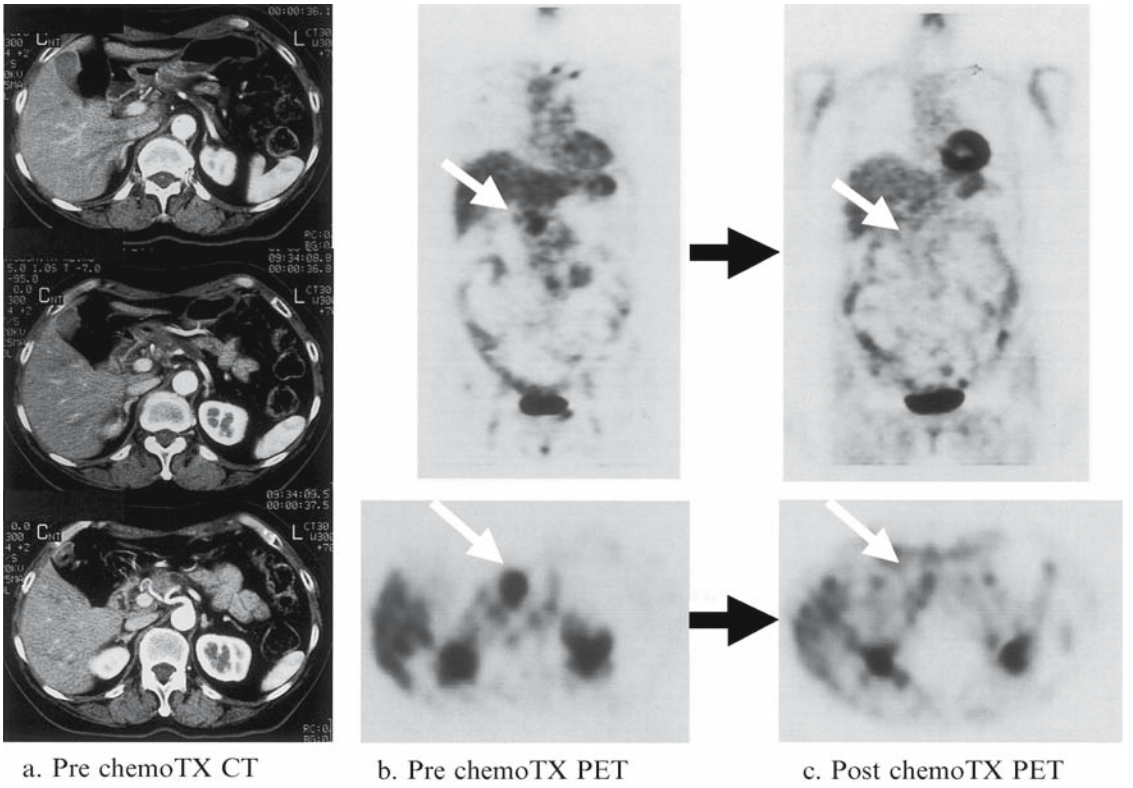

FIGURE 19.1. Evaluation of therapeutic effect of chemotherapy using FDG-PET. Sixty-six years old female, 3-years-survivor with pancreatic cancer. (a) CT findings show direct infiltration to the surrounding arteries and retroperitoneal tissues at the time of initial diagnosis. This tumor was diagnosed as unresectable and chemotherapy with weekly-based venous-infusion of gemcitabine was performed. (b) FDG-PET before chemotherapy shows intense uptake in the pancreatic head (white arrow). Semiquantitative analysis revealed that SUV at 1 and 2 h after injection were calculated as 5.4 and 7.3, respectively, with retention index (RI) 36%. High RI means a possibility of long survival. (c) FDG-PET was performed 1 month after the beginning of chemotherapy. The uptake observed before the chemotherapy in the pancreatic head remarkably disappeared (white arrow), although CT findings of cancer did not show any change in shape of the tumor at that time (not shown). Chemotherapy using weekly-based gemcitabine had shown effective therapeutic outcome for 2 years, and then multiple lung metastases were detected finally. *chemoTx: chemotherapy*

relationship with survival ($p = 0.2$ and 0.5, respectively). The single-variate analysis also showed that thresholds of RI = 10%, 15%, and 20% could make a significant difference in prognosis, but that RI = 10% was the strongest value for survival. The RI = 10% was also a significant prognostic factor in several clinical subgroups, such as histologically confirmed postoperative cancer patients ($p < 0.05$), patients diagnosed at stage I–III ($p < 0.01$), and patients diagnosed at stage IV ($p < 0.05$). In order to analyze the discrepancy between these five reports, it is necessary to focus on the following three important aspects: (1) clinical staging, (2) cut-off value of SUV, and (3) correlation with other cellular characteristics.

Prognostic parameters for pancreatic cancers, including clinical staging, have been evaluated from several clinical points of view. The close relationship between prognosis and clinical staging has been reported by several studies with large patient numbers (Morganti *et al*., 2005). A meta-analysis revealed that surgical resection is the only significant prognostic factor for longer survival in patients with pancreatic cancer, which suggests that the evaluation of the resectability is an important prognostic parameter (Stojadinovic *et al*., 2003). Other studies showed that curative resection with the grade of LN metastasis has prognostic significance (Gebhardt *et al*., 2000; Kuhlmann *et al*., 2004). Tumor size was reported to be the primary prognosticator for pancreatic cancer by several reports (Morganti *et al*., 2005; Gebhardt *et al*., 2000; Kuhlmann *et al*., 2004). These data suggest the importance of TNM classification as a prognostic parameter. Thus, clinical staging including each factor of TNM classification has a solid prognostic value in these large-scale studies. From this standpoint, the studies by Nakata *et al*. (2001) and Zimny *et al*. (2000) are not convincing, because their results lack the statistical significance in the factor of clinical staging. On the other hand, data by Sperti *et al*. (2003) and Lyshchik *et al*. (2005) seem to be plausible. It was reported in several institutes that SUV has a tendency to show a positive linear progression with tumor size or tumor staging in the diagnosis of preoperative pancreatic cancers (Higashi *et al*., 2003). Therefore, these factors may affect prognostic value of SUV because the factor of clinical staging may counterbalance the factor of SUV in the multivariate analysis. It would be fair to compare SUVs of tumors only in patients with cancer of a similar size or with the same clinical stage.

Higashi *et al*. (2002) reported a similar positive relation between prognosis and SUVs in lung cancers. In their study, they separated the patients into several groups according to the clinical stages and showed a similar correlation in each group. This is the same approach as that taken by Sperti *et al*. (2003) and Lyshchik *et al*. (2005) for pancreatic cancers. The former study showed that the threshold of SUV = 4 had a predicting value not only in total cases, but also in stratification for the following factors; clinical stage III to IVa, stage IVb, tumor resection, and others. The latter study revealed that RI = 10% was a significant prognostic factor not only in total cases but also in several clinical subgroups, such as histologically confirmed postoperative cancer patients, patients diagnosed at stage I–III, and patients diagnosed at stage IV. In order to evaluate the malignant potential or

aggressiveness of this cancer, this kind of approach is important in the prognostic evaluation of cancers in general. Further investigations with this approach are needed for the improvement of prognosis of pancreatic cancer patients.

In addition, cut-off values between better and worse prognosis should be discussed because each cut-off value is different between these reports. Absolute values of SUV can be influenced by several institution-dependant factors, such as method of reconstruction and the size and shape of the ROI or others. Keyes (1995) suggested that most of the currently published findings on SUV in tumors are of little or no value for investigators in other laboratories. An average SUV of total cases may have a universal value and is easy to apply as a threshold value. However, there should be a wide borderline area around the cut-off line, and a minor error or change in average SUV may affect the results. In a clinical situation, it is impossible to apply strictly this kind of threshold value to all cancer patients with all stages or all sizes in a prospective manner. For example, it is difficult to predict which one has a better prognosis; a cancer with SUV of 2.0 and size of 6 cm or a cancer with SUV of 6.0 and size of 1 cm. It is unclear whether a cancer with SUV of 2.0 and liver metastasis or a cancer with SUV of 6.0 without distant metastasis would show better prognosis. Again, evaluation of clinical staging (T- or M-factor) is important for the prognostic prediction in FDG-PET.

RI is an index measuring changes between 1 and 2 h; therefore, it is supposed to have a universal value. As for the borderline area around the cut-off line, Lyshchik *et al.* (2005) also showed convincing statistical evidence. In our data, the single-variate analysis showed that not only thresholds of RI = 10%, but also thresholds of RI = 15% and 20% could perform a significant difference in prognosis. One of the drawbacks in the study by Lyshchik *et al.* (2005) is its methodological quality. In our study, we included two different data sets obtained by two different PET machines; PCT3600W (1997–1999) and GE Advance (1999–2003). There might be a distribution bias in SUV which could affect the prognostic value of SUV or RI in the total results. In order to determine an appropriate cut-off value in SUV or RI, further study with larger population of patients with pancreatic cancer are needed.

Furthermore, the correlation of FDG uptake with other cellular characteristics is important. There are many factors that are related to the prognosis of pancreatic cancer. Among these factors, glucose transporter-1 (GLUT-1) expression is the most important. FDG uptake of tumor is related to GLUT-1 expression in the membrane of cancer cells in a variety of cancers, including pancreatic cancer (Higashi *et al.*, 1997). Some studies also support the positive correlation of GLUT-1 expression and proliferative activity or aggressiveness of the cancer. In pancreatic cancer, Ito *et al.* (2004) reported that GLUT-1 gene expression is associated with invasiveness of the tumor. This result may support the data from Nakata *et al.* (2001), Zimny *et al.* (2000), and Sperti *et al.* (2003). On the other hand, there has been no established biochemical or histopathological marker reported so far that could explain the biological meaning of RI as a prognostic parameter. Our recent data revealed that hexokinase-II (HK-II) expression in the cytosol of pancreatic cancer cells has a close relationship

with RI of FDG-PET and survival of patients, while GLUT-1 has no correlation with survival (Higashi T. *et al*., 2002; Lyshchik *et al*., 2007). These data suggest the possible role of RI in glucose metabolism and cancer aggressiveness in pancreatic cancer. As a histopathological background, we hypothesize that RI is also related to lymphocytic-immune response to cancer, because several studies have already reported the prognostic value of intratumoral CD4 and CD8 lymphocyte infiltration in a variety of cancers, including pancreatic cancer (Fukunaga *et al*., 2004). Further evaluation concerning RI in dual-phase FDG-PET and lymphocytic immune response is now ongoing in our university.

Tumor cell cellularity is also an indispensable histopathological factor of FDG uptake in pancreatic cancers. Several *in vitro* and *in vivo* studies reported that tumor cell cellularity was an important factor for FDG tumor uptake in a variety of tumors (Higashi *et al*., 1998). Especially in pancreatic cancer, which is known to be rich in desmoplastic reaction, it is necessary to be aware of the possibility of low FDG uptake due to poor cellularity even when tumor size is fairly large. It is still controversial whether cancer cells use the extracellular matrix for growth factor storage and for their progression, or if this reaction is a defense mechanism of the human body against cancer cell spread (Armstrong *et al*., 2004; Hartel *et al*., 2004). If desmoplastic reaction plays an invasive role in pancreatic cancer progression, FDG uptake may be lower in a cancer with higher progressive nature. Further investigation is needed to clarify this problem in pancreatic cancers.

IMPROVING ACCURACY IN THE EVALUATION OF CLINICAL STAGING

Approximately, 40% of patients with pancreatic cancer that is diagnosed as resectable by preoperative imaging modalities turned out to be unresectable at the time of operation. Clinical staging is supposed to be the most important prognostic factor in predicting prognosis in pancreatic cancer because, as mentioned earlier, meta-analysis revealed that surgical resection is the only prognostic significance for longer survival in patients with pancreatic cancer (Morganti *et al*., 2005). These data suggest the importance of accurate preoperative diagnosis of T-, N- and M-factors in TNM classification as prognostic parameters. Hicks *et al*. (2001) reported the high impact and powerful prognostic stratification of FDG-PET in clinical staging of lung cancer. They concluded that staging that incorporated PET provided a more accurate prognostic stratification than did staging based on conventional investigations. Evaluation of prognostic stratification in staging of pancreatic cancer by PET should be discussed in T-, M-, and N-factors.

Detection of direct invasion to large vessels or to adjacent visceral structures (T-factor) is one of the most important aspects for the staging of pancreatic cancer. Positron emission tomography (PET) is not supposed to be useful in the diagnosis of T-factor because of its relatively low resolution. Recently, the introduction of multi-detector row (MD)-CT technology has changed the situation in the staging of pancreatic cancer. This technology has the capability of whole body scanning with a single breath-hold, and can easily

cover the patient body from the neck to the thigh. It possesses a definite superiority over FDG-PET because the resolution of MD-CT with the multi-axis or curved planar image reformations can provide detailed information of direct invasion of pancreatic cancer to large vessels or adjacent organs easily (Prokesch *et al*., 2002b). Despite the higher resolution, differential diagnosis between pancreatic cancer and chronic pancreatitis, and detection of LN metastasis in supraclaviclar area, bone metastasis or peritoneal dissemination are often difficult even by the use of MD-CT (Prokesch *et al*., 2002a, b; Beyer *et al*., 2002). Therefore, the development of PET/CT occurred in order to combine the usefulness of morphological and functional imaging modalities. PET/CT, a dual-modality scanner that has a capability of latest PET and MD-CT alone, is now the most promising imaging tool in the diagnosis of pancreatic cancer (Heinrich *et al*., 2005). In addition, the use of digital image fusion of PET and CT is now in progress (Lemke *et al*., 2004). However, the clinical usefulness of these multi-modality imaging procedures is not yet established in the diagnosis of pancreatic cancers (see other chapters in this volume).

Liver or other distant metastasis is usually suggested as a contraindication of pancreatic cancer resection (M-factor). Fujino *et al*. (2003) also concluded that liver metastasis and peritoneal dissemination were significant prognostic factors for survival of patients with unresectable pancreatic cancer in their multivariate analysis of 187 cases. FDG-PET can show a powerful prognostic value by the detection of liver and distant metastasis. Frohlich *et al*. (1999) reported that the detection rate for metastatic liver lesions > 1 cm was 97% while that for lesions < or = 1 cm was 43%. On the other hand, FDG-PET can often detect a small lesion that CT scan cannot differentiate, because even if a small lesion with a size of 5 mm has strong radioactivity, it can be detected as a relatively larger lesion by FDG-PET. Nakamoto *et al*. (1999) reported that FDG-PET accurately differentiated metastatic lesions from cysts when the diagnosis using US or CT was unreliable because of the small size of the lesion (< or = 1 cm). The introduction of multi-detector row CT (MD-CT) has raised the detectability of pancreatic cancer much higher than that by single-detector CT (McNulty *et al*., 2001). Recent report of PET/CT revealed that PET/CT staging of distant metastasis showed higher sensitivity and specificity than those of CT and other standard modalities (Heinrich *et al*., 2005). Further evaluation is needed in the detection of liver or other distant metastasis by PET/CT (see other chapters in this volume).

It is also known that LN metastasis (N-factor) is one of the most important factors of clinical management as an independent prognostic indicator for pancreatic cancer patients (Benassai *et al*., 1999). However, there has been no imaging modality that can detect lymph node metastasis in the diagnosis of pancreatic cancer with high accuracy. Zimny *et al*. (1997) reported an accuracy rate of FDG-PET for the detection of LN metastasis of only 46%. Even the use of PET/CT machine or digital image fusion of PET and CT did not improve the detectablity of lymph node metastasis, where sensitivity of LN metastasis was < 40% (Heinrich *et al*., 2005; Lemke *et al*., 2004). It was reported that polymerase chain reaction

(PCR) amplification could detect occult LN metastases that were not detected by routine histopathological examination (Demeure *et al*., 1998). There is little hope as yet in the diagnosis of lymph node metastasis from pancreatic cancers.

MONITORING THERAPEUTIC EFFECT

Monitoring cancer therapy and thereby predicting outcome is one of the most promising roles for FDG-PET. This type of approach to prognostic prediction using FDG-PET is commonly performed and believed to be useful in various cancers (Weber *et al*., 2005). The use of FDG-PET for this purpose, however, has not been thoroughly evaluated in pancreatic cancer. This is partly because there has been no established treatment procedure for pancreatic cancer, except for surgical resection, and partly because the prognosis of patients with pancreatic cancer is poor only with short follow-up period.

In post-operative patients with pancreatic cancer, the use of chemoradiotherapy after operation is an important factor affecting prognosis, however, its role is still controversial (Oya, 2004). A large randomized phase III trial (n = 218) was conducted by European Organization for Research and Treatment of Cancer (EORTC), comparing two aspects, curative operation alone vs. curative operation with chemoradiation (40 Gy with 5-FU based chemotherapy) (Klinkenbijl *et al*., 1999). They concluded that there was no significant difference between the two aspects. Another large randomized trial (n = 289) with similar treatment methods was conducted by European Study Group for Pancreatic Cancer (ESPAC-1), in which they concluded that post-operative chemoradiotherapy had a negative effect on survival in patients with resected pancreatic cancer (Neoptolemos *et al*., 2004). On the other hand, a retrospective cohort study (n = 396) of registered patients in the National Cancer Institute's (NCI) Surveillance, Epidemiology, and End Results (SEER) program analyzed the prognostic factors following curative resection for pancreatic cancer (Lim *et al*., 2003). Their conclusion using multivariate analysis was that the strongest predictor of survival was the factor of adjuvant combined chemoradiotherapy. These studies were performed without the use of gemcitabine (GEM), one of the most feasible chemotherapeutic agents. The trends in chemoradiotherapy have already been changed to the GEM-based chemoradiotherapy. Several trials are under evaluation using GEM. In the near future, there may be a great need of FDG-PET to evaluate the therapeutic effect of post-operative chemoradiotherapy.

In patients with locally-advanced unresectable pancreatic cancer, chemoradiotherapy is the first choice of treatment method. Various dose and regimen have been reported, but not established yet (Oya, 2004). Our previous study reported the usefulness of FDG-PET in the evaluation of the therapeutic effect of IORT (intraoperative radiation therapy)–based treatment in unresectable pancreatic cancers, in which FDG-PET showed that the metabolic change in irradiated cancer after IORT was significantly earlier than the morphological change detected by CT scan (Higashi *et al*., 1999) (Figure 19.2). However, although FDG-PET effectively evaluated the local control of the primary site, there was no

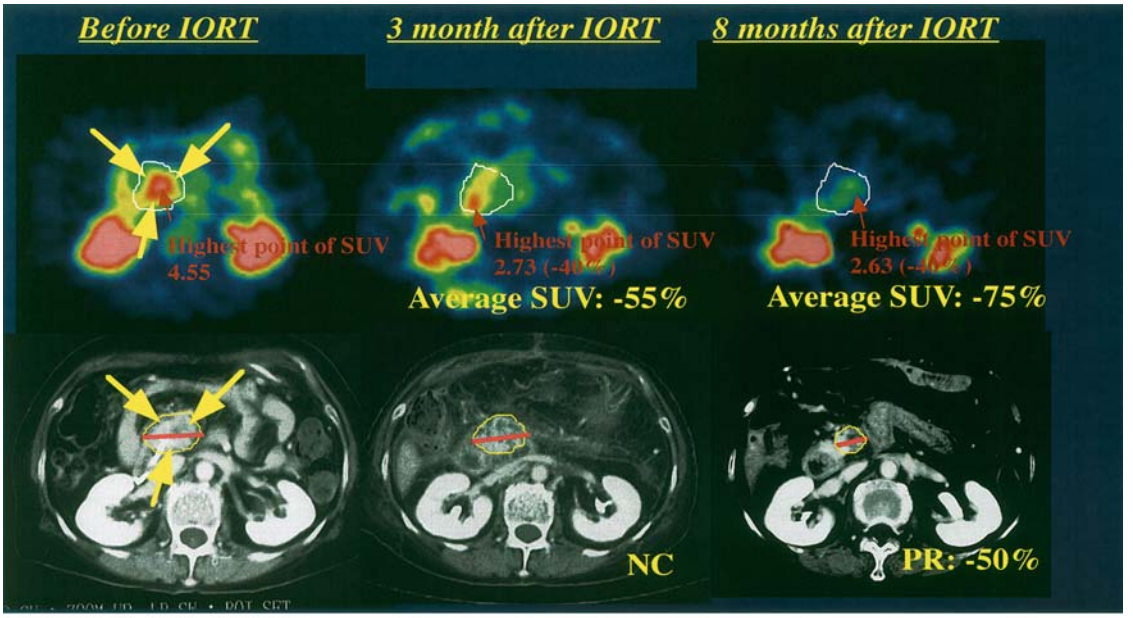

FIGURE 19.2. Evaluation of therapeutic effect of IORT and EBRT by FDG-PET. Seventy-three years old female patient with unresectable pancreatic cancer without distant metastasis was initially treated with IORT (30 Gy) and then followed with EBRT (50.4 Gy). PET and CT studies were performed before treatment (a) 3 months after IORT and just after the end of EBRT (b) and 8 months after the IORT (c). The decreased FDG uptake was observed at 3 months after IORT, whereas CT findings did not show any change in size at that time. Eight months after IORT, tumor finally showed decrease in size at CT. PET showed marked decrease in FDG uptake around the pancreatic head in general, but there was an intense hot spot remained, which suggest viability within the irradiated mass. This patient died 4 months later after this PET study because of multiple liver metastasis. *IORT: intraoperative radiation therapy EBRT: external beam radiation therapy*

relation between FDG-PET results and prognosis in the patient population.

Recently, we evaluated 27 patients with locally-advanced unresectable pancreatic cancer (age: 58 ± 10 years-old, male: 19 cases, female: 8 cases), who received external-beam radiation treatment (EBRT/total 50.4 Gy with 20–30 fraction) or EBRT with chemotherapy (5-FU daily venous infusion) (not published). Before treatment and after the end of treatment, FDG-PET studies were performed with the results of SUV 7.2 ± 4.6 and 4.3 ± 2.2, respectively. In all cases, SUV showed a decrease from pre- to post-treatment at the primary site, and it was diagnosed that local control of cancer was excellent. However, survival of the patients (mean: 277 days) was defined not by local control of the primary tumor, but by the appearance of distant metastasis, mainly liver metastasis. Therefore, we evaluated prognostic factors in these patients according to the separation of two groups as follows; short-time survivor (STS: survival days < 300 days/mean ± SD: 192 ± 57 days/stage III: n = 0, stage IV: n = 10) and intermediate- and long-time survivor (ILTS: survival days > 300

days/mean ± SD: 437 ± 208 days/stage III: n = 3, stage IV: n = 8). Multivariate analysis revealed that decreased rate of serum CA19-9 was the only significant prognostic factor, whereas SUV or its change rate did not show any significant difference between STS and ILTS. Average SUV before treatment was higher in ILTS (8.2) than that in STS (6.1); therefore, pretreatment SUV did not show any prognostic value.

We also evaluated the same patients using Kaplan-Meier analysis with the difference between high-response group (HRG) and low response group of serum CA19-9 (LRG), which revealed that HRG survived significantly longer than LRG ($p < 0.05$). Thus, local change of FDG uptake in the primary tumor may not have prognostic value for radiation or chemoradiation. Franke *et al*. (1999) also reported the diagnostic benefit of follow-up of pancreatic cancers in their brief reports with 19 cases, but the benefit was basically limited in the detection of distant metastasis by FDG PET. Further evaluation is needed (see other chapters in this volume).

Maisey *et al*. (2003) reported in their pilot study that the absence of FDG uptake at 1 month following chemotherapy for pancreatic carcinoma is an indicator of improved overall survival. This is a promising study, but the patient number is only 11. Further investigation is necessary. Chemotherapy alone with gemcitabine or combination of other agents is considered as an acceptable alternative of chemoradiation (Louvet *et al*., 2005). Our limited data also suggest its efficacy (Figure 19.1). Several clinical trials are now under investigation. Much still remained to be done for the treatment of pancreatic cancer.

CONCLUSION

As a prognostic parameter, FDG-PET is promising, but not established yet. FDG uptake (SUV) and/or its uptake pattern (RI: retention index) are supposed to be feasible in pretreatment prediction of malignant potential. Further investigation with more patient number or with additional indications of histopathological backgrounds is needed. Clinical staging by FDG-PET is a useful predictive tool in the evaluation of resectability and thereby prognosis of pancreatic cancer, especially by the detection of distant metastasis. PET/CT will be a great help in this respect in the near future. Monitoring cancer therapy is one of the most promising roles for FDG-PET, but there has been little information so far. There is a real need for systemic treatment approaches to the devastating survival of patients with pancreatic cancer.

Acknowledgments. I wish to express my gratitude to the staff of Radio-Isotope Ward and the staff of the Department of Surgical Oncology and Basic Science, Kyoto University Hospital for their clinical advice and to Ms. Mayumi Takeuchi for her valuable editorial assistance.

REFERENCES

Armstrong, T., Packham, G., Murphy, L.B., Bateman, A.C., Conti, J.A., Fine, D.R., Johnson, C.D., Benyon, R.C., and Iredale, J.P. 2004. Type I collagen promotes the malignant phenotype of pancreatic ductal adenocarcinoma. *Clin. Cancer Res. 10*: 7427–7437.

Benassai, G., Mastrorilli, M., Mosella, F., and Mosella, G. 1999. Significance of lymph node metastases in the surgical management of pancreatic head carcinoma. *J. Exp. Clin. Cancer Res. 18*: 23–28.

Beyer, T., Townsend, D.W., and Blodgett, T.M. 2002. Dual-modality PET/CT tomography for clinical oncology. *Q. J. Nucl. Med. 46*: 24–34.

Demeure, M.J., Doffek, K.M., Komorowski, R.A., and Wilson, S.D. 1998. Adenocarcinoma of the pancreas: detection of occult metastases in regional lymph nodes by a polymerase chain reaction-based assay. *Cancer 83*: 1328–1334.

Franke, C., Klapdor, R., Meyerhoff, K., and Schauman, M. 1999. 18-FDG positron emission tomography of the pancreas: diagnostic benefit in the follow-up of pancreatic carcinoma. *Anticancer Res. 19*: 2437–2442.

Frohlich, A., Diederichs, C.G., Staib, L., Vogel, J., Beger, H.G., and Reske, S.N. 1999. Detection of liver metastases from pancreatic cancer using FDG PET. *J. Nucl. Med. 40*: 250–255.

Fujino, Y., Suzuki, Y., Ajiki, T., Ku, Y., and Kuroda, Y. 2003. Predicting factors for survival of patients with unresectable pancreatic cancer: a management guideline. *Hepatogastroenterology 50*: 250–253.

Fukunaga, A., Miyamoto, M., Cho, Y., Murakami, S., Kawarada, Y., Oshikiri, T., Kato, K., Kurokawa, T., Suzuoki, M., Nakakubo, Y., Hiraoka, K., Itoh, T., Morikawa, T., Okushiba, S., Kondo, S., and Katoh, H. 2004. CD8+ tumor-infiltrating lymphocytes together with CD4+ tumor-infiltrating lymphocytes and dendritic cells improve the prognosis of patients with pancreatic adenocarcinoma. *Pancreas 28*: e26–e31.

Gebhardt, C., Meyer, W., Reichel, M., and Wunsch, P.H. 2000. Prognostic factors in the operative treatment of ductal pancreatic carcinoma. *Langenbecks Arch. Surg. 385*: 14–20.

Hartel, M., Di Mola, F.F., Gardini, A., Zimmermann, A., Di Sebastiano, P., Guweidhi, A., Innocenti, P., Giese, T., Giese, N., Buchler, M.W., and Friess, H. 2004. Desmoplastic eaction influences pancreatic cancer growth behavior. *World J. Surg. 28*: 818–825.

Heinrich, S., Goerres, G.W., Schafer, M., Sagmeister, M., Bauerfeind, P., Pestalozzi, B.C., Hany, T.F., von Schulthess, G.K., and Clavien, P.A. 2005. Positron emission tomography/computed tomography influences on the management of resectable pancreatic cancer and its cost-effectiveness. *Ann. Surg. 242*: 235–243.

Hicks, R.J., Kalff, V., MacManus, M.P., Ware, R.E., Hogg, A., McKenzie, A.F., Matthews, J.P., and Ball, D.L. 2001. (18)F-FDG PET provides high-impact and powerful prognostic stratification in staging newly diagnosed non-small cell lung cancer. *J. Nucl. Med. 42*: 1596–1604.

Higashi, K., Ueda, Y., Arisaka, Y., Sakuma, T., Nambu, Y., Oguchi, M., Seki, H., Taki, S., Tonami, H., and Yamamoto, I. 2002. 18F-FDG uptake as a biologic prognostic factor for recurrence in patients with surgically resected non-small cell lung cancer. *J. Nucl. Med. 43*:39–45.

Higashi, T., Tamaki, N., Honda, T., Torizuka, T., Kimura, T., Inokuma, T., Ohshio, G., Hosotani, R., Imamura, M., and Konishi, J. 1997. Expression of glucose transporters in human pancreatic tumors compared with increased FDG accumulation in PET study. *J. Nucl. Med. 38*: 1337–1344.

Higashi, T., Tamaki, N., Torizuka, T., Nakamoto, Y., Sakahara, H., Kimura, T., Honda, T., Inokuma, T., Katsushima, S., Ohshio, G., Imamura, M., and Konishi, J. 1998. FDG uptake, GLUT-1 glucose transporter and cellularity in human pancreatic tumors. *J. Nucl. Med. 39*: 1727–1735.

Higashi, T., Sakahara, H., Torizuka, T., Nakamoto, Y., Kanamori, S., Hiraoka, M., Imamura, M., Nishimura, Y., Tamaki, N., and Konishi, J. 1999. Evaluation of intraoperative radiation therapy for unresectable pancreatic cancer with FDG PET. *J. Nucl. Med. 40*: 1424–1433.

Higashi, T., Saga, T., Nakamoto, Y., Ishimori, T., Mamede, M.H., Wada, M., Doi, R., Hosotani, R., Imamura, M., and Konishi, J. 2002. Relationship between retention index in dual-phase (18)F-FDG PET, and hexokinase-II and glucose transporter-1 expression in pancreatic cancer. *J. Nucl. Med. 43*: 173–180.

Higashi, T., Saga, T., Nakamoto, Y., Ishimori, T., Fujimoto, K., Doi, R., Imamura, M., and Konishi, J. 2003. Diagnosis of pancreatic cancer using fluorine-18 fluorodeoxyglucose positron emission tomography (FDG PET) –usefulness and limitations in "clinical reality". *Ann. Nucl. Med. 17*: 261–279.

Ito, H., Duxbury, M., Zinner, M.J., Ashley, S.W., and Whang, E.E. 2004. Glucose transporter-1 gene expression is associated with pancreatic cancer invasiveness and MMP-2 activity. *Surgery 136*: 548–556.

Jeong, H.J., Min, J.J., Park, J.M., Chung, J.K., Kim, B.T., Jeong, J.M., Lee, D.S., Lee, M.C., Han, S.K., and Shim, Y.S. 2002. Determination of the

prognostic value of [(18)F]fluorodeoxyglucose uptake by using positron emission tomography in patients with non-small cell lung cancer. *Nucl. Med. Commun. 23*: 865–870.

Keyes, J.W. Jr. 1995. SUV: standard uptake or silly useless value? *J. Nucl. Med. 36*: 1836–1839.

Klinkenbijl, J.H., Jeekel, J., Sahmoud, T., van Pel, R., Couvreur, M.L., Veenhof, C.H., Arnaud, J.P., Gonzalez, D.G., de Wit, L.T., Hennipman, A., and Wils, J. 1999. Adjuvant radiotherapy and 5-fluorouracil after curative resection of cancer of the pancreas and periampullary region: phase III trial of the EORTC gastrointestinal tract cancer cooperative group. *Ann. Surg. 230*: 776–782.

Kuhlmann, K.F., de Castro, S.M., Wesseling, J.G., ten Kate, F.J., Offerhaus, G.J., Busch, O.R., van Gulik, T.M., Obertop, H., and Gouma, D.J. 2004. Surgical treatment of pancreatic adenocarcinoma; actual survival and prognostic factors in 343 patients. *Eur. J. Cancer 40*: 549–558.

Lemke, A.J., Niehues, S.M., Hosten, N., Amthauer, H., Boehmig, M., Stroszczynski, C., Rohlfing, T., Rosewicz, S., and Felix, R. 2004. Retrospective digital image fusion of multidetector CT and 18F-FDG PET: clinical value in pancreatic lesions–a prospective study with 104 patients. *J. Nucl. Med. 45*: 1279–1286.

Lim, J.E., Chien, M.W., and Earle, C.C. 2003. Prognostic factors following curative resection for pancreatic adenocarcinoma: a population-based, linked database analysis of 396 patients. *Ann. Surg. 237*: 74–85.

Louvet, C., Labianca, R., Hammel, P., Lledo, G., Zampino, M.G., Andre, T., Zaniboni, A., Ducreux, M., Aitini, E., Taieb, J., Faroux, R., Lepere, C., and de Gramont, A.; GERCOR; GISCAD. 2005. Gemcitabine in combination with oxaliplatin compared with gemcitabine alone in locally advanced or metastatic pancreatic cancer: results of a GERCOR and GISCAD phase III trial. *J. Clin. Oncol. 23*: 3509–3516.

Lyshchik, A., Higashi, T., Nakamoto, Y., Fujimoto, K., Doi, R., Imamura, M., and Saga, T. 2005. Dual-phase 18F-fluoro-2-deoxy-D-glucose positron emission tomography as a prognostic parameter in patients with pancreatic cancer. *Eur. J. Nucl. Med. Mol. Imaging. 32*: 389–397.

Lyshchik, A., Higashi, T., Hara, T., Nakamoto, Y., Fujimoto, K., Doi, R., Imamura, M., Saga, T., and Togashi, K. 2007. Expression of glucose transporter-1, hexokinase, proliferating nuclear antigen and survival of the patients with pancreatic cancer. *Cancer Invest. 25*: 154–162.

Maisey, N.R., Webb, A., Flux, G.D., Padhani, A., Cunningham, D.C., Ott, R.J., and Norman, A. 2000. FDG-PET in the prediction of survival of patients with cancer of the pancreas: a pilot study. *Br. J, Cancer. 83*: 287–293.

McNulty, N.J., Francis, I.R., Platt, J.F., Cohan, R.H., Korobkin, M., and Gebremariam, A. 2001. Multi–detector row helical CT of the pancreas: effect of contrast-enhanced multiphasic imaging on enhancement of the pancreas, peripancreatic vasculature, and pancreatic adenocarcinoma. *Radiology 220*: 97–102.

Minn, H., Lapela, M., Klemi, P.J., Grenman, R., Leskinen, S., Lindholm, P., Bergman, J., Eronen, E., Haaparanta, M., and Joensuu, H. 1997. Prediction of survival with fluorine-18-fluoro-deoxyglucose and PET in head and neck cancer. *J. Nucl. Med. 38*: 1907–1911.

Morganti, A.G., Brizi, M.G., Macchia, G., Sallustio, G., Costamagna, G., Alfieri, S., Mattiucci, G.C., Valentini, V., Natale, L., Deodato, F., Mutignani, M., Doglietto, G.B., and Cellini, N. 2005. The prognostic effect of clinical staging in pancreatic adenocarcinoma. *Ann. Surg. Oncol. 12*: 145–151.

Nakamoto, Y., Higashi, T., Sakahara, H., Tamaki, N., Kogire, M., Imamura, M., and Konishi, J. 1999. Contribution of PET in the detection of liver metastases from pancreatic tumours. *Clin. Radiol. 54*: 248–252.

Nakata, B., Chung, Y.S., Nishimura, S., Nishihara, T., Sakurai, Y., Sawada, T., Okamura, T., Kawabe, J., Ochi, H., and Sowa, M. 1997. 18F-fluorodeoxyglucose positron emission tomography and the prognosis of patients with pancreatic adenocarcinoma. *Cancer 79*: 695–699.

Nakata, B., Nishimura, S., Ishikawa, T., Ohira, M., Nishino, H., Kawabe, J., Ochi, H., and Hirakawa, K. 2001. Prognostic predictive value of 18F-fluorodeoxyglucose positron emission tomography for patients with pancreatic cancer. *Int. J. Oncol. 19*: 53–58.

National Cancer Center. 2001. The 2001 edition of Cancer Statistics in Japan. http//www.ncc.go.jp/en/statistics/2001/index.html.

National Cancer Institute. 1999. SEER cancer statistics review 1973–1996. NIH Publication No.

99-2789. Bethesda, Department of Health and Human Services.

Neoptolemos, J.P., Stocken, D.D., Friess, H., Bassi, C., Dunn, J.A., Hickey, H., Beger, H., Fernandez-Cruz, L., Dervenis, C., Lacaine, F., Falconi, M., Pederzoli, P., Pap, A., Spooner, D., Kerr, D.J., and Buchler, M.W.; European Study Group for Pancreatic Cancer. 2004. A randomized trial of chemoradiotherapy and chemotherapy after resection of pancreatic cancer. *N. Engl. J. Med. 350*: 1200–1210.

Oya, N. 2004. Chemoradiotherapy for pancreatic cancer: current status and perspectives. *Int. J. Clin. Oncol. 9*: 451–457.

Prokesch, R.W., Chow, L.C., Beaulieu, C.F., Bammer, R., and Jeffrey, R.B. Jr. 2002a. Isoattenuating pancreatic adenocarcinoma at multi-detector row CT: secondary signs. *Radiology 224*: 764–768.

Prokesch, R.W., Chow, L.C., Beaulieu, C.F., Nino-Murcia, M., Mindelzun, R.E., Bammer, R., Huang, J., and Jeffrey, R.B. Jr. 2002b. Local staging of pancreatic carcinoma with multi-detector row CT: use of curved planar reformations initial experience. *Radiology 225*: 759–765.

Sperti, C., Pasquali, C., Chierichetti, F., Ferronato, A., Decet, G., and Pedrazzoli, S. 2003. 18-Fluorodeoxyglucose positron emission tomography in predicting survival of patients with pancreatic carcinoma. *J. Gastrointest. Surg. 7*: 953–959.

Stojadinovic, A., Brooks, A., Hoos, A., Jaques, D.P., Conlon, K.C., and Brennan, M.F. 2003. An evidence-based approach to the surgical management of resectable pancreatic adenocarcinoma. *J. Am. Coll. Surg. 196*: 954–964.

Weber, W.A. 2005. Use of PET for monitoring cancer therapy and for predicting outcome. *J. Nucl. Med. 46*: 983–995.

Zimny, M., Bares, R., Fass, J., Adam, G., Cremerius, U., Dohmen, B., Klever, P., Sabri, O., Schumpelick, V., and Buell, U. 1997. Fluorine-18 fluorodeoxyglucose positron tomography in the differential diagnosis of pancreatic carcinoma: a report of 106 cases. *Eur. J. Nucl. Med. 24*: 678–682.

Zimny, M., Fass, J., Bares, R., Cremerius, U., Sabri, O., Buechin, P., Schumpelick, V., and Buell, U. 2000. Fluorodeoxyglucose positron emission tomography and the prognosis of pancreatic carcinoma. *Scand. J. Gastroenterol. 35*: 883–888.

20
Imaging and Pathologic Findings of Peculiar Histologic Variants of Pancreatic Endocrine Tumors

Nobuyuki Ohike, Masaaki Kawahara, Manabu Takahashi, Ayako Sugihara, Takehiko Gokan, and Toshio Morohoshi

INTRODUCTION

Pancreatic endocrine tumors (PETs) are relatively uncommon, representing 1–2% of all pancreatic neoplasms. The detection of PETs has increased due to the development of sensitive diagnostic tools such as imaging techniques and reliable laboratory tests. This increased detection has resulted in the identification of a clinical and morphologic variety of PETs and a variety of histologic alterations including oncocytic changes, rhabdoid features, clear cytoplasm, mucin accumulation resulting in goblet cell formation, and spindle cell morphology (Chetty and Asa., 2004; Frankel, 2006), although they are rare. Such peculiar histologic features may make diagnosis difficult, especially in biopsy specimens. Therefore, diagnosis of PETs may better be performed according to radiologic findings. There are few reports concerning imaging findings of peculiar PETs. We report three cases, with imaging and pathologic findings: oncocytic PET, PET with rhabdoid features, and PET with clear cell cytology.

CASE 1

This case was reported by Sugihara *et al*. (2006). A 65-year-old woman consulted a doctor because of occasional symptoms of nausea, diarrhea, and discomfort in the stomach after meals. She received a diagnosis of nonfunctioning tumor in the body of the pancreas and metastases in segments 6 and 8 of the liver, for which she underwent distal pancreatectomy and partial hepatectomy. The postoperative course was favorable, and there have been no signs of recurrence 5 months after surgery.

Imaging Findings

Computed tomography (CT) imaging showed a solitary, well-circumscribed mass extending from the body to the head of the pancreas. The tumor was identified by contrast-enhanced CT (CE-CT) imaging as a mildly enhancing, somewhat heterogeneous mass in the early phase (Figure 20.1) that enhanced equally to the surrounding pancreas in the late phase. Metastatic lesions to the liver were strongly enhanced in the early phase (Figure 20.1).

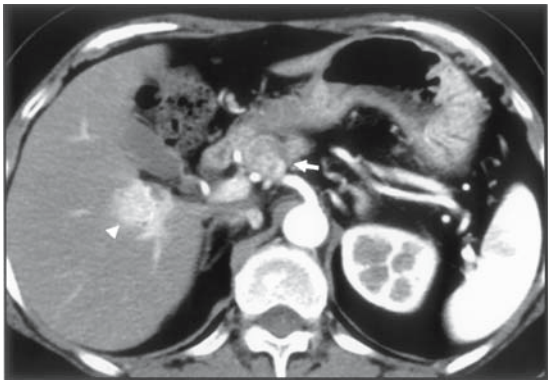

FIGURE 20.1. Imaging findings of an oncocytic pancreatic endocrine tumor (PET) (Contrast-enhanced CT (CE-CT), early phase). A solitary mass (arrow) extending from the body to the head of the pancreas is identified by contrast-enhanced CT imaging as a mildly enhancing mass. Metastatic lesion in the liver is strongly enhanced (arrowhead).

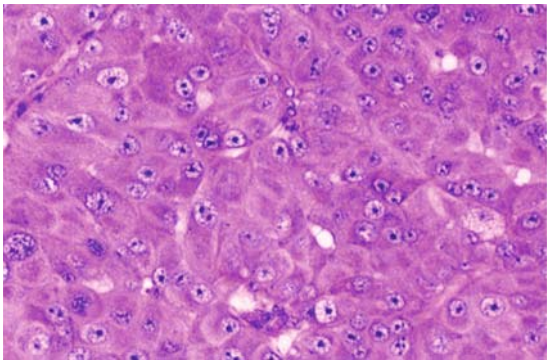

FIGURE 20.2. Pathological findings of an oncocytic PET (Histology, hematoxylin and eosin (HE) stain). Tumor cells are large, and have an eosinophilic cytoplasm and a large nucleus with one or two prominent nucleoli.

Pathologic Findings

The pancreatic tumor was well demarcated, 4.8 × 5.5 cm in size, and yellowish-white on the cut surface. The tumor cells were arranged in trabeculae or solid nests separated by a fibrous or loose fibrovascular stroma. All tumor cells were large and polygonal in shape with abundant, eosinophilic, and finely granular cytoplasm (Figure 20.2). The nuclei were large, round, and vesicular, containing one or two prominent nucleoli. The number of mitoses was 1 per 10 high-power fields (HPFs). There was no tumor necrosis. Electron microscopy showed that the abundant cytoplasm of the tumor cells was packed with mitochondria varying in size and shape and also contained some electron-dense neuroendocrine granules. Immunohistochemically, tumor cells stained intensely for mitochondrial antigen and were positive for chromogranin A but were negative for hormones and enzymes such as amylase and trypsin. The tumor was diagnosed as a nonfunctioning oncocytic PET and classified as a well-differentiated endocrine carcinoma according to the World Health Organization (WHO) histologic classification (Heitz *et al*., 2004).

CASE 2

A 76-year-old woman was found to have a mass in the pancreatic head with direct invasion to the second portion of the duodenum, causing a duodenal ulcer and hemorrhagic anemia, and another mass extending from the third portion of the duodenum to the jejunum. Atypical signet ring cells were detected by preoperative duodenal biopsy. Pancreatic cancer and jejunal stromal tumor were diagnosed, and pancreatoduodenojejunectomy was performed. There have been no signs of recurrence 5 years after surgery.

Imaging Findings

CT imaging showed a comparatively well-circumscribed mass in the head of the pancreas that appeared to protrude into the body of the pancreas or the third portion of the duodenum. CE-CT imaging showed the tumor to be strongly enhanced in both the early and late phases (Figure 20.3). Hemorrhage

or necrosis was considered in the areas of the tumor that were not enhanced. True fast imaging with steady precession magnetic resonance imaging (True FISP MRI) of the pancreas showed a heterogeneous mass in the head of the pancreas and in the body of the pancreas or along the third portion of the duodenum. The mass in the head pressed against the common bile duct. A celiac angiogram showed a highly abnormal stain in the pancreas head with vascularization of small vessels and feeding by a dilated superior pancreaticoduodenal artery, indicating a hypervascular tumor.

Pathologic Findings

The pancreatic head tumor was 3.0 × 3.0 cm in size, yellowish-white on the cut surface, and directly invaded the second portion of the duodenum. In addition, a metastatic mass of 10 × 6 cm was identified in the third portion of the duodenum. Histologically, the tumors were lobulated by a fibrous stroma and tumor cells were arranged predominantly in a trabecular or solid pattern. Approximately, one-third of the tumor cells showed prominent pale or eosinophilic intracytoplasmic inclusions resulting in a rhabdoid, plasmacytoid, or signet ring-like appearance (Figure 20.4). The inclusions were negative when stained with periodic acid Schiff stain. Tumor cells without inclusions showed the typical, finely granular, eosinophilic cytoplasm of classic endocrine cells. The mitotic count was 1 per 10 HPFs. Widespread tumor necrosis was not present. Electron microscopy showed that the inclusions consisted of aggregates of juxtanuclear intermediate filaments with entrapped neurosecretory granules. Immunohistochemically, the rhabdoid cells were positive for keratin as well as chromogranin A (endocrine marker) but were negative for vimentin, indicating that the main component of the juxtanuclear intermediate filaments was keratin. The tumor was diagnosed as a nonfunctioning PET with rhabdoid features and classified as a well-differentiated endocrine carcinoma according to the WHO histologic classification (Heitz *et al.*, 2004).

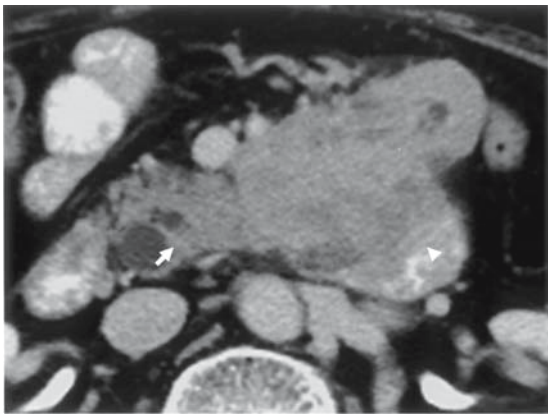

FIGURE 20.3. Imaging findings of a PET with rhabdoid features (CE-CT, early phase). A well-circumscribed mass (arrow) in the head of the pancreas appears to protrude into the body of the pancreas or the third portion of the duodenum (arrowhead). CE-CT imaging shows the tumor to be strongly enhanced in the early phase.

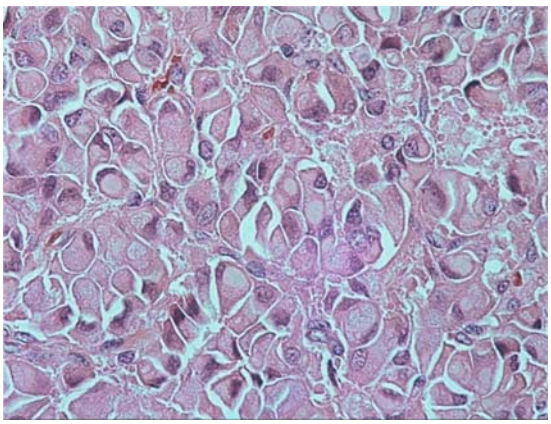

FIGURE 20.4. Pathological findings of a PET with rhabdoid features (Histology, HE stain). Tumor cells show prominent pale intracytoplasmic inclusions resulting in a rhabdoid, plasmacytoid, or signet ring-like appearance.

CASE 3

A 51-year-old man with von Hippel-Lindau (VHL) disease had nonfunctioning tumors in the head of the pancreas, for which a pylorus-preserving pancreatoduodenectomy was performed. The patient died of hemorrhage of a hemangioblastoma of the central nervous system 2 months after surgery.

Imaging Findings

CT imaging showed a comparatively well-circumscribed mass in the head of the pancreas. Postcontrast CT imaging perfomed in the early phase showed that the tumor was highly enhancing, heterogeneous and clearly distinguished from the surrounding pancreatic tissue (Figure 20.5). The enhancement continued into the late phase. A T1-weighted MRI scan of the pancreas showed a low-signal-intensity mass that was mildly increased in intensity with respect to the normal pancreas on T2-weighted images.

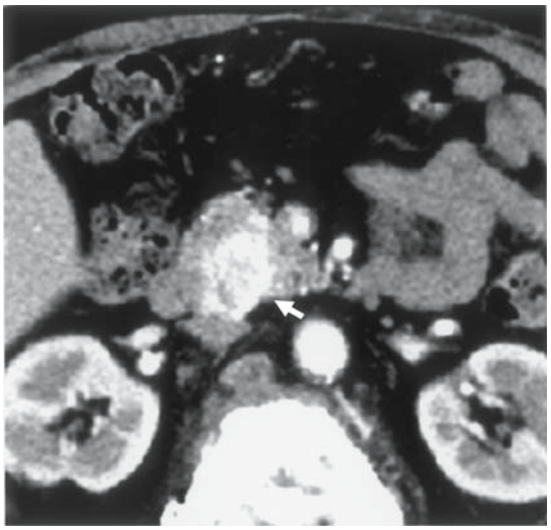

FIGURE 20.5. Imaging findings of a PET with clear cell cytology (CE-CT, early phase). Postcontrast CT imaging perfomed in the early phase shows that a well-circumscribed mass (arrow) in the head is highly enhancing and clearly distinguished from the surrounding pancreatic tissue.

Pathologic Findings

A 2.5 cm firm tumor was noted in the head. The surroundings contained multiple smaller tumors of various sizes and colors including bright yellow. Microscopically, all of the tumor cells were arranged in a solid or trabecular architecture, and they showed typical cytology. However, tumor cells in the bright yellow lesions showed a lipid-rich, multivacuolated, clear cytoplasm (Figure 20.6) accompanied by prominent stromal collagen bands. Involvement of tumor cells to peripancreatic lymph nodes was obsereved. In addition, minute serous cysts or adenomas were found incidentally. The mitotic count was 0 per 10 HPFs. Tumor necrosis was not present. Immunohistochemical studies showed expression of endocrine markers but not of hormone markers. The tumors were diagnosed as nonfunctioning PETs with clear cell cytology associated with VHL and classified as well-differentiated endocrine

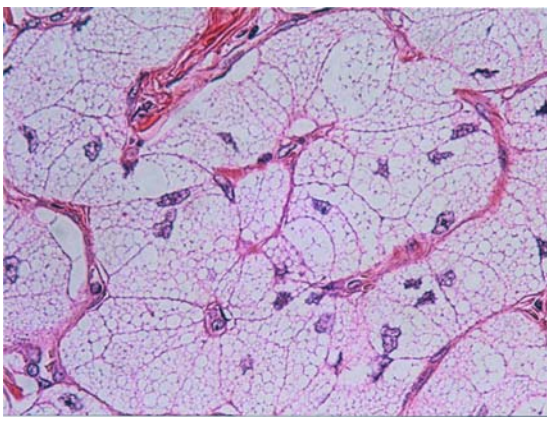

FIGURE 20.6. Pathological findings of a PET with clear cell cytology (Histology, HE stain). Tumor cells in the bright yellow lesions show a lipid-rich, multivacuolated, clear cytoplasm.

carcinoma according to the WHO histologic classification (Heitz *et al*., 2004).

DISCUSSION

Oncocytic changes occur infrequently in PETs. Volante *et al*. (2006) examined 227 PETs and found that 11 (4.85%) were oncocytic. Of 18 reported oncocytic PETs (Volante *et al*., 2006; Sugihara *et al*., 2006), 15 were nonfunctioning, and 14 were malignant, indicating that oncocytic PETs may be more aggressive than most PETs. Oncocytes are traditionally defined by the presence of an abundant, granular, acidophilic cytoplasm. These cells are also rich in mitochondria as determined by special cytochemical or immunohistochemical stains or ultrastructural studies. Therefore, the histologic diagnosis of oncocytic PETs should involve determination of both abundant mitochondria and endocrine differentiation. Differential histologic diagnoses are acinar cell carcinoma or mixed acinar-endocrine carcinoma with oncocytic or acidophilic degeneration and extremely rare oncocytoma of the pancreas. Primary hepatocellular carcinoma and metastatic oncocytic tumors from other sites should also be considered.

Rhabdoid phenotype is defined by the presence of cells containing inclusion-like masses of acidophilic, homogeneous, cytoplasmic material that characteristically displace the nucleus toward the cell periphery. The rhabdoid inclusions are composed of whorls of intermediate filaments and variable numbers of entrapped neurosecretory granules. Serra *et al*. (2006) reported a characteristic rhabdoid morphology in 5 of 84 (5.95%) PET cases. Of a total of 11 reported cases (Serra *et al*., 2006; Perez-Montiel *et al*., 2003; Stokes *et al*., 1998; Shia *et al*., 2004) including our present case (case 2), 10 were nonfunctioning, and eight were malignant, indicating that rhabdoid PETs may also be more aggressive than most PETs. However, rhabdoid PETs are typically well-differentiated, low-grade malignancies and differ from poorly differentiated or dedifferentiated malignancies in which rhabdoid features are thought to portend highly aggressive behavior. Differential histologic diagnoses include signet ring cell carcinoma, poorly differentiated adenocarcinoma, and anaplastic carcinoma with rhabdoid features, and metastatic melanoma with rhabdoid phenotype.

Clear cell changes are rarely found in larger PETs and are frequently found in PETs in patients with VHL disease (Lubensky *et al*., 1998). PETs arise in 8–17% of these patients. Tumors tend to occur in young patients (mean age, 35 years) and in a multicentric fashion (Lonser *et al*., 2003). The fact that the majority of VHL-associated PETs are nonfunctioning can be used to distinguish them from PETs of multiple endocrine neoplasia type 1. Progression of PETs can be a cause of death in VHL patients, but VHL-associated PETs are usually slow growing, similar to common PETs. The clear cytoplasm is finely vacuolated, representing abundant intracytoplasmic lipid droplets or glycogen deposition. The reason for clear cells in tumors in VHL patients is uncertain, but it is speculated that the tumor cells are exposed to ischemia by multicentric occurrence and a fibrous stroma due to the slow tumor growth or that the microvasculature may be delicate due to VHL-associated abnormalities. A clear cell appearance is also characteristic of other neoplasms in VHL patients such as renal cell carcinoma and pancreatic serous cystadenoma. This is also important with respect to differential diagnosis.

The three peculiar PETs described in this report were larger than 2.5 cm and were read-

ily detected by contrast-enhanced CT. The imaging features were of well-circumscribed and enhancing hypervascular masses, similar to common PETs. Several other types of radiologic examinations, including MRI and angiography, also supported these features. Thus, there were no specific imaging findings for these three cases. Generally, PETs are strongly enhanced during the arterial (early) phase in several imaging techniques. The mass reported in case 1 of the present study did not show strong enhancement in the early phase of contrast-enhanced CT but was clearly enhanced in the late phase. However, this does not appear to be specific to oncocytic PETs; fibrosis associated with slow-growing PETs may result in differential enhancement and heterogeneous imaging features. Compared to more common PETs, PETs with peculiar histology appear to have a high malignancy rate, and the present cases were also malignant. One reason may be that almost all such tumors are nonfunctional (asymptomatic) and are detected late. Thus, the histology alone may not explain the high rate of malignancy. Analysis of additional cases will aid in the elucidation of the biologic behavior of these types of tumors. It is also important to localize not only the primary tumors but also metastatic tumors in peculiar PETs. Differential diagnoses include all hypervascular primary and metastatic tumors. Differential diagnosis with respect to metastatic renal cell carcinoma and pancreatic serous cystadenoma may be difficult in VHL patients. In VHL patients, multicentric tumors must be considered upon radiologic examination.

REFERENCES

Chetty, R., and Asa, S.L. 2004. Pancreatic endocrine tumour with cytoplasmic keratin whorls. Is the term "rhabdoid" appropriate? *J. Clin. Pathol. 57*: 1106–1110.

Frankel, W.L. 2006. Update on pancreatic endocrine tumors. *Arch. Pathol. Lab. Med. 130*: 963–966.

Heitz, Ph. U., Komminoth, P., Perren, A., Klimstra, D.S., Dayal, Y., Bordi, C., Lechago, J., Centeno, B.A., and Kloppel, G. 2004. Pancreatic endocrine tumors: introduction. In DeLellis RA, Lloyd RV, Heitz Ph.U, Eng C, eds. *Pathology and Genetics of Tumours of Endocrine Organs*. WHO Classification of Tumours. IARC Press, Lyon.

Lonser, R.R., Glenn, G.M., Walther, M., Chew, E.Y., Libutti, S.K., Linehan, W.M., and Oldfield, E.H. 2003. von Hippel-Lindau disease. *Lancet 361*: 2059–2067.

Lubensky, I.A., Pack, S., Ault, D., Vortmeyer, A.O., Libutti, S.K., Choyke, P.L., Walther, M.M., Linehan, W.M., and Zhuang, Z. 1998. Multiple neuroendocrine tumors of the pancreas in von Hippel-Lindau disease patients: histopathological and molecular genetic analysis. *Am. J. Pathol. 153*: 223–231.

Perez-Montiel, M.D., Frankel, W.L., and Suster, S. 2003. Neuroendocrine carcinomas of the pancreas with 'Rhabdoid' features. *Am. J. Surg. Pathol. 27*: 642–649.

Serra, S., Asa, S.L., and Chetty, R. 2006. Intracytoplasmic inclusions (including the so-called "rhabdoid" phenotype) in pancreatic endocrine tumors. *Endocr. Pathol. 17*: 75–81.

Shia, J., Erlandson, R.A., and Klimstra, D.S. 2004. Whorls of intermediate filaments with entrapped neurosecretory granules correspond to the "rhabdoid" inclusions seen in pancreatic endocrine neoplasms. *Am. J. Surg. Pathol. 28*: 271–273.

Stokes, M.B., Kumar, A., Symmans, W.F., Scholes, J.V., and Melamed, J. 1998. Pancreatic endocrine tumor with signet ring cell features: a case report with novel ultrastructural observations. *Ultrastruct. Pathol. 22*: 147–152.

Sugihara, A., Nakasho, K., Ikuta, S., Aihara, T., Kawai, T., Iida, H., Yoshie, H., Yasui, C., Mitsunobu, M., Kishi, K., Mori, T., Yamada, N., Yamanegi, K., Ohyama, H., Terada, N., Ohike, N., Morohoshi, T., and Yamanaka, N. 2006. Oncocytic non-functioning endocrine tumor of the pancreas. *Pathol. Int. 56*: 755–759.

Volante, M., La Rosa, S., Castellano, I., Finzi, G., Capella, C., and Bussolati, G. 2006. Clinicopathological features of a series of 11 oncocytic endocrine tumours of the pancreas. *Virchows Arch. 448*: 545–551.

21
Periampullary Adenocarcinoma: Diagnosis and Survival After Pancreaticoduodenectomy

Kanika A. Bowen and Taylor S. Riall

INTRODUCTION

Periampullary adenocarcinomas arise within 2 cm of the major papilla in the duodenum. They arise from different tissues in the periampullary region: the head/neck/uncinate process of the pancreas, the distal common bile duct, the duodenum, and the ampulla of Vater. Pancreatic cancer is the most common periampullary adenocarcinoma, followed by distal bile duct cancers, ampullary cancers, and duodenal cancers (Jemal *et al*., 2007). There are an estimated 40,000 incident cases of periampullary cancer annually in the United States with pancreatic cancer accounting for over 33,000 cases annually (Jemal *et al*., 2007). The overall 5-year survival for all patients with pancreatic cancer is > 5%.

Because of their close proximity, periampullary cancers have similar clinical presentations with jaundice, abdominal pain, nausea, and vomiting. However, the 5-year survival following surgical resection differs greatly based on the tissue of origin. At the current time, surgical treatment is the only potentially curative option for periampullary adenocarcinoma. In a large series of resected patients, pancreatic cancers account for ~ 60% of resected periampullary cancers, while distal bile duct cancers account for 10–20%, ampullary cancers account for 10–20%, and duodenal cancers account for 3–7% (Riall *et al*., 2006a).

Resectability is based on the presence or absence of distant metastasis and the extent of locoregional disease at the time of presentation. Patients with distant metastatic disease including liver metastases, lung metastases, and lymph node metastases outside the resection field are considered unresectable. Locally advanced periampullary cancer, which includes invasion of the surrounding major vessels and the retroperitoneal nerve plexus, is also considered to be unresectable. This chapter will discuss the risk factors, clinical presentation, diagnostic workup, resection rates, and long-term prognosis for resected and unresected periampullary cancers.

RISK FACTORS

Pancreatic cancer is the fourth leading cause of cancer related deaths in men and women in the United States. Increasing age is a risk factor for pancreatic cancer,

with 80% of cases occurring in patients aged 60–80 years. The gender distribution is roughly equal, with the incidence being slightly higher in males. African-American patients have a 30–40% higher risk of developing pancreatic cancer than Caucasians (Jemal *et al*., 2007). Smoking increases the risk of pancreatic cancer nearly two-fold and is associated with point mutations in codon 12 of the *K-ras* oncogene which is a known early event in the molecular progression of pancreatic cancer (Tada *et al*., 1990; Wilentz *et al*., 2000). Genetic alterations of the *K-ras* oncogene and loss of tumor suppressor genes *p53*, *p16*, and *BRCA-2* have also been implicated in pancreatic cancer. The molecular progression of the development of pancreatic cancer from noninvasive precursor lesions is shown in Figure 21.1 (Wilentz *et al*., 2000).

There are six known genetic syndromes that are risk factors for pancreatic cancer, which include Familial Atypical Multiple Mole Melanoma (FAMMM) syndrome, familial breast cancer associated with BRCA-2 mutations, Peutz-Jeghers syndrome, hereditary nonpolyposis colorectal cancer, ataxia telangiectasia, and hereditary pancreatitis. Family history accounts for ~10% of pancreatic cancers. Even without identification of a known genetic syndrome, there is an 18-fold increased risk with a first degree relative with pancreatic cancer and a 30-fold risk with two first degree relatives. In the subset of familial pancreatic cancer, kindreds with three or more affected family members at the time of enrollment produced a 57-fold increased risk of pancreatic cancer (Tersmette *et al*., 2001).

The risk of common bile duct cancer increases with conditions that cause chronic inflammation of the bile duct. The majority of these cancers are found in persons older than 65. Sclerosing cholangitis and common bile duct stones are risk factors for common bile duct cancer (Chapman, 1999). Other diseases with associated risk are choledochal cysts, Caroli's disease, polycystic liver disease, and cirrhosis (Dayton *et al*., 1983; Lipsett *et al*., 1994). In Asian countries with poor water purification, liver flukes Clonorchis sinensis and Opisthorchis viverrini invade the bile duct, leading to chronic inflammation and bile duct cancer (Watanapa, 1996; Watanapa and Watanapa, 2002). Obesity causes an increased risk due to its association with gallstones and common

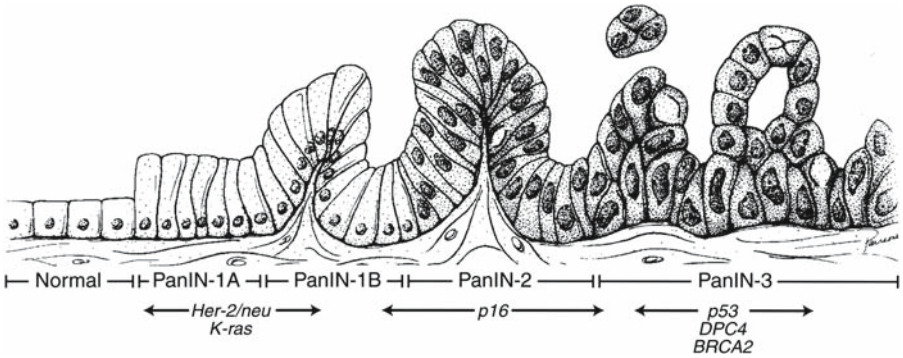

FIGURE 21.1. Progression model for duct adenocarcinoma of the pancreas (From Wilentz et al., 2000; with permission.)

bile duct stones, which are independent risk factors. Patients with inherited hereditary nonpolyposis colon cancer (HNPCC) have an increased risk for bile duct cancer (Mecklin *et al*., 1992). Thorotrast, dioxin, nitrosamines, and polychlorinated biphenyls also increase the risk of cholangiocarcinoma. This is true for all cholangiocarcinomas and not just those arising in the distal common bile duct.

Ampullary cancers can arise from ampullary adenomas, which are a premalignant precursor lesion displaying a similar adenoma-carcinoma sequence to that observed in colorectal neoplasia. Moreover, patients with Familial Adenomatous Polyposis (FAP) have a significantly increased incidence of both ampullary and colorectal cancers relative to the general population, suggesting that the mechanism of ampullary and colorectal carcinogenesis may be similar (Kadmon *et al*., 2001). FAP patients often develop benign ampullary adenomas, which may progress to cancer. The incidence of periampullary cancer is 200–300 times greater in this group than in the general population (Jagelman *et al*., 1988). Environmental risk factors include the use of cigars, pipes, or cigarettes.

TABLE 21.1. Frequency of the presenting symptoms of pancreatic cancer.

Head		Body and tail	
Symptoms	Patients (%)	Symptoms	Patients (%)
Weight loss	92	Weight loss	100
Jaundice	82	Pain	87
Pain	72	Weakness	42
Anorexia	64	Nausea	43
Dark urine	63	Vomiting	37
Light stools	62	Anorexia	33
Nausea	45	Constipation	27
Vomiting	37	Food intolerance	7
Weakness	35	Jaundice	7

(From Dimagno EP: Cancer of the Pancreas and Biliary Tract. In Winawer SJ, editor: Management of Gastrointestinal Diseases, 1992, Crower.)

Cancer of the duodenum is rare when compared with other gastrointestinal malignancies. Crohn's disease and celiac disease are associated with an increased risk of duodenal cancer. FAP, HNPCC, Peutz-Jeghers syndrome, and Gardner's syndrome are familial syndromes associated with the development of duodenal cancer (Delaunoit *et al*., 2005). Radiation exposure has also been linked to development of this cancer and frequent consumption of red meat and salt-cured/smoked foods have been linked with increases in risk (Chow *et al*., 1993).

CLINICAL PRESENTATION

The most common presenting signs and symptoms in patients with periampullary adenocarcinoma are jaundice, abdominal pain, weight loss, nausea, and vomiting (Table 21.1). Intractable back pain is an indication that the cancer has invaded the retroperitoneal nerve plexus. Jaundice is caused by obstruction of the bile duct by tumor. Nausea and vomiting may represent enlarged tumor size impeding on the gastric/duodenal outflow. New onset diabetes is seen in 15% of patients and is a sign of tumor infiltration of the normal pancreas. A sign of incurable periampullary cancer is ascites or a palpable abdominal mass which can represent omental caking or locally advanced disease. Palpable supraclavicular, umbilical, or rectovesicular/rectovaginal nodes may be present with distant lymph node metastasis.

DIAGNOSIS

Patients presenting with jaundice will usually have initial evaluation with abdominal

ultrasonography. Abdominal ultrasound will detect a dilated extrahepatic biliary tree and a mass in the periampullary region, which will then prompt computed tomography (CT) or magnetic resonance imaging (MRI). High resolution 3-D spiral CT has a sensitivity and specificity, of 72% and 100%, respectively, in detecting tumors arising within the periampullary region that are 2 cm or smaller in size (Bronstein *et al*., 2004). High resolution 3-D spiral CT today is considered reliable at evaluating vascular involvement prior to laparotomy and angiographic evaluation is no longer necessary. The ability of a high-quality CT to determine vascular invasion, distant metastasis, and retroperitoneal lymph node involvement approaches 100% (Mortele *et al*., 2002). An evaluation of high resolution 3-D spiral CT to determine diagnosis and resectability of pancreatic cancer was found to have a diagnostic sensitivity, specificity, and accuracy of 97%, 80%, and 96%, respectively, and provided a diagnosis of unresectability with a sensitivity of 96%, specificity of 86%, and accuracy of 93% (Catalano *et al*., 2003).

Endoscopic retrograde cholangiopancreatography (ERCP) is used to evaluate the biliary anatomy. However, the need for ERCP is lessened with the advent of (MRCP) and improved quality CT scans. Approximately, 95% of pancreatic cancers will be detected with ERCP, but tissue diagnosis by ERCP is less reliable. ERCP brush cytology will only produce a diagnosis in ~ 50% of pancreatic cancers. Differentiation between signs of chronic pancreatitis and pancreatic cancer can also be difficult with ERCP. ERCP is performed less commonly for diagnostic purposes and should now be reserved for the palliation of obstructive jaundice in patients with intractable itching, cholangitis, or unresectable cancer.

A reliable test to obtain tissue diagnosis is endoscopic ultrasound (EUS). EUS is the most sensitive and specific test for pancreatic cancer. It has a 99–100% detection rate for pancreatic cancer and EUS-guided core needle biopsy can be performed simultaneously. Vascular invasion by the tumor can also be delineated by EUS. Although EUS has a high detection rate for periampullary cancers, it is often unnecessary. The presentation is often pathognomonic with obstructive jaundice and a mass in the head of the pancreas or periampullary region. Biopsy adds little information if resection is planned. It is most useful in the setting of neoadjuvant therapy or palliative therapy when a tissue diagnosis is critical prior to treatment. EUS is also useful in the setting of cystic lesions. EUS aspiration can help differentiate mucinous and serous lesions, as mucin-containing lesions have malignant potential.

Positron emission tomography (PET) using the radiolabeled glucose analogue 18-fluorodeoxyglucose (FDG) has been suggested as a promising method for noninvasive differentiation between benign and malignant tissue (Avril *et al*., 1996; Strauss and Conti, 1991; Wahl *et al*., 1994). A drawback to PET scan is an association with false-positives in chronic pancreatitis. Some false-positive PET findings may be explained by nonspecific inflammatory reactions after diagnostic procedures such as ERCP and by stenting of the bile duct (Sendler *et al*., 2000).

CA19-9 is a laboratory modality that is frequently tested with the suspicion of pancreatic cancer. CA 19-9 is a tumor marker that was first used in the detection

of colon cancer, but was found to be sensitive for pancreatic cancer. Although it is not a screening tool for pancreatic cancer, in patients that have been found to have an undiagnosed pancreatic mass, the tumor marker provides important information. It is commonly used to monitor a patient's response to chemotherapy, radiation, and/or surgical treatment. Levels higher than 37 U/ml are considered abnormal and the higher the number, the more advanced the disease may be.

STAGING

The current American Joint Committee on Cancer (AJCC) TNM (tumor, nodes, metastasis) staging system for pancreatic cancer is currently the most widely accepted forum for staging of pancreatic cancer (Table 21.2). Stage I disease includes tumors localized to the pancreas without lymph node or distant metastasis. Stage II disease includes larger tumors with invasion into adjacent organs within the resection field. Patients with Stage I or II disease are considered resectable.

Patients with Stage III disease have locally advanced disease involving major vascular structures and are considered unresectable. Nearly two-thirds of patients with pancreatic cancer present with stage IV or metastatic disease defined as disease involving spread to distant organs such as the liver, lungs, or peritoneal surfaces

TABLE 21.2. American Joint Committee on Cancer (AJCC) pancreatic cancer staging, SEER historic staging, and technical resectability.

Primary tumor(P)

TX: Primary tumor cannot be assessed
T0: No evidence of primary tumor
Tis: Carcinoma *in situ*
T1: Tumor is limited to the pancreas and is 2 cm or less in greatest dimension
T2: Tumor is limited to the pancreas and is more than 2 cm in greatest dimension
T3: Tumor extends beyond the pancreas without involvement of the celiac axis or superior mesenteric artery
T4: Tumor involves the celiac axis or the superior mesenteric artery (unresectable primary tumor)

Regional lymph Nodes (N)

NX: Regional lymph nodes cannot be assessed
N0: No regional lymph node metastasis
N1: Regional lymph node metastasis

Distant metastasis (M)

MX: Distant metastasis cannot be assessed
M0: No distant metastasis
M1: Distant metastasis

AJCC staging groups	SEER historic staging	Resectability
Stage 0: Tis, N0, M0	Localized	Resectable
Stage IA: T1, N0, M0	Localized	Resectable
Stage IB: T2, N0, M0	Localized	Resectable
Stage IIA: T3, N0, M0	Regional	Resectable
Stage IIB: T1-3, N1, M0	Regional	Resectable
Stage III: T4, any N, M0	Regional	Unresectable
Stage IV: Any T , any N, M1	Distant	Unresectable

(Jemal *et al*., 2007; Riall *et al*., 2006b). One-third of patients present with stage I, II, or III (locoregional) disease.

The Surveillance, Epidemiology, and End Results (SEER) database uses historic staging which includes three categories: localized, regional, and distant pancreatic cancer. Localized pancreatic cancer includes stage 0 and I disease. It is defined as disease confined to the pancreas. Regional disease includes stage II and III pancreatic cancer. Stage II includes larger pancreatic cancers that may directly involve adjacent organs such as the duodenum, ampulla of Vater, distal bile duct, stomach, peripancreatic soft tissue, regional lymph nodes, portal vein, superior mesenteric vein, splenic artery, splenic vein, or spleen. Involvement of the celiac axis or superior mesenteric artery indicates a cancer stage III, which is classified as unresectable.

PANCREATICODUODENECTOMY

At the current time, surgical resection is the only hope for cure. Surgical resection is achieved via pancreaticoduodenectomy. This treatment involves the enbloc resection of the head of the pancreas, the duodenum, the gallbladder, with or without resection of the first portion of the gastric antrum, and the common bile duct (Figure 21.2). The extensive operation is required for cancer of the periampullary region due to the vascular supply. The vascular network of the pancreas and duodenum are interconnected to the degree that excision of one segment would likely lead to devascularization of the other. Pancreaticoduodenectomy was described by Alessandro Codivilla in 1898 and Kausch in 1912. Kausch performed the first successful pancreaticoduodenectomy and provided the surgical building blocks

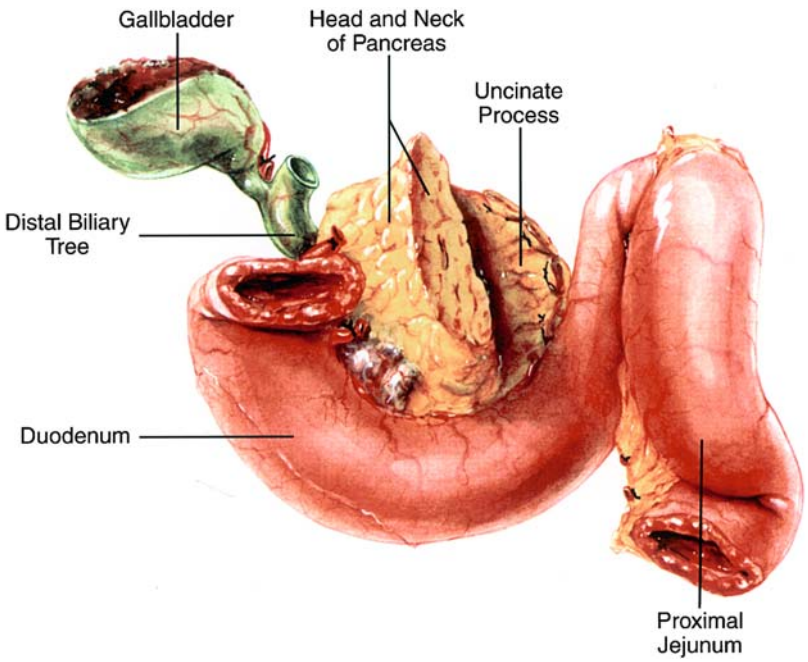

FIGURE 21.2. Pancreaticoduodenectomy specimen (with permission CAmeron JL. (1990). Atlas of Surgery, Volume 1. Toronto, B.C. Decter. p. 399)

for a successful operation. Allen Oldfather Whipple popularized the procedure in the 1930s. Mortality rates of > 25% and 5-year survival rates of < 5% led many surgeons to abandon this procedure in the 1960s and 1970s (Crile *et al*., 1970; Herter *et al*., 1982; Nakase *et al*., 1977). During the last 3 decades, the mortality following surgical resection has decreased to < 5%. The 5-year survival has improved significantly to 15–20% for pancreatic cancer, 20–25% for distal common bile duct cancer, 30–40% for ampullary cancer, and 50–60% for duodenal cancer (Cleary *et al*., 2004; Riall *et al*., 2006a; Sohn *et al*., 1998; Talamini *et al*., 1997; Winter *et al*., 2006).

A midline incision or bilateral subcostal incision is made to gain entry into the abdomen. A complete exploratory laparotomy is performed. Careful examination of the omentum and peritoneum is required to assess for possible metastatic disease. Suspicious lesions are sent for frozen section and if found to be cancerous, the operation is aborted. Enlarged lymph nodes should also be sent for frozen section, but the finding of cancer within lymph nodes in the planned resection field is not an indication for termination of the procedure. Inspection and palpation of the liver is important in the surgical evaluation of the abdomen to evaluate for liver metastasis. If there is a question of liver metastasis after palpation and visual inspection, intraoperative ultrasonography should be utilized. Liver metastasis is a contraindication to pancreaticoduodenectomy.

The hepatic flexure of the colon is first mobilized from its attachments to allow for visualization of the duodenum. A Kocher maneuver is performed to allow inspection of the duodenum, pancreas, and other retroperitoneal structures. The duodenum and the head of the pancreas are separated from their retroperitoneal attachments to create a plane for the palpation of the superior mesenteric artery and to evaluate for possible vascular invasion by the tumor. The gallbladder is removed from the gallbladder fossa at this time and the common bile duct is carefully dissected away from the portal structures and transected above the entry of the cystic duct. Division of the gastroduodenal artery allows for extended visualization and room for the dissection of the portal vein behind the pancreatic neck. After the left gastric and gastroepoploic vessels are divided in close approximation with the gastric wall, an antrectomy or pylorus preserving technique is performed. A pancreatic line of transection is determined based on tumor size. A Penrose drain is placed posterior to the neck of the pancreas and stay sutures are placed around the planned area of transection. Electrocautery is then used to slowly transect the pancreas. The ligament of Treitz is mobilized and the jejunum is transected with a stapler, ~ 10 cm past the ligament of Treitz. The last step in removal of the specimen from the abdomen is to divide branches from the uncinate process of the pancreas to the superior mesenteric artery and vein. This includes dissection of the lymphatics. Once the specimen is removed, metal clips at the tumor field margins should be placed in the event that focused radiation therapy is needed.

Pancreatic, biliary, and bowel reconstruction follows. The pancreaticojejunostomy is usually created in an end to side fashion and distal to this anastomosis an end to side hepaticojejunostomy is fashioned. The last step in bowel continuity is the gastro- or duodenojejunostomy anastomosis. Drains are placed in the abdomen

posterior to biliary and pancreatic anastomosis prior to abdominal closure. The drains help to identify biliary or pancreatic leaks that may occur (Figure 21.2).

In the early 1900s, Kausch (1912) and Whipple *et al*. (1935) reported pancreaticoduodenectomy resections involving pylorus preservation, but by the 1970s the majority of pancreaticoduodenectomies involved distal gastric resection. The change to distal gastrectomy was based on the premise that: (1) distal gastric resection led to better oncologic therapy, with obligate resection of the peripyloric and perigastric lymph nodes, (2) the need to resect the duodenum and proximal stomach because of close tumor proximity, and (3) the reduction in marginal ulceration at the site of gastrojejunostomy by performing antrectomy, thereby decreasing circulating gastrin levels and reducing acid secretion (Sohn *et al*., 1998). Through various studies, it has been shown that although distal gastric resection results in decreased delayed gastric emptying in the early postoperative period, there is no significant long term difference between pylorus preservation and distal gastrectomy in delayed gastric emptying, quality of life, or survival (Di Carlo *et al*., 1999; Mosca *et al*., 1997; Warshaw and Torchiana, 1985).

Tumor invasion of the superior mesenteric-portal vein (SMPV) confluence is often considered a contraindication to pancreaticoduodenectomy for patients with malignant tumors of the pancreas or periampullary region. Most centers report higher rates of positive margins in the retroperitoneal area. When positive margins are present after a pancreaticoduodenectomy is performed, there till remains a significant increase in survival when compared to palliative treatment. Studies conducted at M.D. Anderson Cancer Center indicate that SMPV resection and reconstruction can be safely performed with no increase in hospital stay, morbidity, mortality, tumor size, margin positivity, nodal positivity, or tumor DNA content (Fuhrman *et al*., 1996). These data suggest that venous involvement is a function of tumor location rather than an indicator of aggressive tumor biology. Tumor involvement of the SMA remains a contraindication to pancreaticoduodenectomy because of the high morbidity and mortality rates associated with arterial resection and reconstruction (Nagakawa *et al*., 1991; Sindelar, 1989).

SURVIVAL

In all localized periampullary cancer types, 5-year survival is improved with surgical resection. Winter *et al*. (2006) reviewed 1,423 patients that underwent pancreaticoduodenectomy for a malignancy originating in the pancreas. Using multivaritate regression, the most important predictors of long term survival included tumor diameter < 3 cm, negative lymph node status, negative resection margin status, well or moderately differentiated cancer, the absence of COPD, the absence of postoperative bile leak, and the administration of adjuvant therapy. Patients that demonstrated all of the above positive predictors of long term survival had a median survival of 44 months. The median survival for all patients with ductal adenocarcinoma was 18 months and 1, 2, and 3-year survival of 65%, 37%, and 18%, respectively.

In a recent, unpublished analysis of the SEER database, 58,735 patients with

periampullary adenocarcinomas were identified between 1988 and 2002. For the overall cohort, 48.9% of patients were male, 80.5% of patients were white, 11.2% were black, and 8.3% were other races. Mean age at presentation for all tumors was 69.6 ± 12.5 years. The distribution of tumor type was predominantly pancreatic in origin (n = 50,140; 85.3%) followed by bile duct type (n = 4,162; 7%), ampullary (n = 2,431; 4%) and duodenal (n = 2,002; 3.4%). At the time of diagnosis, the majority of periampullary cancers were found at an advanced stage. Only 35.9% of patients were found to have locoregional disease. The demographics and tumor characteristics by site of primary tumor are shown in Table 21.3. Patients with duodenal adenocarcinoma were younger (66.7 vs. 69–70 years for

TABLE 21.3. Demographics and tumor characteristics for entire cohort by tumor type.

	All groups	Pancreatic	Bile duct	Ampullary	Duodenum	P-value*
Age in years	69.6 ± 12.5	69.6 ± 12.3	70.9 ± 13.0	69.3 ± 13.2	66.7 ± 14.1	<0.0001
Gender (% Male)	48.9	48.4	50.2	52.7	52.3	<0.0001
Race						
White	80.5	81.0	80.2	80.1	69.7	<0.0001
Black						
Other						
Married (%)	53.7	53.4	54.2	57.4	54.9	0.0012
SEER region						
San Francisco-Oakland	9.7%	9.8%	8.5%	10.1%	9.3%	<0.0001
Connecticut	10.1%	10.3%	9.2%	9.2%	8.6%	
Metropolitan Detroit	11.9%	11.9%	11.7%	9.0%	14.0%	
Hawaii	3.3%	3.2%	4.3%	3.9%	3.7%	
Iowa	8.0%	8.1%	8.4%	7.6%	7.3%	
New Mexico	3.6%	3.7%	3.4%	3.6%	3.8%	
Seattle-Puget Sound	8.9%	9.0%	9.0%	7.1%	7.4%	
Utah	3.0%	3.0%	2.7%	2.9%	2.5%	
Metropolitan Atlanta	4.3%	4.3%	4.3%	4.0%	5.0%	
Alaska	0.2%	0.1%	0.3%	0.2%	0.2%	
San Jose-Monterey	3.3%	3.4%	2.8%	4.3%	1.9%	
Los Angeles	14.6%	14.1%	16.8%	18.7%	15.0%	
Rural Georgia	0.2%	0.2%	0.1%	0.1%	0.3%	
Greater California	8.9%	8.9%	9.1%	10.0%	8.3%	
Kentucky	2.1%	2.1%	2.3%	2.6%	2.5%	
Lousiana	2.7%	2.7%	2.3%	2.1%	3.5%	
New Jersey	5.2%	5.2%	4.8%	4.6%	6.7%	
Tumor Stage						
Locoregional	35.9%	31.9%	50.4%	74.8%	59.7%	<0.0001
Distant	46.6%	51.2%	22.3%	10.0%	24.4%	
Unstaged	17.5%	16.9%	27.2%	15.2%	15.8%	
Nodal Status						
Positive	18.7%	19.3%	6.2%	18.9%	26.3%	<0.0001
Negative	25.0%	22.9%	33.5%	38.1%	44.4%	
Unknown	56.3%	57.8%	60.3%	43.0%	29.3%	
Percent Resected	14.0%	11.5%	19.3%	38.8%	35.9%	<0.0001

*Chi-square p-value for overall differences among all four groups

other tumor types, $P < 0.0001$) and less likely to be white (69.7% vs. ~ 80% for other tumor types, $P < 0.0001$). The distribution by SEER region differed slightly for each tumor type. Only 31.9% of patients with pancreatic cancer had locoregional disease at the time of resection, while 50.4% of patients with bile duct cancer, 59.8% of patients with ampullary cancer, and 74.8% of patients with duodenal cancer presented with locoregional disease (Table 21.3, $P < 0.0001$). In addition, patients with bile duct cancer were more likely to have unstaged disease than patients with other types of periampullary adenocarcinomas. Similarly, patients with bile duct cancer were most likely to have unknown lymph node status, consistent with unstaged tumors. The positive, negative, and unknown status of lymph nodes for each tumor type is shown in Table 21.2. However, these data are more meaningful for resected patients and are shown later. The overall survival for each tumor type is shown in Figure 21.3-A. Actuarial 5-year survival for resected locoregional pancreatic cancer was found to be 17.2% and unresected locoregional pancreatic cancer had a 5-year survival rate of 2.3% (Figure 21.3B). Five-year survival was also increased in patients that underwent surgical resection versus unresected locoregional bile duct cancer (22.9% vs. 7.2%), ampullary cancer (35.7% vs. 22.7%), and duodenal cancer (58.1% vs. 27.1%) (Figures 21.3C–E).

Many studies have reported actuarial 5-year survival data after pancreaticoduodenectomy for periampullary adenocarcinoma, but a recent study evaluates actual 5-year survival and the subsequent 10-year survival in patients surviving 5 years after initial surgery (Riall *et al*., 2006a). The 5-year actuarial survival rates in this study were 55% for pancreatic, 74% for bile duct, 66% for ampullary, and 85% for duodenal cancer. Similar rates were found in the SEER analysis. When patients attain 5-year survival after resection for pancreatic adenocarcinoma, there is a favorable outcome for the subsequent 5 years; 65% of initial 5-year survivors lived for another 5 years, bringing them to a 10-year post resection landmark. Positive predictors for the 201 patients who survived 5 years or longer included a younger age at diagnosis, negative margins, negative lymph node status, and well differentiated tumors. Adjuvant therapy was not associated with an increase in survival in this study.

ADJUVANT THERAPY

Adjuvant therapy involves the use of chemotherapeutic agents and radiation in the postoperative period. There is still much debate upon the best adjuvant therapy in the treatment of pancreatic cancer. 5-Fluorouricil (5-FU) has been the clinical chemotherapeutic treatment for pancreatic cancer for several years. The Gastrointestinal Tumor Study Group (GITSG) was a prospective, randomized trial which used split course irradiation with concurrent bolus 5-FU, followed by maintenance 5-FU for a duration of up to 2 years (Kalser and Ellenberg, 1985). The trial showed a survival advantage for adjuvant chemoradiotherapy (median survival 20 months) in comparison to surgery alone (median survival 11 months). The GITSG was the first trial to document a survival advantage in pancreatic adenocarcinoma. Several other studies have confirmed the improved survival with modification

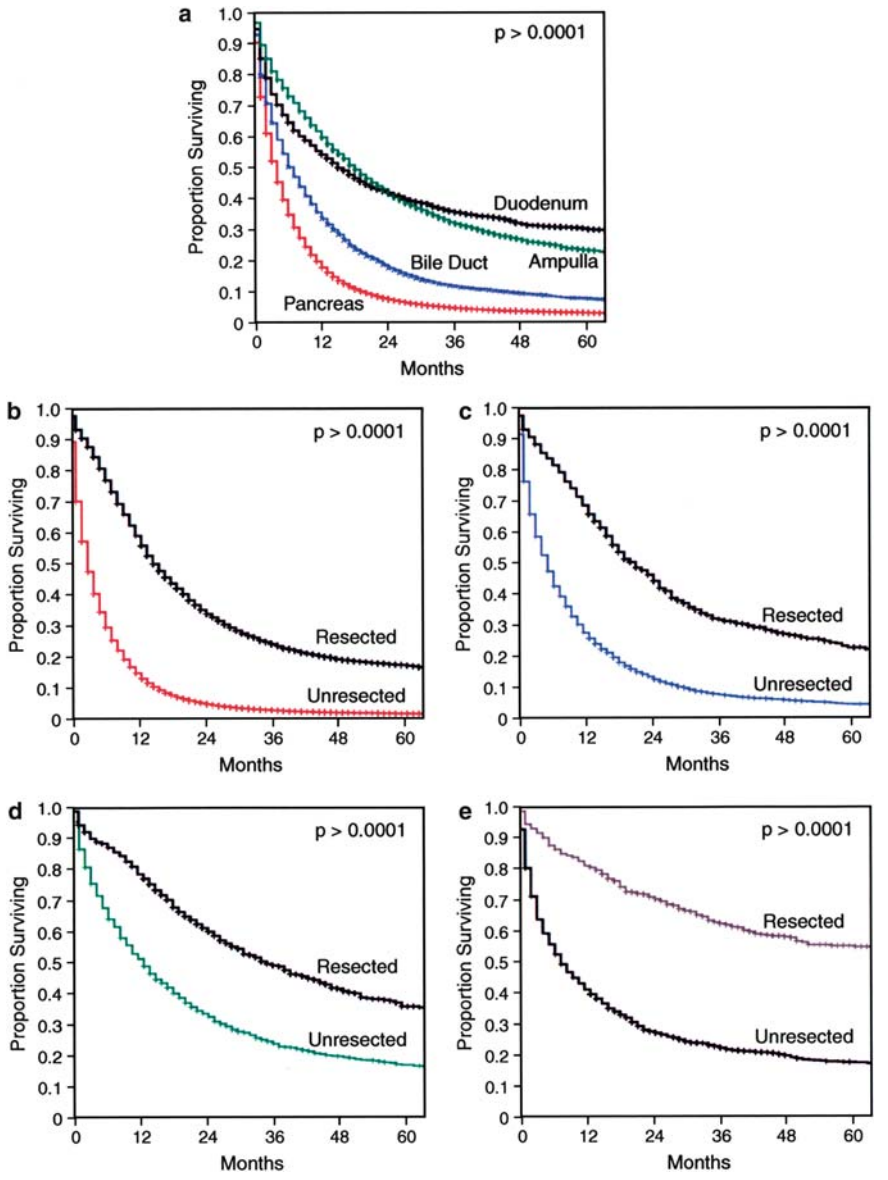

FIGURE 21.3 (a) The Kaplan-Meier actuarial 5-year survival by site of tumor origin for the cohort of 58,735 patients with periampullary cancer (includes resected and unresected patients). Pancreatic cancer (n = 50,140) shown in red; bile duct cancer (n = 4,162), shown in blue; ampullary cancer (n = 2,431) shown in green; duodenal cancer (n = 2,002), shown in black. The 5-year actuarial survival rates: 3.2% for pancreas, 7.8% for bile duct, 23.3% for ampulla, and 30.0% for duodenum. (b). Kaplan-Meier actuarial survival for resected and unresected patients with locoregional pancreatic cancer. Resected patients are shown in black (n = 4,925) with a 5-year survival rate of 17.2%, unresected patients are shown in red (n = 11,070, p-value < 0.0001) with a 5-year survival rate of 2.3%. (c) Kaplan-Meier actuarial survival for resected and unresected patients with locoregional bile duct cancer. Resected patients are shown in black (n = 730) with a 5-year survival rate of 22.9%, unresected patients are shown in green (n = 1,369, p-value < 0.0001) with a 5-year survival rate of 7.2%. (d) Kaplan-Meier actuarial survival for resected and unresected patients with locoregional ampullary cancer. Resected patients are shown in black (n = 911) with a 5-year survival rate of 35.7%, unresected patients are shown in green (n = 907, p-value < 0.0001) with a 5-year survival rate of 22.7%. (e) Kaplan-Meier actuarial survival for resected and unresected patients with locoregional duodenal cancer. Resected patients are shown in gray (n = 629) with a 5-year survival rate of 58.1%, unresected patients are shown in black (n = 568, p-value < 0.0001) with a 5-year survival rate of 27.1%.

of the amount and cycles of 5-FU and radiotherapy for pancreatic cancer (Kalser and Ellenberg, 1985; Whittington *et al*., 1991; Yeo *et al*., 1997). Currently, chemoradiation is considered the standard of care in the United States.

The European Study Group for Pancreatic Cancer (ESPAC) was designed to test whether postoperative treatment with 5-FU chemoradiotherapy, 5-FU chemotherapy alone, chemoradiotherapy and chemotherapy, or observation would result in a significant difference in survival. It is currently the largest randomized clinical study investigating chemoradiotherapy in pancreatic cancer (Neoptolemos *et al*., 2004). The median survival for patients in the chemotherapy group was 19.7 months versus 14.0 months for the no-chemotherapy group. The median survival for the chemoradiation group was 15.5 months versus 16.1 months for the no-chemoradiation, which was not statistically significant (Chu *et al*., 2003). There are currently ESPAC trials being conducted to investigate the effect of gemcitabine and radiation therapy on survival, but to date chemotherapy alone is considered the standard of care in European countries.

NEOADJUVANT THERAPY

A drawback of adjuvant therapy is that ~ 20–30% of patients who undergo pancreaticoduodenectomy do not receive postoperative chemoradiation (Spitz *et al*., 1997; Yeo *et al*., 1997). A few of the arguments for neoadjuvant use of chemoradiation are: neoadjuvant therapy provides systemic treatment within days of diagnosis, patients undergo systemic therapy prior to pancreatic resection, and are, therefore, more likely to complete their therapy and less likely to have complications or delays associated with being in the early postoperative period. Neoadjuvant therapy might decrease the risk of disseminating microscopic tumor during resection and also result in fewer positive margins, and radiation therapy generally is more effective as well. The concerns of neoadjuvant therapy are the risk of making the surgery more difficult because of an irradiated field and the possibility that a resectable patient may progress during the course of therapy and miss the 'window of opportunity' for curative resection. Prior to neoadjuvant therapy a tissue diagnosis is required.

Recent studies suggest that neoadjuvant chemoradiation can downstage locally advanced pancreatic tumors, but a large randomized prospective trial has not been performed. Most current studies agree that although chemoradiation is associated with improved overall survival in locally advanced disease, it rarely leads to surgical "downstaging" allowing for potentially curative pancreatic resections (Kim *et al*., 2002). Chemoradiation therapy prior to pancreatic cancer surgery is still clinically debated and at the current time chemoradiation is most commonly given postoperatively. At this time, there are no prospectively randomized studies for neoadjuvant therapy, but the Interdisciplinary Study Group of Gastrointestinal Tumours of the German Cancer Aid is investigating the effect of neoadjuvant chemoradiation in locally resectable and probable respectable cancer of the pancreatic head on overall survival compared to surgery alone (Brunner *et al*., 2007). This trial also analyzes adjuvant chemotherapy. If the hypothesis that neoadjuvant chemoradiation leads to improved survival proves true, this

would be the first prospective, randomized clinical trial to establish a role for neoadjuvant chemotherapy in the treatment of pancreatic cancer.

UNDERUTILIZATION OF SURGICAL RESECTION

A review of the SEER data indicates that surgical resection for pancreatic cancer is underutilized in comparison with other periampullary cancers. In a recent analysis of the SEER database, 31.9% of patients with pancreatic cancer had locoregional disease at the time of presentation, while 50.4% of patients with bile duct cancer, 59.8% of patients with ampullary cancer, and 74.8% of patients with duodenal cancer presented with locoregional disease. For patients with locoregional disease, ampullary and duodenal cancers were more likely to be resected (50.1% and 52.6% respectively) than patients with pancreatic (30.8%) and distal bile duct (34.8%) cancer. Pancreatic cancer was the least likely of the periampullary locoregional cancers to be resected, with only 30.8% undergoing resection.

While we continue to strive for earlier diagnostic techniques and improved therapy, we can improve outcomes in patients with periampullary cancer by maximizing surgical resection rates. Recent studies show that surgical resection is underutilized in patients with pancreatic and other periampullary cancers. In the SEER database, the percentage of patients undergoing curative resection for pancreatic cancer increased from 19% in 1988 to 30% in 2001 ($p < 0.0001$) However, fewer than 1/3 of patients with locoregional pancreatic cancer underwent surgical resection (Riall *et al*., 2006b). A recent study using the National Caner Database (NCDB) shows similar findings (Bilimoria *et al*., 2007). Bilimoria *et al*. (2007) evaluated 9,559 patients with clinical stage I (T1-2N0M0) disease. Only 28.6% of patients with stage I disease underwent cancer-directed surgery. This difference may be explained by the fact that duodenal and ampullary cancers may be treated more aggressively due to their increased 5-year survival post resection. Pancreatic cancer does see an increase in survival after resection, but the result is not as profound as the survival for duodenal and ampullary cancers. This may lead some surgeons and physicians not to explore the option of surgical resection for locoregional pancreatic cancer. It is our hope that making this information available will lead to a change in attitude towards pancreatic resection.

REFERENCES

Avril, N., Dose, J., Janicke, F., Bense, S., Ziegler, S., Laubenbacher, C., Romer, W., Pache, H., Herz, M., Allgayer, B., Nathrath, W., Graeff, H., and Schwaiger, M. 1996. Metabolic characterization of breast tumors with positron emission tomography using F-18 fluorodeoxyglucose. *J. Clin. Oncol. 14*: 1848–1857.

Bilimoria, K. Y., Bentrem, D. J., Ko, C. Y., Stewart, A. K., Winchester, D. P., and Talamonti, M. S. 2007. National failure to operate on early stage pancreatic cancer. *Ann Surg. 246*: 173–180.

Bronstein, Y. L., Loyer, E. M., Kaur, H., Choi, H., David, C., DuBrow, R. A., Broemeling, L. D., Cleary, K. R., and Charnsangavej, C. 2004. Detection of small pancreatic tumors with multiphasic helical CT. *A.J.R. Am. J. Roentgenol. 182*: 619–623.

Brunner, T. B., Grabenbauer, G. G., Meyer, T., Golcher, H., Sauer, R., and Hohenberger, W. 2007. Primary resection versus neoadjuvant chemoradiation followed by resection for locally resectable or potentially resectable pancreatic carcinoma without distant metastasis: a multicentre prospectively randomised phase II-study

of the interdisciplinary working group gastrointestinal tumours (AIO, ARO, and CAO). *B.M.C. Cancer 7*: 41.

Catalano, C., Laghi, A., Fraioli, F., Pediconi, F., Napoli, A., Danti, M., Reitano, I., and Passariello, R. 2003. Pancreatic carcinoma: the role of high-resolution multislice spiral CT in the diagnosis and assessment of resectability. *Eur. Radiol. 13*: 149–156.

Chapman, R. W. 1999. Risk factors for biliary tract carcinogenesis. *Ann. Oncol. 10 Suppl 4*: 308–311.

Chow, W. H., Linet, M. S., McLaughlin, J. K., Hsing, A. W., Chien, H. T., and Blot, W. J. 1993. Risk factors for small intestine cancer. *Cancer Causes Control. 4*: 163–169.

Chu, Q. D., Khushalani, N., Javle, M. M., Douglass, H. O., Jr., and Gibbs, J. F. 2003. Should adjuvant therapy remain the standard of care for patients with resected adenocarcinoma of the pancreas? *Ann. Surg. Oncol. 10*: 539–545.

Cleary, S. P., Gryfe, R., Guindi, M., Greig, P., Smith, L., Mackenzie, R., Strasberg, S., Hanna, S., Taylor, B., Langer, B., and Gallinger, S. 2004. Prognostic factors in resected pancreatic adenocarcinoma: analysis of actual 5-year survivors. *J. Am. Coll. Surg. 198*: 722–731.

Crile, G., Jr., Isbister, W. H., and Hawk, W. A. 1970. Carcinoma of the ampulla of Vater and the terminal bile and pancreatic ducts. *Surg. Gynecol. Obstet. 131*: 1052–1054.

Dayton, M. T., Longmire, W. P., Jr., and Tompkins, R. K. 1983. Caroli's disease: a premalignant condition? *Am. J. Surg. 145*: 41–48.

Delaunoit, T., Neczyporenko, F., Limburg, P. J., and Erlichman, C. 2005. Pathogenesis and risk factors of small bowel adenocarcinoma: a colorectal cancer sibling? *Am. J. Gastroenterol. 100*: 703–710.

Di Carlo, V., Zerbi, A., Balzano, G., and Corso, V. 1999. Pylorus-preserving pancreaticoduodenectomy versus conventional whipple operation. *World J. Surg. 23*: 920–925.

Fuhrman, G. M., Leach, S. D., Staley, C. A., Cusack, J. C., Charnsangavej, C., Cleary, K. R., El-Naggar, A. K., Fenoglio, C. J., Lee, J. E., and Evans, D. B. 1996. Rationale for en bloc vein resection in the treatment of pancreatic adenocarcinoma adherent to the superior mesenteric-portal vein confluence. Pancreatic Tumor Study Group. *Ann. Surg. 223*: 154–162.

Herter, F. P., Cooperman, A. M., Ahlborn, T. N., and Antinori, C. 1982. Surgical experience with pancreatic and periampullary cancer. *Ann. Surg. 195*: 274–281.

Jagelman, D. G., DeCosse, J. J., and Bussey, H. J. 1988. Upper gastrointestinal cancer in familial adenomatous polyposis. *Lancet 1*: 1149–1151.

Jemal, A., Siegel, R., Ward, E., Murray, T., Xu, J., and Thun, M. J. 2007. Cancer statistics. 2007. *CA Cancer J. Clin. 57*: 43–66.

Kadmon, M., Tandara, A., and Herfarth, C. 2001. Duodenal adenomatosis in familial adenomatous polyposis coli: a review of the literature and results from the Heidelberg Polyposis Register. *Int. J. Colorectal Dis. 16*: 63–75.

Kalser, M. H., and Ellenberg, S. S. 1985. Pancreatic cancer: adjuvant combined radiation and chemotherapy following curative resection. *Arch. Surg. 120*: 899–903.

Kausch, W. 1912. Carcinoma of the duodenal papilla and its radical excision [Das Carcinom der Papilla duodeni und seine radikale Entfernung]. *Beitrage zur Klinischen Chirurgie 78*: 439–486.

Kim, H. J., Czischke, K., Brennan, M. F., and Conlon, K. C. 2002. Does neoadjuvant chemoradiation downstage locally advanced pancreatic cancer? *J. Gastrointest. Surg. 6*: 763–769.

Lipsett, P. A., Pitt, H. A., Colombani, P. M., Boitnott, J. K., and Cameron, J. L. 1994. Choledochal cyst disease: a changing pattern of presentation. *Ann. Surg. 220*: 644–652.

Mecklin, J. P., Jarvinen, H. J., and Virolainen, M. 1992. The association between cholangiocarcinoma and hereditary nonpolyposis colorectal carcinoma. *Cancer 69*: 1112–1114.

Mortele, K. J., Ji, H., and Ros, P. R. 2002. CT and magnetic resonance imaging in pancreatic and biliary tract malignancies. *Gastrointest. Endosc. 56*: S206–S212.

Mosca, F., Giulianotti, P. C., Balestracci, T., Di Candio, G., Pietrabissa, A., Sbrana, F., and Rossi, G. 1997. Long-term survival in pancreatic cancer: pylorus-preserving versus Whipple pancreatoduodenectomy. *Surgery 122*: 553–566.

Nagakawa, T., Konishi, I., Ueno, K., Ohta, T., Akiyama, T., Kanno, M., Kayahara, M., and Miyazaki, I. 1991. The results and problems of extensive radical surgery for carcinoma of the head of the pancreas. *Jpn. J. Surg. 21*: 262–267.

Nakase, A., Matsumoto, Y., Uchida, K., and Honjo, I. 1977. Surgical treatment of cancer of the

pancreas and the periampullary region: cumulative results in 57 institutions in Japan. *Ann. Surg. 185*: 52–57.

Neoptolemos, J. P., Stocken, D. D., Friess, H., Bassi, C., Dunn, J. A., Hickey, H., Beger, H., Fernandez-Cruz, L., Dervenis, C., Lacaine, F., Falconi, M., Pederzoli, P., Pap, A., Spooner, D., Kerr, D. J., and Buchler, M. W. 2004. A randomized trial of chemoradiotherapy and chemotherapy after resection of pancreatic cancer. *N. Engl. J. Med. 350*: 1200–1210.

Riall, T. S., Cameron, J. L., Lillemoe, K. D., Winter, J. M., Campbell, K. A., Hruban, R. H., Chang, D., and Yeo, C. J. 2006a. Resected periampullary adenocarcinoma: 5-year survivors and their 6- to 10-year follow-up. *Surgery 140*: 764–772.

Riall, T. S., Nealon, W. H., Goodwin, J. S., Zhang, D., Kuo, Y. F., Townsend, C. M., Jr., and Freeman, J. L. 2006b. Pancreatic cancer in the general population: Improvements in survival over the last decade. *J. Gastrointest. Surg. 10*: 1212–1223; discussion 1223–1214.

Sendler, A., Avril, N., Helmberger, H., Stollfuss, J., Weber, W., Bengel, F., Schwaiger, M., Roder, J. D., and Siewert, J. R. 2000. Preoperative evaluation of pancreatic masses with positron emission tomography using 18F-fluorodeoxyglucose: diagnostic limitations. *World J. Surg. 24*: 1121–1129.

Sindelar, W. F. 1989. Clinical experience with regional pancreatectomy for adenocarcinoma of the pancreas. *Arch. Surg. 124*: 127–132.

Sohn, T. A., Lillemoe, K. D., Cameron, J. L., Pitt, H. A., Kaufman, H. S., Hruban, R. H., and Yeo, C. J. 1998. Adenocarcinoma of the duodenum: factors influencing long-term survival. *J. Gastrointest. Surg. 2*: 79–87.

Spitz, F. R., Abbruzzese, J. L., Lee, J. E., Pisters, P. W., Lowy, A. M., Fenoglio, C. J., Cleary, K. R., Janjan, N. A., Goswitz, M. S., Rich, T. A., and Evans, D. B. 1997. Preoperative and postoperative chemoradiation strategies in patients treated with pancreaticoduodenectomy for adenocarcinoma of the pancreas. *J. Clin. Oncol. 15*: 928–937.

Strauss, L. G., and Conti, P. S. 1991. The applications of PET in clinical oncology. *J. Nucl. Med. 32*: 623–648; discussion 649–650.

Tada, M., Yokosuka, O., Omata, M., Ohto, M., and Isono, K. 1990. Analysis of ras gene mutations in biliary and pancreatic tumors by polymerase chain reaction and direct sequencing. *Cancer 66*: 930–935.

Talamini, M. A., Moesinger, R. C., Pitt, H. A., Sohn, T. A., Hruban, R. H., Lillemoe, K. D., Yeo, C. J., and Cameron, J. L. 1997. Adenocarcinoma of the ampulla of Vater: a 28-year experience. *Ann. Surg. 225*: 590–599; discussion 599–600.

Tersmette, A. C., Petersen, G. M., Offerhaus, G. J., Falatko, F. C., Brune, K. A., Goggins, M., Rozenblum, E., Wilentz, R. E., Yeo, C. J., Cameron, J. L., Kern, S. E., and Hruban, R. H. 2001. Increased risk of incident pancreatic cancer among first-degree relatives of patients with familial pancreatic cancer. *Clin. Cancer. Res. 7*: 738–744.

Wahl, R. L., Hawkins, R. A., Larson, S. M., Hendee, W. R., Coleman, R. E., Holden, R. W., Frick, M. P., Gatsonis, C., Brown, G. S., and Shtern, F. 1994. Proceedings of a National Cancer Institute workshop: PET in oncology–a clinical research agenda. *Radiology 193*: 604–606.

Warshaw, A. L., and Torchiana, D. L. 1985. Delayed gastric emptying after pylorus-preserving pancreaticoduodenectomy. *Surg. Gynecol. Obstet. 160*: 1–4.

Watanapa, P. 1996. Cholangiocarcinoma in patients with opisthorchiasis. *Br. J. Surg. 83*: 1062–1064.

Watanapa, P., and Watanapa, W. B. 2002. Liver fluke-associated cholangiocarcinoma. *Br. J. Surg. 89*: 962–970.

Whipple, A. O., Parsons, W. B., and Mullins, C. R. 1935. Treatment of carcinoma of the ampulla of Vater. *Ann. Surg. 102*: 763–779.

Whittington, R., Bryer, M. P., Haller, D. G., Solin, L. J., and Rosato, E. F. 1991. Adjuvant therapy of resected adenocarcinoma of the pancreas. *Int. J. Radiat. Oncol. Biol. Phys. 21*: 1137–1143.

Wilentz, R. E., Iacobuzio-Donahue, C. A., Argani, P., McCarthy, D. M., Parsons, J. L., Yeo, C. J., Kern, S. E., and Hruban, R. H. 2000. Loss of expression of Dpc4 in pancreatic intraepithelial neoplasia: evidence that DPC4 inactivation occurs late in neoplastic progression. *Cancer Res. 60*: 2002–2006.

Winter, J. M., Cameron, J. L., Campbell, K. A., Arnold, M. A., Chang, D. C., Coleman, J., Hodgin, M. B., Sauter, P. K., Hruban, R. H., Riall, T. S., Schulick, R. D., Choti, M. A., Lillemoe, K. D., and Yeo, C. J. 2006. 1423 pancreaticoduodenectomies for pancreatic

cancer: a single-institution experience. *J. Gastrointest. Surg. 10*: 1199–1210; discussion 1210–1191.

Yeo, C. J., Abrams, R. A., Grochow, L. B., Sohn, T. A., Ord, S. E., Hruban, R. H., Zahurak, M. L., Dooley, W. C., Coleman, J., Sauter, P. K., Pitt, H. A., Lillemoe, K. D., and Cameron, J. L. 1997. Pancreaticoduodenectomy for pancreatic adenocarcinoma: postoperative adjuvant chemoradiation improves survival: a prospective, single-institution experience. *Ann. Surg. 225*: 621–633; discussion 633–626.

22
Unresectable Locally Advanced Pancreatic Cancer: Concurrent Chemotherapy

Ender Kurt, Meral Kurt, Turkkan Evrensel, Lutfi Ozkan, and Osman Manavoglu

INTRODUCTION

Pancreatic cancer (PC) is one of the most troublesome solid tumors, and remains a major challenge to oncologists. Approximately 40% of patients with PC present with locally advanced disease, and generally the treatment of this situation is not curative. Locally advanced PC (LAPC) is commonly defined as the tumor invading the celiac axis, superior mesenteric artery, inferior vena cava, aorta, or the encasement or occlusion of the superior mesenteric vein-portal vein confluence. The most common clinical evaluations for the determination of disease extension are obtained from the computed tomography scan and magnetic resonance imaging of the abdomen, endoscopic ultrasound with fine needle aspiration biopsy, angiography, and endoscopic retrograde cholangiopancreatography. Being an effective diagnostic intervention, 18-fluorodeoxyglucose-positron emission tomography gives additional information on the findings of these more conventional examinations. More invasive diagnostic utilities, such as laparoscopy and laparoscopic ultrasonography, may be helpful in selected cases, which are able to show the hepatic and peritoneal dissemination as well as the vascular invasion of a pancreatic tumor more accurately (Russo *et al*., 2007).

TREATMENT OF LOCALLY ADVANCED PANCREATIC CANCER

The optimal treatment of LAPC is still being debated. However, concurrent administration of chemotherapy (CT) and radiotherapy (RT) is generally accepted as the standard treatment for patients with unresectable LAPC, based on the results of the several randomized studies. The effectiveness of chemoradiotherapy (CRT) was first demonstrated in a landmark study by Moertel *et al*. (1969) from the Mayo Clinic, in which patients with locally advanced gastrointestinal cancer were randomized to receive either RT (35–40 Gy) alone or with 5-fluorouracil (5-FU). The study demonstrated a statistically meaningful positive effect of concurrent CRT over RT alone in terms of median survival. This study was followed by a number of studies that started to define the exact role of CRT in LAPC. In the Gastrointestinal Tumor Study Group (GITSG) trial

(Moertel *et al*., 1981), patients with LAPC were randomized into three arms; high-dose irradiation alone (60 Gy, split course), moderate-dose irradiaton (40 Gy, split course) plus 5-FU, and high-dose irradiation plus 5-FU. The patients in the combined-modality arms received several months of maintenance 5-FU after CRT. Both moderate-dose RT plus 5-FU and high-dose RT plus 5-FU groups had similar survival rates, which were significantly better than those from irradiation therapy alone. The study, therefore, confirmed the superiority of CRT over RT alone. Another GITSG trial compared concurrent bolus 5-FU and RT (54 Gy) followed by adjuvant SMF (streptozotocin, mitomycin-C, 5-FU) to the same CT alone, and showed the difference for survival in favor of the combined-modality treatment (GITSG, 1988). Subsequent reports, as well as meta-analyses, confirmed the fact that CRT improves upon the survival rates achieved by best supportive care or RT alone (Yip *et al*., 2006; Sultana *et al*., 2007). In an attempt to investigate the effectiveness of the other chemotherapeutic agents, doxorubicin was compared with 5-FU; both were given with 60 Gy split course of RT in unresectable, LAPC in a study by GITSG (1985). The study showed that survival times were similar in both groups, but the doxorubicin group exhibited unacceptable treatment-related toxicities.

The above-mentioned studies made 5-FU-based concurrent CRT the most widely used treatment modality in the treatment of LAPC. On the other hand, there are some contradictory reports in the literature, in particular when CRT or CT alone has been compared in locally advanced disease. An Eastern Oncology Group (ECOG) study that was reported by Klaassen *et al*. (1985), in which RT (40 Gy) plus 5-FU (600 mg/m^2/day for 3 days in week one of the RT) was compared 5-FU alone (600 mg/m^2, weekly) in patients with locally advanced gastrointestinal cancer, suggested that concurrent 5-FU-based CRT and 5-FU alone have equal efficacy with respect to time to progression and median survival of the patients. In fact, as stated in a meta-analysis by Yip *et al*. (2006), there is no clear evidence to propose CRT as a distinctly superior treatment modality over CT, and there is still a need to perform well-designed, randomized studies comparing CRT and CT. However, presently most authors agree that CT alone is a suboptimal treatment that has to be reserved for unfit patients only, and CRT should be added into the treatment schedule for LAPC (Mancuso *et al*., 2006). In support of this belief, a recent retrospective analysis by Huguet *et al*. (2007) delineated that concurrent CRT given after initial CT improves survival in patients with LAPC compared to those who received CT alone. Actually, the majority of the reports regarding the treatment of LAPC have consistently pointed out the importance of CRT in this situation, although the best schedule for the integrating of EBRT and CT remains to be elucidated. Taken together, it is conceivable to recommend the use of CRT in LAPC. Additionally, the question is not whether EBRT should be added to CT, but rather how.

Radiotherapy

With regard to RT, external-beam RT techniques using high-energy photons with conventional fractionation are usually employed in PC. A typical protocol delivers a total dose of 45–50.4 Gy in

1.8 Gy daily fractions (5 days per week) to gross tumor plus regional lymphatics with a usual 2–3 cm margin using three or four fields. These are followed by a boost dose delivered to gross tumor only with 1–2 cm margin. The stomach, small intestine, liver, kidneys, and spinal cord are the main dose-limiting organs in patients with LAPC receiving RT (Calvo *et al*., 2004; Wilkowski *et al*., 2005). Therefore, a computed tomography-based treatment plan is required to minimize the irradiation exposure to these adjacent organs, which yields lower treatment-related toxicities, and permits the application of effective irradiation doses on the involved sites. During the last few decades, conformal RT techniques such as three-dimensional RT, intensity-modulated RT (IMRT), and stereotactic RT have increasingly been studied in many tumors, including LAPC. These modalities allow more precise application of irradiation and optimization of the dose intensity onto specific target volumes while sparing the doses to critical normal structures. The use of IMRT in the treatment of LAPC conferred lower acute and chronic treatment-related toxicities with no increase in loco-regional failures, despite highly conformal radiation treatment (Milano *et al*., 2004).

Apart from the conventional fractionation schedule, altered fractionations have also been examined in PC. With hypofractionation, higher daily fraction dose of irradiation is given one to three times per week for a shorter treatment period than conventional fractionation. With hyperfractionation, the total dose and the total daily dose of irradiation are higher than conventional fractionation by using smaller per fraction dose for two times a day. Hence, ~ 10–15% more irradiation doses can be delivered compared to standard fractionations. In PC, it has been reported by Ashamalla *et al*. (2003) that hyperfractionated RT (63.8 Gy) and concurrent weekly paclitaxel with a maximum tolerated dose (MTD) of $60\,mg/m^2/week$ was an active regimen, and needed to be explored in further trials. To date, there is no randomized study showing that altered fractionations are associated with better survival rates in patients with LAPC compared with the use of conventional fractionation.

To improve local control rates, specialized irradiation techniques, including interstitial brachytherapy with Iodine-125 and palladium-103, intraoperative electrons alone, or in combination with external-beam RT (EBRT) as a boost dose, have been introduced into the treatment of LAPC. Generally, the application of these modalities revealed increased local control rates, but at the cost of increased procedure-related toxicities, and with no impact on overall survival (Calvo *et al*., 2004; Dobelbower *et al*., 1986; Mohiuddin *et al*., 1988). An important question is whether or not higher local control rates, which would be best achieved with minimal morbidity by recent conformal RT techniques, are associated with improved survival. In a phase II study by Koong *et al*. (2005), the efficacy of concurrent CRT consisting of IMRT (45 Gy) plus 5-FU followed by a 25 Gy stereotactic radiosurgery boost was examined in patients with LAPC. Albeit the results concerning local control were promising, the median overall survival was only 33 weeks, and most patients succumbed to the occurrence of distant metastasis. Accordingly, it is apparent that the higher RT doses (> 50.4 Gy) to tumor delivered via specialized irradiation

techniques may improve local control, but overall survival is unlikely to be affected by this approach, because PC has a tendency towards the development of systemic metastases, which justifies the application of more effective systemic therapies. However, considering the increased local control rates obtained by these modalities, the small but unresectable or marginally resectable tumors may particularly benefit from the use of specialized irradiation techniques (Russo *et al*., 2007).

Concurrent Chemotherapy

The most frequently used concurrent chemotherapeutic agent during the course of RT for LAPC is 5-FU, which has been extensively studied, and has been demonstrated to be effective in many randomized trials as summarized earlier. In fact, there are many different ways to administer 5-FU in this situation; a protracted intravenous infusion at the doses of 200–250 mg/m^2/day during the entire RT course, continuous intravenous infusion at the dose of 300 mg/m^2/day, 5 days per week, or 500 mg/m^2/day intravenous bolus given on the first and last 3 days of RT. Among these schedules, protracted intravenous infusion has gained a wide acceptance by most practitioners, although there has been no randomized study comparing protracted intravenous infusion with intravenous bolus administration. However, a retrospective study by Poen *et al*. (1998) showed that concurrent CRT with protracted intravenous infusion of 5-FU was better tolerated, and permitted more CT and RT dose intensity when compared to intravenous bolus administration.

Given the fact that the impact of 5-FU-based CRT on the outcome of patients with LAPC is modest and distant metastases are the major causes of treatment failures, attempts have been directed toward the development of different CRT regimens exhibiting more systemic activity. For this purpose, various modalities, such as substitution of another effective drug instead of 5-FU for concurrent treatment, using a number of CT cycles before and/or after CRT, using a combination CT regimen during RT, and the application of the targeted therapies into the CRT, have been investigated in LAPC.

Gemcitabine has become the most attractive agent for concurrent CRT after its beneficial effects were observed in patients with advanced stage PC in an important randomized study by Burris *et al*. (1997). Along with the cytotoxic activity, gemcitabine also has radiosensitizing properties in PC (Lawrence *et al*., 1996). In concurrent treatment of LAPC, gemcitabine has been administered in different ways and schedules, none of which are considered a standard approach. While various doses and schedules have been examined in many trials, weekly and twice weekly doses as 30-min intravenous infusion are usually preferred. With conventionally fractionated RT, the MTD of twice weekly gemcitabine was documented to be 40 mg/m^2 in a phase I study by Blackstock *et al*. (1999). Weekly doses between 200 to 600 mg/m^2 have been used in different trials. In general, the clinical efficacy obtained by the use of gemcitabine-based CRT has been comparable to those achieved by 5-FU-based CRT. Presently, there has been no randomized study comparing gemcitabine-based CRT with protracted intravenous infusional 5-FU-based CRT in LAPC, although a small randomized study suggested that

gemcitabine-based approach was more effective than bolus 5-FU-based CRT (Li *et al*., 2003).

The major obstacle for using gemcitabine as a concurrent agent with RT is the toxicity of the treatment. Indeed, the therapeutic index of concurrent gemcitabine-based CRT is very narrow, and severe gastrointestinal toxicities may occur, especially if uninvolved regional lymphatics are included in the RT target volume (Crane *et al*., 2002). Several factors contribute to the development of the toxicities resulting from concurrent gemcitabine-based CRT, including the dose and the administration schedule of the drug, and the dose fractionation and field size of irradiation (Crane *et al*., 2001; Murphy *et al*., 2007). The severe gastrointestinal toxicities are especially encountered if irradiation fraction dose is > 2.2–2.4 Gy (Wilkowski *et al*., 2005). Among various factors influencing the therapeutic index of gemcitabine-based CRT, one of the most important is the irradiation field size. It is impossible to give the full cytotoxic dose of gemcitabine if the irradiation field size contains both gross tumor and draining lymph nodes areas. In the case of elective nodal irradiation, either gemcitabine dose or RT should be reduced to prevent the severe toxicity of treatment, which means the diminished systemic or local effectiveness of the concurrent therapy as can be expected. In order to solve this problem, researches have focused on the application of the limited treatment volume of RT concurrently with full cytotoxic dose of gemcitabine, which is able to exert better systemic activity.

In a phase I study, McGinn *et al*. (2001) established a concurrent CRT approach consisting of full cytotoxic dose of gemcitabine (1,000 mg/m^2 on days 1, 8, 15 of each 28-day cycle) plus escalating doses of conformal RT (24–42 Gy) with 1.6–2.8 Gy fractions. RT volume covered gross tumor volume only with 1 cm margin, leaving the regional lymph node areas outside the treatment target volume. This study and subsequent studies have clearly proven that the use of conformal RT with avoidance of elective nodal irradiation permits the application of full cytotoxic doses of gemcitabine with acceptable toxicity profile without compromising loco-regional efficacy (Talamonti *et al*., 2006; Yamazaki *et al*., 2007). Presently, the irradiation of the uninvolved regional lymphatics is unnecessary in the treatment of LAPC regardless of the concurrent chemotherapeutic agent used, because excessive gastrointestinal toxicity may occur while there is no meaningful effect on overall survival (Crane *et al*., 2007).

Besides 5-FU and gemcitabine, the role of the other chemotherapeutic agents has also been investigated in LAPC. Capecitabine, a prodrug taken by oral route, mimics the effects of protracted intravenous infusional 5-FU, and has been used in a wide variety of solid tumors. In LAPC, concurrent treatment with capecitabine and EBRT has been demonstrated as a well-tolerated regimen, and the efficacy data were comparable 5-FU-based CRT (Schneider *et al*., 2005). Ben-Josef *et al*. (2004) suggested that concurrent CRT with capecitabine (1,600 mg/m^2/day) plus IMRT revealed excellent preliminary efficacy with low toxicity in patients with PC. For eight patients who had unresectable disease, 1-year actuarial survival rate was 69%, and the disease converted to the resectable stage in two out of eight patients. Hence, capecitabine should replace 5-FU after phase III non-inferiority studies have

been accomplished, owing to the more convenient usage of the drug in comparison to protracted intravenous infusional 5-FU that is required for the replacement of a venous pump for the drug infusion.

Another chemotherapeutic agent, paclitaxel, has been studied in LAPC in a phase II study by the Radiation Therapy Oncology Group (RTOG) (Rich *et al*., 2004). In this study, weekly paclitaxel at the dose of 50 mg/m^2 was given with 50.4 Gy EBRT in patients with LAPC. In spite of the use of elective nodal irradiation, toxicity of the treatment was acceptable and the efficacy of the treatment was encouraging.

Because distant metastases are the main causes of treatment failures for LAPC, much attention has been focused on the use of more systemic treatments. Some authors examined the efficacy of the numerous cycles of CT before and/or after concurrent CRT. It seems that this approach gives no additional benefit over concurrent CRT alone (Schneider *et al*., 2005; Mishra *et al*., 2005; Kurt *et al*., 2006). In addition, CT after CRT has been found to be difficult to administer due to poor compliance of the patients (Schneider *et al*., 2005; Kurt *et al*., 2006). However, induction CT may discern the patients with LAPC, who could optimally benefit from concurrent consolidative CRT (Krishnan *et al*., 2007). Another strategy to exhibit more systemic efficacy is a combination CT regimen for concurrent treatment. However, it should be kept in mind that the toxicity of such treatment may be considerable as demonstrated by an ECOG trial (Talamonti *et al*., 2000), and most of the studies examining this issue reported similar efficacy as with more traditional CRT approaches (Haddock *et al*., 2007).

Novel Approaches

Apart from the classical chemotherapeutic agents, the targeted therapies seem to be attractive interventions for the treatment of PC. The expression of both epidermal growth factor receptor (EGFR) and its ligands is one of the most important molecular abnormalities in PC, and is associated with malignant and aggressive phenotypes. This led to clinical studies integrating EGFR inhibitors into the treatment of advanced PC.

In advanced stage PC, addition of an EGFR tyrosine kinase inhibitor (TKI) erlotinib to gemcitabine exerted significant survival advantage over gemcitabine alone in a randomized study by Moore *et al*. (2007). The experience concerning the use of the small molecule EGFR TKIs in LAPC is premature. Although another EGFR TKI gefitinib resulted in significant toxicity or limited activity in LAPC in different studies (Czito *et al*., 2006; Maurel *et al*., 2006), erlotinib seems to be a valuable therapeutic agent that can be administered concurrently with EBRT. In a phase I study by Iannitti *et al*. (2005), a novel CRT approach consisted of EBRT (50.4 Gy to the primary tumor and draining lymph nodes), erlotinib (50–100 mg/day), paclitaxel (40 mg/m^2, weekly for 6 weeks), and gemcitabine (75 mg/m^2, weekly for 6 weeks), followed by maintenance erlotinib (150 mg/day), was examined in LAPC. Authors concluded that the MTD of erlotinib for concurrent CRT with the presented schedule was 50 mg/day, and full dose maintenance erlotinib was well tolerated. Moreover, the preliminary activity of the regimen was found to be promising with a median survival of 14 months and an objective response rate of 46% for 13 patients with LAPC. Accordingly, it is

apparent that targeted therapies, especially EGFR inhibitors have noticeable clinical activity for the treatment of advanced PC. Trials evaluating the role of EGFR inhibitors as well as a broad spectrum of the targeted therapies, in particular, vascular endothelial growth factor (VEGF) inhibitors and the multitargeted agents in advanced PC are currently underway, and it is hoped that these agents will provide a safer and more effective ways of administering CRT in PC.

Recently, interesting chemobiologic approaches have evolved in the treatment of LAPC. TNFerade, a replication deficient adenoviral vector carrying the human tumor necrosis factor (TNF)-α gene regulated by the radiation inducible promoter, Egr-1, plus concurrent 5-FU-based CRT showed encouraging efficacy in LAPC according to the first interim analysis of a recent trial by Posner *et al*. (2007). These results should be confirmed by the second interim analysis of the study and by further studies.

CONCLUSIONS AND FURTHER CONSIDERATIONS

As a consequent, it can be concluded that currently available treatments have only modest influence on the outcome of patients with LAPC. Briefly, 5-FU-based CRT remains the treatment of choice according to most practitioners worldwide. Certain chemotherapeutic agents including gemcitabine, capecitabine, and paclitaxel, seem to be plausible alternatives to 5-FU as concurrent chemotherapeutic agents for the CRT of LAPC. However, it is emphasized that the administration of these newer drugs has not been demonstrated to be associated with better survival rates in comparison to the use of protracted intravenous infusional 5-FU. The routine use of elective nodal irradiation appears to be unnecessary, the avoidance of which does not result in excessive loco-regional failures, and does not compromise overall survival. In this way, effective cytotoxic doses of CT could be given to the patients receiving RT with acceptable treatment-related toxicities. It is likely that the novel agents targeting the important molecular abnormalities involved in the PC will take an important place in the CRT for LAPC in the future. One of the most suitable candidates of these agents seems to be erlotinib, an EGFR TKI, which has been the first targeted therapy to show an extended survival time among patients with advanced PC. The activity of erlotinib as well as TNFerade, cetuximab, bevacizumab, and other agents belonging to the family of multitargeted TKIs needs to be tested in further trials in locally advanced disease.

REFERENCES

Ashamalla, H., Zaki, B., Mokhtar, B., Colella, F., Selim, H., Krishnamurthy, M., and Ross, P. 2003. Hyperfractionated radiotherapy and paclitaxel for locally advanced/unresectable pancreatic cancer. *Int. J. Radiat. Oncol. Biol. Phys. 55*: 679–687.

Ben-Josef, E., Shields, A.F., Vaishampayan, U., Vaitkevicius, V., El-Rayes, B.F., McDermott, P., Burmeister, J., Bossenberger, T., and Philip, P.A. 2004. Intensity-modulated radiotherapy (IMRT) and concurrent capecitabine for pancreatic cancer. *Int. J. Radiat. Oncol. Biol. Phys. 59*: 454–459.

Blackstock, A.W., Bernard, S.A., Richards, F., Eagle, K.S., Case, L.D., Poole, M.E., Savage, P.D., and Tepper, J.E. 1999. Phase I trial of twice-weekly gemcitabine and concurrent radiation in patients with advanced pancreatic cancer. *J. Clin. Oncol. 17*: 2208–2212.

Burris, H.A., Moore, M.J., Andersen, J., Green, M.R., Rothenberg, M.L., Modiano, M.R., Cripps, M.C., Portenoy, R.K., Storniolo, A.M., Tarassoff, P., Nelson, R., Dorr, F.A., Stephens, C.D., and Von Hoff, D.D. 1997. Improvements in survival and clinical benefit with gemcitabine as first-line therapy for patients with advanced pancreas cancer: a randomized trial. *J. Clin. Oncol. 15*: 2403–2413.

Calvo, F.A., Viera, J.C., Gunderson, L.L., and Willett, C.G. Cancer of the pancreas. 2004. In: *Principles and Practice of Radiation Oncology*. Perez, C.A., Brady, L.W., Halperin, E.C., and Schmidt-Ullrich, R.K. (eds.). Lippincott Williams&Wilkins, Philadelphia, PA: pp. 1574–1588.

Crane, C.H., Wolff, R.A., Abbruzzese, J.L., Evans, D.B., Milas, L., Mason, K., Charnsangavej, C., Pisters, P.W., Lee, J.E., Lenzi, R., Lahoti, S., Vauthey, J.N., and Janjan, N.A. 2001. Combining gemcitabine with radiation in pancreatic cancer: understanding important variables influencing the therapeutic index. *Semin. Oncol. 28*: 25–33.

Crane, C.H., Abbruzzese, J.L., Evans, D.B., Wolff, R.A., Ballo, M.T., Delclos, M., Milas, L., Mason, K., Charnsangavej, C., Pisters, P.W., Lee, J.E., Lenzi, R., Vauthey, J.N., Wong, A.B., Phan, T., Nguyen, Q., and Janjan, N.A. 2002. Is the therapeutic index better with gemcitabine-based chemoradiation than with 5-fluorouracil-based chemoradiation in locally advanced pancreatic cancer? *Int. J. Radiat. Oncol. Biol. Phys. 52*: 1293–1302.

Crane, C.H., Varadhachary, G., Pisters, P.W., Evans, D.B., and Wolff, R.A. 2007. Future chemoradiation strategies in pancreatic cancer. *Semin. Oncol. 34*: 335–346.

Czito, B.G., Willett, C.G., Bendell, J.C., Morse, M.A., Tyler, D.S., Fernando, N.H., Mantyh, C.R., Blobe, G.C., Honeycutt, W., Yu, D., Clary, B.M., Pappas, T.N., Ludwig, K.A., and Hurwitz, H.I. 2006. Increased toxicity with gefitinib, capecitabine, and radiation therapy in pancreatic and rectal cancer: phase I trial results. *J. Clin. Oncol. 24*: 656–662.

Dobelbower, R.R., Merrick, H.W., Ahuja, R.K., and Skeel, R.T. 1986. 125I interstitial implant, precision high-dose external beam therapy, and 5-FU for unresectable adenocarcinoma of pancreas and extrahepatic biliary tree. *Cancer 58*: 2185–2195.

Gastrointestinal Tumor Study Group. 1988. Treatment of locally unresectable carcinoma of the pancreas: comparison of combined-modality therapy (chemotherapy plus radiotherapy) to chemotherapy alone. Gastrointestinal Tumor Study Group. *J. Natl. Cancer Inst. 80*: 751–755.

Gastrointestinal Tumor Study Group. 1985. Radiation therapy combined with adriamycin or 5-fluorouracil for the treatment of locally unresectable pancreatic carcinoma. Gastrointestinal Tumor Study Group. Gastrointestinal Tumor Study Group. *Cancer 56*: 2563–2568.

Haddock, M.G., Swaminathan, R., Foster, N.R., Hauge, M.D., Martenson, J.A., Camoriano, J.K., Stella, P.J., Tenglin, R.C., Schaefer, P.L., Moore, D.F., and Alberts, S.R. 2007. Gemcitabine, cisplatin, and radiotherapy for patients with locally advanced pancreatic adenocarcinoma: results of the North Central Cancer Treatment Group Phase II Study N9942. *J. Clin. Oncol. 25*: 2567–2572.

Huguet, F., André, T., Hammel, P., Artru, P., Balosso, J., Selle, F., Deniaud-Alexandre, E., Ruszniewski, P., Touboul, E., Labianca, R., de Gramont, A., and Louvet, C. 2007. Impact of chemoradiotherapy after disease control with chemotherapy in locally advanced pancreatic adenocarcinoma in GERCOR phase II and III studies. *J. Clin. Oncol. 25*: 326–331.

Iannitti, D., Dipetrillo, T., Akerman, P., Barnett, J.M., Maia-Acuna, C., Cruff, D., Miner, T., Martel, D., Cioffi, W., Remis, M., Kennedy, T., and Safran, H. 2005. Erlotinib and chemoradiation followed by maintenance erlotinib for locally advanced pancreatic cancer: a phase I study. *Am. J. Clin. Oncol. 28*: 570–575.

Klaassen, D.J., MacIntyre, J.M., Catton, G.E., Engstrom, P.F., and Moertel, C.G. 1985. Treatment of locally unresectable cancer of the stomach and pancreas: a randomized comparison of 5-fluorouracil alone with radiation plus concurrent and maintenance 5-fluorouracil–an Eastern Cooperative Oncology Group study. *J. Clin. Oncol. 3*: 375–378.

Koong, A.C., Christofferson, E., Le, Q.T., Goodman, K.A., Ho, A., Kuo, T., Ford, J.M., Fisher, G.A., Greco, R., Norton, J., and Yang, G.P. 2005. Phase II study to assess the efficacy of conventionally

fractionated radiotherapy followed by a stereotactic radiosurgery boost in patients with locally advanced pancreatic cancer. *Int. J. Radiat. Oncol. Biol. Phys. 63*: 320–323.

Krishnan, S., Rana, V., Janjan, N.A., Varadhachary, G.R., Abbruzzese, J.L., Das, P., Delclos, M.E., Gould, M.S., Evans, D.B., Wolff, R.A., and Crane, C.H. 2007. Induction chemotherapy selects patients with locally advanced, unresectable pancreatic cancer for optimal benefit from consolidative chemoradiation therapy. *Cancer 110*: 47–55.

Kurt, E., Kurt, M., Kanat, O., Cetintas, S.K., Aygun, S., Palazoglu, T., Ozkan, L., Evrensel, T., Kaya, E., and Manavoglu, O. 2006. Phase II study of induction chemotherapy with gemcitabine plus 5-fluorouracil followed by gemcitabine-based concurrent chemoradiotherapy for unresectable locally advanced pancreatic cancer. *Tumori 92*: 481–486.

Lawrence, T.S., Chang, E.Y., Hahn, T.M., Hertel, L.W., and Shewach, D.S. 1996. Radiosensitization of pancreatic cancer cells by 2',2'-difluoro-2'-deoxycytidine. *Int. J. Radiat. Oncol. Biol. Phys. 34*: 867–872.

Li, C.P., Chao, Y., Chi, K.H., Chan, W.K., Teng, H.C., Lee, R.C., Chang, F.Y., Lee, S.D., and Yen, S.H. 2003. Concurrent chemoradiotherapy treatment of locally advanced pancreatic cancer: gemcitabine versus 5-fluorouracil, a randomized controlled study. *Int. J. Radiat. Oncol. Biol. Phys. 57*: 98–104.

Mancuso, A., Calabrò, F., and Sternberg, C.N. 2006. Current therapies and advances in the treatment of pancreatic cancer. *Crit. Rev. Oncol. Hematol. 58*: 231–241.

Maurel, J., Martin-Richard, M., Conill, C., Sánchez, M., Petriz, L., Ginès, A., Miquel, R., Gallego, R., Cajal, R., Ayuso, C., Navarro, S., Marmol, M., Nadal, C., Augé, J.M., Fernández-Cruz, L., and Gascón, P. 2006. Phase I trial of gefitinib with concurrent radiotherapy and fixed 2-h gemcitabine infusion, in locally advanced pancreatic cancer. *Int. J. Radiat. Oncol. Biol. Phys. 66*: 1391–1398.

McGinn, C.J., Zalupski, M.M., Shureiqi, I., Robertson, J.M., Eckhauser, F.E., Smith, D.C., Brown, D., Hejna, G., Strawderman, M., Normolle, D., and Lawrence, T.S. 2001. Phase I trial of radiation dose escalation with concurrent weekly full-dose gemcitabine in patients with advanced pancreatic cancer. *J. Clin. Oncol. 19*: 4202–4208.

Milano, M.T., Chmura, S.J., Garofalo, M.C., Rash, C., Roeske, J.C., Connell, P.P., Kwon, O.H., Jani, A.B., and Heimann, R. 2004. Intensity-modulated radiotherapy in treatment of pancreatic and bile duct malignancies: toxicity and clinical outcome. *Int. J. Radiat. Oncol. Biol. Phys. 59*: 445–453.

Mishra, G., Butler, J., Ho, C., Melin, S., Case, L.D., Ennever, P.R., Magrinat, G.C., Bearden, J.D., Minotto, D.C., Howerton, R., Levine, E., and Blackstock, A.W. 2005. Phase II trial of induction gemcitabine/CPT-11 followed by a twice-weekly infusion of gemcitabine and concurrent external beam radiation for the treatment of locally advanced pancreatic cancer. *Am. J. Clin. Oncol. 28*: 345–350.

Moertel, C.G., Childs, D.S., Reitemeier, R.J., Colby, M.Y., and Holbrook, M.A. 1969. Combined 5-fluorouracil and supervoltage radiation therapy of locally unresectable gastrointestinal cancer. *Lancet 2*: 865–867.

Moertel, C.G., Frytak, S., Hahn, R.G., O'Connell, M.Y., Reitemeier, R.J., Rubin, J., Schutt, A.J., Weiland, L.H., Childs, D.S., Holbrook, M.A., Lavin, P.T., Livstone, E., Spiro, H., Knowlton, A., Kalser, M., Barkin, J., Lessner, H., Mann-Kaplan, R., Ramming, K., Douglas, H.O., Thomas, P., Nave, H., Bateman, J., Lokich, J., Brooks, J., Chaffey, J., Corson, J.M., Zamcheck, N., and Novak, J.W. 1981. Therapy of locally unresectable pancreatic carcinoma: a randomized comparison of high dose (6000 rads) radiation alone, moderate dose radiation (4000 rads + 5-fluorouracil), and high dose radiation + 5-fluorouracil: The Gastrointestinal Tumor Study Group. *Cancer 48*: 1705–1710.

Mohiuddin, M., Cantor, R.J., Biermann, W., Weiss, S.M., Barbot, D., and Rosato, F.E. 1988. Combined modality treatment of localized unresectable adenocarcinoma of the pancreas. *Int. J. Radiat. Oncol. Biol. Phys. 14*: 79–84.

Moore, M.J., Goldstein, D., Hamm, J., Figer, A., Hecht, J.R., Gallinger, S., Au, H.J., Murawa, P., Walde, D., Wolff, R.A., Campos, D., Lim, R., Ding, K., Clark, G., Voskoglou-Nomikos, T., Ptasynski, M., and Parulekar, W.; National Cancer Institute of Canada Clinical Trials Group. 2007. Erlotinib plus gemcitabine compared with

gemcitabine alone in patients with advanced pancreatic cancer: a phase III trial of the National Cancer Institute of Canada Clinical Trials Group. *J. Clin. Oncol. 25*: 1960–1966.

Murphy, J.D., Adusumilli, S., Griffith, K.A., Ray, M.E., Zalupski, M.M., Lawrence, T.S., and Ben-Josef, E. 2007. Full-dose gemcitabine and concurrent radiotherapy for unresectable pancreatic cancer. *Int. J. Radiat. Oncol. Biol. Phys. 68*: 801–808.

Poen, J.C., Collins, H.L., Niederhuber, J.E., Oberhelman, H.A., Vierra, M.A., Bastidas, A.J., Young, H.S., Slosberg, E.A., Jeffrey, B.R., Longacre, T.A., Fisher, G.A., and Goffinet, D.R. 1998. Chemo-radiotherapy for localized pancreatic cancer: increased dose intensity and reduced acute toxicity with concomitant radiotherapy and protracted venous infusion 5-fluorouracil. *Int. J. Radiat. Oncol. Biol. Phys. 40*: 93–99.

Posner, M., Chang, K.J., Rosemurgy, A., Stephenson, J., Khan, M., Reid, T., Fisher, W.E., Waxman, I., Von Hoff, D., and Hecht, R. 2007. Multi-center phase II/III randomized controlled clinical trial using TNFerade combined with chemoradiation in patients with locally advanced pancreatic cancer (LAPC). *American Society of Clinical Oncology (ASCO) 2007 Annual Meeting: A4518*.

Rich, T., Harris, J., Abrams, R., Erickson, B., Doherty, M., Paradelo, J., Small, W., Safran, H., and Wanebo, H.J. 2004. Phase II study of external irradiation and weekly paclitaxel for nonmetastatic, unresectable pancreatic cancer: RTOG-98-12. *Am. J. Clin. Oncol. 27*: 51–56.

Russo, S., Butler, J., Ove, R., and Blackstock, A.W. 2007. Locally advanced pancreatic cancer: a review. *Semin. Oncol. 34*: 327–334.

Schneider, B.J., Ben-Josef, E., McGinn, C.J., Chang, A.E., Colletti, L.M., Normolle, D.P., Hejna, G.F., Lawrence, T.S., and Zalupski, M.M. 2005. Capecitabine and radiation therapy preceded and followed by combination chemotherapy in advanced pancreatic cancer. *Int. J. Radiat. Oncol. Biol. Phys. 63*: 1325–1330.

Sultana, A., Tudur, S.C., Cunningham, D., Starling, N., Tait, D., Neoptolemos, J.P., and Ghaneh, P. 2007. Systematic review, including meta-analyses, on the management of locally advanced pancreatic cancer using radiation/combined modality therapy.. *Br. J. Cancer 96*: 1183–1190.

Talamonti, M.S., Catalano, P.J., Vaughn, D.J., Whittington, R., Beauchamp, R.D., Berlin, J., and Benson, A.B. 2000. Eastern Cooperative Oncology Group Phase I trial of protracted venous infusion fluorouracil plus weekly gemcitabine with concurrent radiation therapy in patients with locally advanced pancreas cancer: a regimen with unexpected early toxicity. *J. Clin. Oncol. 18*: 3384–3389.

Talamonti, M.S., Small, W., Mulcahy, M.F., Wayne, J.D., Attaluri, V., Colletti, L.M., Zalupski, M.M., Hoffman, J.P., Freedman, G.M., Kinsella, T.J., Philip, P.A., and McGinn, C.J. 2006. A multiinstitutional phase II trial of preoperative full-dose gemcitabine and concurrent radiation for patients with potentially resectable pancreatic carcinoma. *Ann. Surg. Oncol. 13*: 150–158.

Wilkowski, R., Thoma, M., Weingandt, H., Dühmke, E., and Heinemann, V. 2005. Chemoradiation for ductal pancreatic carcinoma: principles of combining chemotherapy with radiation, definition of target volume and radiation dose. *J. Pancreas 6*: 216–230.

Yamazaki, H., Nishiyama, K., Koizumi, M., Tanaka, E., Ioka, T., Uehara, H., Iishi, H., Nakaizumi, A., Ohigashi, H., and Ishikawa, O. 2007. Concurrent chemoradiotherapy for advanced pancreatic cancer: 1,000 mg/m2 gemcitabine can be administered using limited-field radiotherapy. *Strahlenther. Onkol. 183*: 301–306.

Yip, D., Karapetis, C., Strickland, A., Steer, C.B., and Goldstein, D. 2006. Chemotherapy and radiotherapy for inoperable advanced pancreatic cancer. *Cochrane Database Syst. Rev. 3*: CD002093.

Index

f: Refers to the keywords cited in figure captions
t: Refers to the keywords cited in tables